Economic Plantwide Control Techniques Applied to a Reactor-Separator-Recycle Process

A thesis submitted

in partial fulfillment of the requirement for the degree of

Doctor of Philosophy
in
Chemical Engineering
by

Vivek Kumar
(Roll No. 11102083)

to the

DEPARTMENT OF CHEMICAL ENGINEERING
INDIAN INSTITUTE OF TECHNOLOGY KANPUR

January, 2019

Department of Chemical Engineering
Indian Institute of Technology Kanpur
Kanpur, India

Certificate

This is to certify that the work contained in the thesis entitled **“Economic Plantwide Control Techniques Applied to a Reactor-Separator-Recycle Process”**, submitted by Vivek Kumar, for the award of the degree of *Doctor of Philosophy* in *Chemical Engineering*, has been carried out under my supervision and this work has not been submitted elsewhere for a degree.

Dr. Nitin Kaistha
Professor
Department of Chemical Engineering
Indian Institute of Technology Kanpur
Kanpur- 208016, India

Date: 7th January, 2019

Synopsis

Name of Student: **Vivek Kumar**

Roll No.: **11102083**

Degree for which submitted: **PhD**

Department: **Chemical Engineering**

Thesis title: **Economic Plantwide Control Techniques Applied to a Reactor-Separator-Recycle Process**

Thesis supervisor: **Dr. Nitin Kaistha** (Professor)
Department of Chemical Engineering, IIT Kanpur

Optimal steady operation of continuous integrated chemical processes requires the design of a plantwide control system that drives the process operation as close as possible to the optimally active constraints and closely tracks the optimum values of controlled variables (CVs) corresponding to any remaining unconstrained degrees of freedom (dofs). The combinatorial flexibility in CV-MV (manipulated variable) pairings is usually gainfully exploited to obtain pairings that achieve tight control of the active constraints. This allows the process to be driven as close as possible to the active constraint limits with negligible back-off. In case the active constraint set changes, overrides or supervisory model predictive control (MPC) effects the necessary reconfiguration in the CV-MV pairings for tight control of the new active constraint set. Given tight active constraint control, the remaining issue is obtaining and tracking the optimum value of CVs corresponding to any unconstrained dofs. Tracking is usually desirable as the optimum value of the unconstrained CV changes with operating conditions and disturbances with significant economic loss for constant setpoint operation. Optimal management of the unconstrained CVs is one of the more challenging issues in economic plantwide control system design. This work evaluates three extant approaches, namely, hill-climbing control, real-time optimization (RTO) and self optimizing control (SOC) for managing optimally unconstrained dofs. These approaches are evaluated for optimal operation of a reactor-separator-recycle process with the $A + B \rightarrow C$ reaction chemistry, which has been used previously in plantwide control studies. Optimal operation is evaluated for two modes of operation. In Mode I, the throughput is given and the column boilup (or sometimes recycle rate) is minimized. In Mode II, the throughput is maximized subject to a capacity bottleneck.

First, Shinskey's hill-climbing controller is evaluated for tracking the optimum value of the reactor composition setpoint in the reactor-separator-recycle process. This is a variant of extremum seeking control, where the process is perturbed to estimate the gradient of the economic objective with respect to the unconstrained CV and feedback is applied to drive this gradient to zero, corresponding to the CV optimum. This is followed by the development of a steady state model and specific parameter estimation method to fit recent plant data for RTO of the reactor composition setpoint. The steady state results show that the RTO economic loss from the actual plant optimum is less than 0.1% suggesting that the proposed RTO method drives the reactor composition very close to the actual plant optimum. The dynamic economic performance of the RTO method developed is then evaluated. In particular, overrides for handling the capacity bottleneck are shown to provide a smooth Mode I ↔ Mode II transition. Also the economic benefit is found to be similar to the results from the steady state analysis. The idea of a globally optimal invariant based control law for tracking the optimum value of the reactor composition is then explored. The invariant is obtained from an analysis of the overall plant material balance. The analysis is performed for alternative reaction kinetic expressions. It reveals that at constant reactor *A/B* ratio, near optimum process operation is achieved over the envisaged disturbance space regardless of the plant reaction kinetic expression. The reactor *A/B* ratio is thus a good self-optimizing CV (SOCV), which by definition, achieves near optimal process operation at constant setpoint. To avoid cumbersome and expensive reactor composition measurements in this SOCV, using the separator distillation column top tray temperature as an inferential replacement of the reactor *A/B* ratio is proposed. The closed loop dynamic and economic performance of the synthesized plantwide control system is then evaluated and quantified. The work concludes with a summary of the main findings from the evaluation of the various approaches for (near) optimal management of an unconstrained dof and pointers for future work.

To My Family

Acknowledgment

I would like to express my heartfelt gratitude to my thesis supervisor **Dr. Nitin Kaistha** for his expert guidance and constant inspiration which made possible the completion of this thesis. Indeed I consider myself very fortunate to have worked under his supervision. He has inspired me at all stages and spared invaluable time for discussion, whenever I needed it.

I gratefully acknowledge IITK for providing excellent environment for academic and research work.

I would like to thank all my lab mates throughout the years when I joined, specially *Rahul Jagtap*, *Ojasvi*, *Abhishek*, *Harish*, *Pallavi*, *Aryan*, *Rishabh*, *Sudhodhan*, *Ashish*, *Ankit*, *Garima*, *Jeeshan*, *Kalp*, *Nikita*, *Shyam*, *Vikas*, *Aditya* and *Dinesh Ji* to make lab environment cheerful.

I would like to thank my friends *Yogendra Nath Prajapati*, *Prateek Khare*, *Abhi Mukherjee* and many more for motivating me to complete this task.

I would like to express my sincere and deepest gratitude to my family for their eternal love and unconditional support. Most importantly, I would like to thank my wife ***Priyanka*** for always being there and motivate me to complete this thesis.

With the blessing of my mother, I am going to submit this thesis.

Vivek Kumar

TABLE OF CONTENTS

Certificate *ii*
Synopsis *iii*
Acknowledgment *vii*
Table of Content *viii*
List of Figures *xi*
List of Tables *xiii*

Chapter 1 **Introduction** 1
1.1. Integration in Process Industry 1
1.2. Plantwide Control of Integrated Processes 2
    1.2.1. Basic Regulatory Plantwide Control System 3
    1.2.2. Economic Plantwide Control 8
    1.2.3. Overall Plantwide Control Hierarchy 10
1.3. Approaches for Managing Unconstrained Setpoints 11
    1.3.1. Extremum-Seeking Control 12
    1.3.2. Real-Time Optimization 12
    1.3.3. Self Optimizing Control 15
1.4. Thesis Motivation and Scope 17
1.5. Reactor-Separator-Recycle Process 18
1.6. Thesis Organization and Style 20
References 21

Chapter 2 **Hill climbing for plant wide control to economic optimum** 27
2.1. Introduction 28
2.2. Process description 29
    2.2.1. Optimum Steady Process Operation 31
2.3. Plantwide Regulatory Control Structure 33
    2.3.1. Regulatory Control Structure for Mode I 34
    2.3.2. Regulatory Control Structure for Mode II 37
    2.3.3. Overrides for Reconfiguring Regulatory Layer Loops 38
    2.3.4. Augmented Control System for Economic Operation 41
2.4. Shinskey's Hill-Climber 44
2.5. Dynamic Simulation and Controller Tuning 46
    2.5.1. Closed Loop Results 47
2.6. Discussion 52

2.7. Conclusion 54

References 54

Chapter 3 Real Time Optimization of a Reactor-Separator-Recycle Process I: steady state modelling 55

3.1. Introduction 56

3.2. Plantwide Process Module 57

    3.2.1. Economic Optimum Steady State Operation 59

3.3. Steady State RTO Modelling 62

    3.3.1. Estimation of Material Stream Component Flows 64

    3.3.2. Estimation of Reaction Kinetic Model Parameters 66

    3.3.3. Estimation of Column Model Parameters 68

    3.3.4. Fitted Model Optimization 71

3.4. Steady State RTO Performance Evaluation 74

    3.4.1. Impact of Kinetic Model on RTO Performance 76

    3.4.2. Impact of Column Model on RTO Performance 79

    3.4.3. Impact of Measurement Bias on RTO Performance 82

    3.4.4. Quantitative Benefit of RTO Over Constant Setpoint Operation 82

3.5. Discussion 83

    3.5.1. Adequacy of Kinetic Models 83

    3.5.2. Minimum Excitation Due to Measurement Uncertainty 86

    3.5.3. Miscellaneous Comments 89

3.6. Conclusion 90

References 91

Chapter 4 Real Time Optimization of a Reactor-Separator-Recycle Process II: Dynamic Evaluation 93

4.1. Introduction 94

4.2. Summary of part 1 results 96

4.3. Regulatory Layer Pairings for Mode I and Mode II 100

    4.3.1 Mode I 100

    4.3.2. Mode II 102

4.4. Overrides for Mode I ↔ Mode II Transition 104

4.5. Mode I ↔ Mode II Switching in RTO Layer 106

4.6. Control System Tuning 107

4.7. Dynamic Results 109

    4.7.1. Regulatory Layer Performance 110

4.7.2. RTO Performance 112
4.8. Discussion 121
4.9. Conclusion 124
References 124

Chapter 5 **Invariants for Optimal Operation of a Reactor-Separator-Recycle Process** 126
5.1. Introduction 127
5.2. Process Description and Optimal Operation 129
5.3. Globally Optimal Invariants from Simplified Analysis 133
5.3.1. Mode I Globally Optimal Invariant 135
5.3.2. Mode II Globally Optimal Invariant 137
5.4. Evaluation of Optimal Operation Policies for the Rigorous Case 140
5.5. Discussion 145
5.6. Conclusion 147
References 147

Chapter 6 **Inferential Self Optimizing Control of a Reactor-Separator-Recycle Process** 149
6.1. Introduction 150
6.2. Process Description 152
6.3. Optimal Operation 154
6.4. Inferential SOCV 159
6.5. Plantwide Control Systems 160
6.6. Closed Loop Dynamic Results 163
6.7. Discussion 175
6.8. Conclusions 177
References 178

Chapter 7 **Summary and future work** 180
References 185

Nomenclature 186

LIST OF FIGURES

Figure 1.1 Schematics of (a) LQ (b) DQ (c) LB and (d) DB control configurations 4
Figure 1.2 Alternate control structures with TPM at (a) L (b) B (c) D and (d) Q 5
Figure 1.3 Plant material balance with TPM at (a) Fresh feed (b) Total feed 6
Figure 1.4 Inventory control loop orientation around TPM 7
Figure 1.5 Illustration of tightness of active constraint control and backoff 8
Figure 1.6 Illustration of (a) Constraint (b) Unconstrained regulatory setpoints 9
Figure 1.7 Hierarchical three-layered control structure 11
Figure 1.8 Schematic of reactor-separator-recycle process 19

Figure 2.1 Conventional regulatory control structure, CS1 (for Mode I) 36
Figure 2.2 Regulatory control structure, CS2 (for Mode II) 38
Figure 2.3 Overrides for switching between CS1 and CS2 39
Figure 2.4 Variation in V with x_{rxrB} and L/F_{col} at design throughput (F_B=100 kmol/h) 42
Figure 2.5 (a) CS1 modifications for economic optimum operation 43
(b) CS2 modifications for economic optimum operation 44
Figure 2.6 Block-diagram of the one-dof hill-climber 45
Figure 2.7 Dynamic response for boilup minimization 48
Figure 2.8 Dynamic response for throughput maximization 49
Figure 2.9 (a) 10% A impurity in F_B 50
(b) 10% B impurity in F_A 51

Figure 3.1 Variation of plant column tray efficiency (η) with F_{factor} 59
Figure 3.2 Column model fitting (a) x_C^R measured (b) x_C^R unmeasured 70
Figure 3.3 Optimization of x_{rxrB}^m for fitted plant model 72
Figure 3.4 Real time optimization cycle 73
Figure 3.5 Deviation in RTO converged steady state from actual plant optimum for various disturbance scenarios using alternative kinetic models (a) Decision variable (b) Economic Objective 77
Figure3.6 Evolution of x_{rxrB}^{SP} and J with RTO iterations for 10% loss in catalyst activity using alternative reaction kinetic models (a) KM I (b) KM II (c) KM III 78
Figure 3.7 Deviation in RTO converged steady state from actual plant optimum for various disturbance scenarios for different column model (a) Decision variable (b) Economic Objective 80
Figure3.8 Evolution of x_{rxrB}^{SP} and J with RTO iterations for 10% loss in catalyst activity in Mode II using alternate column model 81
Figure 3.9 Contrasting point-wise adequacy of KM II vs inadequacy of KM I for (a) Mode I (b) Mode II 84
Figure 3.10 Variation in $\Delta\alpha/\alpha$ with Δx_{rxrB} for various measurement uncertainty levels using up to 4 recent steady states (SS) for parameter fitting 88

Figure 4.1 Conventional control structure, CS1 for Mode I 101
Figure 4.2 Back-off illustration 103
Figure 4.3 Control structure, CS2 for Mode II 103
Figure 4.4 Override control structure for Mode I ↔ Mode II transition 104
Figure 4.5 Mode I ↔ Mode II transition without RTO 111
Figure 4.6 Transient approach to optimum for $k_{90\%}$ for (a) Mode I (b) Mode II 113
Figure 4.7 Mode I operation for slow decay in catalyst activity over 6 months 118
Figure 4.8 Mode II operation for slow decay in catalyst activity over one year 119
Figure 4.9 Mode I → Mode II → Mode I transition 122

Figure 5.1 % Economic loss with principal disturbance for (a) Mode I (b) Mode II 142
Figure 5.2 Loss$_{\%}$ for global invariant and *[A/B]* for KM III for (a) Mode I (b) Mode II 144
Figure 5.3 Loss% for invariant control law, polynomial control law and constant ER operation for (a) Mode I (b) Mode II 146

Figure 6.1 % Economic loss for four alternative CVs (a) Mode Ib (b) Mode IIb 158
Figure 6.2 Plantwide control structure, CS1 162
Figure 6.3 Plantwide control structure, CS2 162
Figure 6.4 Transient response for a ±20% Mode Ib throughput change (a) CS1 (b) CS2 166
Figure 6.5 Mode Ib transient response for 10 mol% A in F_B (a) CS1 (b) CS2 168
Figure 6.6 Mode Ib transient response for 20% catalyst activity decay (a) CS1 (b) CS2 169
Figure 6.7 30% activity decay for Mode IIb (a) CS1 (b) CS2 170
Figure 6.8 Variation in $\Delta[V/P]_{\mathrm{av}}\%$ and $\Delta P_{\mathrm{av}}\%$ for different sinusoid time periods for considered sinusoid disturbances for (a) Mode Ib (b) Mode IIb 172
Figure 6.9 Mode Ib → Mode IIb → Mode Ib transition for constant x_C^R 173
Figure 6.10 Economic objective at backed-off ΔT (a) Mode Ib (b) Mode IIb 175
Figure 6.11 Transient response to a ±20% Mode Ib throughput change at backed-off ΔT for (a) CS1$^{\Delta T}$ (b) CS2$^{\Delta T}$ 176

LIST OF TABLES

Table 2.1 Recycle process base-case operating conditions for Mode I 30
Table 2.2 Modeling details of recycle process 30
Table 2.3 Process Optimization Summary 32
Table 2.4 V at throughput of F_B = 125 kmol/h 42
Table 2.5 Salient controller parameters for CS1/CS2 48

Table 3.1 The salient base-case process operating conditions 58
Table 3.2 Modeling details of recycle process 58
Table 3.3 Plant Optimization Summary 63
Table 3.4 RTO performance with ± 5% bias in key measurements 82
Table 3.5 Quantitative comparison of RTO with constant setpoint operation for different disturbance scenarios 83
Table 3.6 RTO performance with different LHHW models 86
Table 3.7 RTO performance with 1% measurement uncertainty 89

Table 4.1 Salient optimum operating conditions for Mode I/Mode II 99
Table 4.2 Salient controller parameters for CS1/CS2 108
Table 4.3 Quantitative comparison of RTO with optimal operation for different disturbance (step change) scenarios 113
Table 4.4 Disturbance scenarios evaluated 114
Table 4.5 Economic comparison for disturbance scenarios 117

Table 5.1 Hypothetical component properties and kinetic parameters 130
Table 5.2 Salient base-case steady state conditions for Mode I/Mode II 133
Table 5.3 Plant globally optimal invariants 140
Table 5.4 Quantitative evaluation of candidate unconstrained CV 143

Table 6.1 The salient base-case process operating conditions 153
Table 6.2 Hypothetical component properties and reaction kinetics 153
Table 6.3 % Loss for the four candidate SOCVs 159
Table 6.4 Salient controller parameters for CS1/CS2 164
Table 6.5 Evaluation of disturbances 164

Chapter 1

Introduction

1.1 Integration in Process Industry

The continuous process industry is the bedrock supporting the modern, consumerist, high standard-of-living lifestyle of today. Petroleum fuel products such as gasoline, diesel and aviation turbine fuel, petrochemicals such as polymers and resins as well as chemicals such as esters, alcohols and ketones, are manufactured in bulk in continuous integrated chemical plants [1]. These are then supplied to downstream processing chains that result in the finished end-products, such as clothing, vinyl floors/tiles, PET beverage bottles, plasticware, fuels etc, for use by the consumer. Market competition as well as long-term sustainability concerns dictate that the continuous processes be designed for maximum possible raw-material and energy utilization efficiency. Material and energy recycle is thus routinely employed to maximize the respective efficiencies. This is also referred to as process integration [2].

For integrated processes involving the transformation of raw materials to value added products via appropriate reaction chemistry, the ideal process takes in only the reactants and gives out only the product with no waste streams, i.e. zero waste discharge, implying 100% raw-material utilization efficiency. In addition to highly selective reaction chemistry, this necessarily requires the separation of the valuable product from the reactor effluent mixture as well as recovery and recycle of the unconverted reactants. Almost all continuous processing plants involving chemical transformations thus have the "reaction followed by separation" topology with at least one material recycle stream between the reaction and separation sections[3]. Even for separations that are complicated by e.g. the presence of azeotropes, it is usually economical to employ more complex separation cum recycle schemes [4] that achieves the (near) perfect raw material utilization efficiency target. This is because raw-materials are usually quite expensive and energy is relatively much cheaper so that the savings due to efficient raw material utilization easily compensates for the higher separation cost (Douglas doctrine [5]). For such systems, the overall plant topology is more involved with potentially multiple material recycle loops.

Given a process topology that achieves the best possible material utilization efficiency, the process economics can be further improved by process-to-process heat exchange so that the external utility (e.g. steam or refrigeration) consumption per kg product is reduced for better energy efficiency. A very common example in reactor-separator-recycle processes is the hot reactor effluent preheating the cold feed. Such process-to-process heat exchange creates an energy recycle loop [6]. It is easy to imagine even the simplest of plants having multiple energy recycle loops for enhanced energy efficiency [7-8].

1.2 Plantwide Control of Integrated Processes

From the economic perspective, process integration with multiple material/energy recycle loops is very appealing. From the plant operations perspective however, the loops create interconnections between different sections of the plant with steady state and dynamic implications. The positive feedback due to recycle results in high steady state non-linearity. Common examples are the high recycle rate sensitivity to fresh feed rate changes (snowball effect [9]) as well as steady state multiplicity [10-12]. At the dynamic level, the loops create multiple pathways over which disturbances can propagate. A "local" disturbance in one section, unless properly managed by a well-designed plantwide control system, may propagate to other plant sections and further on, to the entire plant with non-linear amplification of the transients due to steady state non-linearity [13-14]. The realization of the economic benefit in integrated chemical plants is thus intimately linked to the plantwide control system.

1.2.1 Basic Regulatory Plantwide Control System

At the most basic level, a plantwide control system is required to close all the independent plant material and energy balances. The corresponding control system is also referred to as the basic regulatory control system. For robustness, usually a decentralized control system with PID controllers is used [15]. The controller manipulates either the input rate or the output rate or the generation rate in the associated material/energy balance equation.

The plant balances to be closed include obvious ones on each of the individual unit operations as well as subtler highly non-linear plantwide balances encompassing the recycle loops[16]. Further, the transients associated with the overall plant balances are plantwide in nature as they must necessarily propagate across the entire recycle loop. Consequently, the open loop dynamics of plantwide balances involving recycle loops is usually quite slow [16-17]. This discussion highlights that one of the key issues in plantwide regulatory control is managing the transients around recycle loops.

The design of a robust regulatory control system is a very interesting problem with several possible pairings due to the curse of dimensionality (combinatorial complexity). For example, at a given feed rate, the simple distillation column has four basic control configurations [18]. These are the well known LQ, DQ, LB and DB configurations (see Figure 1.1), the latter being applied in superfractionators [19]. Instead of fixing the fresh feed rate, if one of the other material streams is fixed (e.g. distillate rate, bottoms rate or steam rate), one would obtain alternative control structures (see Figure 1.2). It is easy to see that for a more complex plant with multiple columns, the number of possible regulatory control structures grows exponentially. How does then one systematically deal with the curse of dimensionality in plantwide regulatory control system design?

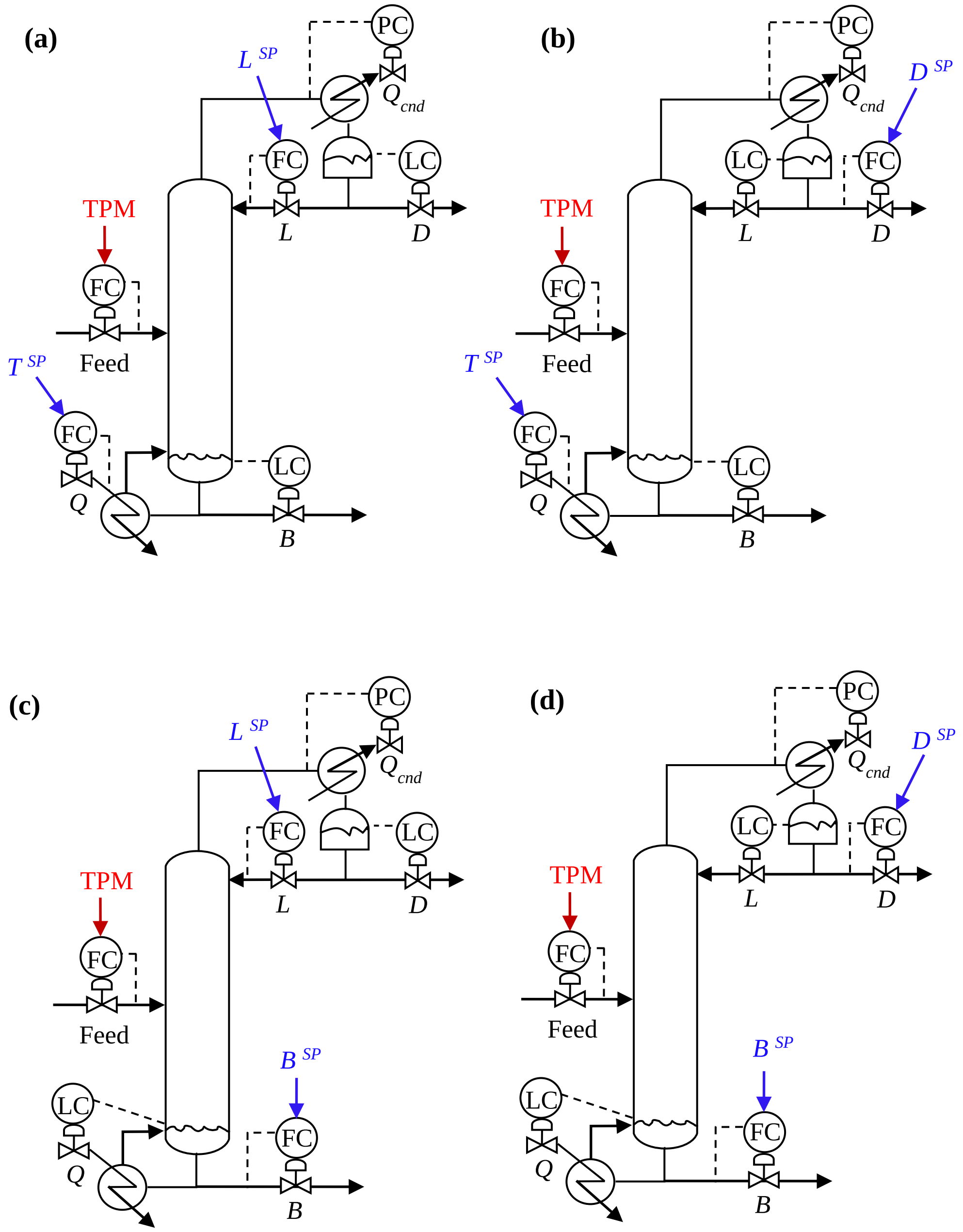
(a)
PC
L^{SP}
Q_{cnd}
FC
LC
L
D
TPM
FC
Feed
T^{SP}
FC
LC
Q
B
(b)
PC
Q_{cnd}
D^{SP}
LC
FC
L
D
TPM
FC
Feed
T^{SP}
FC
LC
Q
B
(c)
PC
L^{SP}
Q_{cnd}
FC
LC
L
D
TPM
FC
Feed
B^{SP}
LC
FC
Q
B
(d)
PC
Q_{cnd}
D^{SP}
LC
FC
L
D
TPM
FC
Feed
B^{SP}
LC
FC
Q
B

Figure 1.1. Schematics of (a) LQ (b) DQ (c) LB and (d) DB control configurations

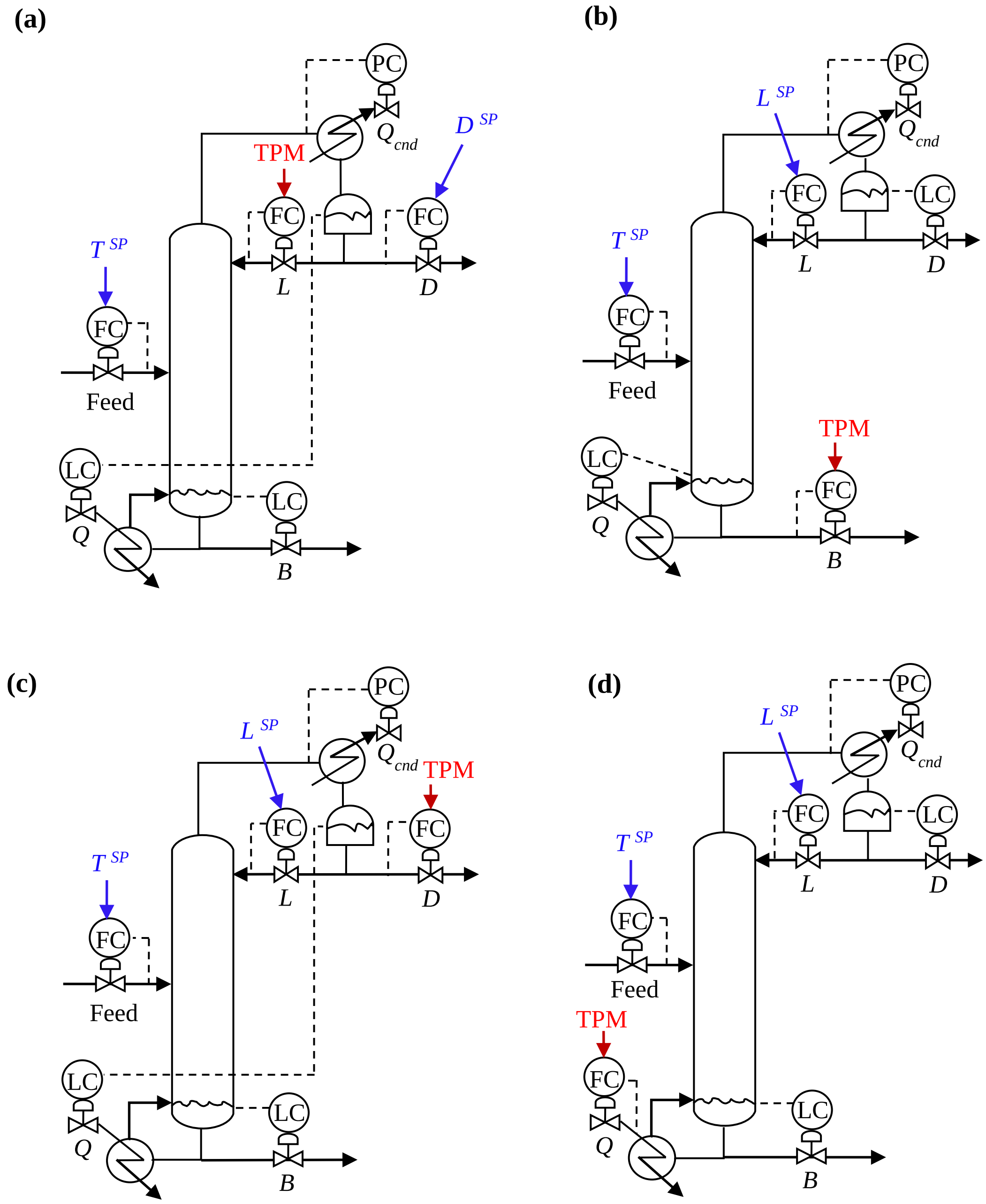
(a)
PC
Q_{cnd}
D^{SP}
TPM
FC
FC
L
D
T^{SP}
FC
Feed
LC
LC
Q
B
(b)
PC
L^{SP}
Q_{cnd}
FC
LC
L
D
T^{SP}
FC
Feed
TPM
LC
FC
Q
B
(c)
PC
L^{SP}
Q_{cnd}
TPM
FC
FC
L
D
T^{SP}
FC
Feed
LC
LC
Q
B
(d)
PC
L^{SP}
Q_{cnd}
FC
LC
L
D
T^{SP}
FC
Feed
TPM
FC
LC
Q
B

Figure 1.2. Alternate control structures with TPM at (a) *L* (b) *B* (c) *D* and (d) *Q*

Over the years, a vast body of literature has emerged on designing a robust plantwide regulatory control system that effectively closes the independent plant material/energy balances. These include several example case-studies (see e.g.[20-30]) as well as step-by-step procedures for synthesizing effective plantwide regulatory control stuctures[31-33]. The key issue in regulatory control of integrated plants is the propagation of transients around recycle loops. The guiding principle is to structure the control system to avoid large swings in the recycle rate, since such swings would end up disturbing all the equipment in the recycle loop. These transients may also get exacerbated by amplification due to steady state non-linearity with the possibility of one or more of the equipment hitting an operational/capacity constraint. Thus, instead of fixing the fresh feed rate into a material recycle loop and letting the recycle rate float in order to close the associated plantwide material balance, it is recommended that the total rate (fresh + recycle) be fixed and let the fresh feed rate float appropriately to close the associated overall plant balance[34-36]. This is schematically illustrated in Figure 1.3. The strategy helps mitigate large swings in the recycle rate by transforming the material imbalance transients out of the loop via appropriate control configuration. Similar ideas are also employed in energy recycle loops where the energy balance control system is structured to transform imbalances in the energy balances out of the recycle loop[37].

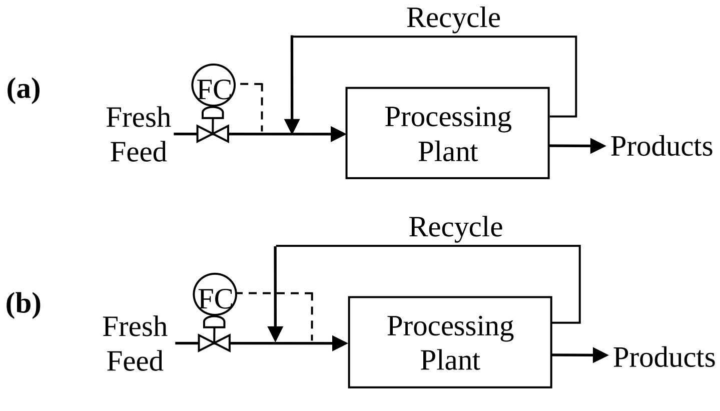

Figure 1.3. Plant material balance with TPM at (a) Fresh feed (b) Total feed

Another key idea in regulatory control system design is the throughput manipulator (TPM), which fixes the processing rate through a train of interconnected units. As illustrated in Figure 1.4, the TPM dictates the orientation of the material balance control system with the upstream material balance controllers oriented in the reverse direction of process flow and downstream controllers oriented in the direction of process flow [38]. When the TPM location is flexible, which is often the case, locating the TPM inside the material recycle loop ensures large swings in the recycle rate are avoided and the fresh feed is brought in as a make-up stream under material balance control [34]. An extension of this TPM heuristic is to locate the TPM at the plant capacity bottleneck, which is often inside the recycle loop due to the high sensitivity of the recycle rate to fresh feed rate changes (snowballing) [39-40]. By locating the TPM at the capacity bottleneck inside the recycle loop, one achieves the twin objectives of tight bottleneck constraint control as well as mitigation of large swings in the recycle rate. As illustrated in Figure 1.5, tight bottleneck constraint control allows the process to be pushed very close to the capacity limit with only a small back-off. The achievable maximum production from the plant can then be significantly higher compared to a conventional structure with the TPM at a fresh feed, which is susceptible to large recycle rate swings with consequently large back-off from the bottleneck capacity limit, a hard constraint.

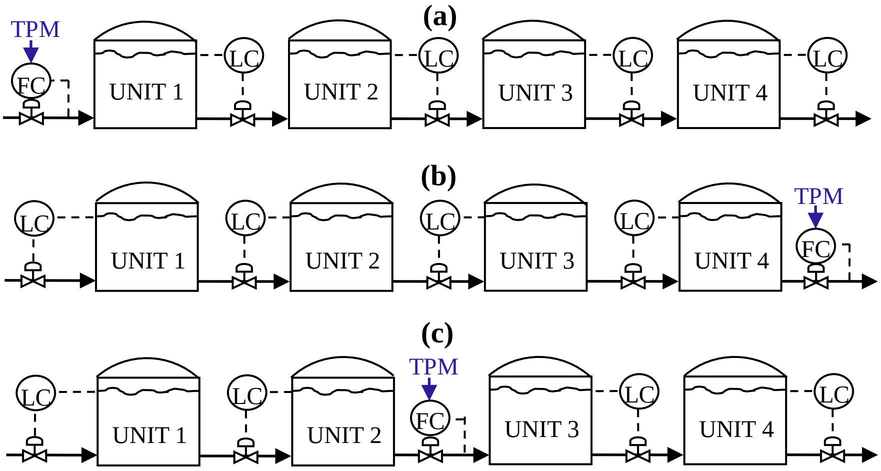

Figure 1.4. Inventory control loop orientation around TPM

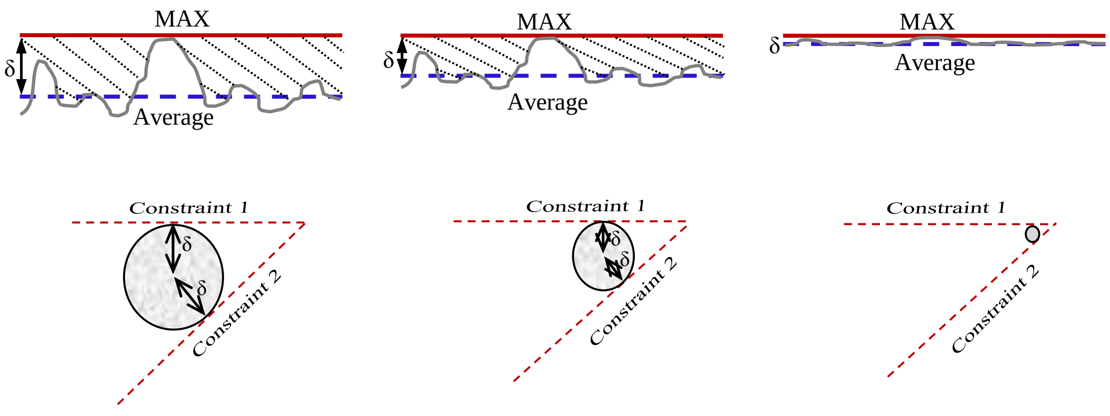

Large backoff Moderate backoff Small backoff

Figure 1.5. Illustration of tightness of active constraint control and backoff

Several articles in the literature demonstrate the application of the above common sense heuristics for robust process regulation as well as tight bottleneck control for achieving higher maximum production from a given plant [41-43]. Given a robust regulatory control system, the process gets operated at the steady state determined by the regulatory loop setpoints. The obvious next question is what should be the values of the regulatory loop setpoints or in other words, what steady state should the process be operated at. Clearly, the regulatory setpoint values should be chosen to optimize an economic objective. Examples include minimizing expensive utility consumption per kg product or maximizing production or yield to desired product (i.e. material efficiency).

1.2.2 Economic Plantwide Control

The optimum steady state with the regulatory setpoints as the decision variables is a non-linear constrained optimization problem. The optimum solution typically has multiple active constraints, the capacity bottleneck being a hard one. For optimality, the process should be driven as close as possible to these active constraints. In other words, all active constraints must be controlled tightly. Out of a total of N steady state degrees of freedom (equivalently, regulatory setpoints with a steady state effect), if there are M optimally active constraints (M ≤ N), then M regulatory setpoints will get used for tight active constraint control. For a given active constraint set, it is usually possible to exploit the input-output pairing flexibility (curse of dimensionality) to configure the regulatory control system for the tightest possible active constraint control. This has been clearly demonstrated in recent literature case studies [44-45]. We then have the M active constraint control loops with their setpoints at the constraint limits, and a small back-off in case an active constraint is a hard one. This leaves N-M unconstrained regulatory setpoints that exhibit a hill/valley shaped optimum with respect to the economic objective. The overall plantwide control system, including active constraint control loops, then has N setpoints that affect the process steady state, of which M setpoints are at their active constraint limits (maximum or minimum), with appropriate back-offs where necessary, and N-M setpoints are unconstrained. This is pictorially depicted in Figure 1.6.

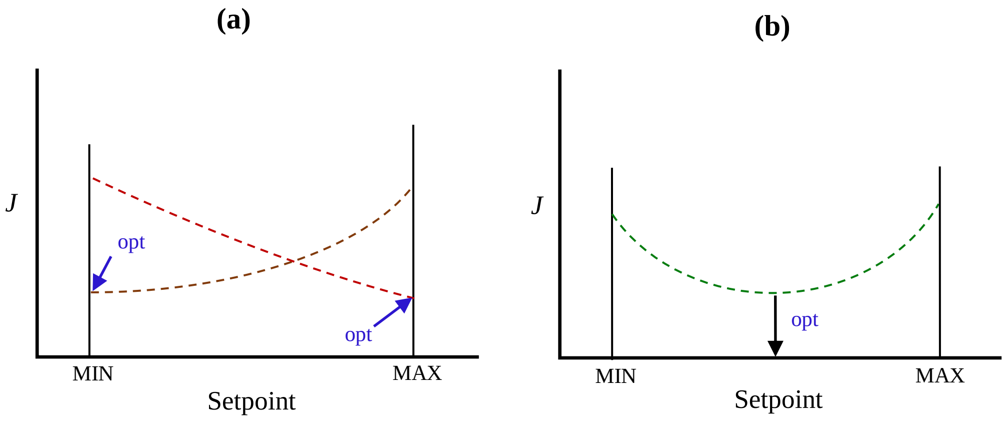

Figure 1.6. Illustration of (a) Constraint (b) Unconstrained regulatory setpoints

The choice of the setpoint value for the active constraints is very obvious, namely, at its maximum or minimum allowed value (with back-off if needed). The same is however not true for the unconstrained setpoints. This is because their unconstrained optimum value is unknown to begin with. Even if the optimum value is somehow obtained, it is liable to change as the plant operating conditions (e.g. production rate) and disturbances (e.g feed quality, catalyst activity etc) vary. An appropriate tracking mechanism is then needed that ensures the unconstrained setpoint is appropriately adjusted to remain near optimum.

1.2.3 Overall Plantwide Control Hierarchy

In light of the above description, the overall plantwide control system has a hierarchical layered structure with the regulatory layer at the bottom effectively closing the plant independent material and energy balances and an economic layer on top calculating the economic optimum steady state, translating it into appropriate regulatory layer setpoint updates and cascading down the updates. This is schematically shown in Figure 1.7. Since it is possible that the optimally active constraint set changes with disturbances and operating conditions, the economic layer is further subdivided into an optimization sub-layer and a supervisory sub-layer. The optimization sub-layer calculates the optimum steady state, usually based on a plant model. The optimum solution gives the optimally active constraint set as well as unconstrained setpoint optimum values. Since the active constraint set dictates the "best" regulatory layer pairings for tight active constraint control, which may require shifting the TPM to a different location in the plant depending on the bottleneck capacity constraint, the role of the supervisory layer is to directly/indirectly effect the reconfiguration of the regulatory inventory control strategy for tight active constraint control. The direct approach is to implement override controllers that take-over / give-up valve manipulation depending on whether a constraint goes active or inactive [46-47]. The indirect approach is to use model predictive control, which is known to be particularly adept at handling multiple active constraints, to effect the required change in the inventory control strategy [48-49]. Given its primary function, the supervisory sub-layer may also be interpreted as the active constraint control manager.

1.3 Approaches for Managing Unconstrained Setpoints

Regardless of the specific implementation in the supervisory sub-layer, the principal challenge in economic optimum operation is "tracking" the optimum value of the unconstrained regulatory layer setpoints. There are three primary approaches propounded in the literature for handling the unconstrained setpoints. These are hill-climbing or extremum seeking control and its variants [50-52], model based real-time optimization [53-55] and self-optimizing control [56-58]. The primary motivation behind this thesis is to evaluate these approaches in tracking an unconstrained regulatory setpoint for an integrated chemical process for typically encountered operating and disturbance scenarios.

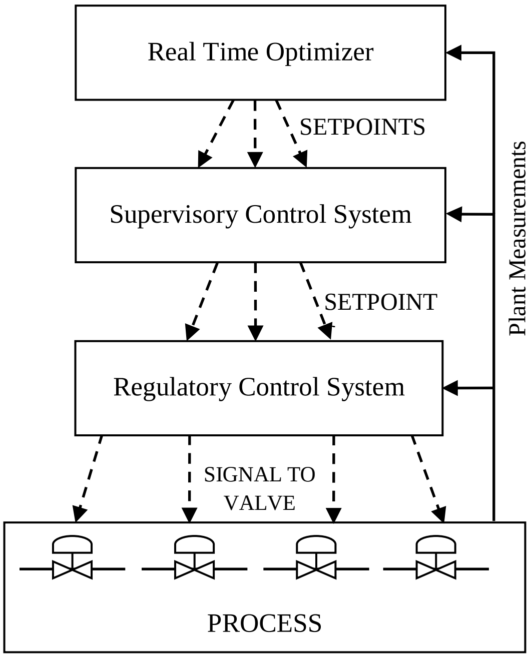
Real Time Optimizer
SETPOINTS
Supervisory Control System
SETPOINT
Regulatory Control System
SIGNAL TO VALVE
PROCESS
Plant Measurements

Figure 1.7. Hierarchical three-layered control structure

1.3.1 Extremum-Seeking Control

Extremum seeking or hill-climbing control, as the phrase indicates, drives the gradient of the objective function with respect to the unconstrained setpoint to zero using a numerical method inspired scheme, such as the Newton Raphson method [59-60] or via feedback [61-63]. Usually, the gradient is directly estimated by perturbing the decision variable and letting the plant settle at the new steady state. The obvious disadvantage is that the extremum seeker or hill climber can be easily confused to move in the wrong direction due to unmeasured disturbances. The advantage, of course, is the economic benefit of driving the unconstrained to near its optimum value. In terms of applications, extremum seeking control has been applied quite widely in the solar power industry to maximize the solar flux captured as the sun moves across the horizon, by adjusting the orientation of the solar panel [64-65]. The application of extremum seeking control in the process industry is, however, quite sparse with very few open literature reports. Almost all of these reports are on standalone processes such as a continuous stirred tank reactor [66], a bioreactor [67], an anaerobic digester [68], a fermenter [69] etc. Quite surprisingly, there are no reports that apply hill-climbing / extremum seeking control to optimize an unconstrained regulatory setpoint in the context of plantwide control of integrated chemical processes. One of the chapters in this thesis is devoted to hill-climbing using Shinskey's simple PID feedback control scheme[70] for driving an unconstrained setpoint to its optimum for alternative disturbance scenarios.

1.3.2 Real-Time Optimization

The idea behind conventional two-step real time optimization (RTO)[71] to drive an unconstrained setpoint to its optimum value is quite simple. Parameters of an appropriate plant model are adjusted to best fit the available recent measurement data from the plant. Assuming a good plant-model fit, the model is then a good representation of the plant. The fitted model is optimized and the calculated optimum value of the unconstrained setpoint is implemented in the plant. The plant is allowed to settle at the new operating condition and the fit-optimize-implement cycle is repeated until the change in the decision variables becomes small.

The RTO approach is very appealing in that the plant is not perturbed unnecessarily simply to estimate a gradient. The feedback for driving the unconstrained setpoints close to the optimum occurs implicitly via changes in the fitted model parameters from one RTO cycle to the next. In practice, since the plant optimum is never known and also due to plant-model mismatch, the optimum to which the model based RTO converges can be noticeably away from the actual plant optimum. A good RTO model is thus required that properly accounts for the principal non-linear effects that influence the optimum. Forbes et al.[72] formally define a model as point-wise "adequate" if there exists a combination of adjustable model parameters for which the plant optimum and the model optimum coincide. Even for "adequate" process models, the RTO may still converge to a suboptimal solution due to the parameter fitting strategy applied. Significant effort must therefore be spent on both developing and maintaining an "adequate" non-linear RTO model as well as an appropriate parameter fitting strategy using the large amount of measurement data available in today's well-instrumented plants.

In terms of RTO applications, some applications have been reported in the open literature. Many of these are on a particular unit such as a catalytic cracker[73], a crude distillation unit in a refinery[74], a fermentation process[75] etc. A few applications are also reported on complete integrated plants such as the Tennessee Eastman process[76], an acetaldehyde process[77], a pulp mill process[78]. Muller et al.[79] claim significant economic benefit due to RTO in an actual plant with multiple reactors, separators and recycle loops. The survey by Darby et al.[80] notes that RTO applications have been very successful in ethylene plants, but much less so in refineries. They further state that, "Today, we find industry split in the acceptance of RTO. Some companies are convinced and continue to invest in applications; other companies have concluded that RTO, as it is currently implemented, is not viable for them." One of the polite reasons offered is the absence of a modeling culture and poor management support for maintaining the applications.

The actual reasons may however be not as simple or banal. Note that the benefits of MPC or alternatively, an override constraint control manager are easily recognizable, as these push the process operation as close as possible to the optimally active constraints. Indeed, Downs[81] clearly states that the economic benefits of MPC are largely attributable to the automatic execution of changes in the regulatory control strategy as the active constraint set changes. On the other hand, the benefits of RTO may not be as direct as it seeks a tradeoff between opposing effects that result in the optimum. Examples of these tradeoffs abound in the process industry and include the classic yield vs conversion tradeoff, throughput versus conversion (or recycle) tradeoff, balancing costs associated with two interacting material recycle loops etc. Usually, for well designed processes, the variation in the objective function with respect to the decision variable is quite flat near the optimum. Thus, only if the deviation in the decision variable away from the optimum is large does one incur a noticeable economic penalty. The economic benefit achieved by RTO can therefore be much harder to discern. It then becomes hard to justify the benefit achieved by RTO, beyond the supervisory MPC layer.

If one carefully examines the literature, in one of the more honest comparisons, Ricker and coworkers[82-84] clearly show that the control performance of non-linear MPC over conventional decentralized control with overrides is very similar, for the celebrated Tennessee Eastman[85] challenge process. The report clearly suggests that a simple conventional decentralized control system with overrides for managing constraints coupled to an RTO optimizing the economically dominant unconstrained setpoints should do as well as, if not better than, the mathematically much more complex and harder to maintain RTO-MPC framework [86-87], including its more recent single layer variants [88-89]. The simplicity and understandability of such an overall economic plantwide control system, would not only help in clear quantification of the RTO benefit, but also come with an associated cost benefit due to the ease of maintainability that comes with the simple control systems. In this thesis, such a simple

RTO based economic plantwide control system is developed and evaluated for an integrated reactor-separator-recycle process.

1.3.3 Self Optimizing Control

The third and final approach for managing unconstrained regulatory setpoints is referred to as self optimizing control (SOC). The basic idea is to control that "magic" variable, whose optimum value remains unchanged with changes in the plant operating conditions and disturbances. Even as several researchers have used the idea in process control research [90-92], Luyben[93] unified them into what he referred to as the "eigenstructure", which is "that configuration which yields a system that is naturally self-regulating and self-optimizing". The paper only presented the basic concept and how it seamlessly unifies the process control approaches of other researchers. It was more than a decade before Skogestad provided a more precise definition of self-optimizing control (SOC) [94-95], including a systematic quantitative methodology for selecting the best possible self optimizing controlled variables (SOCVs) [96-97]. Skogestad[94] defines SOC as "when we can achieve an acceptable loss with constant setpoint values for the controlled variables (without the need to reoptimize when disturbances occur)." By definition, the optimum SOCV value remains nearly the same regardless of disturbances so that process operation at a constant setpoint results in near optimum operation over the envisaged disturbance space. A related concept is that of an "optimal invariant"[98]; that measurement combination (equivalent to the gradient) whose optimum value does not change with disturbances. An optimal invariant held constant at that value guarantees zero-loss operation regardless of disturbances. The invariant is thus the perfect SOCV. The idea behind SOC is very appealing in that it transforms an optimization problem into a simpler control problem. Quite simply, near optimal operation is achieved by holding the SOCV constant at the appropriate value via feedback adjustment of the unconstrained regulatory setpoint. An RTO may be needed to find this appropriate setpoint value, but beyond that SOCV eliminates the need for RTO.

Since the seminal articles by Skogestad, the SOC literature has grown to be quite vast and it is not the intention to review it all but only highlight relevant salient aspects. Several applications of the SOC methodology have been demonstrated on complete integrated chemical plants [99-105]. These include the celebrated Tennessee Eastman challenge[99] and toluene hydrodealkylation[100] processes, a reactor separator recycle process[101], an air-separation unit[102], a Fischer Tropsch gas-to-liquids process[103], a refrigeration cycle[104] etc. One of the major issues in SOC is coming up with a "good" candidate SOCV for an unconstrained dof. It usually requires good engineering judgment and process insight. While systematic approaches using "local" steady state analyses to combine measurements for SOC have been developed[105-106], their usefulness is debatable due to the high non-linearity inherent in integrated chemical processes and also the fact that these measurement combinations are likely to exhibit strange open loop dynamics. Regardless of these limitations, the quest for the perfect SOCV (or invariant) to manage an unconstrained dof has its own appeal. To the best of our knowledge, there are no literature reports that attempt obtaining an invariant or perfect SOCV for an unconstrained dof in the plantwide control of an integrated process. Further, there is the need for evaluating the economic performance of a conventional two-step RTO and SOC for typical disturbance scenarios to ascertain the suitability of the approaches for specific scenarios. This thesis addresses these issues for an integrated reactor-separator-recycle process.

1.4 Thesis Motivation and Scope

The brief overview of plantwide control along with the relevant literature review highlights that tracking the optimum value of unconstrained regulatory layer setpoints is one of the challenging issues in economic process operation. The available options include extremum seeking control, real-time optimization and self-optimizing control. Of these, the application of extremum seeking control in the plantwide control context is not well explored in the extant literature. On the other hand, the application of RTO-MPC, which requires significant mathematical formulation, modeling, solution and maintenance effort, is quite well espoused in the literature. The jury however is still out on its real benefits compared to conventional common sense driven decentralized regulatory control with overrides for managing constraints and an optimizer solving the unconstrained setpoint optimization problem in the reduced operating space, after eliminating active constraints. In fact, the mathematical complexity of the RTO-MPC paradigm has driven academics to developing innovative formulations, solution techniques and their demonstration on simulation examples. A natural consequence is that the common sense driven approach, which is much more practical, easy to understand and appealing to operators, seems woefully neglected in the literature. Finally, while the SOC literature has grown to be quite vast, there are very few literature reports that provide a physical basis for why a particular CV is self-optimizing in nature. Further, the evaluation of when one technique makes sense over others is also inadequately addressed. This thesis is motivated by the need to address these lacunae apparent from an evaluation of the extant plantwide control literature.

In order to address these lacunae, the thesis develops and applies the techniques to a specific reactor-separator-recycle process used in the literature as a benchmark problem on robust regulatory control. The principal idea behind using this process is that while being simple, it has the essential feature of a material recycle stream between the reactor and the separator, which is the main source of non-linearity and unfavorable dynamic interaction in all "reaction followed by separation" processes. At least some of the insights obtained from studying this process should be extendable to other more complex "reaction followed by separation" processes. Also, the familiarity with the process would also be helpful in interpreting the economic trade-offs associated with an unconstrained regulatory setpoint.

The scope of the thesis spans evaluation of Shinskey's hill-climber for tracking the optimum of an unconstrained regulatory setpoint, development and dynamic evaluation of a model based RTO method for tracking the unconstrained setpoint, synthesis and evaluation of a global optimal invariant (the perfect SOCV) for the unconstrained setpoint and evaluation of the performance of RTO and SOC for typical disturbance scenarios encountered in practice. Throughout the thesis, the engineering common sense driven approach for designing the overall plantwide control system is used, as it clearly brings out the thinking behind why certain control system design decisions are taken over other possibilities. It is emphasized that this thinking is at the core of good process engineering and control.

1.5 Reactor-Separator-Recycle Process

Figure 1.8 shows a schematic of the reactor-separator-recycle process studied here. It consists of a continuous stirred tank reactor (CSTR) followed by a simple distillation column. The irreversible exothermic liquid-phase reaction $A + B \rightarrow C$ occurs in the CSTR. Fresh A and fresh B are mixed and fed to the cooled CSTR. The reactor effluent, which is a mixture of A, B and C, is distilled in the downstream column that recovers C down the bottoms, since C is heavy as it is formed by the addition of B to A. The unreacted A and B are recovered up the top of the column and recycled to the CSTR.

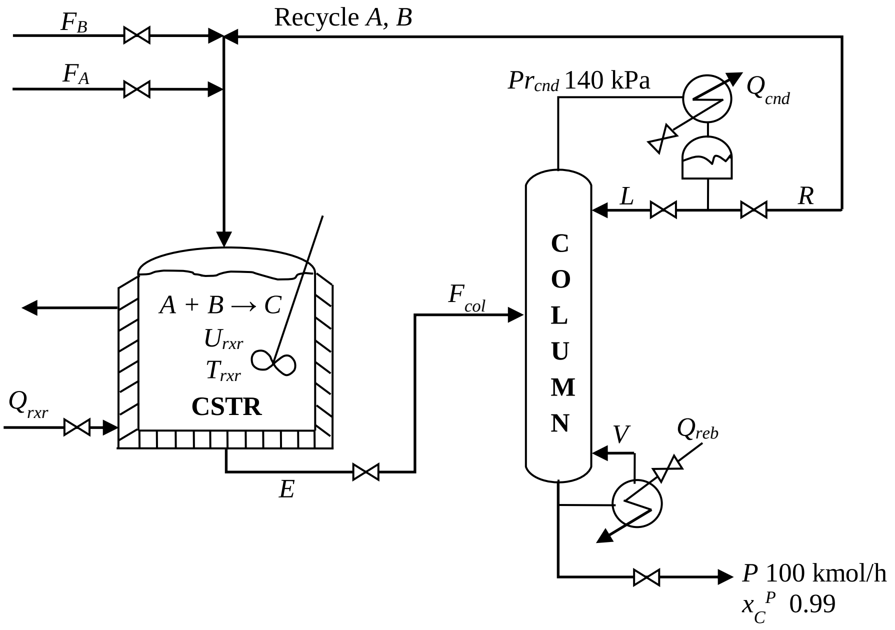

Figure 1.8. Schematic of reactor-separator-recycle process

The hypothetical components *A*, *B* and *C* are chosen such that *A* is lighter than *B*. The component relative volatilities are then in the order $\alpha_A > \alpha_B > \alpha_C$. The reaction chemistry is assumed to be perfect with no side reactions. The reaction kinetic expression varies from simple elementary reaction kinetics to Langmuir-Hinshelwood (LH) with non-elementary order. We thus have $r = k\ x_{rxrA}\ x_{rxrB}$ (elementary), $r = k.x_{rxrA}{}^{a}.x_{rxrB}{}^{b}$ (non-elementary), $r = k.x_{rxrA}.x_{rxrB}/(1+K_Ax_{rxrA}+K_Bx_{rxrB})$ (elementary LH) and $r = k.x_{rxrA}{}^{a}.x_{rxrB}{}^{b}/(1+K_Ax_{rxrA}+K_Bx_{rxrB})$ (non-elementary LH), where *r* is the reaction rate, *k* is the reaction rate constant, x_{rxrA} and x_{rxrB} are the CSTR liquid-phase *A* and *B* mol fractions respectively, *a* and *b* are reaction order with respect to x_{rxrA} and x_{rxrB} respectively and K_A and K_B are component *A* and component *B* adsorption equilibrium constants, respectively. The particular hypothetical component properties, reaction kinetics used and base-case process design are noted in the relevant chapters. Aspen Hysys is used for steady state and dynamic modeling with the hydrocarbons method used for estimating the thermodynamic parameters of the hypotheticals. The SRK equation of state is used for modeling the thermodynamic properties.

The process has a total of six steady state degrees of freedom, two for the two fresh feeds, two for the CSTR (hold-up and temperature) and two for the distillation column, assuming it operates at the design pressure. Optimal steady state operation is considered for two operating modes, namely Mode I and Mode II. In Mode I, the throughput is given and the remaining five dofs are optimized to minimize the column boilup or recycle rate. In Mode II, all six dofs are optimized to maximize production. The optimization is a constrained non-linear optimization problem and solved using the Matlab NLP solver, fmincon using the active set method with Hysys as the background steady state solver.

1.6 Thesis Organization and Style

This thesis contains a total of seven chapters, including this one. Moving forward, the next chapter (Chapter 2), evaluates Shinskey's feedback hill-climber for tracking an unconstrained regulatory layer setpoint in the reactor-separator-recycle process with elementary kinetics. In the absence of disturbances, the hill-climber is shown to effectively track the optimum for both Mode I and Mode II operation. Chapter 3 develops a robust steady state RTO model with a robust parameter fitting method using available routine measurement data for the process. The RTO is developed for both Mode I and Mode II operation. Plant-model mismatch occurs in the reaction kinetics with the actual kinetics being LH type and the fitted kinetic model being of the power-law type. Also, a simplified ideal VLE column model is used. It is shown that the developed RTO method drives the unconstrained setpoint close to the actual plant optimum and achieves significant economic benefit compared to constant setpoint operation. The suitability of the proposed approach is also demonstrated for reaction kinetics of the general LH type. In Chapter 4, the economic benefit of the developed RTO approach is demonstrated both for Mode I and Mode II operation in dynamics, where the process is never truly at steady state and routine process variability is omnipresent. A robust override control system for reconfiguring the regulatory control loops between Mode I ↔ Mode II transitions is also developed and shown to work effectively. Chapter 5 develops globally optimal invariants for the considered reaction kinetic expressions to manage the unconstrained reactor *B* composition setpoint in Mode I and Mode II. In Mode I, the recycle rate is minimized while in Mode II, production is maximized subject to maximum recycle rate as the bottleneck constraint. The application of these invariants for minimizing boil-up or maximizing production subject to maximum boil-up as the bottleneck constraint shows negligible loss due to no reoptimization, clearly demonstrating good SOC performance. In Chapter 6, the application of SOC using invariants inspired inferential SOCV for optimal operation of the process is evaluated in dynamics for typical disturbance scenarios. Finally, the thesis concludes with a summary of the learnings from the various techniques for near optimal management of the unconstrained dofs and pointers for future work.

The thesis is organized as a series of self-contained chapters which are either published or have been submitted to reputed peer reviewed international journals. There is thus material that gets repeated from chapter-to-chapter, e.g. process description, degrees of freedom etc. The familiar reader may skip these and get to the main technical content in each chapter. Further, the reader may also read these chapters (excluding concluding chapter) in any order as independent entities. The overall context of the work has been presented in this Chapter while the last chapter summarizes the main findings.

References

(1) Meyers, R. A. *Handbook of petrochemicals production processes*. McGraw-Hill: New York, 2005.

(2) Morud, J.; Skogestad, S. Dynamic behaviour of integrated plants. *J. Process Control* 1996, 6 (2/3), 145-156.

(3) Luyben, M.L.; Luyben, W. L. Design and control of a complex process involving two reaction steps, three distillation columns, and two recycle streams. *Ind. Eng. Chem. Res.*1995, 34(11), 3885-3898.

(4) Sahu, A.; Kumar, V.; Kaistha, N. Conceptual design and plantwide control of an ethyl acetate process, *Chem. Eng. Process. Process Intensif.* 2018, 126, 45-61.

(5) Douglas, J. M. *Conceptual design of chemical processes*. McGraw-Hill: New York, 1988.

(6) Luyben, W. L. Design and control of gas-phase reactor/recycle processes with reversible Exothermic Reactions. *Ind. Eng. Chem. Res.* 2000, 39, 1529-1538.

(7) Collura, M. A., Luyben, W. L. Energy-saving distillation designs in ethanol production. *Ind. Eng. Chem. Res.* 1988, 27(9), 1686-1696.

(8) Pathak, A. S.; Agarwal, S.; Gera, V.; Kaistha, N. Design and control of a vapor-phase conventional process and reactive distillation process for cumene production. *Ind. Eng. Chem. Res.* 2011, 50, 3312-3326.

(9) Luyben, W. L. Snowball effects in reactor/separator processes with recycle. *Ind. Eng. Chem. Res.* 1994, 33, 299-305.

(10) Güttinger, T. E.; Morari, M. Predicting multiple steady-states in distillation: Singularity analysis and reactive systems. *Comput. Chem. Eng.* 1997, 21 (SUPPL1), S995.

(11) Ojasvi; Kaistha, N. Plantwide control for maximum throughput operation of an ester purification process. *Ind. Eng. Chem. Res.* 2016, 55(47), 12242-12255.

(12) Gupta, R.; Kaistha, N. Role of nonlinear effects in benzene-toluene-xylene dividing wall column control system design. *Ind. Eng. Chem. Res.* 2015, 54(38), 9407-9420.

(13) Downs, J.J.; Caveness, M.H. Influence of process variability propagation in plantwide control. Eds: Rangaiah G.P.; Kariwala, V. *Plantwide Control: Recent Developments and Applications*. Chichester, West Sussex: John Wiley and Sons, 2012.

(14) Ojasvi; Kaistha, N. Design and Operating Strategy Innovations for Energy Efficient Process Operations, *The Water-Food-Energy-Nexus: Processes, Technologies, and Challenges*, CRC Press, Taylor and Francis, 2017, 717-735.

(15) Luyben, M. L.; Tyreus, B. D.; Luyben, W. L. *Plantwide process control.* New York: McGraw-Hill 1998.

(16) Belanger, P. W.; Luyben, W. L. Inventory control in processes with recycle. *Ind. Eng. Chem. Res.* 1997, 36(3), 706-716.

(17) Luyben, W. L. Dynamics and control of recycle systems. 1. simple open-loop and closed-loop systems. *Ind. Eng. Chem. Res.* 1993, 32(3), 466-475.

(18) Skogestad, S.; Morari, M. Control configuration selection for distillation columns, *AIChE Journal,* 1987, 33 (10)-1620-1635.

(19) Fingo, M. V.; Luyben, W. L. Control of distillation columns with low relative volatilities. *Ind. Eng. Chem. Res.* 1989, 28(1), 75-83.

(20) Luyben, W. L. Design and Control of an Autorefrigerated Alkylation Process. *Ind. Eng. Chem. Res.* 2009, 48, 11081-11093.

(21) Chen, R.; McAvoy, T. Plant-Wide Control System Design: Methodology and Application to a Vinyl Acetate Process. *Ind. Eng. Chem. Res.* 2003, 42, 4753-4771.

(22) Jha, A.; Okorafor, O. C. Optimal Plantwide Process Control Applied to the Tennessee Eastman Problem. *Ind. Eng. Chem. Res.* 2014, 53, 738−751.

(23) Banerjee, A.; Arkun, Y. Control Configuration Design Applied to the Tennessee Eastman Plant-Wide Control Problem. *Comput. Chem. Eng*. 1995, 19, 453-480.

(24) Downs, J. J.; Vogel, E. F. A Plant-Wide Industrial Process Control Problem. *Comput. Chem. Eng*. 1993, 17, 245-255.

(25) Lyman, P. R.; Georgakis, C. Plant-Wide Control of the Tennessee Eastman Problem. *Comput. Chem. Eng*. 1995, 19, 321-331.

(26) Maity, D.; Kaistha, N. Systematic top-down economic plantwide control of the cumene process. *J. Process Control* 2013, 23, 1426-1440.

(27) Hovd, M.; Skogestad, S. Procedure for regulatory control structure selection with application to the FCC process. *AIChE J.* 1993, 39 (12), 1938-1953.

(28) Konda, N. V. S. N. M.; Rangaiah, G. P. Plantwide control of industrial processes: An integrated framework of simulation and heuristics. *Ind. Eng. Chem. Res.* 2005, 44(22), 8300-8313.

(29) Luppi, P. A.; Zumoffen, D. A. R.; Basualdo, M. S. Decentralized plantwide control strategy for large-scale processes. Case study: Pulp mill benchmark problem. *Comput. Chem. Eng.* 2013, 52, 272-285.

(30) Jagtap, R.; Kaistha, N.; Skogestad, S. Plantwide control for economic optimum operation of a recycle process with side reaction. *Ind. Eng. Chem. Res.* 2011, 50(14), 8571-8584.

(31) Luyben M. L.; Tyreus B. D.; Luyben W. L. Plantwide Control Design Procedure. *AIChE J.* 1997, 43(12), 3161-3174.

(32) Skogestad S. Control Structure Design for Complete Chemical Plants. *Comput. Chem. Eng.* 2004, 28(1-2), 219-234.

(33) Ng, C. S.; Stephanopoulos, G. Synthesis of control system for chemical plants. *Comput. Chem. Eng.* 1996, 20, S999-S1004.

(34) Jagtap, R.; Kaistha, N. Throughput Manipulator Location Selection for Economic Plantwide Control. In: Rangaiah, G. P.; Kariwala, V. A, editors. *Advances in Plantwide Control*. Upper Saddle River, NJ: John Wiley and Sons, 2012.

(35) Wu, K. L.; Yu, C. C. Reactor/Separator Processes with Recycle 1. Candidate Control Structure for Operability. *Comput. Chem. Eng.* 1996, 20, 1291-1316.

(36) Bildea, C. S.; Dimian, A. C. Fixing flow rates in recycle systems: Luyben's rule revisited. *Ind. Eng. Chem. Res.* 2003, 42(20), 4578-4585.

(37) Reyes, F.; Luyben, W. L. Steady-state and dynamic effects of design alternatives in heat-exchanger/furnace/reactor processes. *Ind. Eng. Chem. Res.* 2000, 39(9), 3335-3346.

(38) Price R. M.; Lyman P. R.; Georgakis, C. Throughput manipulation in plantwide control structures. *Ind. Eng. Chem. Res*. 1994, 33(5), 1197- 1207.

(39) Buckley P. S. *Techniques of Process Control*. Upper Saddle River, NJ: Wiley, 1964.

(40) Minasidis, V.; Skogestad, S.; Kaistha, N. Simple rules for economic plantwide control. *Comp. Aided Chem. Eng*. 2015, 37, 101-108.

(41) Gera, V.; Panahi, M.; Skogestad, S.; Kaistha, N. Economic Plantwide Control of the Cumene Process. *Ind. Eng. Chem. Res.* 2013, 52, 830-846.

(42) Araújo, A. C.B. de.; Hori, E. S.; Skogestad, S. Application of plantwide control to the HDA process. II- Regulatory control. *Ind. Eng. Chem. Res.* 2007, 46, 5159-5179.

(43) Kanodia, R.; Kaistha, N. Plantwide control for throughput maximization: A case study. *Ind. Eng. Chem. Res.* 2010, 49, 210-221.

(44) Narraway, L. T.; Perkins, J. D. Selection of Control Structures based on Economics. *Comput. Chem. Eng.* 1993, 18, S511-S515.

(45) Percell, E.; Moore, C.F. Analysis of the Operation and Control of a Simple Plantwide Module. *Proceed. Amer. Cont. Conf.* 1995, 1, 230-234.

(46) Jagtap, R.; Pathak, A. S.; Kaistha, N. Economic Plantwide Control of the Ethyl Benzene Process. *AIChE J*. 2013, 59 (6), 1996-2014.

(47) Jagtap, R.; Kaistha, N.; Luyben, W. L. External reset feedback for constrained economic process, *Ind. Eng. Chem. Res.* 2013, 52(28), 9654-9664.

(48) Aske, E. M. B.; Strand, S.; Skogestad, S. Coordinator MPC for Maximizing Plant Throughput. *Comput. Chem. Eng*. 2008, 32, 195-204.

(49) Amrit, R.; Rawlings, J. B.; Angeli, D. Economic Optimization Using Model Predictive Control with a Terminal Cost. *Annual Reviews in Control.* 2011, 35, 178-186.

(50) Ariyur, K. B.; Krstic, M. *Real-time optimization by extremum-seeking control*. Wiley-Interscience, Hoboken, NJ, 2003.

(51) Cougnon, P.; Dochain, D.; Guay, M.; Perrier, M. On-line optimization of fedbatch bioreactors by adaptive extremum seeking control. *J. Process Control* 2011, 21(10), 1526-1532.

(52) Popp, J.; Deutscher, J. Optimizing a hybrid diesel power unit using extremum-seeking control. *IEEE T. Contr. Sys. T.* 2018, In press.

(53) Marchetti, A.; Chachuat, B.; Bonvin, D. Modifier-adaptation methodology for real-time optimization. *Ind. Eng. Chem. Res.* 2009, 48(13), 6022-6033.

(54) Diehl, M.; Bock, H. G.; Schlöder, J. P.; Findeisen, R.; Nagy, Z; Allgöwer, F. Real-time optimization and nonlinear model predictive control of processes governed by differential-algebraic equations. *J. Process Control* 2002, 12(4), 577-585.

(55) Lacks, D. J. Real-time optimization in nonlinear chemical processes: need for global optimizer. *AIChE J.* 2003, 49 (11), 2980-2983.

(56) Jäschke, J.; Skogestad, S. NCO tracking and self-optimizing control in the context of real-time optimization. *J. Process Control* 2011, 21(10), 1407-1416.

(57) Ye, L.; Cao, Y.; Li, Y.; Song, Z. Approximating necessary conditions of optimality as controlled variables. *Ind. Eng. Chem. Res.* 2013, 52 (2), 798-808.

(58) Kariwala, V. Optimal measurement combination for local self-optimizing. *Ind. Eng. Chem. Res.* 2007, 46 (11), 3629-3634.

(59) Spall, J. C. Multivariate stochastic approximation using a simultaneous perturbation gradient approximation. *IEEE Trans. Automat. Contr.* 1992, 37(3), 332-341.

(60) Wang, K.; Shao, Z.; Lang, Y.; Qian, J.; Biegler, L. T. Barrier NLP methods with structured regularization for optimization of degenerate optimization problems. *Comput. Chem. Eng*. 2013, 57(5), 24-29.

(61) Fletcher, R. *Practical methods of optimization*. John Wiley and Sons, Chichester, 1987

(62) Garcia, C. E.; Morari, M. Optimal operation of integrated processing systems. Part I: Open-loop on-line optimizing control. *AIChE J.* 1981, 27(6), 960-968.

(63) Kumar, V.; Kaistha, N. Hill climbing for plantwide control to economic optimum. *Ind. Eng. Chem. Res.* 2014, 53 (42), 16465-16475.

(64) Roth, P.; Georgiev, A.; Boudinov, H. Design and construction of a system for sun-tracking. *Renew Energ* 2004, 29(3), 393-402.

(65) Mousazadeh, H.; Keyhani, A.; Javadi, A.; Mobli, H.; Abrinia, K.; Sharifi, A. A review of principle and sun-tracking methods for maximizing solar systems output. *Renew. Sust. Energ. Rev.* 2009, 13(8), 1800-1818.

(66) Zhang, T.; Guay, M.; Dochain, D. Adaptive extremum seeking control of continuous stirred-tank bioreactors. *AIChE J.* 2003, 49(1), 113-123.

(67) Bastin, G.; Nešić, D.; Tan, Y.; Mareels, I. On extremum seeking in bioprocesses with multivalued cost functions. *Biotechnol. Prog*r. 2009, 25(3), 683-689.

(68) Lara-Cisneros, G.; Aguilar-López, R.; Femat, R. On the dynamic optimization of methane production in anaerobic digestion via extremum-seeking control approach. *Comput. Chem. Eng.* 2015, 75, 49-59.

(69) Dewasme, L.; Srinivasan, B.; Perrier, M.; Vande Wouwer, A. Extremum-seeking algorithm design for fed-batch cultures of microorganisms with overflow metabolism. *J. Process Control* 2011, 21(7), 1092-1104.

(70) Shinskey, F. G. *Process Control Systems: Application, Design and Adjustment*. McGraw-Hill, New York, 1967.

(71) Kumar, V.; Kaistha, N. Real time optimization of a reactor-separator-recycle process I: Steady state modelling. *Ind. Eng. Chem. Res.* 2018, 57 (37), 12429-12443.

(72) Forbes, J. F.; Marlin, T. E.; Macgregor, J. F. Model adequacy requirement for optimizing plant operations. *Comput. Chem. Eng.* 1994, 18(6), 497-510.

(73) Lid, T.; Strand, S. Real-time optimization of a cat cracker unit. *Comput. Chem. Eng.* 1997, 21, S887-S892.

(74) Zanin, A. C.; De Gouvêa, M. T.; Odloak, D. Industrial implementation of a real-time optimization strategy for maximizing production of LPG in a FCC unit. *Comput. Chem. Eng*. 2000, 24 (2-7), 525-531.

(75) Paul, G.; Hawkins, C. The real-time optimisation of an industrial fermentation process. *IFAC Papers-OnLine* 2004, 37(3), 529-534.

(76) Duvall, P. M.; Riggs, J. B. On-line optimization of the Tennessee Eastman challenge problem. *J. Process Control* 2000, 10, 19-33.

(77) Zhijiang, S.; Jinlin, W.; Jixin, Q. Real-time optimization of acetaldehyde production process. *Dev. Chem. Eng. Mineral Process* 2005, 13(3/4), 249-258.

(78) Mercangöz, M.; Doyle III, F. J. Real-time optimization of the pulp mill benchmark problem. *Comput. Chem. Eng.* 2008, 32, 789-804.

(79) Müller, D.; Dercks, B.; Nabati, E.; Blazek, M.; Eifert, T.; Schallenberg, J.; Piechottka, U.; Dadhe, K. Real-time optimization in the chemical processing industry. *Chem. Ing. Tech.* 2017, 89(11), 1464-1470.

(80) Darby, M. L.; Nikolaou, M.; Jones, J.; Nicholson, D. RTO: An overview and assessment of current practice. *J. Process Control* 2011, 21 (6), 874-884.

(81) Downs, J.J. Linking control strategy design and model predictive control, *AIChE Symposium Series*. 2002, 98 (326), 328-341.

(82) Ricker, N. L. Model predictive control with state estimation. *Ind. Eng. Chem. Res.* 1990, 29(3), 374-382.

(83) Ricker, N. L.; Lee, J. H. Nonlinear Model Predictive Control of the Tennessee Eastman Challenge Process. *Comput. Chem. Eng.* 1995, 19, 961-981.

(84) Srinivasan, B.; Primus, C. J.; Bonvin, D.; Ricker, N. L. Run-to-run optimization via control of generalized constraints. *Control Eng. Pract.* 2001, 9 (8), 911-919.

(85) Ricker, N. L. Decentralized control of the Tennessee Eastman challenge process. *J. Process Control* 1996, 6, 205-221.

(86) De Souza, G.; Odloak, D.; Zanin, A. C. Real time optimization (RTO) with model predictive control (MPC). *Comput. Chem. Eng.* 2010, 34 (12), 1999-2006.

(87) Marchetti, A. G.; Ferramosca, A.; González, A. H. Steady-state target optimization designs for integrating real-time optimization and model predictive control. *J. Process Control* 2014, 24 (1), 129-145.

(88) Costello, S.; François, G.; Bonvin, D. A directional modifier-adaptation algorithm for real-time optimization. *J. Process Control* 2016, 39, 64-76.

(89) D'Jorge, A.; Ferramosca, A.; González, A. H. A robust gradient-based MPC for integrating real time optimizer (RTO) with control. *J. Process Control* 2017, 54, 65-80.

(90) Loeblein, C.; Perkins, J. D. Economic analysis of different structures of on-line process optimization systems. *Comput. Chem. Eng.* 1998, 22, 125-1269.

(91) Heldt, S. Dealing with structural constraints in self-optimizing control engineering. *J. Process Control* 2010, 20, 1049-1058.

(92) Marchetti, A. G.; Zumoffen, D. Self-optimizing control structure with minimum number of process-dependent controlled variables. *Ind. Eng. Chem. Res.* 2014, 53 (24), 10177-10193.

(93) Luyben, W.L. The concept of "Eigenstructure" in process control. *Ind. Eng. Chem. Res.* 1988, 27(1), 206-208.

(94) Skogestad, S. Plantwide Control: The Search for the Self Optimizing Control Structure. *J. Process Control* 2000, 10, 487-507.

(95) Skogestad, S. Self-optimizing control: the missing link between steady-state optimization and control. *Comput. Chem. Eng.* 2000, 24, 569-575.

(96) Halvorsen, I. J.; Skogestad, S.; Morud, J. C.; Alstad, V. Optimal selection of controlled variables. *Ind. Eng. Chem. Res.* 2003, 42(14), 3273–3284.

(97) Govatsmark, M. S.; Skogestad, S. Selection of controlled variables and robust setpoints. *Ind. Eng. Chem. Res.* 2005, 44(7), 2207-2217.

(98) Jäschke, J. E. P.; skogestad, S. Optimally invariant variable combinations for nonlinear systems. *IFAC Papers-OnLine* 2009, 7, 530-535.

(99) Larsson, T.; Hestetun, K.; Hovland, E.; Skogestad, S. Selfoptimizing Control of a Large-Scale Plant: The Tennessee Eastman Process. *Ind. Eng. Chem. Res.* 2001, 40, 4889-4901.

(100) Araújo, A. C.B. de.; Govatsmark, M.; Skogestad, S. Application of plantwide control to the HDA process. I- steady-state optimization and self-optimizing control. *Control Eng. Pract.* 2007, 15, 1222-1237.

(101) Larsson, T.; Govatsmark, M.S.; Skogestad, S.; Yu, C. C. Control Structure Selection for Reactor, Separator and Recycle Processes. *Ind. Eng. Chem. Res.*, 2003, 42 (6), 1225-1234.

(102) Panahi, M.; Skogestad, S. Economically efficient operation of CO_2 capturing process part I: Self-optimizing procedure for selecting the best controlled variables. *Chem. Eng. and Process.* 2011, 50(3), 247-253.

(103) Panahi, M.; Skogestad, S. Selection of Controlled Variables for a Natural Gas to liquids (GTL) Process. *Ind. Eng. Chem. Res.* 2012, 51, 10179-10190.

(104) Jensen, J. B.; Skogestad, S. Optimal Operation of Simple Refrigeration Cycles. Part II: Selection of Controlled Variables. *Comput. Chem. Eng*, 2007, 31, 1590-1601.

(105) Alstad, V.; Skogestad, S. Null space method for selecting optimal measurement combinations as controlled variables. *Ind. Eng. Chem. Res.* 2007, 46(3), 846-853.

(106) Manum, H.; Skogestad, S. Self-optimizing control with active set changes. *J. Process Control* 2012, 22 (5), 873-883.

Chapter 2

Hill-Climbing for Plantwide Control to Economic Optimum

This Chapter is based on a published paper “Hill Climbing for Plantwide Control to Economic Optimum” in Industrial Engineering and Chemistry Research, 2014, 53 (42), 16465-16475

In this Chapter, the application of hill-climbing control to ‘seek’ and drive the unconstrained setpoint of a controlled variable (CV) to its economic optimum is proposed for economic plantwide control. Its application is demonstrated on a reactor-column recycle process for energy efficiency maximization at given throughput (Mode I) and also for maximizing process throughput (Mode II). In Mode I, a one degree-of-freedom (dof) hill-climbing feedback controller on top of the regulatory layer is shown to reduce reboiler duty by 3.7% for a 25% throughput increase compared to constant setpoint operation. Similarly, in Mode II, a one-dof hill-climber achieves 3.0% throughput increase compared to constant setpoint operation. These results highlight the effectiveness of hill-climbing for economic plantwide control.

2.1 Introduction

One of the key issues in economic plantwide control is driving and maintaining an unconstrained controlled variable (CV) setpoint at its optimum value, where the optimum value changes due to disturbances and operating condition changes. Ideally, the gradient of the economic objective function with respect to the unconstrained regulatory layer setpoint should be driven to zero for optimality. A possible approach is to directly apply feedback control to drive the gradient or its estimate to zero. The basic idea is to keep adjusting the unconstrained setpoint till the steady state slope of the economic objective function with respect to the unconstrained setpoint is driven to zero. For maximization problems, we thus attempt hill-climbing via feedback. Even as hill-climbing control has been applied for optimal operation of stand-alone isolated units, e.g. maximizing solar flux utilization in solar panels power[1] or minimizing expensive buffer usage in pH control[2], its application to the economic plantwide control of a complete chemical process with material recycle has not been evaluated before, at least to our knowledge. A systematic evaluation of the same for an example process is the major novel contribution of this work.

We note that in real-time optimization (RTO), the estimated gradient of the process model (first principles or statistical) is driven to zero whereas in hill-climbing, the estimated gradient of the actual process is driven to zero via feedback. Also, the feedback in the RTO/EVOP approaches occurs indirectly through the plant model fitting cum setpoint update exercise. Lastly in RTO, the plant is not perturbed and the available plant data is used to update the plant model. In contrast, hill-climbing requires that small perturbations be made to the plant.

In this work, we consider Shinskey's hill-climbing feedback controller[3] for seeking and driving an economically significant unconstrained regulatory layer setpoint to its economic optimum for a reactor-separator-recycle process and quantify its economic benefit over constant setpoint operation. Economic optimality is sought for two operating modes. In Mode I, the reboiler steam (expensive utility) consumption is minimized for a fixed throughput. In Mode II, the plant throughput is maximized.

In the following, we briefly describe the process along with optimal steady state operation results for the two operating modes. The regulatory control structures for the two modes are then synthesized systematically in light of the optimally active constraints. We also present the override controls necessary for switching between the two structures. This is followed by a brief description of Shinskey's one-dof dynamic hill-climber and its application to the example process. Closed loop dynamic control results for both modes are then presented and the economic benefit is compared to constant set-point operation. The article ends with the conclusions that can be drawn from the work.

2.2 Process Description

The reactor-separator-recycle process flowsheet studied here is shown in Figure 1.8 . The salient base-case operating conditions are noted in Table 2.1. This process module has been widely used in the plantwide control literature to highlight and address key issues in plantwide control (see e.g. [4-5]). Fresh *A* (F_A) and fresh *B* (F_B) are mixed with the recycle stream and fed to a heated CSTR. The irreversible exothermic reaction $A + B \rightarrow C$ occurs in the boiling reactor. The reactor effluent is sent to a simple distillation column to recover 99 mol% pure *C* as the bottoms product and recycle the distillate containing unreacted *A* and *B* with some *C* impurity, back to the CSTR. The hypothetical component properties, reaction kinetics and thermodynamic package used in the Hysys process simulation are noted in Table 2.2.

The process has 9 independent control valves (control dofs). Of these 2 valves would be used for controlling the column reflux drum and bottom sump levels, which are non-reactive liquid inventories with no steady state effect. Another valve would be used for column operation at given design pressure. This leaves 6 remaining valves that may be adjusted to move the process to a particular steady state. The process steady state operating dof is then 6. These correspond to two dofs for the fresh feeds (F_A and F_B), two for reactor and two for the column. We use the following six specification variables to exhaust the steady state process dofs and converge the flowsheet: fresh *B* feed rate (F_B), reactor level and temperature (U_{rxr} and T_{rxr}), column reflux to feed ratio and bottoms purity (L/F_{col} and x_C^P) and reactor *B* mol fraction (x_{rxrB}).

Table 2.1 Recycle process base-case operating conditions for Mode I

Process Variables	**Temperature (°C)**	**Molar Flow (kmol/h)**	x_A	x_B	x_C
F_A	26	99	1	0	0
F_B	26	100	0	1	0
F_{col}	108	400.6	0.40	0.22	0.38
R	94	300.6	0.53	0.29	0.17
P	137	100	0.0	0.01	0.99
L	94	240.6	0.53	0.29	0.17
Other Variables					
No. of trays	18				
Feed tray	5				
Pr_{cnd}	1.4 atm				
U_{rxr}	6 m^3				
T_{rxr}	108 °C				
Q_{rxr}	190 kW				
Q_{cnd}	4706 kW				
Q_{reb}	4722 kW				

See Figure 1.8 and Nomenclature for variable descriptions

Table 2.2. Modeling details of recycle process

Kinetics	A+B→C	$r = k.x_{rxrA}.x_{rxrB}$
		$k = 2\times10^8.\exp(-70000/RT)$
Hypotheticals[#]	MW	NBP(°C)
A	50	70
B	80	100
C	130	120
VLE	Soave-Redlich-Kwong	

Reaction rate units: $kmol.m^{-3}.s^{-1}$

#: Hydrocarbon estimation procedure used to estimate parameters for thermodynamic property calculations

2.2.1 Optimum Steady Process Operation

The available steady state dofs should be exploited for economically optimal process operation. We consider two modes of process operation. In Mode I, the throughput (F_B) is given, fixed e.g. by market demand-supply considerations, and the remaining five steady state dofs are optimized to maximize the process energy efficiency. Since steam is the expensive utility here, optimal Mode I operation corresponds to minimizing column boil-up, V. The steam consumption in the reactor is ignored here as it is a small fraction (<5%) of the reboiler duty. In Mode II, all the six dofs, including F_B, are optimized to maximize the process throughput (F_B). Mode II operation is usually desired in a seller's market, where the product demand far exceeds supply.

The steady state optimization must seek solutions that are within the feasible process operating space constrained by maximum/minimum material/energy flows, temperatures etc. For both Mode I and Mode II, we then have a non-linear constrained optimization problem with continuous variables. The optimization is performed using the Matlab *fmincon* routine with Hysys as the background steady state flowsheet solver. Object oriented protocols are used to link Matlab and Hysys. Table 2.3 summarizes the steady state optimization and the results obtained. Mode I results are presented at two process throughputs, F_B = 100 kmol/h (design throughput) and F_B = 125 kmol/h (increased throughput). In both modes, the minimum product quality constraint ($x_C^{P,MIN}$), the maximum reactor temperature (T_{rxr}^{MAX}) constraint and the maximum reactor level (U_{rxr}^{MAX}) constraint are always active. These make economic sense with the $x_C^{P,MIN}$ constraint minimizing product give-away, and the other two constraints maximizing the single pass reactor conversion.

Table 2.3. Process Optimization Summary

Objective	Mode I Max (-V)		Mode II Max (F_B)
Constraints	$0 <$ Material flow < 2(base-case) $0 <$ Energy flow < 2(base-case) $0 < U_{rxr} < 6\text{m}^3$ $0 < V <$700kmol/h $90^{o}\text{C} < T_{rxr} < 108\ ^{\circ}\text{C}$ $x_C^P \geq 0.99$		
	Optimized operating condition		
Variable			
F_B (kmol/h)	100*	125*	133.7
U_{rxr} (m^3)	6 $_{\text{max}}$	6 $_{\text{max}}$	6 $_{\text{max}}$
T_{rxr} (^{o}C)	108 $_{\text{max}}$	108 $_{\text{max}}$	108 $_{\text{max}}$
x_{rxrB}	0.172	.205	.218
L/F_{col}	0.55	0.55	0.55
x_C^P	0.99 $_{\text{min}}$	0.99 $_{\text{min}}$	0.99 $_{\text{min}}$
$V^{\#}$ (kmol/h)	421.3	616.7	700 $_{\text{max}}$

*Specified ; # calculated (not a decision variable)

For a specified Mode I throughput, the active constraints leave 2 (6 dofs – 3 active constraints – 1 F_B specification) unconstrained steady state dofs. In Mode II, to achieve maximum throughput, the maximum column boil-up (V^{MAX}) constraint corresponding to column flooding additionally goes active. The unconstrained Mode II steady state dof then remains 2 (6 dofs – 4 active constraints) with F_B (throughput) as an additional decision variable. Note that V^{MAX} is a hard constraint and its violation is not acceptable as a flooded column represents a severe hydraulic problem requiring laborious manual intervention to drive the column back to its normal operation flow regime. The other three active constraints (T_{rxr}^{MAX}, U_{rxr}^{MAX} and $x_C^{P,MIN}$) are soft ones with small short-term deviations beyond the constraint being acceptable.

2.3 Plantwide Regulatory Control Structure

In this work, we synthesize the plantwide regulatory control structure that reflects industrial practice and has its TPM at a fresh process feed. The same is usually not the best structure from the perspective of handling hard equipment capacity constraint(s) on increasing throughput or minimizing the back-off in the economically dominant active constraint etc. In this work, since the objective is to quantify the economic benefit of hill climbing control, working with a conventional control system is considered acceptable.

Conventionally, the plantwide regulatory control structure is designed with the TPM at a fresh feed with 'local' pairings on the individual unit operations for closing its unit specific material and energy balances. Such a control structure provides robust process regulation as long as an equipment capacity constraint is not encountered. On sufficiently increasing throughput however, equipment capacity constraints such as a column approaching flooding or a furnace approaching its maximum duty etc are encountered. A hard equipment capacity constraint going active usually implies loss of a control dof with consequent loss of the associated regulatory control task. The conventional control structure must then be reconfigured using overrides to ensure proper process regulation with the bottleneck unit operating at its capacity constraint. We then naturally obtain the regulatory control structure for Mode I (no hard constraints) operation with the TPM at the fresh feed and a different regulatory structure for Mode II (hard equipment capacity constrained) operation, where the equipment capacity constraint sets the throughput. Conventionally, overrides are used to effect the control structure reconfiguration due to the equipment capacity constraint. In the following we synthesize the Mode I and Mode II regulatory control structures along with the override control structure reconfiguration scheme.

2.3.1 Regulatory Control Structure for Mode I

The process control dof is 9, corresponding to the 9 independent control valves as in Figure 1.8. These valves must be used to set the process throughput and to regulate the unit specific material and energy balances as well as the overall plantwide balances. In other words the 9 valves must be used to regulate 9 control objectives (including throughput) that ensure the process inventories remain well regulated within an acceptable band and do not drift unmitigated.

For Mode I, we use a conventional regulatory control structure with the TPM at F_B, a process fresh feed, (objective 1). The remaining control objectives include controlling the reactor level (U_{rxr}) and temperature (T_{rxr}), which must be regulated to close the reactor total material and energy balances (objectives 2 and 3). The obvious 'local' manipulated variables (MVs) for a fast dynamic response are reactor exit flow rate (F_{col}) for U_{rxr} control and reactor heating duty (Q_{rxr}) for T_{rxr} control.

On the column, the reflux drum and bottom sump levels (U_{rd} and U_{bot}) must be controlled to close the material balance on the condenser and the reboiler (objectives 4 and 5), respectively. We control U_{rd} using the distillate flow (R) and U_{bot} using the bottoms flow (P), which are fast 'local' pairings. For a given boilup, the column pressure (Pr_{col}) must also be controlled to close the column vapor balance (objective 6). This is effectively accomplished by adjusting column condenser duty (Q_{cnd}).

The other 2 column regulatory objectives are the key component balances corresponding to the heavy key leakage in the distillate (x_C^R) and the light key leak leakage in the bottoms (x_B^P). Since composition measurements are cumbersome, we choose to control the reflux to feed ratio, L/F_{col} (objective 7) and a sensitive stripping tray temperature, T^S_{col} (objective 8) instead. L/F_{col} is maintained by directly adjusting L while T^S_{col} is maintained by manipulating the reboiler duty (Q_{reb}) for 'local', dynamically fast, conventional pairings. Note that by maintaining L/F_{col}, the distillate (im)purity is loosely regulated, which is acceptable since it is a recycle stream. On the other hand, regulating T^S_{col} provides much tighter control of the bottoms purity, which is crucial since the bottoms is the product stream.

The last control objective is subtler and corresponds to stoichiometric balancing of the two fresh feeds as dictated by the reaction chemistry (objective 9). The process topology is such that fresh A and fresh B are taken in and only near pure C product is discharged. Since 1 mole of A reacts with 1 mole of B to give 1 mole of C, for the asymptotic case of pure C being discharged from the process, if F_B = 100 kmol/h (design throughput), F_A must be exactly 100 kmol/h as dictated by the overall plant material balance. Even for the slightest mismatch, the component fed in excess (A or B) would build up unmitigated in the recycle loop. This unmitigated build-up can only be avoided when the fresh feeds are fed such that the reaction stoichiometry is satisfied down to the last molecule. The balancing must necessarily be done in a feedback arrangement by inferring/measuring the A or B circulating around in the recycle loop. This is because flow measurements are never exact and have small biases so that even with the two fresh feed flow setpoints fixed to equal molar flows, a slight mismatch is guaranteed. Since the recycle stream is mixed and contains both A and B in large amounts, inferring the recycle loop inventory of A or B requires a composition measurement inside the recycle loop. Here, we choose to regulate the B mol fraction in the reactor, x_{rxrB} (objective 9). In addition to stoichiometric feed balancing, maintaining x_{rxrB} also helps to mitigate composition variability in the reactor, the most non-linear unit operation in the process. To ensure F_A and F_B move in tandem, F_A is maintained in ratio with F_B and the ratio setpoint is manipulated by the x_{rxrB} controller.

The nine regulatory loops, corresponding to the 9 control dofs, complete the regulatory control structure for Mode I operation. The structure is shown in Figure 2.1 and is referred to as CS1. We note that in this conventional control structure (CS1), all the flows in the recycle loop are under level control. Snowballing [13], where the recycle flow increases in a significantly larger proportion for a small increase in the TPM setpoint, is thus possible. The same is however not an issue since if the recycle rate increase is too large, the column would approach its flooding limit triggering overrides that reconfigure the control structure to cut the fresh feed rate. The consequent regulatory control structure with the column at its flooding limit (bottleneck constraint) setting the maximum throughput (Mode II) is described next.

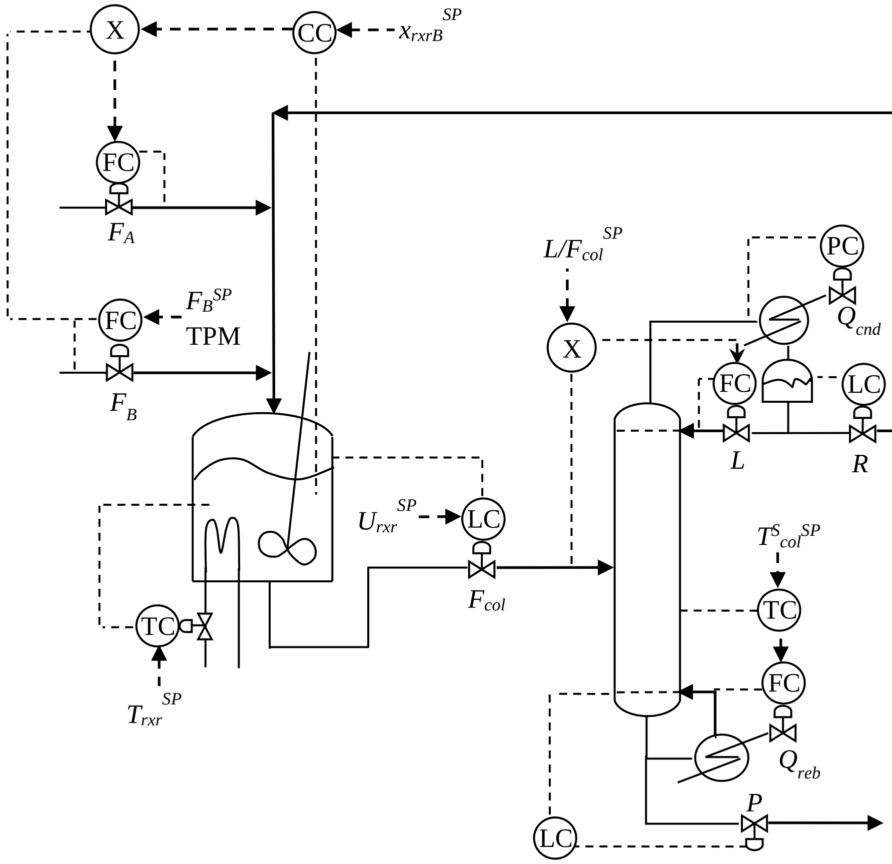
X
CC
x_{rxrB}^{SP}
FC
F_A
FC
F_B^{SP}
TPM
F_B
U_{rxr}^{SP}
LC
F_{col}
TC
T_{rxr}^{SP}
L/F_{col}^{SP}
X
PC
Q_{cnd}
FC
LC
L
R
$T^S{}_{col}^{SP}$
TC
FC
Q_{reb}
P
LC

Figure 2.1. Conventional regulatory control structure, CS1 (for Mode I)

2.3.2 Regulatory Control Structure for Mode II

In Mode II, V^{MAX} acts as the bottleneck equipment capacity constraint. If we use CS1 for maximum throughput operation, the TPM setpoint (F_B^{SP}) will have to be adjusted so that V (bottleneck constraint) is maintained near its constrained value, V^{MAX}. The bottleneck constraint controller thus uses the V-F_B^{SP} pairing. The pairing is dynamically slow (long loop) so that the V control cannot be very tight. Since V^{MAX} is a hard constraint that must not be violated, the bottleneck controller setpoint must necessarily have a large back-off from V^{MAX}. In other words, for Mode II operation, $V^{SP} = V^{MAX} - \Delta$, where Δ is the large back-off representing the unrecoverable production (economic) loss.

As recommended in Kanodia and Kaistha,[5] the back-off can be dramatically reduced by shifting the TPM to the bottleneck constraint and reconfiguring the regulatory control system around it. Accordingly, we use Q_{reb} to control V. With this 'local' pairing, V control would be very tight so that the back-off from V^{MAX} would be negligibly small and we can set $V^{SP} = V^{MAX}$ (negligible back-off) for maximum throughput (Mode II) operation. With Q_{reb} paired for V control, it cannot be used for conventional T^S_{col} control so that the column feed, F_{col} is manipulated instead. With F_{col} already paired, we need an alternative manipulated variable for reactor level (U_{rxr}) control. The reactor fresh feed F_B is used for the purpose. The rest of the regulatory control structure remains the same as CS1.

The revised regulatory control structure for Mode II operation is shown in Figure 2.2 and is referred to as CS2. It differs from CS1 in that the inventory controllers upstream of the TPM are oriented in the reverse direction of process flow. On the other hand, all CS1 inventory controllers are oriented in the direction of process flow. Note that maintaining F_A in ratio with F_B helps U_{rxr} control with both fresh feeds moving in tandem to bring the deviating reactor level back to its setpoint. Also, to reduce throughput below maximum, V^{SP} is reduced below V^{MAX} making V^{SP} the TPM for this structure.

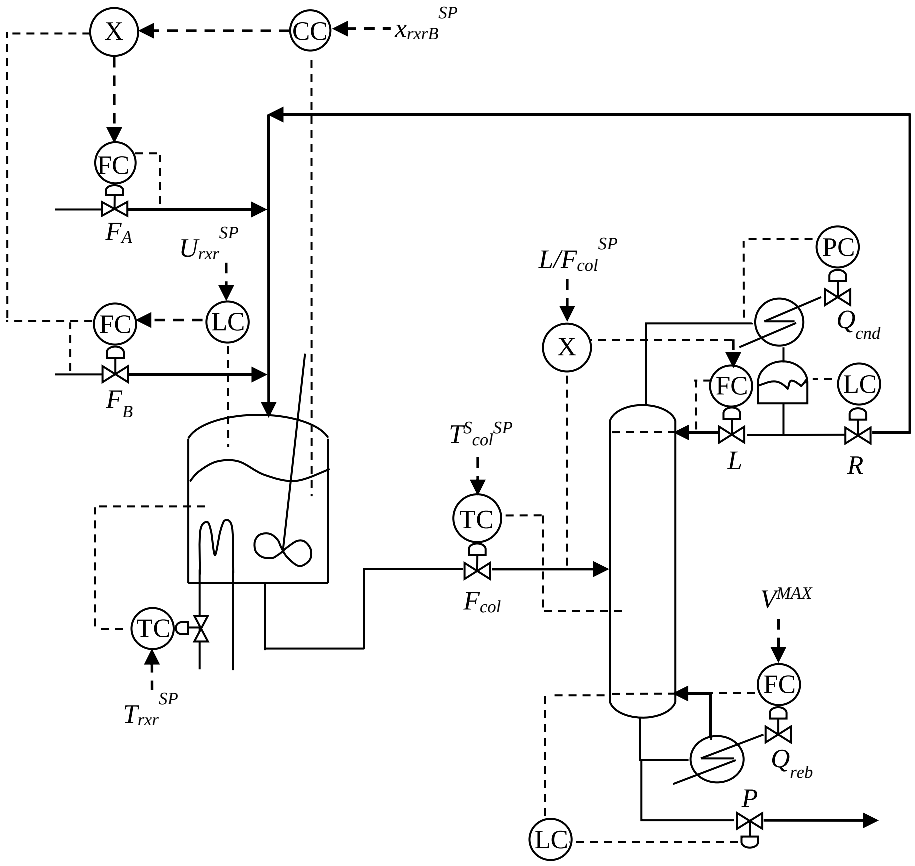
X
CC
x_{rxrB}^{SP}
FC
F_A
U_{rxr}^{SP}
FC
LC
F_B
TC
T_{rxr}^{SP}
$T^S_{col}{}^{SP}$
TC
F_{col}
L/F_{col}^{SP}
X
PC
Q_{cnd}
FC
LC
L
R
V^{MAX}
FC
Q_{reb}
P
LC

Figure 2.2. Regulatory control structure, CS2 (for Mode II)

2.3.3 Overrides for Reconfiguring Regulatory Layer Loops

The override scheme necessary for reconfiguring the regulatory loops to transition between CS1 and CS2 is shown in Figure 2.3. It consists of an override temperature controller (OTC) on the column and an override level controller (OLC) on the reactor with three low selectors (LS_1 – LS_3). The OTC setpoint is slightly lower than the nominal temperature controller setpoint while the OLC setpoint is somewhat higher than the nominal reactor level controller setpoint. Consider increasing the throughput from its nominal value (Mode I) to the maximum achievable (Mode II). At the nominal steady state, since V is less than V^{MAX}, LS_1 passes the nominal temperature controller output so that Q_{reb} is under nominal column temperature control. Since the OTC setpoint is slightly lower and the fast nominal temperature controller effectively maintains the column temperature close to its nominal setpoint, the direct acting OTC output is high so that LS_2 passes the nominal reactor level controller output to the column feed valve. With reactor level controlled at its nominal setpoint, the OLC output is high so that LS_3 passes the operator input F_B^{SP} value. Thus, at the nominal throughput, the low selected outputs emulate CS1.

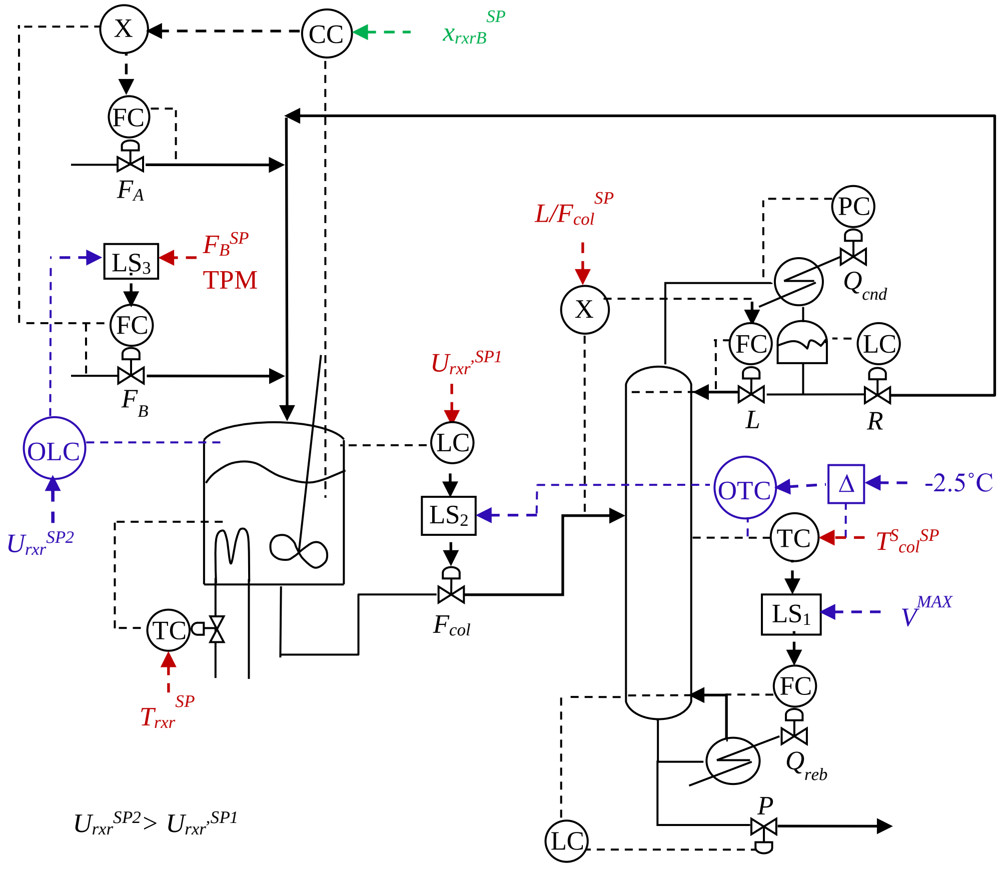
X
CC
x_{rxrB}^{SP}
FC
F_A
LS_3
F_B^{SP}
TPM
FC
F_B
OLC
U_{rxr}^{SP2}
TC
T_{rxr}^{SP}
$U_{rxr}^{SP2} > U_{rxr}'^{SP1}$
$U_{rxr}'^{SP1}$
LC
LS_2
F_{col}
L/F_{col}^{SP}
X
PC
Q_{cnd}
FC
LC
L
R
OTC
Δ
-2.5°C
TC
$T^{S}_{col}{}^{SP}$
LS_1
V^{MAX}
FC
Q_{reb}
P
LC

Figure 2.3. Overrides for switching between CS1 and CS2

Now as F_B^{SP} is increased to transition to maximum throughput (Mode II), V eventually increases beyond V^{MAX} so that LS_1 passes V^{MAX}. Nominal column temperature control is then lost and the column temperature starts to drop as more feed is being input than can be boiled off. As the temperature reduces, the OTC output decreases till it reduces below the nominal reactor level controller output. LS_2 then passes F_{col} manipulation to the OTC. Column temperature control is thus regained while reactor level control is lost. The unregulated reactor level then increases, since F_B^{SP} is increasing while the OTC is decreasing F_{col}. This causes the OLC output to decrease and eventually, LS_3 passes the OLC output to the F_B valve which cuts the fresh B feed to the process. F_B thus floats and settles at the appropriate value corresponding to V^{MAX}, which is the maximum achievable throughput. The overrides thus act to cut the process feed with V constrained at V^{MAX}. Note that the low selected outputs cause emulation of CS2. A complementary logic applies to untriggering of the overrides as F_B^{SP} is reduced. The overrides thus switch the control structure between CS1 and CS2. Purely for reasons of convenience, in this work, we evaluate the two regulatory control structures separately.

It is appropriate to note that when it is well established that the bottleneck constraint is always column flooding, the control system can be significantly simplified by using V^{SP} as the TPM over the entire throughput range. $V^{SP} = V^{MAX}$ then fixes maximum production (Mode II) while lower V^{SP} values correspond to lower production (Mode I). The reconfiguration between CS1 and CS2 using the overrides is then not necessary and CS2 provides smooth operation over the entire throughput range. In this work however, we consider CS1 for Mode I and CS2 for Mode II, as this is typical industrial practice.

2.3.4 Augmented Control System for Economic Operation

In this section we augment the regulatory control structures, CS1 and CS2, for optimal steady economic operation, in line with the optimization results obtained earlier. In both Mode I and Mode II, U_{rxr}^{MAX}, T_{rxr}^{MAX} and $x_C^{P,MIN}$ soft constraints are active. The first two constraints correspond to setting $U_{rxr}^{SP} = U_{rxr}^{MAX}$ and $T_{rxr}^{SP} = T_{rxr}^{MAX}$ in both CS1 and CS2. The product quality measurement, x_C^P, would typically be available in industrial practice. To regulate it, an additional composition controller is implemented which manipulates $T^S{}_{col}^{SP}$ to hold x_C^P. For optimality, we set $x_C^{P,SP} = x_C^{P,MIN}$. In Mode II, CS2 is the regulatory control structure and we set $V^{SP} = V^{MAX}$ for achieving maximum throughput. The average process operation then is at the hard V^{MAX} constraint limit with negligible back-off.

The setpoints, x_{rxrB}^{SP} and $L/F_{col}{}^{SP}$, correspond to the remaining 2 unconstrained steady state dofs in Mode I and Mode II. The simplest operating policy is to keep these set-points constant at their optimized value for the base-case (design throughput) steady state. As throughput changes, the optimum value of these setpoints would, strictly speaking, change. If the economic loss with no re-optimization is small, the constant setpoint policy would be deemed acceptable. If however the loss is large, a hill-climber should be used to drive the operation to the optimum and mitigate the loss.

To evaluate the economic impact of x_{rxrB} and L/F_{col}, Figure 2.4 compares the variation in V (Mode I objective) with x_{rxrB} and L/F_{col} at the design throughput (F_B = 100 kmol/h) optimum values. It is observed that the optimum with respect to L/F_{col} is quite flat with large changes in L/F_{col} around its optimum value causing only a small increase in V. The optimum with respect to x_{rxrB}, on the other hand, is noticeably sharper with larger increase in V as x_{rxrB} is moved away from its optimum value. The optimum solution is thus significantly more sensitive to x_{rxrB} compared to L/F_{col}. The economic loss due to no re-optimization as e.g. the process throughput changes, is then expected to be significant for constant x_{rxrB} while a constant L/F_{col} is likely to result in an acceptably small loss. To quantify the same, Table 2.4 compares V at an increased throughput of F_B = 125 kmol/h with both x_{rxrB} and L/F_{col} held constant at their base-case values (optimum values for F_B = 100 kmol/h), only x_{rxrB} or L/F_{col} reoptimized, and both x_{rxrB} and L/F_{col} reoptimized. The data shows that the increase in boilup above the optimum is primarily attributable to no reoptimization of x_{rxrB} with very little increase (<0.1%) being attributable to no reoptimization of L/F_{col}.

Table 2.4. V at throughput of F_B = 125 kmol/h

	x_{rxrB} and L/F_{col} at base-case	Only x_{rxrB} reoptimised	Only L/F_{col} reoptimised	Both reoptimised
V	639.5	616.7	538.9	616.7
x_{rxrB}	0.172	0.206	0.172	0.21
L/F_{col}	0.55	0.55	0.50	0.55

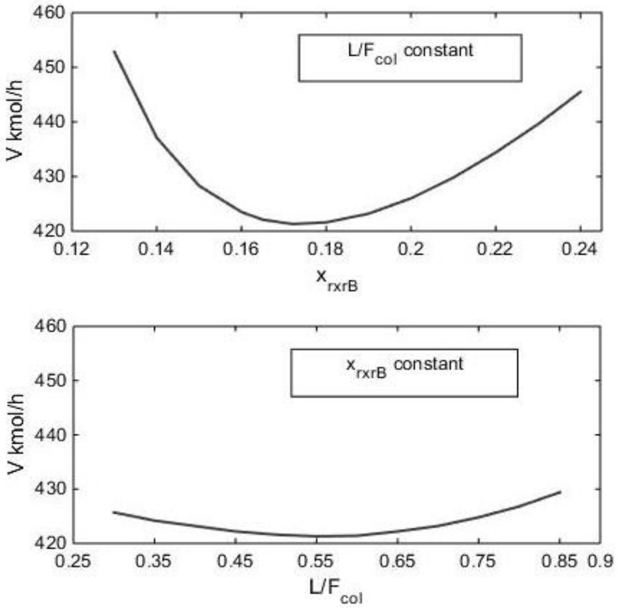

Figure 2.4. Variation in V with x_{rxrB} and L/F_{col} at design throughput (F_B=100 kmol/h)

These results suggest that a hill-climber is worthwhile for optimizing x_{rxrB} in Mode I since the increase in the Mode I objective function, $J = -V$, over the optimum (i.e. economic penalty), due to constant setpoint operation, as throughput is varied, is significant. This climber adjusts the CS1 x_{rxrB}^{SP} to maximize $-V$, which is equivalent to minimizing V. In Mode II, since V^{MAX} is the bottleneck constraint that limits throughput and x_{rxrB}^{SP} significantly affects V, a hill-climber that optimizes the CS2 x_{rxrB}^{SP} is also considered worthwhile. This hill-climber adjusts x_{rxrB}^{SP} to maximize F_B with $V^{SP} = V^{MAX}$. The hill-climber, the x_C^P quality control loop and the regulatory layer setpoint values for economic operation are shown in red in Figure 2.5 (a) for CS1 and Figure 2.5 (b) for CS2. Note that the simple constant setpoint operating policy for L/F_{col}^{SP} is appropriate for both Mode I and Mode II as the economic objective function is quite insensitive to its choice in both Mode I and Mode II.

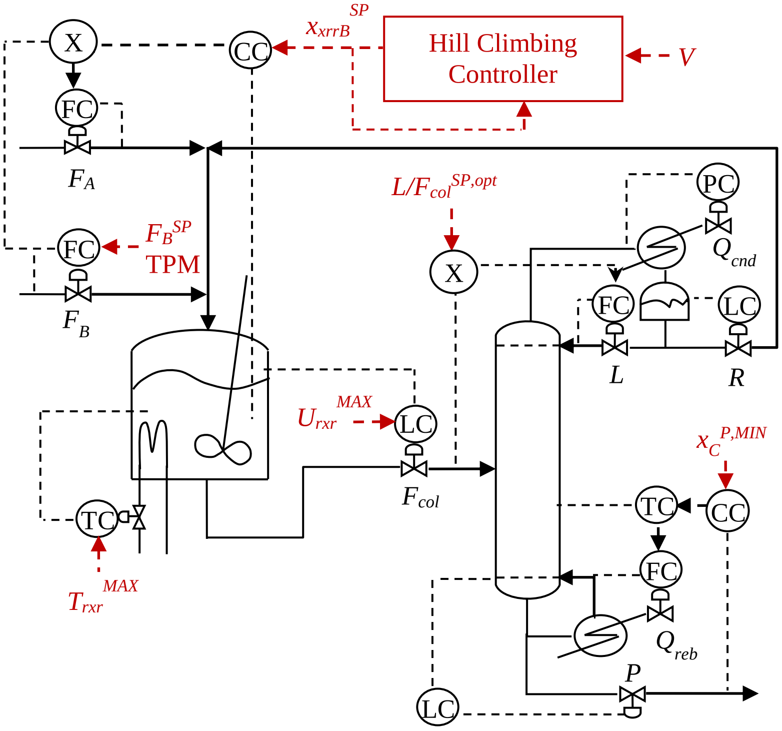
X
CC
x_{xrrB}^{SP}
Hill Climbing Controller
V
FC
F_A
FC
F_B^{SP}
TPM
F_B
$L/F_{col}^{SP,opt}$
X
PC
Q_{cnd}
FC
LC
L
R
U_{rxr}^{MAX}
LC
F_{col}
$x_C^{P,MIN}$
TC
CC
FC
TC
T_{rxr}^{MAX}
Q_{reb}
P
LC

Figure 2.5 (a). CS1 modifications for economic optimum operation

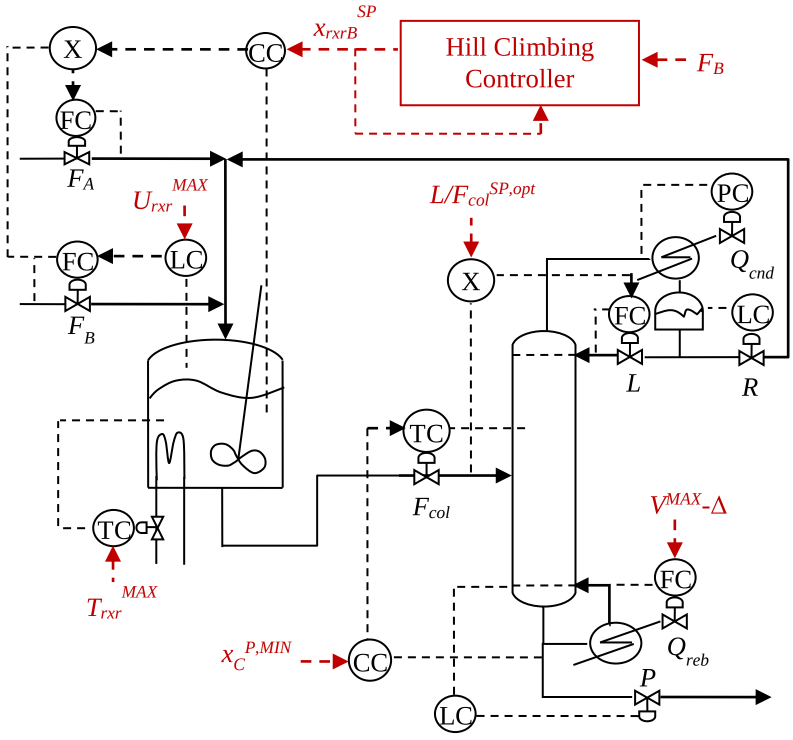
X
CC
x_{rxrB}^{SP}
Hill Climbing Controller
F_B
FC
F_A
U_{rxr}^{MAX}
FC
LC
F_B
$L/F_{col}^{SP,opt}$
PC
Q_{cnd}
X
FC
LC
L
R
TC
F_{col}
V^{MAX}-Δ
FC
Q_{reb}
TC
T_{rxr}^{MAX}
$x_C^{P,MIN}$
CC
P
LC

Figure 2.5 (b). CS2 modifications for economic optimum operation

2.4 Shinskey's Hill-Climber

The one-dof hill-climber, was originally proposed by Shinskey[3] and is shown in Figure 2.6. In general, we want to manipulate the regulatory layer setpoint u such that the economic objective J is driven to its maximum. In other words, u must be adjusted to drive the steady state slope $y = dJ/du$ to zero. No direct measurement is however available for y and it must be inferred from J and u, measurements of which are available. Process dynamics, G_P, get in the way of estimating y. We therefore use a filter to smoothen the transients in J to obtain its long term variation post filtering, J_f. The long-term changes, ΔJ, is then conveniently obtained by sampling J_f. The control input u is maintained constant between two consecutive sampling/control time points. Dividing ΔJ by Δu then gives an estimate of the slope y. This estimate is driven to zero by using a feedback PI controller. The setpoint of the PI controller is zero, corresponding to the zero slope at the top of the hill (optimum). The output of the PI controller is sampled.

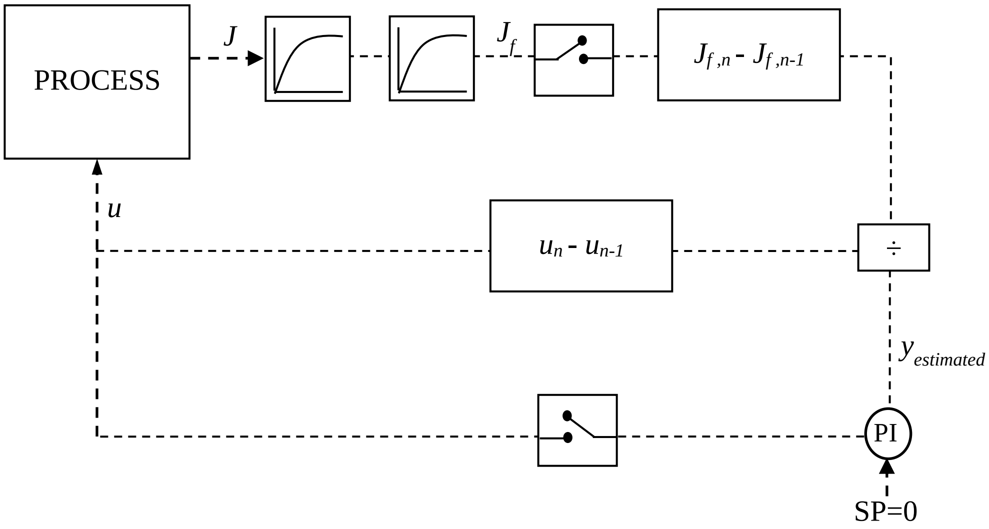

Figure 2.6. Block-diagram of the one-dof hill-climber

We note that since the hill-climber has a division operation, the output of the divider is trimmed to be between a maximum and minimum to guard against large slope estimates due to division by small numbers. Also, the estimation is not self-starting and needs a perturbation that gives a large enough derivative for division. As insightfully noted during the review process, unmeasured disturbances can confuse the hill-climber and cause it to move the manipulated regulatory setpoint in the wrong (suboptimal) direction. In the presence of the disturbance, the change ΔJ_f in the objective function gets wrongly attributed to Δu so that the hill slope estimate becomes erroneous causing the hill climber to move the setpoint in the wrong direction (i.e. away from the actual optimum). However, as the unmeasured disturbance is rejected by the regulatory control system, the slope estimates improve and the hill-climber would then move the process towards the optimum. To mitigate performance deterioration due to disturbanes, it is important that the filtering parameters and sampling period are chosen such that the fast transients due to disturbances are smoothened out so that the ΔJ_f used for estimating the hill slope is largely attributable to Δu. Alternatively, one can turn on the hill-climber during relatively calm operation periods and turn it off during periods with severe transients.

We believe that the confusion due to unmeasured disturbances is unavoidable and all approaches seeking to drive a setpoint to its unconstrained optimum (RTO, EVOP or hill climbing) suffer from the flaw, to a greater or lesser degree, perhaps. The confusion may be significantly mitigated by using a model and available process measurements to estimate the disturbances and partition the total change ΔJ_f into that attributable to Δd (disturbance change) and that attributable to Δu (regulatory layer setpoint change). We would then likely get better hill slope estimates and avoid movement away from the optimum due to disturbances. In the current work, we evaluate simple hill climbing with no modeling of disturbance effects and intend to explore model based hill climbing in follow-up work.

2.5 Dynamic Simulation and Controller Tuning

A rigorous dynamic simulation of CS1 and CS2 along with the respective hill-climbers as described above is built in Hysys. The column drum and sump levels are set for 5 min liquid residence time at the design steady state at 50% level. A consistent tuning procedure is followed for both CS1 and CS2. The column pressure controller is PI and tuned for tight pressure control. All flow controllers are PI and use a reset time of 0.5 mins and a controller gain of 0.3. All non-reactive liquid level controllers are P only and use a gain of 2. The reactor level controller is PI and is tuned for a slightly oscillatory servo response. The reactor temperature and column temperature controller gain is adjusted for a slightly oscillatory servo response with the reset time set to the time it takes for 2/3rd completion of the open loop step response. For realism, all temperature sensor readings are lagged by 2 mins. Also, a lag of 2 mins is applied to all ‘direct Q’ energy duty valves to account for heat transfer dynamics.

In the economic layer, the x_C^P PI controller is tuned by hit-and-trial for a slightly underdamped servo response. The composition sensor uses a sampling time of 5 mins and a dead-time of 5 mins. In our work, the one dof PI hill-climber is implemented in Matlab and linked with Hysys dynamics using object oriented protocols. Both the Mode I and Mode II hill-climbers are tuned by hit-and-trial. Two 2 hr first order lags are applied in series to J to filter out fast transients and obtain their long-term trends. We also apply a 5 hour sampling on the $x_C^{P,SP}$ adjustments by the hill-climber as well as to J_f. The salient parameters of the regulatory / economic loops in CS1 and CS2 simulations are noted in Table 2.5.

2.5.1 Closed Loop Results

The closed loop performance of the economic plantwide control system with the one-dof hill-climber for updating x_{rxrB}^{SP} is now obtained. In Mode I (CS1) operation, the throughput (F_B^{SP}) is changed as a ±25kmol/h step around the design throughput (F_B = 100 kmol/h) and simultaneously the hill-climber is switched on. The plantwide dynamic response of salient process variables is shown in Figure 2.7. The product quality control is observed to be quite tight for the entire duration of the transient response. The hill-climber readjusts x_{rxrB}^{SP} towards its optimum value and in response, V reaches its optimum value in 8 moves. It thus takes about 40 hrs for the minimum V to be closely approached. For a +25kmol/h throughput change, the action of the hill-climber causes V to reduce to 616.7 kmol/h compared to 639.5 kmol/h at constant x_{rxrB}^{SP} operation. This corresponds to~3.7% energy saving, which is not negligible. For a -25kmol/h throughput change, the energy saving is somewhat lower at ~2.6%. These savings are significant enough to justify the additional cost of the hill-climber.

Table 2.5. Salient controller parameters for CS1/CS2*, #, $

CV	CS1/CS2		PV Range&	MV Range&
	K_C	τ_i(min)		
$[A/B]_{rxr}$	1.2/1.2	80/80	0.05-0.40	0.5-1.5
T_{rxr}	3/3	30/30	100-120^{o}C	2x10^{6}kJ/h
U_{rxr}	2/2	20/20	10-100%	0-100%
T^{S}_{col}	0.5/0.5	30/40	110-140^{o}C	4x10^{7}kJ/h
x_C^{P}	0.35/0.35	40/40	0.98-0.995	110-140^{o}C

*All level loops use $K_C = 2$ unless otherwise specified. #Pressure/flow controllers tuned for tight control. & Minimum value is 0, unless specified otherwise. $ All compositions have a 5 min dead time and sampling time. All temperature measurements are lagged by 2 min.

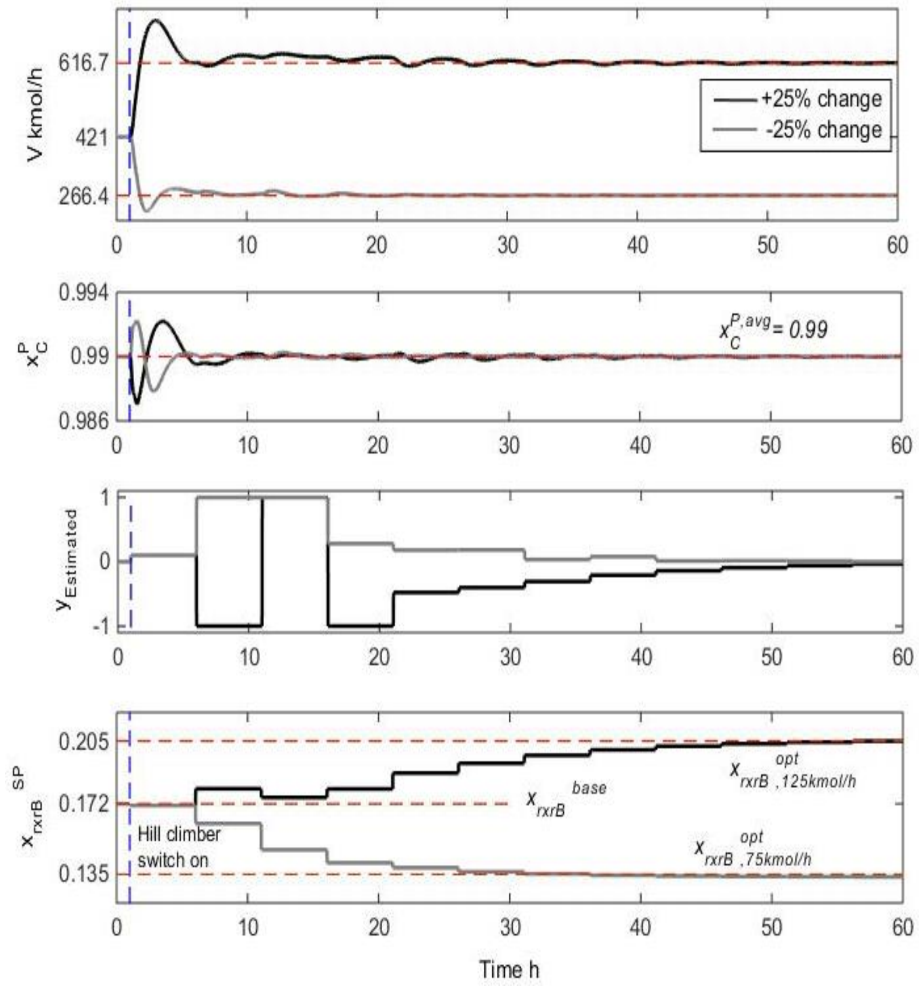

Figure 2.7. Dynamic response for boilup minimization

For Mode II (CS2) operation, the x_{rxrB}^{SP} is kept fixed at its optimum value at the design throughput and the CS2 V^{SP} is set at its constraint value of V^{MAX}. The plant is then allowed to settle to steady state. This initial steady state corresponds to the maximum throughput with constant x_{rxrB}^{SP} (no reoptimization). At this steady state, F_B = 129.9 kmol/h. The one-dof hill-climber is then switched on and it adjusts x_{rxrB}^{SP} to seek the value of x_{rxrB}^{SP} that maximizes F_B. The transient response of salient process variables in Figure 2.8 shows that tight product quality control is achieved during the transient period. The x_{rxrB}^{SP} hill-climber causes F_B to increase towards the maximum achievable throughput value of 133.7 kmol/h. In about 40 hrs (8 control moves), this maximum value is approached quite closely. The hill-climber thus achieves a substantial ~3.0% increase in the maximum throughput. For a product-raw material price differential of $30 per kmol, the increased throughput translates to ~$1.0x10^6 additional yearly sales revenue, which is significant. This shows that a hill-climber to optimize an economically important unconstrained regulatory setpoint results in substantial economic benefit compared to constant setpoint operation.

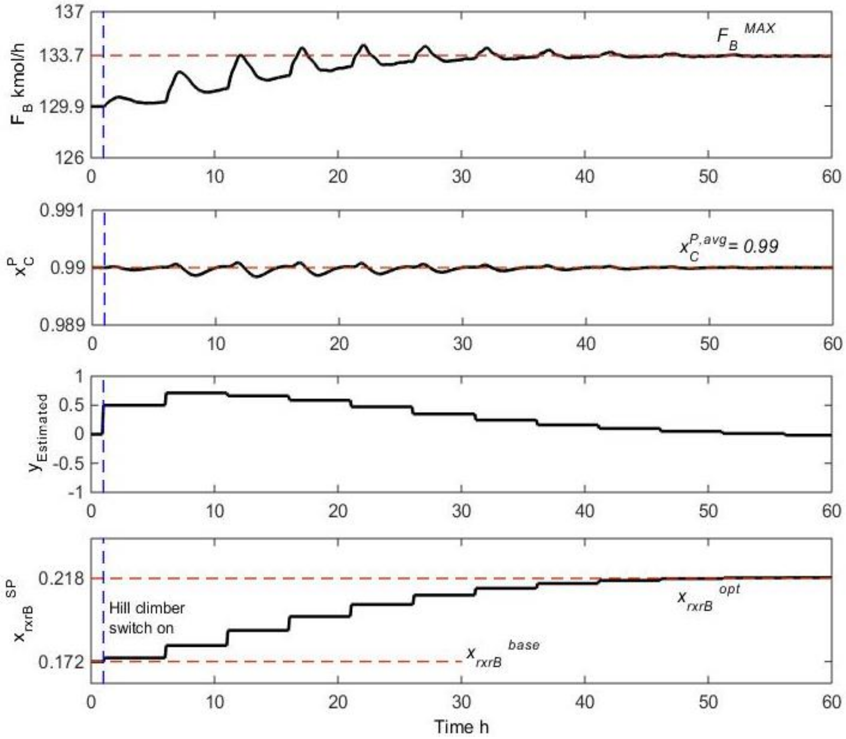

Figure 2.8. Dynamic response for throughput maximization

We also tested the performance of the hill-climber in response to unmeasured feed composition disturbances for both Mode I (given F_B) and Mode II (given V^{MAX}) operation. Two step disturbances are tested; 10% *A* in F_B and 10% *B* in F_A. The initial steady state corresponds to x_{rxrB} at its base-case Mode I optimum value. Further, for Mode II, V^{SP} is set equal to V^{MAX} and the process allowed to settle at the steady state. With this initial steady state, the fresh feed composition change step disturbance is introduced with the hill-climber enabled. The corresponding dynamic responses for Mode I or Mode II operation for the two feed composition disturbances are shown in Figure 2.9. In all cases a stable response is obtained with x_{rxrB} settling at its final optimum value in 8-10 moves (40-50 hrs). Also the product quality control is acceptability tight during the transients, as before.

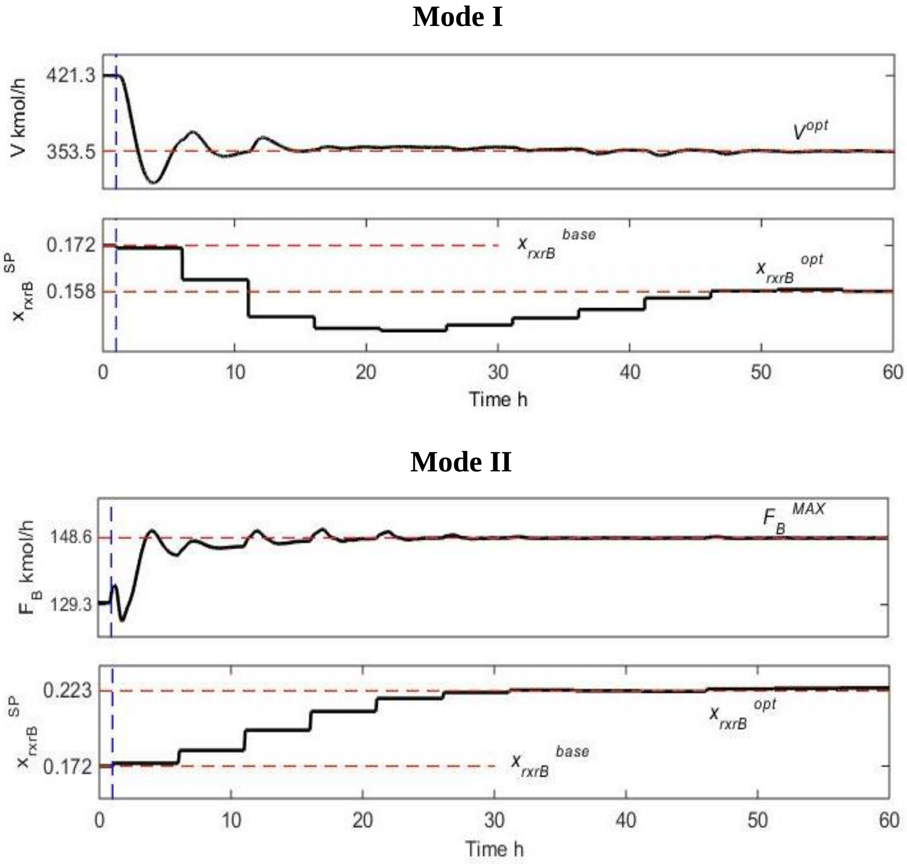

Figure 2.9. (a) 10% *A* impurity in F_B

Mode I

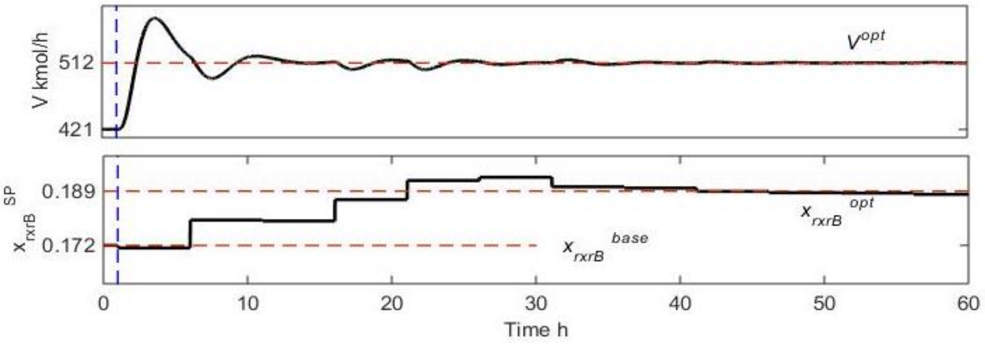

Mode II

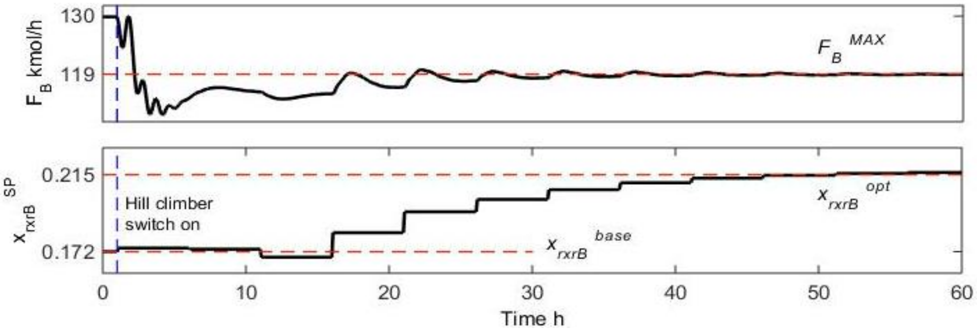

Figure 2.9. (b) 10% *B* impurity in F_A

Note that for Mode I, since F_B^{SP} is fixed, the feed composition disturbances are equivalent to a 10% increase/decrease in throughput. The hill-climber then seeks out the optimum x_{rxrB}^{SP} for the altered throughput. In Mode II, on the other hand, since V^{MAX} sets the throughput, the optimum x_{rxrB}^{SP} remains fixed at 0.218 and the hill-climber seeks it out via feedback. The maximum production rate thus remains constant at 133.7 kmol/h with F_B adjusting appropriately to compensate for the feed composition change.

2.6 Discussion

During the review process, it was pointed out that the column pressure may be an additional dof for further increasing the maximum achievable throughput (Mode II). Since the flooding boilup (V^{MAX}) is proportional to the vapor density (ρ) times the flooding velocity (u^{MAX}), we have at column pressures P_1 and P_2,

$$V_2^{MAX} = (\rho_2/\rho_1).(u_2^{MAX}/u_1^{MAX}).V_1^{MAX}$$

Assuming constant F factor at flooding ($\rho\ \mathrm{u}^{\mathrm{MAX}\ 0.5}$) we have

$$u_2^{MAX}/u_1^{MAX} = (\rho_1/\rho_2)^{0.5}$$

Therefore we get

$$V_2^{MAX} = (\rho_2/\rho_1)^{0.5}.V_1^{MAX}$$

Thus, if $P_2 < P_1$, we will have $\rho_2 < \rho_1$ so that $V_2^{MAX} < V_1^{MAX}$. In other words, the flooding boilup decreases with pressure. As the pressure is decreased, the relative volatility increases and the separation becomes easier so that the boilup for the same split decreases. If this decrease in boilup is greater than the decrease in V^{MAX} at lower pressures, the column pressure should be minimized so that the column is away from its flooding limit, which may then be exploited for further increase in throughput. However for the system studied, it turns out that the decrease in boilup due to improved relative volatility is only marginal and is much smaller than the decrease in V^{MAX} at lower pressures. There is then no incentive for minimum pressure column operation with the condenser duty valve fully open. Column operation at increased pressures is not considered as equipment are typically designed for a certain design pressure and sustained operation above the design pressure would normally not be allowed. At least for this system, column operation at design pressure is the recommended operation policy.

A note on proper tuning of the hill-climber is in order. One may argue that it be tuned as aggressively as possible for the quickest possible approach to the optimum. Aggressive tuning can however lead to a large limit cycle with the hill-climber overshooting the optimum and then back-tracking, repeatedly. Moreover, the hill-climber causes adjustments in a regulatory setpoint, which results in additional servo transients. In the plantwide control context, if these additional servo transients are too severe due to aggressive tuning, operating issues such as more severe and undesirable variability in the product quality, can result. Thus e.g., the higher maximum throughput using the hill-climber may come at the expense of poorer product quality control. The higher variability in the product quality (compared to constant setpoint operation with no hill-climber) may or may not be acceptable depending on the specific process. For example, many a times the final product quality guarantee to the customer is achieved via blending of different streams from a product-tank farm to achieve very specific quality targets. An aggressive hill-climber even to the extent of causing a small limit cycle may then be acceptable, since the plant product would anyway be blended to achieve specific quality targets for the customer. On the other hand, if the product is directly sold to the customer, the quality give-away due to the higher variability may negate the production/energy saving benefit. The point is that the tuning of the hill-climber must duly consider and respect the plantwide context of the specific process.

In this work, a one-dof hill-climber was sufficient, since the optimum was quite flat and insensitive with respect to the other unconstrained controlled variable (CV), L/F_{col}. It is possible that two or more unconstrained CVs require reoptimization with changes in operating conditions as the economic objective surface with respect to the CVs is not flat but much sharper. We then need a higher order hill-climber. The simplest approach is to use decentralized multiple one-dof hill-climbers. Alternatively, a multivariable MPC hill-climber may be applied for a faster approach to the optimum with smoother (not too severe) transients in the regulatory setpoints. In further research, we hope to evaluate higher order hill-climbers in economic plantwide control applications.

2.7 Conclusions

In conclusion, this work has demonstrated the design and dynamic evaluation of an economic plantwide control system that optimizes unconstrained regulatory setpoints via hill-climbing control for a simple recycle process. For the specific example, even as there are two unconstrained CVs, x_{rxrB} and L/F_{col}, economic incentive exists only for reoptimizing x_{rxrB} via feedback as the optimum is quite flat with respect to L/F_{col}. Closed loop results show that Shinskey's one-dof hill-climber effectively drives the process operation towards minimum energy consumption at given throughput (Mode I) and maximum achievable throughput (Mode II) for a given bottleneck constraint (V^{MAX}). Hill-climbing control causes the Mode I reboiler steam consumption to reduce by ~3.7% for a 25% throughput increase. Also, the Mode II maximum achievable throughput increases by ~3% compared to constant setpoint operation. Overall, these results demonstrate hill-climbing control to be a simple and effective tool for seeking and driving the economically important unconstrained regulatory setpoint(s) to the economic optimum steady state for realizing significant economic/sustainability benefit.

References

(1) Roth, P.; Georgiev, A.; Boudinov, H. Design and construction of a system for sun-tracking. *Renew Energ* 2004, 29, 393-402.

(2) Hensen, M. A.; Seborg, D. E. Adaptive non-linear control of a pH neutralization process. *IEEE T. Contr. Sys. T.* 1994, 2, 169-182.

(3) Shinskey, F. G. *Process Control Systems: Application, Design and Adjustment*. McGraw Hill, New York, 1967.

(4) Kanodia, R.; Kaistha, N. Plantwide control for throughput maximization: A case study. *Ind. Eng. Chem. Res.* 2010, 49, 210-221.

(5) Luyben, W.L. Snowball effects in reactor/separator processes with recycle. *Ind. Eng. Chem. Res.* 1994, 33, 299-305.

Chapter 3

Real Time Optimization of a Reactor-Separator-Recycle Process I: Steady State Modelling

This Chapter is based on the published paper “Real Time Optimization of a Reactor-Separator-Recycle Process I: Steady State Modelling” in Industrial Engineering and Chemistry Research, 2018, 57 (37), 12429-12443

In this Chapter, steady state real time optimization (RTO) of the reactor-separator-recycle process is studied. The reaction $A + B \rightarrow C$ occurs in the reactor with the separator recycling unreacted A and B and recovering nearly pure C bottoms product. Two operating scenarios, Mode I (fixed throughput) and Mode II (maximum throughput), are considered. In Mode I, the column boil-up is minimized using available degrees-of-freedom (dofs). In Mode II, the dofs are optimized for maximizing throughput. It is shown that the reactor B composition setpoint is unconstrained and economically dominant in both Mode I and Mode II. Its optimum value is efficiently obtained by fitting a simple reaction kinetic model to the available plant flow and reactor composition data (current and past) and adjusting the separator tray section efficiencies to best fit the current temperature profile. Results show that RTO improves economic benefit by up to 10% over constant setpoint operation.

3.1 Introduction

Proper adjustment of an economically important unconstrained controlled variable (CV) setpoint so that the steady state process operation is (near) optimal with respect to the setpoint is one of the key issues to be addressed in the economic plantwide control of integrated chemical processes. In direct optimization approaches, the optimum value of the unconstrained setpoint is sought by directly perturbing the unconstrained setpoint to estimate the gradient of the economic objective and applying feedback to drive the estimate to zero (extremum seeking or hill-climbing control[1-2]). The perturbation must be large enough to reliably estimate the gradient, unconfounded by plant noise/disturbances. A major criticism of the approach is that disturbances can easily confuse it to move the setpoint away from optimum.

Instead of perturbing the plant to estimate gradients, a steady state plant model may be fitted to recent plant data and the fitted model optimized with respect to the unconstrained setpoint, which then is updated to the regulatory layer. This fit-optimize-update real-time optimization (RTO)[3] cycle is repeated after the plant settles at the new operating condition. RTO is appealing in that deliberate plant perturbation is avoided. The optimum however is only as good as the model and for large plant-model mismatch, may differ significantly from the actual optimum. Model fidelity[4] and adequacy[5] considerations for convergence of the model optimum to (near) the actual optimum are then crucial. Naturally, significant effort is necessary to ensure that the model properly accounts for the principal phenomena that affect the plant economics. Process understanding and insights then are key to successful RTO applications.

In the literature, several RTO applications have been reported. Many of these are on stand-alone units (see e.g.[6-8]) while others, apply RTO to integrated chemical plants (see e.g.[9-12]). Given the unique non-linear characteristics of each process, each application develops and evaluates customized modelling and optimization algorithms. Here, we develop and evaluate RTO for the benchmark $A + B \rightarrow C$ reactor-separator-recycle process[13-14]. The novel contribution of the work is in (a) the specific approach for updating model parameters using steady state plant material balances; and (b) quantitative evaluation of the role of reaction kinetics and column model on the RTO benefit.

In the following, the plantwide process module and its base-case design are first described. Two common plant operating modes are then considered. In Mode I, the throughput is below maximum and the RTO must optimize the unconstrained setpoint(s) to minimize the reboiler steam consumption. In Mode II, the unconstrained setpoint(s) is adjusted to maximize throughput subject to column flooding as the bottleneck constraint limiting production. An appropriate process model and parameter fitting technique that converges to near the actual plant optimum is then developed. Three distinct reaction kinetic models and distillation column models are explored. Quantitative results are then presented on the economic benefit of RTO using the different models for common disturbances. The article ends with a summary of the main findings.

3.2 Plantwide Process Module

The reactor-separator-recycle process shown in Figure 1.8 is studied here. The salient base-case process operating conditions are noted in the Table 3.1. The process produces C via the irreversible exothermic addition of A to B as $A + B \rightarrow C$. Fresh A and fresh B are mixed with the recycle stream and sent to a CSTR. The reactor effluent is distilled to obtain near pure C product as the bottoms with unreacted A and B leaving as distillate, which is recycled to the CSTR. Aspen Hysys is used for steady state and dynamic process modelling. The hypothetical component properties are as in Table 3.2. The SRK equation of state is used for thermodynamic property modelling. The Langmuir-Hinshelwood reaction rate kinetic parameters are as in Table 3.2. For a more realistic distillation column, a Murphree tray efficiency (η) curve is imposed with η nominally varying with respect to the vapour rate into the tray as in Figure 3.1.

Table 3.1 The salient base-case process operating conditions

Material Streams	**Temperature (°C)**	**Molar Flow (kmol/h)**	x_A	x_B	x_C
F_A	26	99	1	0	0
F_B	26	100	0	1	0
F_{rxr}	58.2	365.8	0.522	0.473	0.005
F_{col}	110	266.8	0.345	0.278	0.377
R	92	166.8	0.55	0.44	0.01
P	137	100	0.0	0.01	0.99
L	92	394.9	0.55	0.44	0.01
Other Variables					
No. of Trays	33				
Feed tray	15				
Pr_{cnd}	140 kPa				
U_{rxr}	6 m^3				
T_{rxr}	110 °C				
Q_{rxr}	176.2 kW				
Q_{cnd}	4760 kW				
Q_{reb}	4826 kW				

See Figure 1.8 and Nomenclature for variable descriptions

Table 3.2. Modeling details of recycle process

Kinetics	$A+B \rightarrow C$	$r = k.x_{rxrA}.x_{rxrB}/(1+K.x_{rxrA})$ $k = 2.7\times10^8.\exp(-70000/RT)$ $K = 2.2\times10^4.\exp(-30000/RT)$
Hypotheticals[#]	MW	NBP(°C)
A	50	70
B	80	100
C	130	120
VLE	Soave-Redlich-Kwong	

Reaction rate units: $kmol.m^{-3}.s^{-1}$

#: Aspen Hysys hydrocarbon estimation procedure used to estimate parameters for thermodynamic property calculations

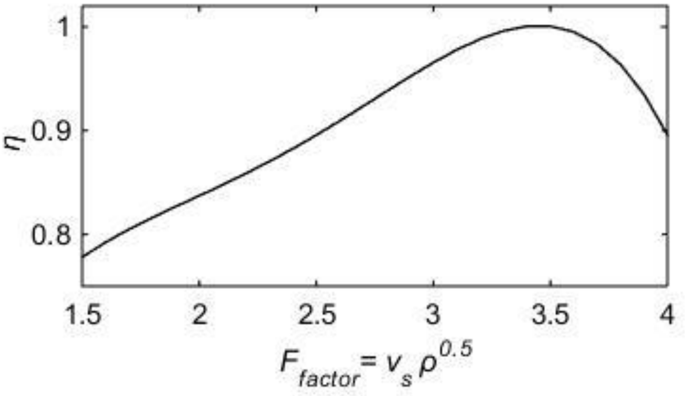

Figure 3.1. Variation of plant column tray efficiency (η) with F_{factor}

3.2.1 Economic Optimum Steady State Operation

The process has 6 steady state degrees of freedom (dofs), two corresponding to the fresh feeds, two for the reactor (hold-up and temperature) and two for the column. Convenient steady state plant specifications corresponding to the six dofs used here are the fresh *B* feed rate (F_B), reactor temperature (T_{rxr}) and hold-up (U_{rxr}), *C* mol fraction in the recycled distillate x_C^R, product *C* purity x_C^P and the reactor feed *A/B* mol ratio, ($[A/B]_{Frxr}$). Let $\mathbf{s}$ = [F_B, T_{rxr}, U_{rxr}, x_C^R, x_C^P $[A/B]_{Frxr}$] represent the plant specification variables. For a chosen value $\mathbf{s} = \mathbf{s_0}$, the converged plant material and energy flows are obtained by solving the Aspen Hysys plant, represented here by the square set of non-linear equations $\boldsymbol{g(x, s_0) = 0}$, where $\boldsymbol{x}$ represents the plant internal state variables.

The specifications are to be adjusted for economic optimum steady process operation for two commonly encountered modes of operation. In Mode I, the process throughput (F_B) is fixed e.g. by market demand-supply considerations and the remaining five specifications are to be adjusted to minimize column boilup, *V*, for minimum steam consumption. In Mode II, the market conditions are extremely favourable and all the available six specifications are to be used for maximizing throughput (F_B). The optimization is subject to process inequality constraints such as maximum/minimum process flows, temperatures, product quality etc. These constraint variables are a function of the converged plant state, $\boldsymbol{x}$, so that all the described inequality constraints may be conveniently represented as $\boldsymbol{c(x, s) \leq 0}$. Specifically, we constrain maximum feasible material flows (F_i; i indexes all material streams) and energy flows (Q_j; j indexes all energy streams) to twice the base-case flows in Table 3.1 so that $0 \leq F_i \leq F_i^{MAX}$ and $0 \leq Q_j \leq Q_j^{MAX}$, respectively. We also have constraints on the maximum reactor temperature (T_{rxr}^{MAX} = 110 °C), maximum column boil-up (V^{MAX} = 800 kmol/h), minimum product C mol fraction ($x_C^{P,MIN}$ = 99 mol%) and distillate maximum C mol fraction leakage ($x_C^{R,MAX}$ = 1 mol%). The need for the former 3 constraints is self-evident. The last constraint reflects the often encountered practical consideration of not letting too much heavy product into the recycle to mitigate e.g. catalyst deactivation or equipment fouling.

Given this background, the plant Mode II constrained optimization is conveniently stated as

$$\text{minimize}_{\mathbf{s}}\ (-F_B)$$

subject to the converged plant equality constraints

$$\boldsymbol{g(x, s) = 0}$$

and the process inequality constraints

$$\boldsymbol{c(x, s) \leq 0}$$

In Mode I, since F_B is specified, the optimization decision variable $\boldsymbol{d} = \boldsymbol{s}(2\ to\ 6)$ (excludes F_B) and the optimization problem is

$$\text{minimize}_{\mathbf{d}}\ (V)$$

subject to the converged plant and specified throughput equality constraints

$$\boldsymbol{g(x, s) = 0} \qquad F_B = F_{B,spec}$$

as well as the process inequality constraints

$$\boldsymbol{c(x, s) \leq 0}$$

The Mode I / Mode II constrained steady state plant optimization is performed using the Matlab function *fmincon* with Aspen Hysys as the background steady state solver. The results of the constrained optimization are summarized in Table 3.3. Note that Mode I optimization results are reported for two specified throughput values, F_B = 100 kmol/h and F_B = 120 kmol/h. For both throughputs, T_{rxr}^{MAX}, U_{rxr}^{MAX} (maximum reactor level), $x_C^{P,MIN}$ and $x_C^{R,MAX}$ constraints are active. The four active constraints and given throughput specification leave one unconstrained steady state dof (6 dofs – 4 active constraints – 1 specification = 1 unconstrained dof). In Mode II, the V^{MAX} constraint is additionally active with throughput being a dependent (calculated) variable. This again leaves one unconstrained steady state dof (6 dofs – 5 active constraints = 1 unconstrained dof).

We note that even as the actual plant has been optimized above, one expects the same set of constraints to be active when optimizing a plant model that well fits the available plant data. Assuming regulatory layer pairings that achieve tight active constraint control, the RTO must seek optimum values for regulatory layer controlled variables (CVs) corresponding to any remaining unconstrained dofs. In this example, we have T_{rxr}^{MAX}, U_{rxr}^{MAX} (maximum reactor level), $x_C^{P,MIN}$ and $x_C^{R,MAX}$ as the active constraints common to both Mode I and Mode II. These four active constraints fix the setpoints on the control loops corresponding to the four steady state dofs for the reactor and the column. This leaves the two dofs corresponding to the two fresh feeds. Of these, one dof gets used to fix throughput at the desired value in Mode I. In Mode II, instead of the throughput specification, the V^{MAX} constraint becomes active, which indirectly fixes the throughput to the maximum achievable. Thus in both Mode I and Mode II, the dof corresponding to the second feed remains unconstrained. This dof must get used to bring in the second feed as a make-up stream for perfect stoichiometric feed balancing (overall plant material balance closure). One of the most common stoichiometric feed balancing strategies is maintaining the mol fraction of a reactant (*A* or *B*) in the CSTR by manipulating the corresponding fresh feed ratio setpoint[15]. Without loss of generality, assume that the reactor *B* mol fraction (x_{rxrB}) is maintained by manipulating the fresh *B* to fresh *A* feed ratio. We then have the reactor composition loop setpoint (x_{rxrB}^{SP}) as the decision variable corresponding to the one unconstrained dof in both Mode I and Mode II. It then follows that the RTO must drive x_{rxrB}^{SP} to its optimum in both Mode I and Mode II.

3.3 Steady State RTO Modelling

Before delving into the RTO modelling details, a brief note on the nomenclature is in order. When no subscript is used, the symbol denotes the actual PV in the plant (e.g. *R* denotes the plant recycle mol flow rate). The use of a component subscript (*A*, *B* or *C*) on a material stream symbol denotes the corresponding component mol flow rate (e.g. R_A denotes *A* component mol flow rate in the plant recycle). Mol fraction of a component (e.g. *B*) in a particular stream (e.g. product stream, *P*) is denoted by the symbol '*x*' with the particular component as subscript and particular stream as superscript (e.g. x_B^P). Other process variables use self explanatory symbols, e.g. T_{rxr} denotes reactor temperature etc. Further, the superscript '*' is used on a PV symbol to explicitly highlight that a plant measurement is available for the PV (e.g. $\boldsymbol{T_{col}}^*$ denotes the array of column tray temperature measurements). In case a PV is calculated using plant balances in conjunction with a model, the superscript '*e*' is added to the PV symbol to explicitly highlight the PV is estimated. The superscript '*m*' on a PV symbol is used to explicitly indicate that it refers to the plant model and not the actual plant. The reader is referred to the nomenclature for clarity on the symbols used here.

The Mode I RTO problem is to adjust the unconstrained setpoint x_{rxrB}^{SP} to minimize the column boil-up, *V*. In Mode II, x_{rxrB}^{SP} is to be adjusted to maximize F_B with the maximum column boil-up, V^{MAX}, as the bottleneck capacity constraint. Note that the limit V^{MAX} is not known in practice and can vary with time. Further, *V* itself is seldom measured and must be estimated.

Table 3.3. Plant Optimization Summary

PV	Mode I Min (V)		Mode II Min ($-F_B$)
F_B (kmol/h)	100^*	120^*	127.2
U_{rxr} (m^3)	6_{max}	6_{max}	6_{max}
T_{rxr} (^{o}C)	110_{max}	110_{max}	110_{max}
x_{rxrB}	0.278^{**}	0.337^{**}	0.358^{**}
x_C^R	0.01_{max}	0.01_{max}	0.01_{max}
x_C^P	0.99_{min}	0.99_{min}	0.99_{min}
$V^\#$ (kmol/h)	531.6	719.1	800_{max}

*Specified; **: Unconstrained optimum; # calculated (not a decision variable)

Physically speaking, the column boil-up prevents B leakage down the bottoms and sends all of the unreacted A and B up the top for recycle to the reactor. The cause-and-effect relationships relating a change in x_{rxrB}^{SP} to column boil-up are as follows. At given T_{rxr}, U_{rxr} (reactor hold-up) and fixed F_B (production) (Mode I), changing x_{rxrB}^{SP} changes the steady state recycle rate required to close the overall plant material balance. The column boil-up also correspondingly changes. In Mode II, x_{rxrB}^{SP} is changed so that the boil-up reduces allowing a throughput to push the boil-up to the bottleneck constraint, V^{MAX}. Since the boil-up is seldom measured, the RTO model must estimate of the same in both Mode I (optimized objective) and Mode II (bottleneck constraint).

The RTO plant model consists of a model reactor and a model column connected as in the actual plant. Here we use a standard CSTR model with alternative parameter adjustable reaction kinetic models and a standard ideal VLE column model with adjustable Murphree stage efficiency for the stripping section and the rectifying section. The unknown parameters for the model reactor and the model column are estimated from the available recent plant data. The model itself requires a good estimate of the input stream state. Usually stream temperature and pressure can be reliably inferred from available routine process instrumentation. This leaves the stream component flow rates to be reliably estimated for fully fixing a stream state. In the absence of direct measurements, appropriate plant material balances must be performed for this estimation. Given material stream component flows (measured or estimated), the model parameters may be appropriately adjusted to best fit the most recent plant data. Post parameter estimation, the fitted model is optimized with respect to x_{rxrB} to obtain its optimum value for implementation in the plant. There are thus four main components to the entire RTO exercise, namely, (a) Estimation of plant stream component flows; (b) Estimation of model reaction kinetic parameters; (c) Estimation of column model parameters; and finally (d) Fitted model optimization. Each of these aspects is now elaborated upon.

3.3.1 Estimation of Material Stream Component Flows

Available plant measurements are used to estimate the material stream component flows using appropriate unit or plantwide material balances. Particularly note the availability of accurate measurements of the product rate (P^*), its B impurity (x_B^{P*}), the recycle rate (R^*) and the reactor B mol fraction (x_{rxrB}^*). Further the column tray temperatures ($\boldsymbol{T_{col}}^*$), reflux rate (L^*), reactor and column feed temperatures (T_{Frxr}^* and T_{Fcol}^*), reactor pressure (Pr_{rxr}^*), column condenser pressure (Pr_{cnd}^*) and column pressure drop (ΔPr_{col}^*) are measured. We first consider the simpler case of a measured recycle stream C impurity mol fraction (x_C^{R*}).

Assuming steady plant operation and negligible A leakage in the product stream ($x_A^P = 0$), an overall plant material balance estimates the fresh feed stream rates as

$$F_A^e = P^* (1 - x_B^{P*}) \qquad 1(a)$$

$$F_B^e = P^* \qquad 1(b)$$

A column component balance estimates the reactor effluent component rates, E_i^e ($i = A, B, C$) as

$$E_A^e = R_A^e \qquad 2(a)$$

$$E_B^e = R_B^e + P^* x_B^{P*} \qquad 2(b)$$

$$E_C^e = R^* x_C^{R\,*} + P^* \left(1 - x_B^{P*}\right) \tag{2(c)}$$

We also have
$$R^* = R_A^e + R_B^e + R^*\, x_C^{R\,*} \tag{3(a)}$$

and
$$x_{rxrB}^{\;*} = E_B^e/(E_A^e + E_B^e + E_C^e) \tag{3(b)}$$

Combining Equation 3(b) with Equation 2, we get

$$x_{rxrB}^{\;*} = (R_B^e + P^* x_B^{P*})/(R_A^e + R_B^e + R^* x_C^{R\,*} + P^*) \tag{3(c)}$$

Simultaneous solution of Equation 3(a) and Equation 3(c) provides the estimates R_A^e and R_B^e, as

$$R_A^e = R^* - x_{rxrB}^{\;*}\,(R^* + P^*) + P^* x_B^{P*} - R^* x_C^{R\,*} \tag{4(a)}$$

$$R_B^e = x_{rxrB}^{\;*}\,(R^* + P^*) - P^* x_B^{P*} \tag{4(b)}$$

Further, we have
$$R_C^e = R^* x_C^{R\,*} \tag{4(c)}$$

All material stream component flows in the plant are thus known (measured or estimated).

For the case where x_C^R is not measured, a simple procedure requiring iterative solution of the column model (described later) gives a reasonable estimate, $x_C^{R,e}$. Initially, $x_C^{R,e}$ is guessed to a small value ($x_C^{R,e}$ = 0.5 to 2 mol%) and R_B^e and R_A^e are obtained from Equation 4 with x_C^{R*} replaced by $x_C^{R,e}$. Equation 2 then fixes the feed component flows to the column. The model column is then converged with x_B^{P*} and the measured reflux rate (L^*) as the two specification variables. When converging the model column, one may also choose to adjust the tray section efficiencies, η_R and η_S, to best match the measured column temperature profile, $\boldsymbol{T_{col}}^{*}$. The converged column model gives a revised estimate of $x_C^{R,e}$ and the calculation cycle is repeated to refine $x_C^{R,e}$ till the change in $x_C^{R,e}$ from one iteration to the next becomes negligible, indicating convergence. Equations 1-4 for the converged $x_C^{R,e}$ give estimates of the plant stream component flows.

3.3.2 Estimation of Reaction Kinetic Model Parameters

The standard CSTR model[16] is used with three of the simplest kinetic models as below:

Kinetic Model I (KM I): $r^m = k^m x_{rxrA} x_{rxrB}$

Kinetic Model II (KM II): $r^m = k^m x_{rxrA}^{\alpha} x_{rxrB}$

Kinetic Model III (KM III): $r^m = k^m x_{rxrA}^{\alpha} x_{rxrB}^{\beta}$

Given that the actual plant reaction rate expression is

$$r = \frac{k x_{rxrA} x_{rxrB}}{1 + K x_{rxrA}}$$

with the Kx_{rxrA} term in the denominator being of the order of 1, there is an inherent plant-model mismatch in the reaction kinetics. KM I, KM II and KM III have, respectively, 1 (k^m), 2 (k^m, α) and 3 (k^m, α, β) unknown parameters. For known reactor feed and effluent component flow estimates for the current and if necessary, previous steady states, the unknown kinetic parameters are adjusted to ensure the model reactor product *C* generation rate matches the difference between the estimated reactor effluent and feed *C* rate. This difference must equal the *C* product rate so that at steady state

$$r^m . U_{rxr}^* = P^*.(1 - x_B^{P*}) \qquad 5(a)$$

We use $U_{rxr}^* = U_{rxr}^{MAX}$ at a steady state assuming optimal operation since maximizing hold up minimizes the unreacted reactant recycle load and is therefore always optimal. The model specific reaction rate r^m depends on the estimated reactor *A* and *B* mol fractions, x_{rxrA}^e and x_{rxrB}^e, easily obtained from the estimated reactor effluent component flows as

$$x_{rxrA}^e = E_A^e/(E_A^e + E_B^e + E_C^e) \qquad 5(b)$$

$$x_{rxrB}^e = E_B^e/(E_A^e + E_B^e + E_C^e) = x_{rxrB}^* \qquad 5(c)$$

In KM I, since there is only one unknown parameter (rate constant k^m) application of Equation 5(a) to the current steady state (subscript '*0*') estimates it as

$$k^{m,e} = P^* \, (1 - x_B{}^{P*})/(x_{rxrA}{}^e \, x_{rxrB}{}^e \, U_{rxr}{}^{MAX}) \tag{6(a)}$$

In KM II, k^m and α, are the two unknown reaction kinetic parameters. Plant data for two most recent steady states, the current steady state (subscript *0*) and the previous steady state (subscript *1*), are then used. Applying Equation 5(a) for both these steady states,

$$k^m \, (x_{rxrA}{}^e{}_0)^\alpha \, (x_{rxrB}{}^e{}_0) \, U_{rxr}{}^{MAX}{}_0 = P^*{}_0 \, (1 - x_B{}^{P*}{}_0)$$

$$k^m \, (x_{rxrA}{}^e{}_1)^\alpha \, (x_{rxrB}{}^e{}_1) \, U_{rxr}{}^{MAX}{}_1 = P^*{}_1 \, (1 - x_B{}^{P*}{}_1)$$

Simultaneous solution provides estimates of the unknown parameters $k^{m,e}$ and α^e for KM II as

$$\alpha^e = \frac{\log\left\{\frac{\left(P_0^*\left(1-x_{B\,0}^{P^*}\right)\left(U_{rxr}{}^{MAX}{}_1\right)\left(x_{rxrB}{}^e{}_1\right)\right)}{\left(P_1^*\left(1-x_{B\,1}^{P^*}\right)\left(U_{rxr}{}^{MAX}{}_0\right)\left(x_{rxrB}{}^e{}_0\right)\right)}\right\}}{\log\left(\frac{x_{rxrA}{}^e{}_0}{x_{rxrA}{}^e{}_1}\right)} \tag{7(a)}$$

$$k^{m,e} = \frac{P_0^*\left(1-x_{B\,0}^{P^*}\right)}{U_{rxr}{}^{MAX}{}_0\left(x_{rxrB}{}^e{}_0\right)\left(x_{rxrA}{}^e{}_0\right)^{\alpha^e}} \tag{7(b)}$$

Note that it is possible to use more than 2 steady states to obtain more robust estimates $k^{m,e}$ and α^e. A simple method for doing the same is described later in the "Discussion" section.

In KM III, k^m, α and β are the three unknown reaction kinetic parameters so that data for three most recent steady states, is needed. The overall material balance for the three latest steady states (subscripts '*0*' for current, '*1*' for previous and '*2*' for one before previous) requires that

$$k^m \, (x_{rxrA}{}^e{}_0)^\alpha \, (x_{rxrB}{}^e{}_0)^\beta \, U_{rxr}{}^{MAX}{}_0 = P^*{}_0 \, (1 - x_B{}^{P*}{}_0)$$

$$k^m \, (x_{rxrA}{}^e{}_1)^\alpha \, (x_{rxrB}{}^e{}_1)^\beta \, U_{rxr}{}^{MAX}{}_1 = P^*{}_1 \, (1 - x_B{}^{P*}{}_1)$$

$$k^m \, (x_{rxrA}{}^e{}_2)^\alpha \, (x_{rxrB}{}^e{}_2)^\beta \, U_{rxr}{}^{MAX}{}_2 = P^*{}_2 \, (1 - x_B{}^{P*}{}_2)$$

For the case where $P^*_0 = P^*_1 = P^*_2$ i.e. production rate is the same at all the three steady states (this is possible in Mode I operation), we get an indeterminate system of equations and k^m, α and β cannot be uniquely determined. We therefore adjust k^m, α and β to minimize the squared sum of the difference between the LHS and RHS of the plantwide material balances above. For the case where any one of the steady state production rates are different (this is usually the case in Mode II operation), one can show that the simultaneous solution of the above equations provides estimates of $k^{m,e}$, α^e, and β^e for KM III as

$$\alpha^e = \frac{\log\left\{\frac{P_0^*\left(1-x_{B\,0}^{P^*}\right)\, {U_{rxr}^{MAX}}_1}{P_1^*\left(1-x_{B\,1}^{P^*}\right)\, {U_{rxr}^{MAX}}_0}\right\}\log\left(\frac{{x_{rxrB}^e}_0}{{x_{rxrB}^e}_2}\right)-\log\left\{\frac{P_0^*\left(1-x_{B\,0}^{P^*}\right)\, {U_{rxr}^{MAX}}_2}{P_2^*\left(1-x_{B\,2}^{P^*}\right)\, {U_{rxr}^{MAX}}_0}\right\}\log\left(\frac{{x_{rxrB}^e}_0}{{x_{rxrB}^e}_1}\right)}{\log\left(\frac{{x_{rxrA}^e}_0}{{x_{rxrA}^e}_1}\right)\log\left(\frac{{x_{rxrB}^e}_0}{{x_{rxrB}^e}_2}\right)-\log\left(\frac{{x_{rxrA}^e}_0}{{x_{rxrA}^e}_2}\right)\log\left(\frac{{x_{rxrB}^e}_0}{{x_{rxrB}^e}_1}\right)} \qquad 8(a)$$

$$\beta^e = \frac{\log\left\{\frac{P_0^*\left(1-x_{B\,0}^{P^*}\right)\, {U_{rxr}^{MAX}}_1}{P_1^*\left(1-x_{B\,1}^{P^*}\right)\, {U_{rxr}^{MAX}}_0}\right\}\log\left(\frac{{x_{rxrA}^e}_0}{{x_{rxrA}^e}_2}\right)-\log\left\{\frac{P_0^*\left(1-x_{B\,0}^{P^*}\right)\, {U_{rxr}^{MAX}}_2}{P_2^*\left(1-x_{B\,2}^{P^*}\right)\, {U_{rxr}^{MAX}}_0}\right\}\log\left(\frac{[{x_{rxrA}^e}_0}{{x_{rxrA}^e}_1}\right)}{\log\left(\frac{{x_{rxrA}^e}_0}{{x_{rxrA}^e}_2}\right)\log\left(\frac{{x_{rxrB}^e}_0}{{x_{rxrB}^e}_1}\right)-\log\left(\frac{{x_{rxrA}^e}_0}{{x_{rxrA}^e}_1}\right)\log\left(\frac{{x_{rxrB}^e}_0}{{x_{rxrB}^e}_2}\right)} \qquad 8(b)$$

$$k^{m,e} = \frac{P_0^*\left(1-x_{B\,0}^{P^*}\right)}{{U_{rxr}^{MAX}}_0\left({x_{rxrA}^e}_0\right)^{\alpha^e}\left({x_{rxrB}^e}_0\right)^{\beta^e}} \qquad 8(c)$$

In this way, the unknown parameters are estimated for KM I, KM II and KM III.

3.3.3 Estimation of Column Model Parameters

The standard Aspen Hysys column model with ideal liquid and vapor phases is applied here. This is a standard equilibrium stage model with a Murphree tray efficiency which is described in detail in textbooks[17] and therefore not repeated here for brevity. The standard Murphree tray efficiency definition based on the vapour composition is used[34]. We consider three model variants - (a) All trays are ideal ($\eta_i = 1$ for all i); (b) All trays have a constant non-ideal stage efficiency ($\eta_i \leq 1$ for all i); and (c) The rectifying and stripping section trays have separate non-ideal stage efficiencies, η_R and η_S, respectively ($\eta_R \leq 1$ and $\eta_S \leq 1$). The modelling is described for variant (c) here, since variants (a) and (b) are simplifications to variant (c). Note that mismatch occurs between the column model and the actual plant column since the column uses the SRK equation of state whereas the ideal solution is used in the model. Further, the actual plant column uses flow dependent Murphree stage efficiency for each tray, as shown in Figure 3.1. Thus, at any given plant steady state, the efficiency of the trays in the column varies over a range, e.g. 0.75 – 0.90. In contrast, all stripping and rectifying trays use a constant tray efficiency ($\eta_S \leq 1$ and $\eta_R \leq 1$).

The model column is simulated as follows. The measured column condenser pressure (Pr_{cnd}^*) and the column pressure drop (ΔPr_{col}^*) fixes the model column tray section pressure profile via linear interpolation. The column feed component flowrates are taken as E_i^e (i = A, B, C). The feed temperature is fixed at the measured column feed temperature (T_{Fcol}^*) and its pressure is fixed at interpolated feed tray pressure. The column feed state is thus fully specified. For the case when x_C^R is accurately measured, the simple column model is converged for the measured C leakage up the top (x_C^{R*}) and the measured B impurity down the bottoms (x_B^{P*}) as the two specifications. The converged column model gives the estimated column temperature profile ($\boldsymbol{T_{col}}^e$). Since the plant column temperature profile is measured ($\boldsymbol{T_{col}}^*$), we adjust the rectifying section Murphree tray efficiency (η_R) and the stripping section Murphree tray efficiency (η_S) to best fit the predicted rectifying and stripping section temperature profiles, respectively, to the corresponding plant temperature profiles. This provides the best fitted estimates, η_R^e and η_S^e. The temperature profile fitted converged column model provides an estimate of the column boil-up, V^e. For greater clarity, Figure 3.2(a) shows the step-by-step algorithm for obtaining V^e when $x_C^R = x_C^{R*}$.

For the case where x_C^R is not known, the simple iterative procedure of refining the $x_C^{R,e}$ guess by repeatedly converging the column model for the column feed state estimated from material balances with L^* and x_B^{P*} as the specifications has been described previously. The column boil-up at convergence ($x_C^{R,e}$ guess stops changing between iterations) is then taken as the model estimated boil-up, V^e. For clarity, Figure 3.2(b) shows the step-by-step algorithm.

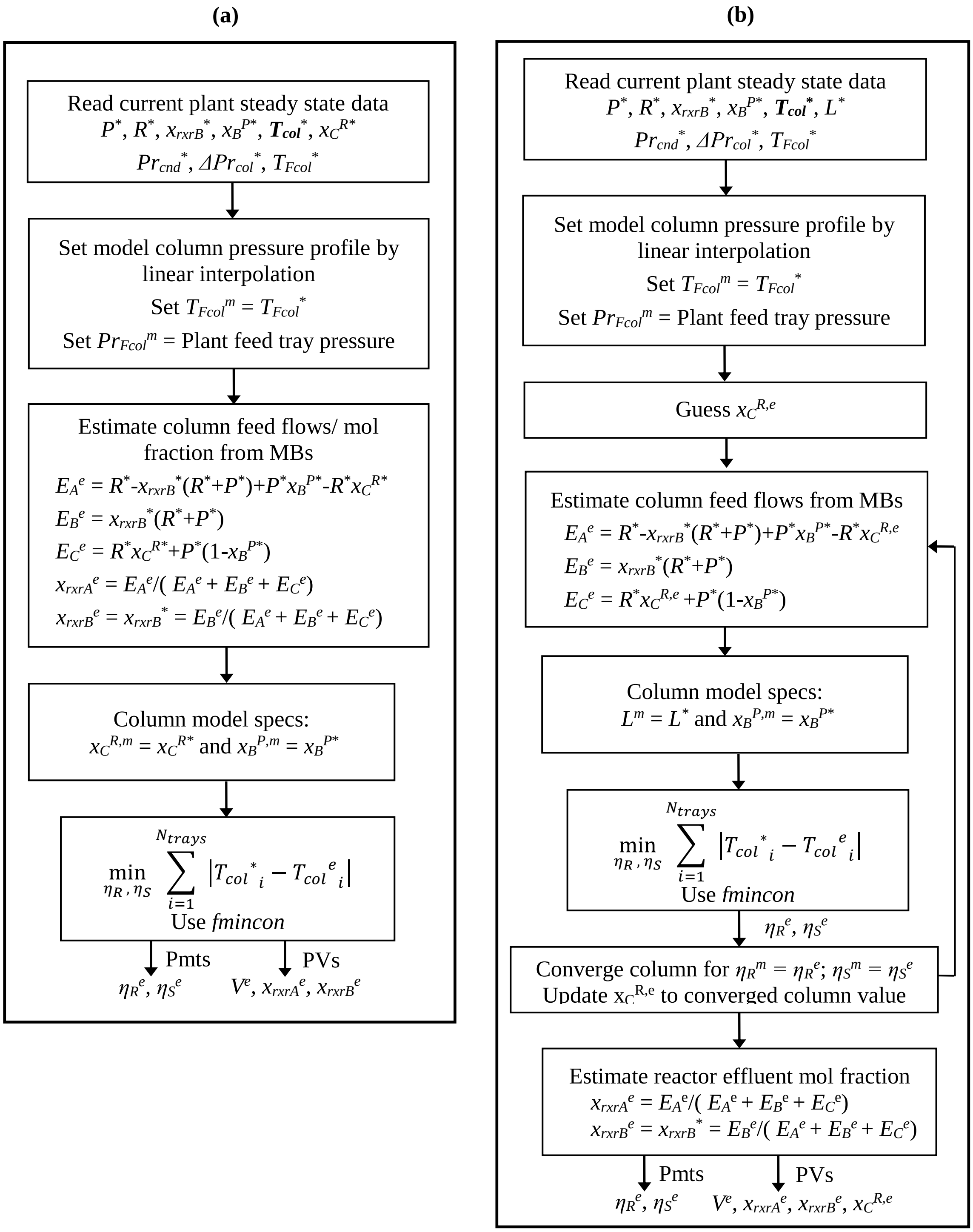

(a)
Read current plant steady state data
$P^*, R^*, x_{rxrB}^*, x_B^{P*}, \boldsymbol{T_{col}}^*, x_C^{R*}$
$Pr_{cnd}^*, \Delta Pr_{col}^*, T_{Fcol}^*$
Set model column pressure profile by linear interpolation
Set $T_{Fcol}^m = T_{Fcol}^*$
Set Pr_{Fcol}^m = Plant feed tray pressure
Estimate column feed flows/ mol fraction from MBs
$E_A^e = R^* - x_{rxrB}^*(R^*+P^*)+P^*x_B^{P*}-R^*x_C^{R*}$
$E_B^e = x_{rxrB}^*(R^*+P^*)$
$E_C^e = R^*x_C^{R*}+P^*(1-x_B^{P*})$
$x_{rxrA}^e = E_A^e/(E_A^e + E_B^e + E_C^e)$
$x_{rxrB}^e = x_{rxrB}^* = E_B^e/(E_A^e + E_B^e + E_C^e)$
Column model specs:
$x_C^{R,m} = x_C^{R*}$ and $x_B^{P,m} = x_B^{P*}$
$\min_{\eta_R,\eta_S} \sum_{i=1}^{N_{trays}} \left|T_{col}{}^*{}_i - T_{col}{}^e{}_i\right|$
Use *fmincon*
Pmts
η_R^e, η_S^e
PVs
$V^e, x_{rxrA}^e, x_{rxrB}^e$
(b)
Read current plant steady state data
$P^*, R^*, x_{rxrB}^*, x_B^{P*}, \boldsymbol{T_{col}}^*, L^*$
$Pr_{cnd}^*, \Delta Pr_{col}^*, T_{Fcol}^*$
Set model column pressure profile by linear interpolation
Set $T_{Fcol}^m = T_{Fcol}^*$
Set Pr_{Fcol}^m = Plant feed tray pressure
Guess $x_C^{R,e}$
Estimate column feed flows from MBs
$E_A^e = R^* - x_{rxrB}^*(R^*+P^*)+P^*x_B^{P*}-R^*x_C^{R,e}$
$E_B^e = x_{rxrB}^*(R^*+P^*)$
$E_C^e = R^*x_C^{R,e}+P^*(1-x_B^{P*})$
Column model specs:
$L^m = L^*$ and $x_B^{P,m} = x_B^{P*}$
$\min_{\eta_R,\eta_S} \sum_{i=1}^{N_{trays}} \left|T_{col}{}^*{}_i - T_{col}{}^e{}_i\right|$
Use *fmincon*
η_R^e, η_S^e
Converge column for $\eta_R^m = \eta_R^e$; $\eta_S^m = \eta_S^e$
Update $x_C^{R,e}$ to converged column value
Estimate reactor effluent mol fraction
$x_{rxrA}^e = E_A^e/(E_A^e + E_B^e + E_C^e)$
$x_{rxrB}^e = x_{rxrB}^* = E_B^e/(E_A^e + E_B^e + E_C^e)$
Pmts
η_R^e, η_S^e
PVs
$V^e, x_{rxrA}^e, x_{rxrB}^e, x_C^{R,e}$

Figure 3.2. Column model fitting (a) x_C^R measured (b) x_C^R unmeasured

3.3.4 Fitted Model Optimization

The plant steady state model with the estimated kinetic parameters and column tray section efficiencies η_R^e and η_S^e (if applicable) is optimized for Mode I or Mode II operation with x_{rxrB}^m as the decision variable. The Matlab NLP constrained optimizer *fmincon* is used here with Hysys as the back ground steady state solver for the plant / model with Matlab – Hysys data exchange. The active-set algorithm applying forward finite difference for gradient/Hessian estimation is applied. Since the J vs x_{rxrB} curve is quite flat near the optimum, a tight convergence tolerance (10^{-4}) is used for a close approach to optimum. The Hysys steady state model uses F_{rxrA}^m and reactor feed B to A ratio, $[B/A]_{Frxr}^m$, as the two specifications corresponding to the two fresh feeds. In Mode I, F_{rxrA}^m is adjusted to hold the throughput, $F_B^m = P^*$. On the other hand, in Mode II, F_{rxrA}^m gets adjusted to hold the model column boil-up $V^m = V^e$, where V^e is the boil-up estimate for the current steady state. A Newton-Raphson Matlab loop is used to converge this adjustment. Note that for the plant column operating at its flooding limit (Mode II), the estimated boil-up at the current steady state, V^e, is a good estimate of V^{MAX}, the bottleneck constraint. For a particular value of F_{rxrA}^m, the other specification, $[B/A]_{Frxr}^m$, fixes the total B going into the reactor as

$$F_{rxrB}^m = F_{rxrA}^m \;.\; [B/A]_{Frxr}^m$$

The two specifications for the reactor are $T_{rxr}^m = T_{rxr}^*$ and $U_{rxr}^m = U_{rxr}^* = U_{rxr}^{MAX}$. Finally on the column, the model specifications are $x_B^{P,m} = x_B^{P*}$ and $x_C^{R,m} = x_C^{R*}$ or $x_C^{R,e}$. The latter assumes that reflux is adjusted to ensure the C impurity in the recycle stream is kept small, possibly using a temperature control loop. Further, the model tray efficiencies are kept fixed at the fitted estimates, i.e., $\eta_R^m = \eta_R^e$ and $\eta_S^m = \eta_S^e$. With these plant model specifications, optimum value of the decision variable $[B/A]_{Frxr}^{m,opt}$ is sought using *fmincon*. The model optimum reactor B mol fraction, $x_{rxrB}^{m,opt}$ is obtained from the optimum steady state to which the optimizer converges (see Figure 3.3). This fitted model optimum is implemented in the plant post smoothing to avoid large changes in x_{rxrB}^{SP} as

$$x_{rxrB}^{SP,new} = a\, x_{rxrB}^{SP,curr} + (1-a)\, x_{rxrB}^{m,opt}$$

where $x_{rxrB}^{SP,curr}$ is the current reactor *B* mol fraction setpoint. The fit-optimize-update cycle is then repeated again after the plant settles at the new steady state corresponding to $x_{rxrB}^{SP,new}$. The major steps of the entire RTO cycle for the reactor-separator-recycle process are shown in Figure 3.4.

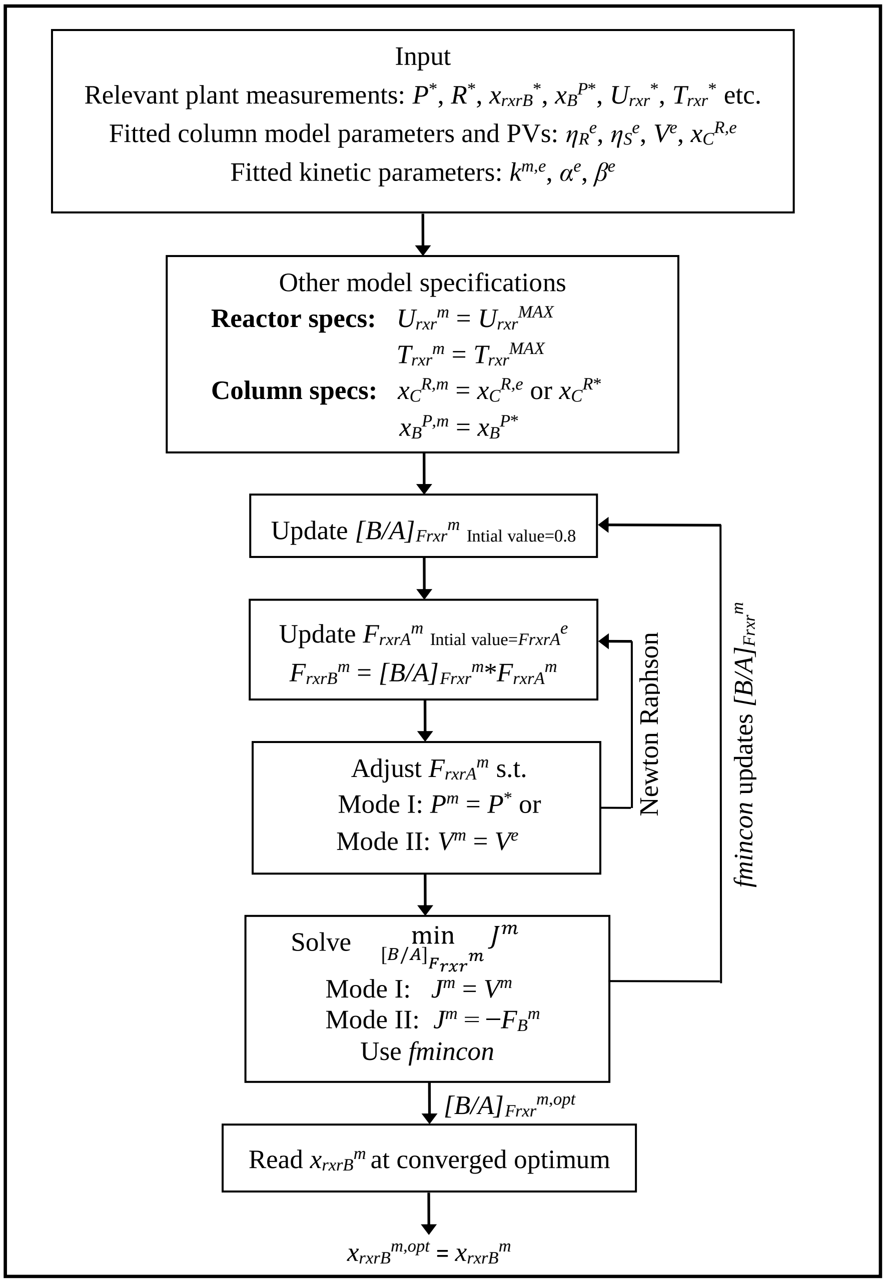
Input
Relevant plant measurements: P^*, R^*, x_{rxrB}^*, x_B^{P*}, U_{rxr}^*, T_{rxr}^* etc.
Fitted column model parameters and PVs: η_R^e, η_S^e, V^e, $x_C^{R,e}$
Fitted kinetic parameters: $k^{m,e}$, α^e, β^e
Other model specifications
Reactor specs: $U_{rxr}^m = U_{rxr}^{MAX}$
$T_{rxr}^m = T_{rxr}^{MAX}$
Column specs: $x_C^{R,m} = x_C^{R,e}$ or x_C^{R*}
$x_B^{P,m} = x_B^{P*}$
Update $[B/A]_{Frxr}^m$ Intial value=0.8
Update F_{rxrA}^m Intial value=F_{rxrA}^e
$F_{rxrB}^m = [B/A]_{Frxr}^m * F_{rxrA}^m$
Adjust F_{rxrA}^m s.t.
Mode I: $P^m = P^*$ or
Mode II: $V^m = V^e$
Newton Raphson
fmincon updates $[B/A]_{Frxr}^m$
Solve $\min_{[B/A]_{Frxr}^m} J^m$
Mode I: $J^m = V^m$
Mode II: $J^m = -F_B^m$
Use fmincon
$[B/A]_{Frxr}^{m,opt}$
Read x_{rxrB}^m at converged optimum
$x_{rxrB}^{m,opt} = x_{rxrB}^m$

Figure 3.3. Optimization of x_{rxrB}^m for fitted plant model

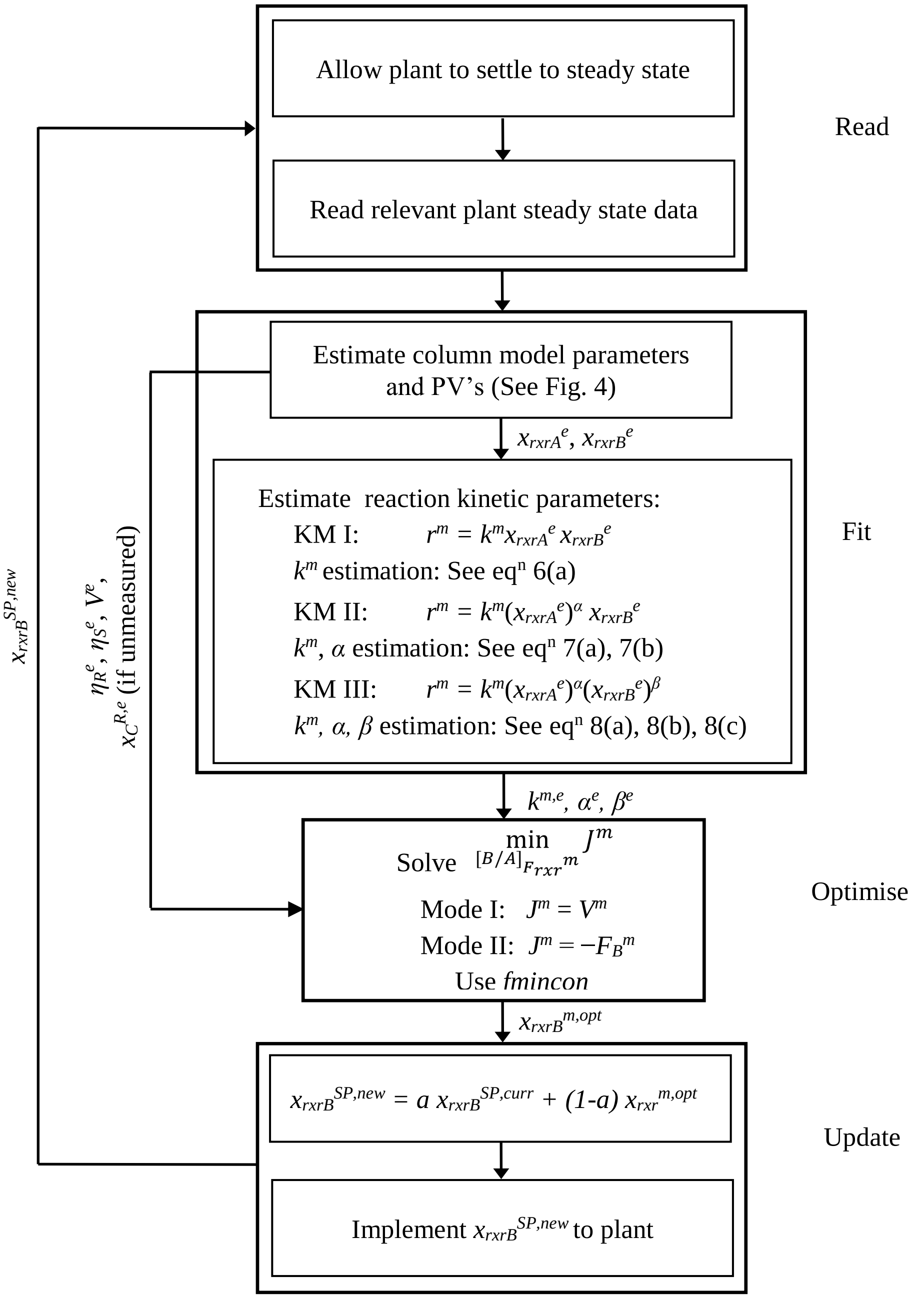
Allow plant to settle to steady state
Read relevant plant steady state data
Read
Estimate column model parameters and PV's (See Fig. 4)
x_{rxrA}^{e}, x_{rxrB}^{e}
Estimate reaction kinetic parameters:
KM I: $r^m = k^m x_{rxrA}^{e} x_{rxrB}^{e}$
k^m estimation: See eq^n 6(a)
KM II: $r^m = k^m (x_{rxrA}^{e})^{\alpha} x_{rxrB}^{e}$
k^m, α estimation: See eq^n 7(a), 7(b)
KM III: $r^m = k^m (x_{rxrA}^{e})^{\alpha} (x_{rxrB}^{e})^{\beta}$
k^m, α, β estimation: See eq^n 8(a), 8(b), 8(c)
Fit
$x_{rxrB}^{SP,new}$
η_R^e, η_S^e, V^e, $x_C^{R,e}$ (if unmeasured)
$k^{m,e}$, α^e, β^e
Solve $\min_{[B/A]_{Frxr}^{m}} J^m$
Mode I: $J^m = V^m$
Mode II: $J^m = -F_B^m$
Use *fmincon*
Optimise
$x_{rxrB}^{m,opt}$
$x_{rxrB}^{SP,new} = a\, x_{rxrB}^{SP,curr} + (1-a)\, x_{rxr}^{m,opt}$
Implement $x_{rxrB}^{SP,new}$ to plant
Update

Figure 3.4. Real time optimization cycle

RTO as described above is implemented on a 3.4 GHz Intel Core i7 processor, 32 GB RAM PC. Each RTO iteration takes about 2-3 mins to execute with the *fmincon* NLP optimizer taking 5-6 iterations to converge. This is acceptable as the plant takes a few hours to settle to the new steady state post implementation of the RTO move, before the next RTO calculation is done.

3.4 Steady State RTO Performance Evaluation

The performance of the developed scheme above for steady state RTO of x_{rxrB} for Mode I and Mode II operation is now evaluated. Here, we limit ourselves to a purely steady state analysis to get an idea of the possible steady state enhancement in plant profitability using RTO. Significant enhancement would then merit further evaluation using rigorous dynamic simulations.

The first and foremost question is if the developed modelling approach pushes the plant operation sufficiently close to the actual plant optimum? A related issue is the role of the model variants in determining how closely the actual plant optimum is approached. Specifically, we have three alternative reaction kinetic models and associated kinetic parameters. We also have the column model variants. To quantify the role of these models (and associated parameters) in closely approaching the actual optimum, we performed the fit-optimize-update RTO cycle for the following:

(a) The three different kinetic models, with fitted rectifying and stripping section efficiencies.

(b) For KM II, a separate tray efficiency is fitted to the rectifying and stripping sections each; or a single tray efficiency is fitted to the entire column; or all model trays are treated as ideal (i.e. all model tray efficiencies = 1).

Each model in (a) or (b) above is tested for the following cases in both Mode I and Mode II

(i) The plant is at steady state with x_{rxrB} at a suboptimal value and the RTO cycle is switched on.

(ii) The plant is at steady state with x_{rxrB} at the optimum value and a step disturbance occurs. RTO is switched on to seek the new optimum for x_{rxrB}.

For Case (i) above, an initial suboptimal x_{rxrB} value on either side of the optimum is considered for Mode I. In Mode II, it is assumed that x_{rxrB} remains fixed at its Mode I optimum ($x_{rxrB} = 0.278$ for a product rate of 100 kmol/h) and the RTO cycle is switched on with the column operating at its flooding limit (bottleneck constraint). For Case (ii), three step disturbances are considered. The first one, applicable to Mode I only, is a ±20% throughput change. The second one is the plant Langmuir Hinshelwood kinetic rate constant decreasing to 90% of its nominal value due to catalyst deactivation. The third one is the fresh *B* (fresh *A*) feed composition changing from pure *B* (*A*) to 90 mol% *B* (*A*) and 10 mol% *A* (*B*). The latter two disturbances are applicable to both operation modes.

The RTO cycles as detailed above were run and the converged optimum $x_{rxrB}^{m,opt}$ and scalar objective function value for each mode of operation (Mode I or Mode II) noted. Since this is a simulation study, the actual plant optimum (x_{rxrB}^{opt}) and the corresponding scalar objective function value (J^{opt}) is known and is therefore compared with the corresponding RTO converged values, $x_{rxrB}^{m,opt}$ and $J^{m,opt}$. The impact of the chosen model (a or b above) on RTO performance can thus be quantified. The % deviation of the converged decision variable (x_{rxrB}) from the actual plant optimum

$$D_{dv\%} = 100 \,.\, (x_{rxrB}^{m,opt} - x_{rxrB}^{opt})/x_{rxrB}^{opt}$$

and the % loss in the economic objective due to the deviation in the economic objective

$$Loss_{J\%} = 100 \,.\, (J^{m,opt} - J^{opt})/J^{opt}$$

are convenient quantitative metrics used here.

3.4.1 Impact of Kinetic Model on RTO Performance

In general, for the different reaction kinetic models, both KM II ($r^m = k^m x_{rxrA}^{\alpha} x_{rxrB}$) and KM III ($r^m = k^m x_{rxrA}^{\alpha} x_{rxrB}^{\beta}$) approach the actual plant optimum closely in Mode I and Mode II. KM I, on the other hand, results in poor performance with $D_{dv\%}$ being substantial. Consequently $Loss_{J\%}$ too then is noticeable. This is clearly evidenced in the bar chart in Figure 3.5. It shows $D_{dv\%}$ and $Loss_{J\%}$ for suboptimal initial x_{rxrB} and other disturbances noted above. Mode I, $Loss_{J\%}$ varies in the range 1.1 - 6% when using KM I. With KM II and KM III on the other hand, $Loss_{J\%}$ is at most 0.2%. Similarly in Mode II, KM I results in a 2.5-3.2% loss in the maximum achievable throughput. With KM II or KM III, the % loss is much smaller at < 0.1%. A closer scrutiny of Figure 3.5 reveals that the performance of KM II and KM III is comparable. The simpler two parameter KM II is thus recommended for RTO.

As an illustration of RTO driving x_{rxrB} towards optimum for the three considered kinetic models, Figure 3.6 plots the variation in $x_{rxrB}{}^{\mathrm{SP}}$ and the plant economic objective (J) with RTO iterations for both Mode I and Model II. The disturbance case of a 10% loss in catalyst activity (plant kinetic constant k reduces to 90% of its base-case value) is considered. Initially x_{rxrB}^{SP} is at its base-case optimum value of 0.278. As RTO is turned on, x_{rxrB} gets driven to its converged value in ~5 iterations for all the three considered kinetic models. While the actual plant optimum is closely approached using KM II and KM III, the converged x_{rxrB} for KM I remains noticeably away from the actual optimum with consequent sub-optimality in the converged economic objective J. For all other disturbance cases, very similar trends are observed (data not shown for brevity).

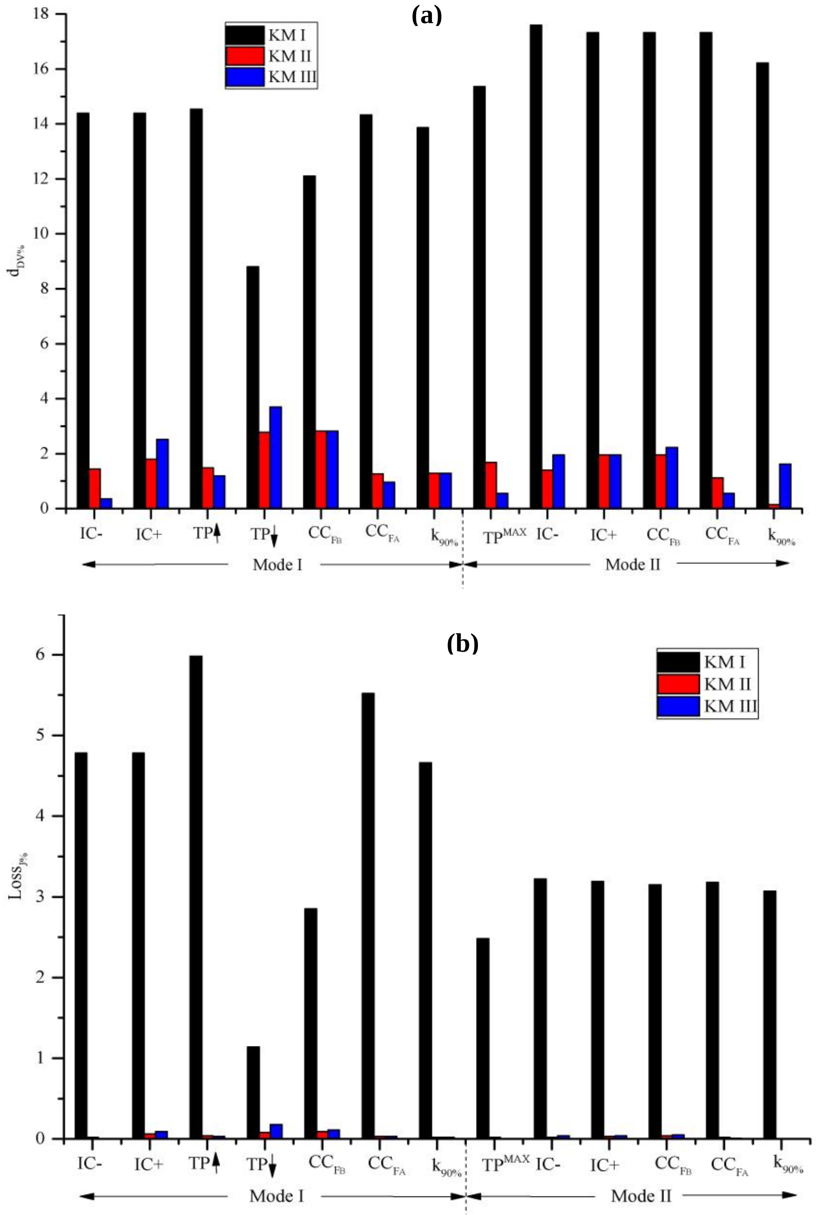

Figure 3.5. Deviation in RTO$^{\#}$ converged steady state from actual plant optimum for various disturbance scenarios using alternative kinetic models

(a) Decision variable (b) Economic Objective

IC: Suboptimal initial x_{rxrB} TP: Throughput CC: Feed composition change $k_{90\%}$: 90% catalyst activity

+: Above optimum −: Below optimum ↑: Increase ↓: Decrease

#: Unmeasured x_C^R; η_R and η_S fitted on column; Similar results for other model variants.

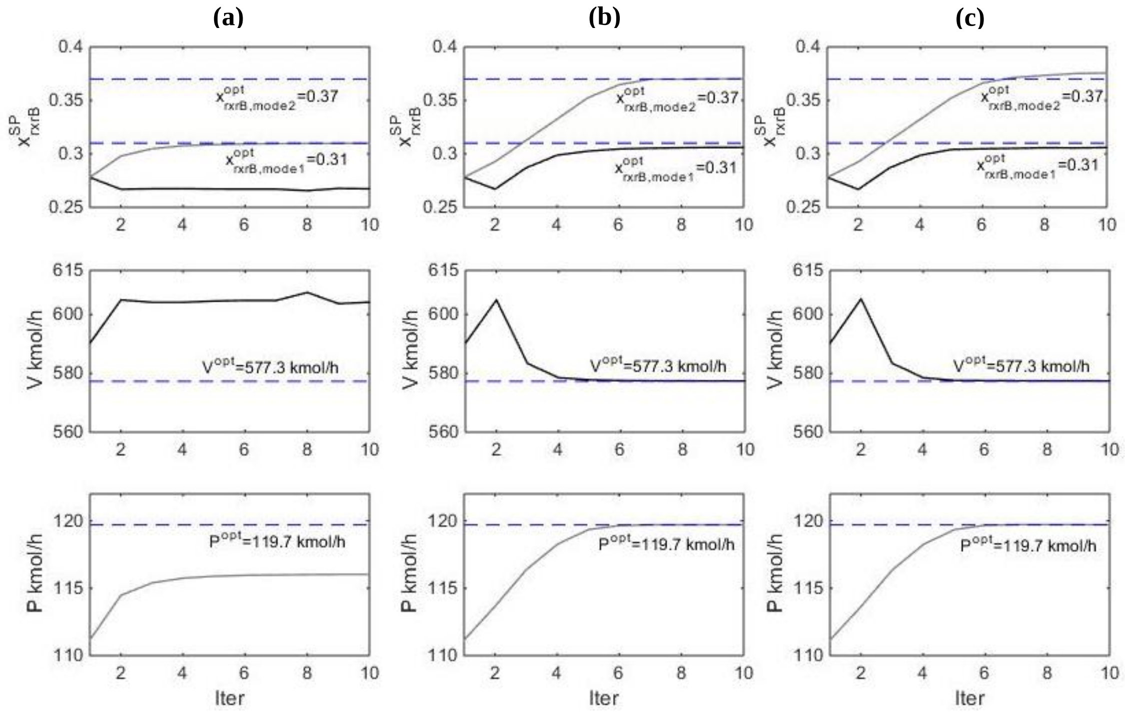

Figure 3.6. Evolution of x_{rxrB}^{SP} and J with RTO iterations for 10% loss in catalyst activity using alternative reaction kinetic models[#] (a) KM I (b) KM II and (c) KM III

#: Unmeasured x_C^R; η_R and η_S fitted on column; Similar results for other model variants.

In practice, higher losses are expected due to imperfect measurements as well as ever-present transient variability. Nevertheless, the results clearly illustrate that the choice of the reaction kinetic model significantly impacts how close an unconstrained plant setpoint can be driven to its actual optimum. Indeed, for perfect measurements and steady state operation, both KM II and KM III drive x_{rxrB} close enough to its actual optimum for a negligibly small economic loss.

3.4.2 Impact of Column Model on RTO Performance

The impact of column model on RTO performance is shown in Figure 3.7. It plots $D_{dv\%}$ and $Loss_{J\%}$ for the three possible column models with KM II for the various disturbance scenarios and suboptimal initial conditions. The bar chart clearly shows that when x_C^R is not measured and is therefore estimated, all three column models approach the plant optimum closely with the maximum loss being < 0.15% for all the considered disturbance scenarios. On the other hand, when x_C^R is measured, a distinct trend is noticed with the ideal trays model performance being noticeably inferior to the other two models. The % loss for the former varies in the range 0.04 – 1% whereas for the latter, the corresponding range is much smaller at 0.00 – 0.13%. This is likely because when x_C^R is estimated, the column model specifies $L^m = L^*$. The curvature in the actual J vs x_{rxrB} curve is then better captured since reflux rate is directly related to the column boil-up via the energy balance.

As an illustration of the convergence of RTO for the case when x_C^R is not measured, Figure 3.8 plots the variation in x_{rxrB} and J with respect to RTO iterations for Mode II operation for the three column models. Initially, x_{rxrB} is at a suboptimal value of 0.278. As RTO is switched on, the actual optimum x_{rxrB} of 0.358 is closely approached for all the three column models in ~5 iterations. These results suggest that for this system, the simplest of column models is appropriate for capturing the curvature in J vs x_{rxrB} curve and thus driving the decision variable, x_{rxrB}, to the actual optimum.

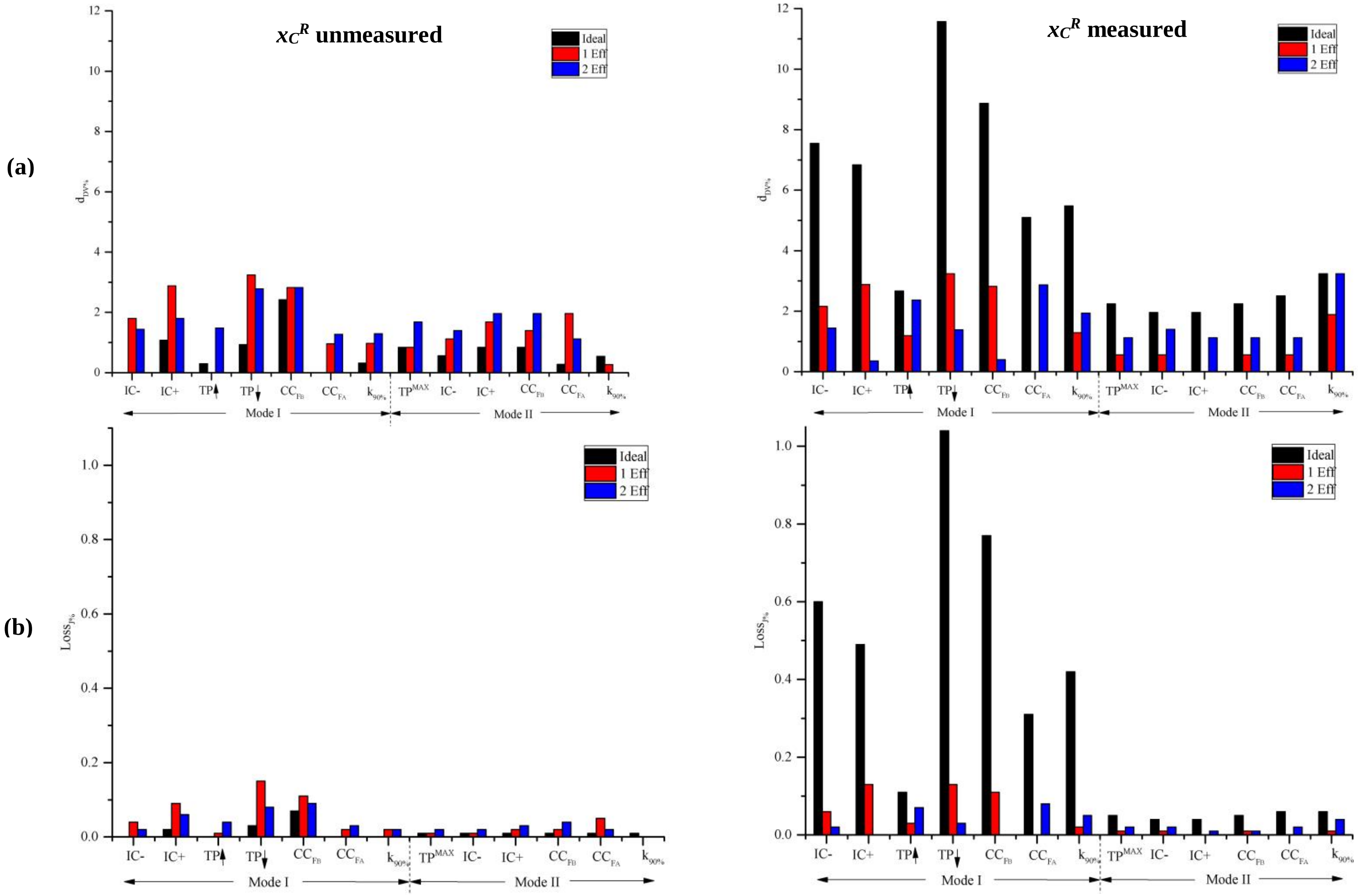

Figure 3.7. Deviation in RTO# converged steady state from actual plant optimum for various disturbance scenarios for different column model

(a) Decision variable (b) Economic Objective

IC: Suboptimal initial x_{rxrB} TP: Throughput CC: Feed composition change $k_{90\%}$: 90% catalyst activity

+: Above optimum −: Below optimum ↑: Increase ↓: Decrease

#: KM II; Similar results for other kinetic models.

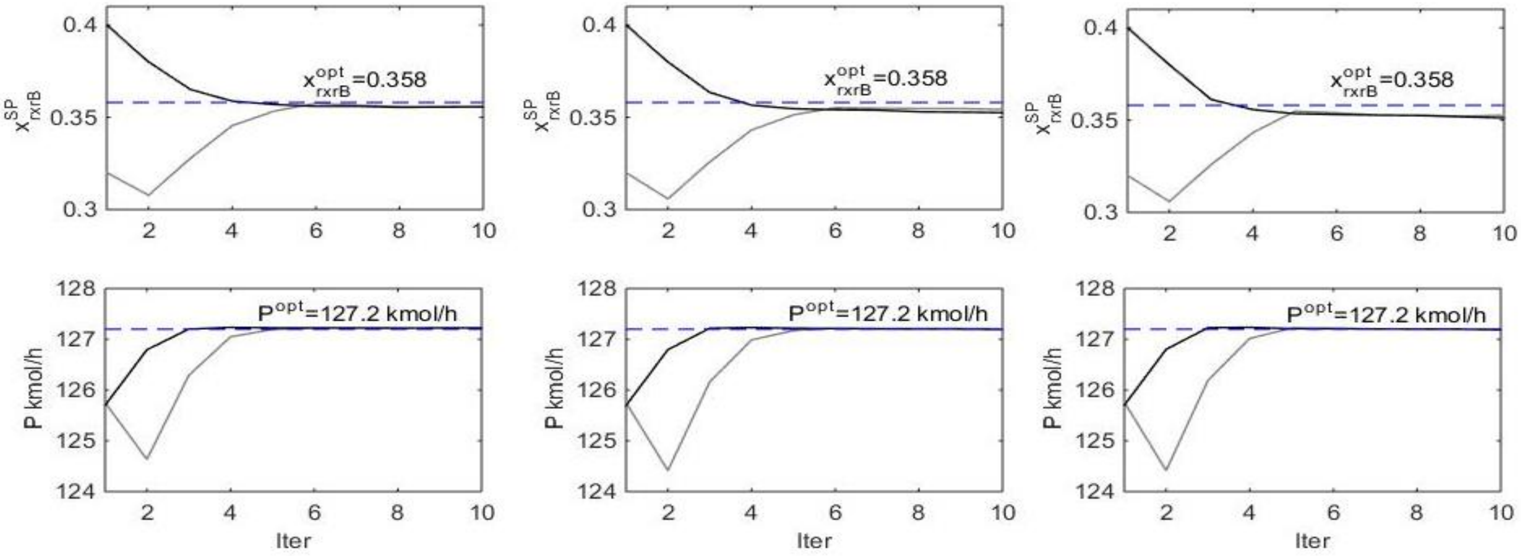

Figure 3.8. Evolution of $x_{rxrB}{}^{SP}$ and J with RTO$^{\#}$ iterations for 10% loss in catalyst activity in Mode II using alternate column model

#: Unmeasured $x_C{}^R$; KM II; Similar results for other kinetic model.

3.4.3 Impact of Measurement Bias on RTO Performance

The plant model fitting exercise requires plant measurements and a sustained bias in the measurement(s) can result in deterioration of RTO performance. To quantify the same, Table 3.4 reports $D_{dv\%}$ and $Loss_{J\%}$ using the proposed RTO scheme for a ±5% bias in the key plant measurements, namely, $x_{rxrB}{}^{*}$, R^{*}, L^{*} and P^{*}. The % economic loss is no more than 0.2% in all the cases. This suggests that the proposed RTO scheme is inherently robust to measurement errors.

3.4.4 Quantitative Benefit of RTO Over Constant Setpoint Operation

To appreciate the RTO benefit, Table 3.5 compares the Mode I and Mode II steady state economic objectives using RTO versus constant setpoint operation (i.e. $x_{rxrB}{}^{SP} = 0.278$, its Mode I optimum value) for the various disturbance / operating scenarios evaluated. The data in the Table 3.5 clearly shows that the recommended RTO approach brings in Mode I energy savings in the range of 1.3-10% and an increase in the maximum production rate in the range 5.5-7.6%. There thus exists significant economic incentive to implement the proposed RTO scheme. Further dynamic analysis will be taken up in Part II of this article series.

Table 3.4. RTO[#] performance with ±5% bias in key measurements

		Mode I $J = \min(V)$				Mode II $J = \min(-F_B)$	
		$TP_{+20\%}$		CC_{F_B}		TP^{MAX}	
		$D_{dv\%}$	$Loss_{J\%}$	$D_{dv\%}$	$Loss_{J\%}$	$D_{dv\%}$	$Loss_{J\%}$
$x_{rxrB}{}^{*}$	+	0.000	0.014	0.134	0.022	0.000	0.000
	-	0.009	0.042	0.139	0.022	0.006	0.008
P^{*}	+	0.003	0.014	0.148	0.000	0.006	0.008
	-	0.003	0.014	0.139	0.022	0.006	0.000
R^{*}	+	0.012	0.028	0.148	0.000	0.011	0.016
	-	0.009	0.028	0.111	0.132	0.011	0.016
L^{*}	+	0.003	0.014	0.120	0.066	0.008	0.008
	-	0.015	0.042	0.162	0.022	0.000	0.000

#: Unmeasured $x_C{}^{R}$; η_R and η_S fitted on column; KM II; Similar results for other model variants.

Table 3.5. Quantitative comparison of RTO# with constant setpoint operation for different disturbance scenarios

	Mode I $J = \min(V)$					Mode II $J = \min(-F_B)$			
	$TP_{+20\%}$	$TP_{-20\%}$	CC_{F_B}	CC_{F_A}	$k_{90\%}$	TP^{Max}	CC_{F_B}	CC_{F_A}	$k_{90\%}$
Constant SP	791.4	410.7	461.8	661.2	590.3	120.4	120.4	120.4	111.2
With RTO#	719.1	393.3	455.9	641.2	577.3	127.2	127.2	127.2	119.7
% Benefits	10.1%	4.4%	1.3%	3.1%	2.2%	5.6%	5.6%	5.6%	7.6%

#: Unmeasured x_C^R; η_R and η_S fitted on column; KM II.

TP: Throughput change $k_{90\%}$: 90% catalyst activity CC_{F_A} or CC_{F_B}: F_A or F_B composition change

Overall, the results indicate that the simple modelling approach using KM II and a tray efficiency each for the rectifying and stripping sections gets the plant very close to the actual x_{rxrB} optimum with negligible (<0.1%) economic loss. In particular, KM I is found to be inadequate with large offset from the actual optimum and consequent economic loss (up to 6%).

3.5 Discussion

In the following, we further try to understand understand why KM I works so poorly compared to KM II or KM III. We also evaluate the suitability of the proposed model for other reaction kinetic scenarios and the minimum excitation required in x_{rxrB} due to measurement noise. Other miscellaneous aspects worth highlighting are also briefly discussed.

3.5.1 Adequacy of Kinetic Models

In one of the first works on point-wise model adequacy for RTO applications, Forbes et al.[5] state that, "a process model is considered adequate if there is a set of adjustable parameters which allow the model based problem to have an extremum which coincides with that of the plant, in the reduced operating space". In our case, the reduced operating space is a simple one degree of freedom optimization problem, i.e. to seek the optimum value of x_{rxrB}. For simplicity, let us assume the model column is ideal so that only the kinetic parameters are to be fitted. In KM I, the parameter k^m gets fixed to match the production at the current steady state. No adjustable parameter is then left so that the model predicted optimum, $x_{rxrB}^{m,opt}$, cannot in general be exactly matched with the plant optimum, x_{rxrB}^{opt}. KM I is then clearly inadequate for RTO. In KM II, if we assume that k_m is fixed to match the current production rate, then α can be adjusted to ensure the $x_{rxrB}^{m,opt}$ exactly matches x_{rxrB}^{opt}. This is illustrated in Figure 3.9 that shows the model predicted and actual plant ΔJ vs x_{rxrB} curves for fitted KM I and KM II parameter values at a particular current Mode I/ Mode II steady state. It is easy to see that in KM II, there is a unique value of α that forces $x_{rxrB}^{m,opt} = x_{rxrB}^{opt}$. KM II is thus "strongly point-wise adequate", as defined in Forbes et al.[5]. In KM III, both α and β can be adjusted so that there are multiple values for which $x_{rxrB}^{m,opt} = x_{rxrB}^{opt}$. KM III is thus only point-wise adequate. Between the three considered kinetic models, recommending KM II for RTO thus has a sound rational basis. Note that even for an adequate model, a poor parameter fitting methodology can always cause the RTO to converge to a model optimum that is not close enough to the actual plant optimum. That both the adequate kinetic models, KM II and KM III, approach the optimum closely implies that the suggested RTO methodology using available plant data is reasonable.

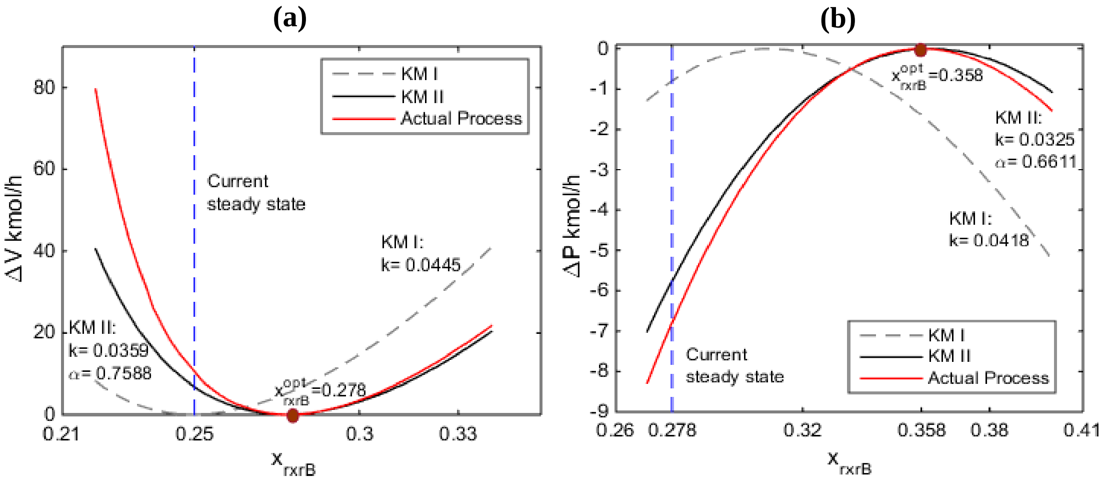

Figure 3.9. Contrasting point-wise adequacy of KM II vs inadequacy of KM I for (a) Mode I (b) Mode II

k is in kmol m^{-3} s^{-1}

A related issue concerns the suitability of the recommended RTO methodology using KM II for the same process but different plant kinetics. Given that the plant optimum is not known in practice, one cannot conclude that the suggested methodology will work well for different reaction kinetics. In order to address this issue, we considered a more general kinetic expression

$$r = k\frac{x_A^a x_B^b}{(1+K_A x_A+K_B x_B)}$$

Since our RTO problem in the reduced operating space is the simplest possible one dof problem, it is easy to see that for all reasonable values of plant reaction kinetic parameters (k, a, b, K_A and K_B), KM II is adequate since with k^m fixed to match production, α can be appropriately adjusted to force $x_{rxrB}^{m,opt} = x_{rxrB}^{opt}$. Clearly, KM II is then point-wise adequate. Now to evaluate if the specific proposed RTO parameter fitting method converges close to the actual plant optimum, we considered 9 different parameter combinations with $a > b$, $a = b$, $a < b$, $K_A x_{rxrA} \approx O(1)$ or 0 and $K_B x_{rxrB} \approx O(1)$ or 0 (K_A and $K_B = 0$ is redundant) and applied the proposed RTO method. The results summarized in Table 3.6 for a Mode I ±20% throughput change clearly suggest that for all considered kinetics, the recommended RTO method approaches the actual plant optimum quite closely with the loss from optimum being small at less than 0.02%. Similar results have also been verified for other Mode I/ Mode II disturbance scenarios (data not shown for brevity). The suggested RTO method may therefore be considered suitable for plant reaction kinetic scenarios of the general form above.

Table 3.6. RTO$^{\#}$ performance with different LHHW models

Models	x_{rxrB}^{opt}	V^{opt}	$x_{rxrB}^{m,opt}$	$V^{m,opt}$	$D_{dv\%}$	$Loss_{J\%}$
$r = 0.0766x_{rxrA}x_{rxrB}/(1+1.78x_{rxrA})$	0.337	719.1	0.338	719.13	0.267	0.004
$r = 0.1701x_{rxrA}^{2}x_{rxrB}/(1+1.78x_{rxrA})$	0.23	742.29	0.229	742.3	0.435	0.001
$r = 0.2127x_{rxrA}x_{rxrB}^{2}//(1+1.78x_{rxrA})$	0.392	707.97	0.39	708.02	0.510	0.006
$r = 0.0827x_{rxrA}x_{rxrB}/(1+2.73x_{rxrB})$	0.204	678.22	0.205	678.23	0.343	0.001
$r = 0.1601x_{rxrA}^{2}x_{rxrB}/(1+2.73x_{rxrB})$	0.151	718.445	0.151	718.44	0.331	0.00
$r = 0.131x_{rxrA}x_{rxrB}^{2}/(1+3.04x_{rxrB})$	0.322	710.8	0.321	710.79	0.311	0.001
$r = 0.105x_{rxrA}x_{rxrB}/(1+1.78x_{rxrA}+3.79x_{rxrB})$	0.292	725.12	0.293	725.12	0.548	0.00
$r = 0.2728x_{rxrA}^{2}x_{rxrB}/(1+1.78x_{rxrA}+3.79x_{rxrB})$	0.164	643.84	0.163	643.89	0.793	0.008
$r = 0.341x_{rxrA}x_{rxrB}^{2}/(1+1.78x_{rxrA}+2.02x_{rxrB})$	0.396	812.07	0.395	812.07	0.177	0.00

#: For +20% TP change; Unmeasured x_C^R; η_R and η_S fitted on column

r units: kmol.m^{-3}.s^{-1}

3.5.2 Minimum Excitation Due to Measurement Uncertainty

In the quantitative RTO analysis, we have assumed perfect measurements, within the tight simulator numerical error tolerance. In practice, there exists uncertainty in the plant steady state measurements. The noisy measurements can cause amplification in the uncertainty associated with parameter estimates. In particular, notice that for the recommended KM II model fitting equations, the expression for α (Equation 7a) tends to 0 by 0 as the two steady states approach each other. To keep the uncertainty in the parameter estimates small, the two steady states must be minimally separated i.e. a minimum excitation is required in x_{rxrB} for reliable kinetic parameter estimation.

To analyze for the minimum excitation in the recommended kinetic model, KM II, we consider the case where x_C^R is measured. Random normal noise is added to the steady state measurements needed in the calculation of k^m and α^m, namely, P, x_C^R, x_B^P, R, x_{rxrB} and U_{rxr}. For convenience, the percentage random error due to noise, $\Delta e_{\%}$, at 99% confidence level (3-sigma limit) in all the measurements is taken to be the same. Adding noise to the true plant steady state PV values, a total of 1000 noisy steady state measurements are generated for plant steady states (current + up to 3 previous steady states). These plant steady states differ from each other in the implemented x_{rxrB} values with the difference between two adjacent steady states being a constant,

Δx_{rxrB}. The KM II parameters are then fitted using the noisy data for a total of 2, 3, or 4 steady states. Equation 7 is applicable for fitting 2 steady states. The fitting for more than 2 steady states is done quite simply as follows. At each of these *i* steady states, we have

$$k^m \, (x_{rxrA}{}^{e}{}_{i})^{\alpha} \, (x_{rxrB}{}^{e}{}_{i}) \, U_{rxr}{}^{MAX}{}_{0} = P^{*}{}_{0} \, (1 - x_B{}^{P^*}{}_{i})$$

Taking log of both sides, rearranging and writing the equations in matrix form, we get

$$\begin{bmatrix} 1 & log\left(x_{rxrB}{}_{0}^{e}\right) \\ 1 & log\left(x_{rxrB}{}_{1}^{e}\right) \\ \vdots & \vdots \\ 1 & log\left(x_{rxrB}{}_{n}^{e}\right) \end{bmatrix} \begin{bmatrix} log(k^m) \\ \alpha \end{bmatrix} = \begin{bmatrix} log\left\{P_0^*\left(1 - x_{B}{}_{0}^{P^*}\right)\right\} - log\left(U_{rxr}{}^{MAX}{}_{0}\right) - \log\left(x_{rxrB}{}_{0}^{e}\right) \\ log\left\{P_0^*\left(1 - x_{B}{}_{1}^{P^*}\right)\right\} - log\left(U_{rxr}{}^{MAX}{}_{1}\right) - \log\left(x_{rxrB}{}_{1}^{e}\right) \\ \vdots \\ log\left\{P_0^*\left(1 - x_{B}{}_{n}^{P^*}\right)\right\} - log\left(U_{rxr}{}^{MAX}{}_{n}\right) - \log\left(x_{rxrB}{}_{n}^{e}\right) \end{bmatrix}$$

Using

$$\boldsymbol{X} = \begin{bmatrix} 1 & log\left(x_{rxrB}{}_{0}^{e}\right) \\ 1 & log\left(x_{rxrB}{}_{1}^{e}\right) \\ \vdots & \vdots \\ 1 & log\left(x_{rxrB}{}_{n}^{e}\right) \end{bmatrix}; \qquad \boldsymbol{\beta} = \begin{bmatrix} log(k^m) \\ \alpha \end{bmatrix}; \, \boldsymbol{y} =$$

$$\begin{bmatrix} log\left\{P_0^*\left(1 - x_{B}{}_{0}^{P^*}\right)\right\} - log\left(U_{rxr}{}^{MAX}{}_{0}\right) - \log\left(x_{rxrB}{}_{0}^{e}\right) \\ log\left\{P_0^*\left(1 - x_{B}{}_{1}^{P^*}\right)\right\} - log\left(U_{rxr}{}^{MAX}{}_{1}\right) - \log\left(x_{rxrB}{}_{1}^{e}\right) \\ \vdots \\ log\left\{P_0^*\left(1 - x_{B}{}_{n}^{P^*}\right)\right\} - log\left(U_{rxr}{}^{MAX}{}_{n}\right) - \log\left(x_{rxrB}{}_{n}^{e}\right) \end{bmatrix}$$

we get $\boldsymbol{X\beta} = \boldsymbol{y}$

The unknown kinetic parameters are then easily obtained from the normal equations as

$$\boldsymbol{\beta} = (\boldsymbol{X}^T\boldsymbol{X})^{-1}\boldsymbol{X}^T\boldsymbol{y}$$

By fitting using the 1000 data with reandom noise, an approximate distribution of the parameter estimates and their 95% confidence limits are obtained. Due to the 0 by 0 form of the α expression (Equation 7a) for nearly equal values of x_{rxrB}, the 95% confidence limit in the α estimate blows up so that it sets the minimum Δx_{rxrB} excitation required. Figure 3.10 plots the variation in the $\Delta\alpha/\alpha$ (95% confidence limit) with Δx_{rxrB} for 3-sigma uncertainty levels of 0.01%, 0.05%, 0.1% and 1% in the steady state measurements. Given that the steady state measurement estimates will be obtained by averaging several hours of past data, we expect the uncertainty in the various measurements to be no more the 1%. From the Figure, for $\Delta\alpha/\alpha$ to be within 20%, Δx_{rxrB} is ~0.01 when data for 4 most recent steady states is fitted. Using steady state data for 4 most recent steady states, The RTO converge x_{rxrB} close to the plant optimum. To confirm, we performed RTO with 1% added measurement noise to the steady state plant data for the disturbance scenarios considered. The results summarized in Table 3.7 clearly suggest that the RTO method approaches the true optimum to within 3% for Mode I and 8% for Mode II. The corresponding economic loss is within 0.15% and 0.9% respectively. The method is therefore robust to small levels of uncertainty in the measurements.

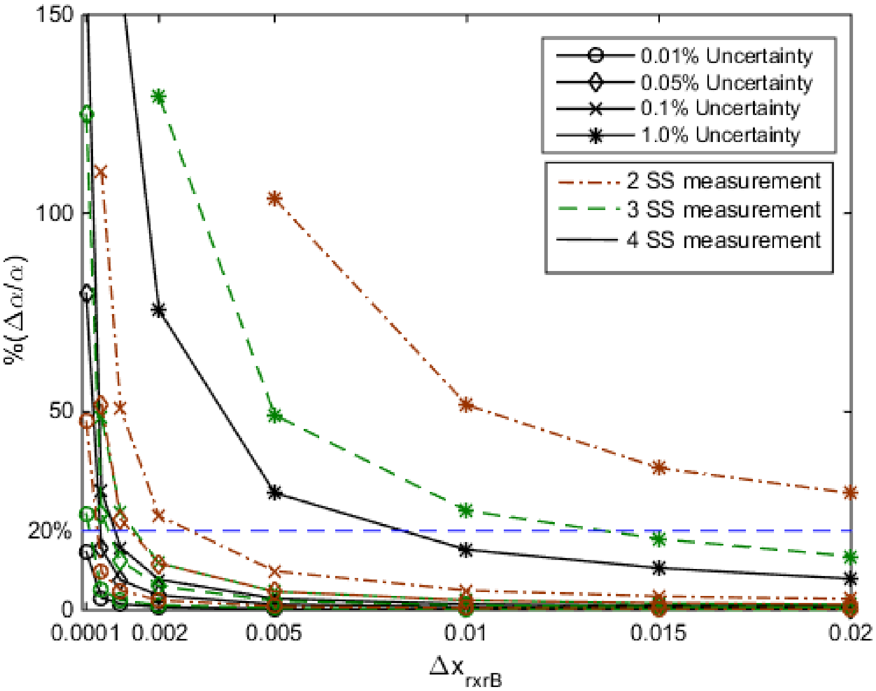

Figure 3.10. Variation in $\Delta\alpha/\alpha$ with Δx_{rxrB} for various measurement uncertainty levels using up to 4 recent steady states (SS) for parameter fitting

Table 3.7. RTO[#] performance with 1% measurement uncertainty

	Mode I $J = \min(V)$					Mode II $J = \min(-F_B)$			
	TP$_{+20\%}$	TP$_{-20\%}$	CC$_{F_B}$	CC$_{F_A}$	k$_{90\%}$	TP^{Max}	CC$_{F_B}$	CC$_{F_A}$	k$_{90\%}$
x_{rxrB}^{opt}	0.337	0.216	0.248	0.314	0.31	0.358	0.358	0.358	0.37
J^{opt}	719.1	393.3	455.9	641.2	577.3	127.23	127.23	127.23	119.71
$x_{rxrB}^{m,opt}$	0.344	0.215	0.241	0.317	0.315	0.333	0.329	0.334	0.340
$J^{m,opt}$	719.6	393.4	456.4	641.3	577.6	126.65	126.48	126.66	118.7
$D_{dv\%}$	2.07	0.46	2.82	0.96	1.61	6.98	8.10	6.70	8.11
Loss$_{J\%}$	0.07	0.02	0.11	0.02	0.05	0.46	0.59	0.45	0.84

#: Unmeasured x_C^R; η_R and η_S fitted on column; KM II.

TP: Throughput change k$_{90\%}$: 90% catalyst activity CC$_{F_A}$ or CC$_{F_B}$: F_A or F_B composition change

3.5.3 Miscellaneous Comments

Here we have demonstrated RTO for a single decision variable. This may be a limitation in that many practical RTO problems are multivariable in nature. It is however our experience that in many multivariable scenarios, the economic sensitivity with respect to a particular decision variable is significantly more than the other decision variables. The problem then reduces to a single variable problem. Nevertheless, extension of the work to multivariable RTO is envisaged as future work.

Lastly, we note that what has been presented here is the conventional two-step fit and optimize model approach for RTO, which is very appealing and is the norm in industry. This approach always suffers from some sub-optimality due to plant-model mismatch. Its major limitation is that the presented parameter adaptation strategy has not been systematically designed for converging to (or near) the plant optimum, in the presence of plant-model mismatch. Even as the sub-optimality in the presented case study is small (< 1% with measurement noise), it is possible that the sub-optimality is large due to model inadequacy (e.g. RTO performance with KM I in this work). To guarantee convergence to optimum, Bonvin and co-workers[18-22] have formalized the concept of modifier adaptation. The key idea is to take the difference in the optimality condition predicted by the model and that estimated from plant data, and use this information in modifiers that are added to the constraints and to the cost function of a modified optimization problem. The modifiers are adapted iteratively and upon convergence the difference in the model predicted and the plant estimated optimality condition is driven to zero. Thus, the scheme converges to the actual plant optimum. Applications of the modifier adaptation RTO method have been reported recently[23-24]. We are now actively engaged in researching modifier adaptation based RTO of reactor-separator-recycle processes and hope to report the findings in the near future.

3.6 Conclusion

In conclusion, this work has demonstrated RTO of the dominant unconstrained economic decision variable for a complete plantwide process module with material recycle. RTO using simple reaction kinetic and distillation column models is shown to approach to actual plant optimum very closely with negligible economic loss. A key modelling requirement is the ability of the model to appropriately capture the curvature in the plant response curve with respect to the decision variable. For the various disturbance scenarios considered, the proposed RTO scheme is shown to result in up to 10% energy savings (Mode I) and up to 7.6% higher maximum throughput (Mode II) compared to constant setpoint operation. Further work will evaluate the dynamic performance of the proposed RTO scheme.

References

(1) Ariyur, K. B.; Krstic, M. *Real-time optimization by extremum-seeking control*. Wiley-Interscience, Hoboken, NJ, 2003.

(2) Kumar, V.; Kaistha, N. Hill climbing for plantwide control to economic optimum. *Ind. Eng. Chem. Res.* 2014, 53 (42), 16465-16475.

(3) Darby, M. L.; Nikolaou, M.; Jones, J.; Nicholson, D. RTO: An overview and assessment of current practice. *J. Process Control* 2011, 21 (6), 874-884.

(4) Forbes, J. F.; Marlin, T. E. Model accuracy for economic optimizing controllers: The bias update case. *Ind. Eng. Chem. Res.* 1994, 33 (8), 1919-1929.

(5) Forbes, J. F.; Marlin, T. E.; Macgregor, J. F. Model adequacy requirement for optimizing plant operations. *Comput. Chem. Eng.* 1994, 18(6), 497-510.

(6) Lacks, D. J. Real-time optimization in nonlinear chemical processes: need for global optimizer. *AIChE J*. 2003, 49 (11), 2980-2983.

(7) Gouvea, M. T.; Odloak, D. One-layer real time optimization of LPG production in the FCC unit: Procedure, advantages and disadvantages. *Comput. Chem. Eng.* 1998, 22, S191-S198.

(8) Mendoza, D. F.; Palacio, L. M.; Graciano, J.E.A.; Riascos, C. A.M.; Vianna, A. S. Jr.; Roux, G. A.C. L. Real-time optimization of an industrial-scale vapour recompression process. Model validation and analysis. *Ind. Eng. Chem. Res.* 2013, 52, 5735-5746.

(9) Duvall, P. M.; Riggs, J. B. On-line optimization of the Tennessee Eastman challenge problem. *J. Process Control* 2000, 10, 19-33.

(10) Mercangöz, M.; Doyle III, F. J. Real-time optimization of the pulp mill benchmark problem. *Comput. Chem. Eng.* 2008, 32, 789-804.

(11) Lid, T.; Strand, S. Real-time optimization of a cat cracker unit. *Comput. Chem. Eng.* 1997, 21, S887-S892.

(12) Zhijiang, S.; Jinlin, W.; Jixin, Q. Real-time optimization of acetaldehyde production process. *Dev. Chem. Eng. Mineral Process* 2005, 13(3/4), 249-258.

(13) Luyben, W. L. Dynamics and control of recycle systems. 1. Simple open-loop and closed-loop systems. *Ind. Eng. Chem. Res.* 1993, 32(3), 466-475.

(14) Wu, K. L.; Yu, C. C. Reactor/separator processes with recycle 1. Candidate control structure for operatibility. *Comput. Chem. Eng.* 1996, *20*, 1291.

(15) Kanodia, R.; Kaistha, N. Plant-wide control for throughput maximization: A case study. *Ind. Eng. Chem. Res.* 2010, 49, 210-221.

(16) Fogler, H. S. *Elements of Chemical Reaction Engineering*. Upper Saddle River, NJ: Prentice Hall, 2006.

(17) Henley, E. J.; Seader, J. D. *Separation Process Principles*. Wiley: New York, 2006.

(18) Marchetti, A.; Chachuat, B.; Bonvin, D. Modifier-adaptation methodology for real-time optimization. *Ind. Eng. Chem. Res.* 2009, 48(13), 6022-6033.

(19) Chachuat, B.; Srinivasan, B.; Bonvin, D. Adaptation strategies for real-time optimization. *Comput. Chem. Eng.* 2009, 33(10), 1557-1567.

(20) Marchetti, A.; Chachuat, B.; Bonvin, D. A dual modifier-adaptation approach for real-time optimization. *J. Process Control* 2010, 20(9), 1027-1037.

(21) François, G.; Bonvin, D. Use of convex model approximations for real-time optimization via modifier adaptation. *Ind. Eng. Chem. Res.* 2013, 52(33), 11614-11625.

(22) Costello, S.; François, G.; Bonvin, D. A directional modifier-adaptation algorithm for real-time optimization. *J. Process Control* 2016, 39, 64-76.

(23) Bunin, G. A.; Wuillemin, Z.; François, G.; Nakajo, A.; Tsikonis, L.; Bonvin, D. Experimental real-time optimization of a solid oxide fuel cell stack via constraint adaptation. *Energy* 2012, 39(1), 54-62.

(24) Costello, S.; François, G.; Bonvin, D. Real-time optimizing control of an experimental crosswind power kite. *IEEE Trans. Automat. Contr*. 2018, 26(2), 507-522.

Chapter 4

Real Time Optimization of a Reactor-Separator-Recycle Process II: Dynamic Evaluation

This Chapter is based on the published paper “Real Time Optimization of a Reactor-Separator-Recycle Process II: Dynamic Evaluation” in Industrial Engineering and Chemistry Research, doi: 10.1021/acs.iecr.8b04274.

In this Chapter dynamic performance of a fully automatic real time optimization (RTO) scheme is evaluated for a reactor-separator-recycle process in Mode I (minimize column boilup at given throughput) and Mode II (maximize production) operation. In both modes, the reactor composition setpoint is the optimized unconstrained degree of freedom. The RTO requires a simple override control scheme to reconfigure the inventory loops as the active constraint set changes between Mode I and Mode II. The overrides reorient inventory loops from in the direction of process flow (CS I) in Mode I to opposite the process flow (CS II) upstream of the bottleneck constraint (column maximum boilup) limiting Mode II production. The set of selected signals in the override scheme allows automatic distinction between Mode I and Mode II optimization. Closed loop results are reported for realistic sustained disturbance scenarios that include sudden fast changes as well as gradual equipment degradation. The RTO scheme significantly improves economic performance with up to 9% and 7% benefit over constant setpoint operation in Mode I and Mode II, respectively. Also, economic loss compared to the optimum gold standard is within 1%, implying excellent performance even as the plant is never truly at steady state.

4.1 Introduction

Real time optimization (RTO) is a promising approach for driving plant operation close to the actual economic optimum steady state in the face of large disturbances[1-2]. Typically, at the optimum steady state, several constraints are active with a few remaining unconstrained degrees of freedom. The optimally active constraints are usually fairly obvious. Examples include operation at minimum product quality (to minimize product giveaway) or at maximum reactor hold-up (to minimize unconverted reactant recycle load) etc. If we assume that the regulatory layer control loop pairings are configured (or can be reconfigured, if required) to drive the process operation as close as possible to the optimally active constraint limits, optimal operation then boils down to obtaining the optimum values of any remaining unconstrained degrees of freedom. These decision variables correspond to unconstrained setpoints in the regulatory layer. The basic RTO cycle thus consists of using recent plant measurement data to best-fit parameters to a steady state model of the plant, optimizing the fitted steady state model to estimate the optimum values of the unconstrained regulatory layer setpoints and implementing the updated setpoints in the plant. The plant is allowed to settle at the new steady state and the fit-optimize-update cycle is then repeated. With an adequate process model that accounts for the major process non-linearities and a proper parameter fitting strategy, this standard model based RTO improves process operation economics and is the state-of-the-art in the process industry[3-6].

In the recent work of our group[7], a simple steady state modeling approach was developed for real time optimization (RTO) of the unconstrained degree of freedom of a reactor-separator-recycle process for Mode I (reboiler duty minimization at given throughput) and Mode II (throughput maximization) plant operation. The steady state results showed that the proposed approach drives the unconstrained setpoint very close to the actual plant optimum in the presence of large disturbances (plant-model mismatch) with potential economic benefit up to 10% over constant setpoint operation for the considered disturbances. It was also shown that the approach works well for a class of reaction kinetics so that the conventional fit-optimize RTO method is appropriate. In view of the promising steady state economic benefit results from the conventional RTO approach, further dynamic evaluation is merited.

There are two major reasons why such a dynamic evaluation is required. Firstly, the process never really settles at a steady state due to ever present transient variability/disturbances. Further, many-a-times the disturbance itself is a slow transient, e.g. decline in catalyst activity over months of reactor operation, implying quasi-steady operation. There is also the economic loss during the RTO iterations till the optimum steady state is closely approached. The economic benefit achieved in an actual operating plant is thus likely to be less than the estimates from a purely steady state analysis, making dynamic evaluation necessary.

The second major reason for dynamic evaluation is the need to change the regulatory layer pairings as the optimally active constraint set changes. A common example of a change in the active constraint set is the transition from Mode I (given throughput) to Mode II (maximum throughput) operation and vice versa[8-9]. Typically in Mode I, none of the equipment capacity constraints are active and the process operates at the desired throughput, as dictated by market considerations. A transition to Mode II may be desired when product demand is exceedingly high (seller's market) and maximizing production maximizes profit. The maximum production is constrained by the bottleneck equipment capacity constraint, which is typically a hard constraint. Alternatively, a transition to Mode II becomes necessary when an equipment hits a capacity constraint (bottleneck) due to process degradation. The process throughput then must be reduced appropriately to ensure the bottleneck capacity constraint hard limit is not violated. In either case, the bottleneck capacity constraint is a new optimally active constraint that sets the throughput. To ensure the back-off from the hard constraint limit is as small as possible, appropriate reconfiguring of regulatory layer loops is usually required.

For the primary reasons enumerated above, this work addresses the dynamic evaluation of the RTO approach developed in previous chapter (Part I) for the reactor-separator-recycle process. In the following, the main results from Part I are first summarized. We then present the Mode I and Mode II regulatory control structures along with an override control system for reconfiguring the loops in Mode I ↔ Mode II transition. Dynamic simulation results for the developed control system (including overrides) with RTO updated unconstrained regulatory setpoint are then presented to quantify economic benefit over constant setpoint for various disturbance scenarios. Results are also presented for scenarios where the process operation must transition between Mode I and Mode II and vice versa. Post a brief discussion of outstanding issues, the article ends with a summary of the main findings from the work.

4.2 Summary of Part I Results

The plantwide reactor-separator-recycle process is shown in Figure 1.8. The liquid-phase, exothermic, irreversible reaction $A + B \rightarrow C$ occurs in the reactor. The reactor effluent is distilled to recover nearly pure C as the bottoms product and unreacted A and B as the distillate. The distillate is recycled back to the reactor. The process has six steady state operating degrees of freedom (dofs); 2 for the two fresh feeds, 2 for the reactor (hold up and temperature) and 2 for the column (assuming given column pressure). These dofs are to be optimized for two modes of process operation. In Mode I, the throughput fixed and the remaining five dofs are to be optimized to minimize the column boilup (V). In Mode II, all six dofs are to be optimized to maximize throughput.

Of the available dofs, maximum reactor temperature (T_{rxr}^{MAX}) and level (U_{rxr}^{MAX}) as well as minimum product purity ($x_C^{P,MIN}$) constraints are always optimally active i.e. three strictly active constraints in both Mode I and Mode II. Further, it is optimal to maintain the C leakage up the column distillate at the maximum limit of 1 mol%. This is treated as a soft constraint with slight deviations being acceptable. A higher *C* leakage in the recycle stream is not permissible for long durations due to practical considerations of accelerated equipment fouling or catalyst deactivation in the presence of too much heavy *C*. Thus in Mode I (minimize boilup at given throughput), the four active constraints as well as the given throughput specification leave one unconstrained dof. In Mode II (maximize throughput), the maximum column boilup (V^{MAX}) is the bottleneck capacity constraint that becomes additionally active to limit throughput. The unconstrained dof in Mode II then remains one as the throughput is no longer specified and gets set indirectly by the V^{MAX} constraint. We take the *B* reactor mol fraction (x_{rxrB}) as the regulatory layer setpoint corresponding to this unconstrained dof in both Mode I and Mode II. For completeness, Table 4.1 lists the salient optimum operating conditions for Mode I and Mode II. At the Mode I optimum, where the throughput is noticeably lower than the maximum throughput (Mode II), the optimum reactor *B* mol fraction is lower than *A*. At the Mode II optimum, the reactor *A* and *B* mol fractions are comparable with *B* being in slight excess. It appears that at lower throughputs (Mode I), the optimum reactor *B* mol fraction is noticeably lower than *A* as *B* is heavier than *A* so that *B* is more expensive to recycle. This gap decreases as throughput is increased and at maximum throughput (Mode II) the reactor *B* mol fraction is slightly higher than the *A* mol fraction.

The optimum value of x_{rxrB} is obtained by RTO on a simple plant model. The recommended model uses two parameter reaction kinetics with the reaction rate given by

$$r^m = k^m \, x_{rxrA}{}^{\alpha} \, x_{rxrB}$$

and an ideal VLE column model with adjustable rectifying section and stripping section tray efficiencies, η_R and η_S. The unknown parameters (k^m, α, η_R and η_S) are fitted using available recent plant measurements. Plant model mismatch occurs with the actual plant reaction kinetics being Langmuir-Hinshelwood and the actual column having vapor rate dependent tray efficiencies and SRK equation-of-state based thermodynamic properties. These details are available in previous chapter. Here we limit ourselves to the case of the recycle stream *C* mol fraction ($x_C{}^R$) being measured. The measurement is necessitated as temperature control of a sensitive rectifying tray temperature results in significant deviation in the recycle stream C leakage above to maximum 1 mol% limit. Distillate composition based update of the tray temperature setpoint then becomes necessary. The RTO proceeds as follows.

1. The plant internal stream component flow rates are estimated for the measured value of x_C^R using material balances and available measurements.
2. For the column feed obtained in Step 1, the ideal VLE column model is converged with plant measured bottoms product purity and distillate C impurity as the specifications. Further η_R and η_S are adjusted to minimize the sum of absolute deviation in the measured and column model predicted tray temperature profiles. Good estimates of η_R and η_S are thus obtained.
3. Good estimates of the kinetic parameters, k^m and α, are obtained by adjusting them so that the throughput at the current and the previous steady state exactly match the plant throughput for the corresponding (estimated) total A and total B (recycle + fresh) component flow rates to the reactor. An algebraic estimation method is given in Part I.
4. With all the model parameters thus estimated (k_m, α, η_R and η_S), the fitted model is optimized to obtain the model estimated optimum $x_{rxrB}^{m,opt}$. Note that in Mode II, the model estimated boilup, V^e, is considered the V^{MAX} constraint (i.e. $V^{MAX} = V^e$) in the optimization.
5. The estimated optimum $x_{rxrB}^{m,opt}$ is used to revise the x_{rxrB} setpoint to the plant.
6. Plant is allowed to settle at new steady state and steps 1 - 6 are repeated.

The Part I steady state results show that the above fit-optimize-update RTO cycle results in up to 10% and 6% additional economic benefit in Mode I and Mode II, respectively, over constant setpoint operation.

Table 4.1. Salient optimum operating conditions for Mode I/Mode II

	Mode I					Mode II				
Material Streams	Molar Flow (kmol/h)	T (˚C)	x_A	x_B	x_C	Molar Flow (kmol/h)	T (˚C)	x_A	x_B	x_C
F_A	99	25	1	0	0	126	25	1	0	0
F_B	100	25	0	1	0	127.2	25	0	1	0
E	266.4	110	0.337	0.285	0.378	431.6	110	0.339	0.362	0.299
R	166.4	92.4	0.54	0.45	0.01	304.3	94.1	0.48	0.51	0.01
P	100	137.8	0.0	0.01	0.99	127.2	140.3	0.0	0.01	0.99
L	378.3	92.4	0.54	0.45	0.01	555.3	94.1	0.48	0.51	0.01
Other Variables										
V	518.2 kmol/h					822 kmol/h				
U_{rxr}	6 m^3					6 m^3				

See Figure 1.8 and Nomenclature for variable descriptions

The active constraint set changes between Mode I and Mode II with four common active constraints (T_{rxr}^{MAX}, U_{rxr}^{MAX}, $x_C^{P,MIN}$ and $x_C^{R,MAX} = 1\%$). The given production rate constraint in Mode I is replaced by the V^{MAX} bottleneck constraint in Mode II. For as close an approach to the optimum as possible, the dynamically fastest regulatory layer pairings should be used for tight active constraint control. It is likely that the best regulatory layer pairings are different between Mode I and Mode II since the active constraint set changes. We thus need to synthesize appropriate best pairings for Mode I and Mode II operation and also a mechanism for reconfiguring the loops, if any, for a transition between Mode I and Mode II and vice versa. Given such a control system, the regulatory layer setpoint x_{rxrB}^{SP} may then be updated using the RTO approach summarized above.

4.3 Regulatory Layer Pairings for Mode I and Mode II

4.3.1 Mode I

In Mode I, we have the following soft constraints in addition to the specified throughput

$$T_{rxr} = T_{rxr}^{MAX},\ U_{rxr} = U_{rxr}^{MAX},\ x_C^P = x_C^{P,MIN} \text{ and } x_C^{R,MAX} = 1 \text{ mol\%}.$$

These constraints are treated as soft in the sense that small short-term constraint violation is acceptable and do not require any operator intervention or alternatively, invoking of overrides. The throughput manipulator (TPM) is conventionally located at a process fresh feed. Of the two fresh feeds, we choose the reactant *B* fresh feed flow setpoint as the TPM. The inventory control system is then oriented in the direction of process flow. We thus have reactor level control by manipulating the reactor outflow and a conventional dual ended composition control system on the column. Dual ended control is needed as a constant feed-to-reflux ratio policy requires significant over-refluxing to ensure the *C* leakage in the recycle stream remains small at ≤ 1 mol% over the envisaged disturbance space. The over-refluxing causes the boilup to be noticeably higher than minimum for nominal conditions implying noticeable suboptimality. Further, the distillate composition must be controlled as rectifying tray temperature control results in unacceptably large variability in the distillate impurity levels. The specific pairings on the column are as follows. The reflux drum and bottom sump levels are maintained by manipulating the distillate rate and bottoms rate, respectively. The column pressure is maintained by manipulating the condenser duty. A sensitive stripping tray temperature is controlled by manipulating the reboiler duty. Since regular product quality measurements are usually available, a composition controller holds x_C^P by manipulating the stripping tray temperature control loop setpoint. Further, a distillate *C* impurity controller adjusts the reflux rate to ensure x_C^R is maintained at its 1 mol% limit. On the reactor, the energy balance is closed by manipulating reactor cooling duty to hold T_{rxr}. Lastly, the fresh *A* feed (F_A) is maintained in ratio with the fresh B feed (F_B) so that F_A moves in tandem with F_B for stoichiometric balance. Any minor imbalance in the fresh feeds due to sensor bias will result in the excess component accumulating in the recycle loop. This slow drift in the recycle loop reactant inventory is prevented by holding x_{rxrB} via adjustments to the F_A/F_B ratio setpoint.

The Mode I regulatory control structure, as described above is shown in Figure 4.1 and is referred to as CS I. Note that the T_{rxr}, U_{rxr} and x_C^P loop pairings are the fastest possible and therefore would achieve tight control of the respective CVs. Simply setting $T_{rxr}^{SP} = T_{rxr}^{MAX}$, $U_{rxr}^{SP} = U_{rxr}^{MAX}$ and $x_C^{P,SP} = x_C^{P,MIN}$, on the corresponding loops, would tightly control these soft active constraints around their constraint limits. Further, by setting $x_C^{R,SP} = 1$ mol%, the C leakage in the recycle gets regulated around its 1 mol% limit.

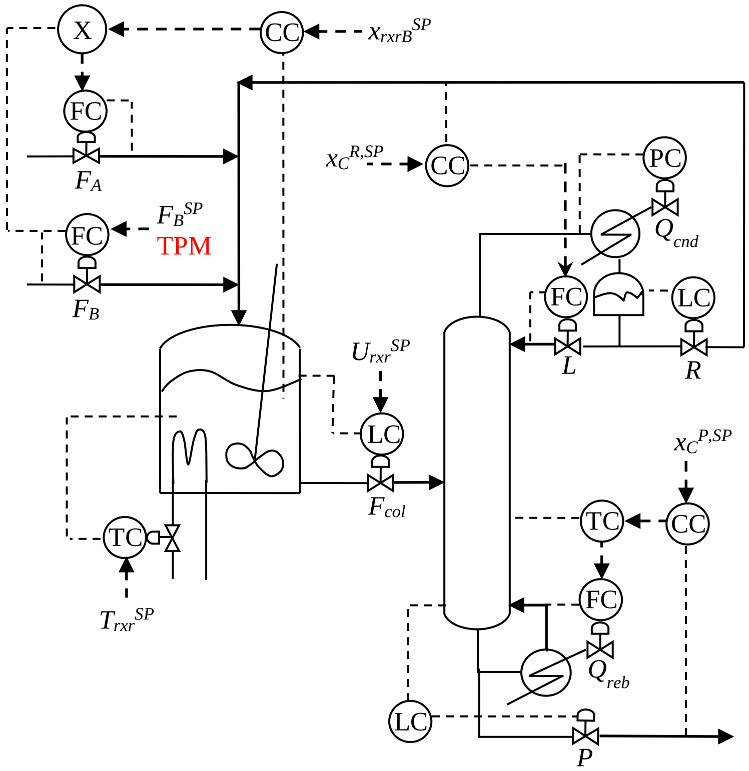
X
CC
x_{rxrB}^{SP}
FC
F_A
FC
F_B^{SP}
TPM
F_B
$x_C^{R,SP}$
CC
PC
Q_{cnd}
FC
LC
L
R
U_{rxr}^{SP}
LC
F_{col}
$x_C^{P,SP}$
TC
TC
CC
T_{rxr}^{SP}
FC
Q_{reb}
LC
P

Figure 4.1. Conventional control structure, CS1 for Mode I

4.3.2 Mode II

In Mode II, the maximum achievable throughput is limited by the column flooding limit, where the boilup exceeding V^{MAX} results in excessive liquid entrainment into the rising vapor, severely compromising the column separation efficiency. V^{MAX} is then a hard equipment capacity limit that must not be breached. For maximizing throughput, the column operation must be pushed as close as possible to the V^{MAX} limit without violating it (hard constraint). The average process operation must have sufficient back-off from the V^{MAX} limit so that the constraint is not breached. Clearly, the magnitude of the back-off is dependent on the severity of the transients in V. The lower the severity, the lower the back-off. In the limiting case of no transients in V, the average column operation boilup can be pushed to be at the V^{MAX} constraint (see Figure 4.2) with no back-off. These simple arguments suggest that the tightest possible control of V is desired so that the column can be operated at the hard bottleneck V^{MAX} constraint with negligible back-off. Such tightest possible control may be achieved by pairing boilup with the reboiler duty valve. With the reboiler duty valve thus paired for bottleneck constraint control, an alternative manipulation handle is needed for regulating the stripping tray temperature. The dynamically fastest manipulation handle, excluding reboiler duty (already paired), is the column feed and it is paired for stripping tray temperature control. Now, with the column feed already paired for stripping tray temperature control, an alternate pairing is needed for reactor level control. The appropriate "close-by" manipulation handle is the fresh B feed rate. With this pairing, as reactor level changes, both fresh feeds change since F_A is maintained in ratio with F_B. Thus, in Mode II, we have reboiler duty tightly regulating boilup for tight bottleneck constraint control and upstream regulatory pairings in the reverse direction of process flow. All other loop pairings are the same as the pairings in CS I. Figure 4.3 shows the Mode II regulatory control structure, also conveniently referred to as CS II.

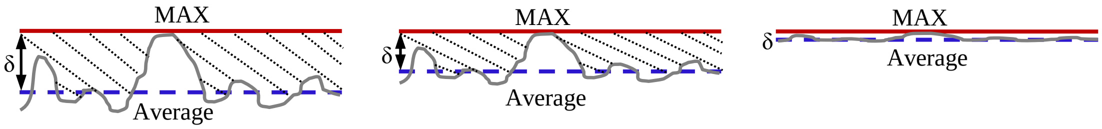

Figure 4.2. Back-off illustration

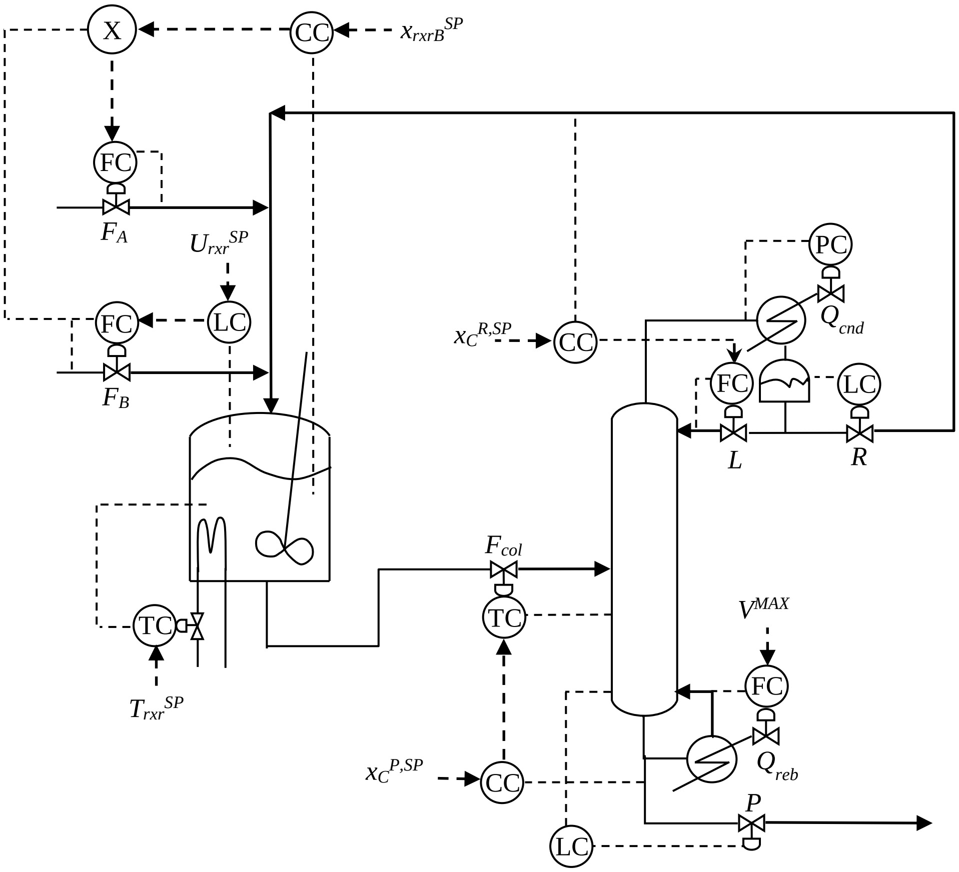
X
CC
x_{rxrB}^{SP}
FC
F_A
U_{rxr}^{SP}
FC
LC
F_B
TC
T_{rxr}^{SP}
PC
Q_{cnd}
$x_C^{R,SP}$
CC
FC
LC
L
R
F_{col}
TC
V^{MAX}
FC
Q_{reb}
$x_C^{P,SP}$
CC
P
LC

Figure 4.3. Control structure, CS2 for Mode II

4.4 Overrides for Mode I ↔ Mode II Transition

The conventional control structure, CS I, functions when the plant is away from the bottleneck capacity constraint, V^{MAX}, i.e. unconstrained operation. When the constraint V^{MAX} is hit, CS I must be reconfigured to CS II to minimize loss due to back-off from the V^{MAX} limit (Mode I to Mode II transition). Similarly, should the process operation move away from V^{MAX}, CS II loops must be reconfigured back to CS I (Mode II to Mode I transition). This CS I ↔ CS II reconfiguration of loops can be accomplished quite simply using overrides. The complete control system with the overrides is shown in Figure 4.4. It consists of three low selector blocks (LS_1, LS_2 and LS_3), a low stripping tray override temperature controller (OTC) on the column and a high reactor level override controller (OLC) on the reactor. The OTC setpoint is slightly below the nominal stripping tray temperature controller setpoint while the OLC setpoint is slightly above the nominal reactor level controller setpoint.

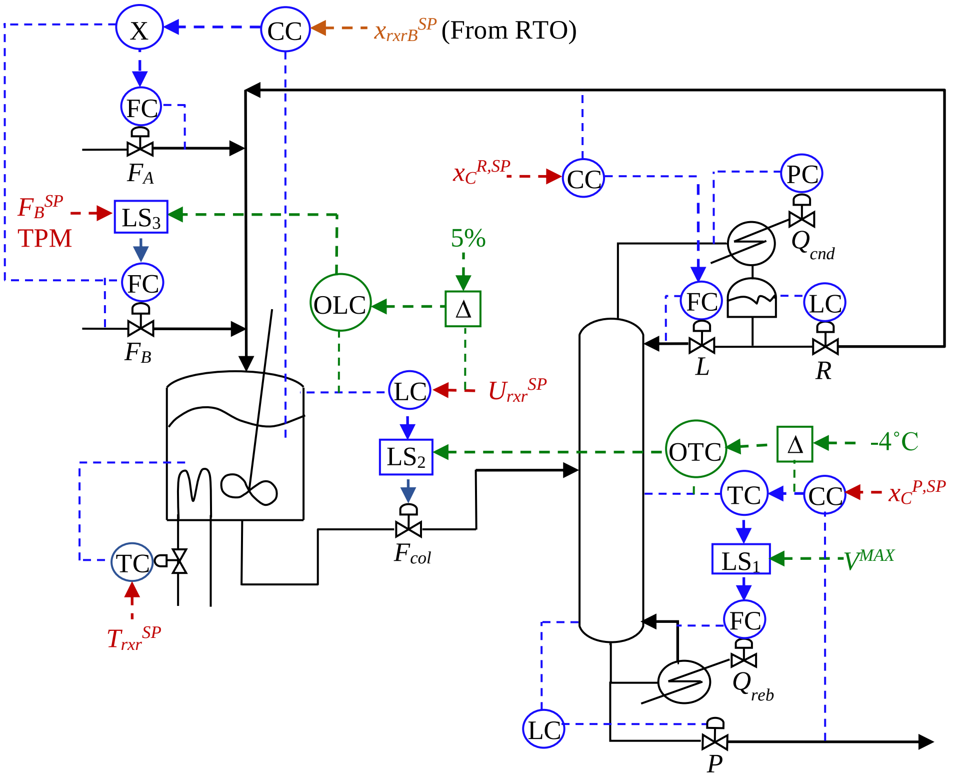
X
CC
x_{rxrB}^{SP} (From RTO)
FC
F_A
F_B^{SP}
TPM
LS_3
FC
F_B
OLC
Δ
5%
LC
U_{rxr}^{SP}
LS_2
F_{col}
TC
T_{rxr}^{SP}
$x_C^{R,SP}$
CC
PC
Q_{cnd}
FC
LC
L
R
OTC
Δ
-4°C
TC
CC
$x_C^{P,SP}$
LS_1
V^{MAX}
FC
Q_{reb}
LC
P

Figure 4.4. Override control structure for Mode I ↔ Mode II transition

To understand the functioning of the override control system, consider nominal Mode I process operation below V^{MAX}. Since $V < V^{MAX}$, LS_1 passes the nominal stripping tray temperature controller signal to the boilup controller. The reboiler duty thus changes to hold the stripping control tray temperature at its nominal setpoint. The OTC output then is high since its setpoint is slightly below nominal so that the column feed rate (OTC output) must be increased to decrease the tray temperature. The low selector, LS_2, then passes the nominal reactor level controller output to the column feed valve and column feed valve is under reactor level control (nominal operation). With the reactor level regulated around its nominal setpoint, the reverse acting high reactor level override controller output is high since level is below the OLC setpoint. The low selector, LS_3, then passes the operator desired F_B as the setpoint to the F_B controller. Thus under nominal conditions, F_B is the TPM with column feed and reboiler duty under nominal reactor level control and nominal tray temperature control respectively.

Now consider the situation where the operator slowly increases F_B to increase production. In consequence, the boilup will increase under nominal stripping tray temperature control. At some stage, the nominal temperature controller demanded boilup will exceed V^{MAX} and LS_1 will pass V^{MAX} as the setpoint to the boilup controller. Since the boilup is now fixed at V^{MAX} and not increasing as demanded, the stripping tray temperature will naturally start decreasing. In response, the OTC output will start decreasing and eventually become less than the nominal reactor level controller output. The manipulation of the column feed valve then passes to OTC which acts to cut the column feed rate. The decrease in the column feed rate would cause the reactor level to increase. In response, the OLC output will decrease to eventually reduce below the operator demanded F_B. LS_3 then passes the OLC output which acts to cut F_B. Thus when V^{MAX} goes active (Mode I to Mode II transition), the nominal CS I pairings are appropriately reconfigured to CS II with column feed under stripping tray temperature control and F_B under reactor level control. The CS II pairings act to appropriately reduce throughput.

Now consider Mode II to Mode I transition. As operator reduces F_B setpoint sufficiently to transition back to Mode I, LS_3 causes the operator input reduced F_B signal to be passed as the setpoint to the F_B controller. The reduced F_B causes the reactor level to decrease and the nominal reactor level controller output decreases sufficiently to eventually take up column feed valve manipulation. The reduction in column feed rate (at fixed boilup) causes the stripping tray temperature to increase and the nominal stripping tray temperature controller output decreases to eventually take up boilup manipulation through LS_1. The control structure configuration thus seamlessly transitions from CS II to CS I to effect the Mode II to Mode I transition.

Note that the OTC and OLC setpoints are, respectively biased slightly below and slightly above the respective nominal controller setpoints. A ramp in the setpoints is triggered to ensure the override setpoints become the same as the nominal setpoints whenever control passes from the nominal controller to the override controller. Similarly a complementary ramp is triggered whenever control passes from the override controller to the nominal controller. The implemented setpoint (override or nominal) then remains the same.

4.5 Mode I ↔ Mode II Switching in RTO Layer

In the RTO layer, the optimizer must switch optimization objectives for a Mode I ↔ Mode II transition in process operation. This switching should be automatic and independent of the operator. Consider process operation in Mode I at a high operator demanded throughput. Since the bottleneck constraint limit itself can change due to equipment degradation, it is entirely conceivable that while operating in Mode I, the bottleneck constraint goes active and the overrides then act to cut the throughput. The process operation has then transitioned from Mode I to Mode II. Even as the operator may believe the process is operating in Mode I, the RTO layer must automatically detect the transition from Mode I to Mode II and appropriately switch the optimization. On the other hand, it is also possible that the overrides get triggered for a short duration due to a transient disturbance and then the nominal controllers take back control as the disturbance subsides. In such cases, what optimization, Mode I or Mode II, should the RTO perform? Should RTO be allowed to make a setpoint update when the distinction between Mode I / Mode II operation is unclear? These simple arguments suggest the need for an algorithm to determine the current operating mode based on the current plant state and relevant immediate plant history. Given a clear indication of the operating mode, the RTO can then perform the appropriate optimization and regulatory layer setpoint update.

In this work, we follow the simplest of procedures for determining which optimization, Mode I or Mode II, is to be performed, based on the selected signal in LS_1, LS_2 and LS_3. In Mode I, LS_1, LS_2 and LS_3 should select, respectively, the nominal column temperature controller output, the nominal reactor level controller output and the operator input nominal throughput setpoint. In Mode II, LS_1, LS_2 and LS_3 should select, respectively, the V^{MAX} constraint signal, column override temperature controller output, and the reactor override level controller output. The current sampling period, is categorized as Mode I or Mode II if the LS_i (i = 1 to 3) selected signals for more than half the sampling period is as per the respective template. The appropriate optimization thus determined is performed by the optimizer.

4.6 Control System Tuning

The control loops are tuned as follows. The column pressure controller is PI and tuned aggressively for tight pressure control. Both the reflux drum and bottom sump level controllers are P only and use a gain of 2 (%/%) for effective filtering of flow transients. All flow controllers are PI and use a gain of 0.5 (%/%) and an integral time of 0.3 mins for a fast and snappy servo response. Similarly, the column boilup controller is PI and is tuned for a fast servo response. The controller output is lagged by 2 mins to account for reboiler heating dynamics. The nominal reactor level controller is PI and tuned for a slightly underdamped servo response. The override level controller is deliberately detuned slightly so that as far as possible, the nominal level controller is active. The override level setpoint is biased to be 5% above the nominal setpoint. On the column, the nominal stripping tray temperature controller is tuned for slightly underdamped response. The temperature measurement is lagged by 2 mins to account for sensor dynamics. The product purity and recycle impurity measurements have a dead time of 5 mins each and a sampling time of 5 mins each. The corresponding composition controllers are tuned for a slightly underdamped servo response. Similar to the reactor override level controller, the override temperature controller is deliberately detuned slightly. Its setpoint is biased to be 4°C below the nominal temperature setpoint. Appropriate triggered ramps are applied to the override/nominal reactor level or column temperature controllers so that the setpoint of the controller that is moving the control valve remains constant (except for the brief duration of the ramp) and there is no unnecessary back-off in the implemented level/temperature setpoint. The ramps get triggered whenever the selector block switches the selected control signal. Note that all controllers that are PI and compete for control through a low select block use external reset feedback [10-11] for bumpless taking over and giving up of control. Table 4.2 reports the salient regulatory layer controller parameters used to generate dynamic results.

Table 4.2. Salient controller parameters for CS1/CS2[*, #, $]

CV	CS1/CS2		PV Range[&]	MV Range[&]
	K_C	τ_i(min)		
x_{rxrB}	1.5/1.5	100/100	0.05-0.44	0.5-1.5
T_{rxr}	3/3	10/10	100-120°C	$2\text{x}10^6$kJ/h
U_{rxr}	2/2	15/30	100%	100%
T_{col}^S	1/1	5/10	120-150°C	200-900kmol/h
x_C^R	0.1/0.1	60/60	0.005-0.03	100-800kmol/h
x_C^P	0.08/0.08	80/80	0.98-0.999	120-150°C

[*] All level loops use $K_C = 2$ unless otherwise specified. [#]Pressure/flow controllers tuned for tight control.

[$] All compositions use 5 min dead time and sampling time. All temperature measurements are lagged by 2 min.

[&] Minimum value is 0, unless specified otherwise.

As discussed earlier, the plant is inherently dynamic in nature and is never truly at steady state. The inherently transient measurement data must therefore be appropriately processed to infer near steady values of process variables that are required in the steady state model fitting exercise for RTO. Here, we take the simplest possible approach of averaging out the measurement over an appropriate time window and simply setting the steady value to this average value. The time window duration is then a parameter that must be chosen appropriately. If it is too small, the process variable steady state estimate will be poor and the RTO moves are likely to be erratic. On the other hand, if the duration is too long, the RTO moves get unnecessarily delayed implying a slower approach to optimum. We tested the RTO scheme using time window durations of 6, 8, 10 and 12 hrs and found an 8 hr window to be a reasonable choice. Thus the average of the process variable measurement data over the past 8 hours is used as an estimate of its current steady state value and the unknown model parameters are adjusted to best fit this current steady state. The details of the fitting exercise have already been presented in previous chapter and therefore not repeated here for brevity.

4.7 Dynamic Results

A crucial requirement for success of the RTO scheme is a robust regulatory layer control system that properly reconfigures regulatory control loops between Mode I and Mode II transitions. Note that the transition may be deliberate, e.g. management instructs maximum production due to favorable market conditions, or inadvertent, e.g. V^{MAX} bottleneck limit reduces below nominal temperature controller requested boilup due to slow clogging of trays. We therefore first test the regulatory layer control system (including overrides) closed loop performance (no RTO) to confirm robustness and follow it up with RTO performance evaluation.

4.7.1 Regulatory Layer Performance

Consider steady process operation in Mode I with F_B^{SP} = 100 kmol/h. To effect a transition to Mode II (maximum throughput operation), F_B^{SP} is ramped up at the rate of 10 kmol/h/h from 100 kmol/h to 140 kmol/h. The process is allowed to settle at the new steady state corresponding to V^{MAX} as the bottleneck constraint. Post settling at the new steady state, F_B^{SP} is ramped back down to 100 kmol/h. The closed loop response to this Mode I → Mode II → Mode I transition sequence is shown in Figure 4.5. As F_B^{SP} is ramped up, nominal column temperature controller output increases beyond V^{MAX} so that LS_1 implements V^{MAX}. The tray temperature then dips and the override temperature controller output reduces to take over column feed manipulation and cut the column feed. Simultaneously, the override and nominal temperature controller setpoints are ramped up so that the override setpoint is the same as the nominal setpoint when the nominal controller has control of the boilup. The reduced column feed rate causes the reactor level to increase and the override reactor level controller output decreases to take over F_B valve manipulation. Simultaneously, the nominal and override level controller outputs are ramped down so that the override setpoint remains the same as the nominal level controller setpoint when it has control of the column feed. In this way the regulatory layer pairings are reconfigured from CS I to CS II with nominal setpoint values. The time points where the override takes over manipulation of a valve/setpoint are clearly shown in the Figure. The process flows settle down smoothly at the new steady state (throughput: 121.2 kmol/h) in about 8 hours.

Post initiation of the F_B^{SP} rampdown back to 100 kmol/h, the nominal reactor level controller and the nominal column temperature controller take over manipulation of the column feed and boil-up respectively to reconfigure the control system back to CS I. The time points where the nominal controller takes up valve/setpoint manipulation is clearly shown in the Figure. An appropriate ramp in the nominal and override setpoints immediately post taking over of control ensures the implemented setpoints remain the same between CS I and CS II. The process flows smoothly settle down at the Mode I steady state in ~ 15 hours. Notice that during the entire period, the product quality remains tightly controlled with ±0.1% of its 99 mol% base-case value. These results clearly show that the regulatory control system is robust with smooth plantwide transients over a large operating window and should respond well to x_{rxrB}^{SP} changes demanded by the RTO layer.

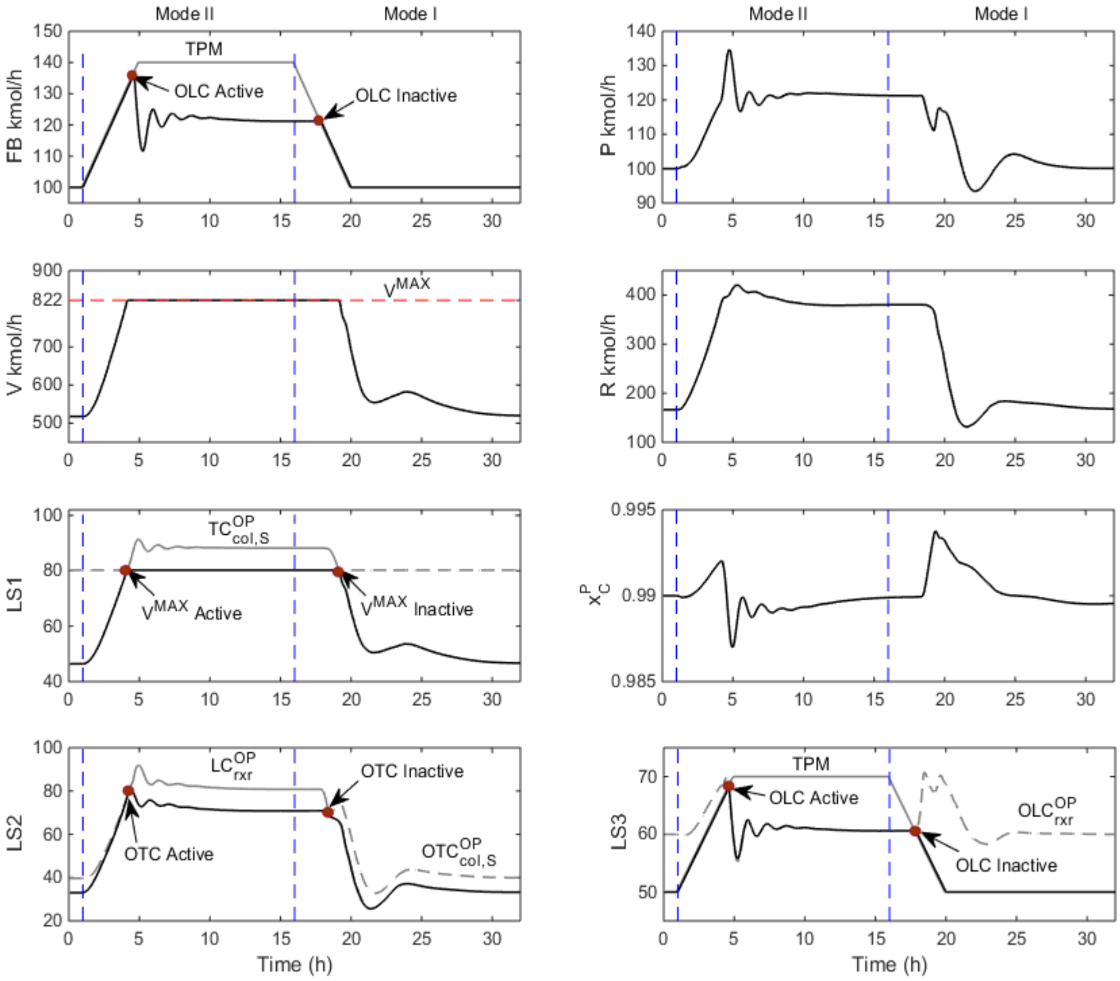

Figure 4.5. Mode I ↔ Mode II transition without RTO

4.7.2 RTO Performance

Dynamic RTO results are now presented for Mode I and Mode II operation for various disturbance scenarios. These disturbance scenarios include a ±20% change in throughput (Mode I only), a ramped decrease in the purity of the fresh *A* feed by 10 mol%, a slow ramped decrease of 30% in the plant reaction rate constant and a ramped 30% decrease in the column V^{MAX} limit to effect an unforeseen Mode I to Mode II transition.

For each of the enumerated disturbance scenarios, we performed rigorous Aspen Hysys dynamic simulations to obtain (a) the plant optimum value, x_{rxrB}^{opt}, and final steady state plant economic objective function J^{opt}_{SS}; (b) the RTO model converged value of $x_{rxrB}^{m,opt}$ and corresponding final steady state plant economic objective function J_{SS}. The number of RTO iterations taken to reach within 5% of $x_{rxrB}^{m,opt}$ are also noted. A simple dynamic simulation is also performed where the disturbance occurs as a step at t = 0 and x_{rxrB}^{SP} is immediately set equal to the plant optimum value (i.e. $x_{rxrB}^{SP} = x_{rxrB}^{opt}$ at t = 0). This corresponds to perfect reoptimization of the unconstrained regulatory layer setpoint, x_{rxrB}^{SP}. If the RTO iterations take *T* hrs to converge to within 5% of $x_{rxrB}^{m,opt}$, then the metric

$$Loss_{\%} = \frac{\left|\left[\int_0^T Jdt\right]^{opt} - \left[\int_0^T Jdt\right]^{RTO}\right|}{\left[\int_0^T Jdt\right]^{opt}} \times 100$$

where the superscripts 'opt' and 'RTO' denote perfect reoptimization and real time optimization of x_{rxrB}^{SP}, respectively, quantifies the % loss from perfect reoptimization in the transient period T.

Table 4.3 reports x_{rxrB}^{opt}, $x_{rxrB}^{m,opt}$, J^{opt}_{SS}, J_{SS} and $\text{Loss}_{\%}$ for the different disturbance scenarios. As observed in Part I, the RTO converged x_{rxrB} is driven quite close to the actual plant optimum so that the steady state economic loss (J_{SS} - J^{opt}_{SS}) is quite small (<0.1%). Further the economic loss during the transient period is also acceptably small with $Loss_{\%}$ being < 1% for all the considered disturbances. These results reconfirm the main finding from Part I, that the proposed

RTO method drives the plant operation very close to the economic optimum. In particular notice that even as 8 hr transient average data are used as estimates for the plant steady state, the RTO still drives x_{rxrB} very close to the actual plant optimum. Further, the loss during the transient period is also acceptably small. As an example, Figure 4.6 contrasts the transient approach to optimum using RTO with perfect reoptimization of x_{rxrB} for a 10% decrease in reaction rate constant in Mode I and Mode II operation.

Table 4.3. Quantitative comparison of RTO with optimal operation for different disturbance (step change) scenarios

	Disturbances	x_{rxrB}^{opt}	$x_{rxrB}^{m,opt}$	J^{opt}_{SS}	$J^{m,opt}_{SS}$	$Loss_{\%}$
Mode I	$TP_{+20\%}$	0.340	0.34	729.08	729.08	0.00
	$TP_{-20\%}$	0.222	0.223	361.18	361.39	0.06
	CC_{F_A}	0.252	0.251	433.33	433.44	0.03
	CC_{F_B}	0.318	0.316	642.03	642.10	0.01
	$k_{90\%}$	0.314	0.308	569.61	570.02	0.07
Mode II	TP^{MAX}	0.362	0.361	127.35	127.35	0.00
	CC_{F_A}	0.362	0.355	127.35	127.30	0.04
	CC_{F_B}	0.362	0.36	127.35	127.35	0.00
	$k_{90\%}$	0.376	0.372	119.71	119.69	0.02

TP: Throughput change CC_{F_A} or CC_{F_B}: F_A or F_B composition change $k_{90\%}$: 90% catalyst activity

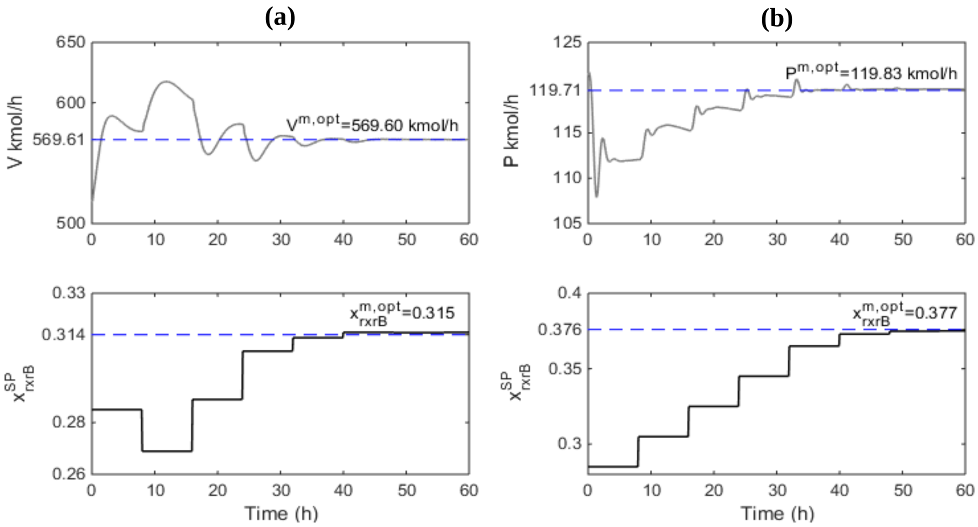

Figure 4.6. Transient approach to optimum for $k_{90\%}$ for (a) Mode I (b) Mode II

For a more realistic evaluation of the proposed RTO scheme, we consider process operation in the presence of routine variability along with sustained disturbances. Process variability in the form of transient time-series variation in the fresh *B* feed composition is simulated. The fresh *B* feed mol fraction is varied as a random walk between 90-100 mol% *B*. In response, all internal plant flows will exhibit transient variability and the plant will operate around a steady state without ever being truly steady. We distinguish between two types of disturbances. In the first type, the disturbance is a fast ramp from one value to another value. An example would be a change in throughput or in a fresh feed composition. In the second type, the disturbance is a very slow ramp implying quasi-steady process operation. Slow equipment degradation such as catalyst deactivation is an example. Table 4.4 tabulates the specific disturbances evaluated with time series variability in the fresh *B* feed composition.

Table 4.4. Disturbance scenarios evaluated

	Disturbances	Period (days)	Type	Step Length/ Ramp Rate
Mode I	TP	10	Step	±20%
	CC_{F_B} or CC_{F_A}	10	Step	-10%
	$k_{100\rightarrow 70\%}$	180	Slow Ramp	-18750 $kmol.m^{-3}.s^{-1}/h$
Mode II	TP^{MAX}	10	-	-
	CC_{F_B} or CC_{F_A}	10	Step	-10%
	$V^{MAX}{}_{70\rightarrow 100\%}$	10	Fast Ramp	+100 kmol/h/h
	$V^{MAX}{}_{100\rightarrow 70\%}$	30/30	Ramp/Constant	-0.3425 kmol/h/h
	$k_{100\rightarrow 40\%}$	360	Slow Ramp	-18750 $kmol.m^{-3}.s^{-1}/h$
Mode I → Mode II → Mode I		5→10→5	Ramp	±10 kmol/h/h

$V^{MAX}{}_{100\%}$ = 822 kmol/h ; $k_{100\%} = 2.7\times 10^8$ $kmol.m^{-3}.s^{-1}$

TP: Throughput change; CC_{F_A} or CC_{F_B}: F_A or F_B composition change; $k_{X\rightarrow Y\%}$: X to Y% catalyst activity change

For the fast ramp disturbance from one value to the other, we simulated the plant for 10 days continuous operation in Mode I or Mode II post disturbance with RTO and without RTO (i.e. no change in x_{rxrB} setpoint). The pre-disturbance x_{rxrB} setpoint is at its pre-disturbance optimum value. As the gold standard of optimal operation for the fast disturbance, we also simulated process operation with x_{rxrB} at its actual optimum value corresponding to the new mean operating condition. Note that since the feed composition exhibits variability over time, strictly speaking, optimal operation would require x_{rxrB} to vary over time. However, since the feed composition variability is short term (small time constant compared to RTO time scale) and around a mean value, a revised constant x_{rxrB} value corresponding to new mean operating condition of the plant is considered a very good approximation of the optimum x_{rxrB} time trajectory. On the other hand, for a very slow ramped disturbance, the optimal operation gold standard would require x_{rxrB} to vary as an appropriate time trajectory. This gold standard is obtained from a look-up table that tabulates the plant optimum x_{rxrB} over the range of the slow ramped disturbance. In the dynamic simulation, the revised optimum x_{rxrB} from the look-up table is input to the plant every 5 mins.

A quantitative comparison of the economic performance of RTO with the gold standard and constant x_{rxrB} setpoint operation is provided in Table 4.5 for both the fast and slow disturbances. For all the fast disturbances in Mode I, namely, a ± 20% throughput change and a 10 mol% additional A (B) impurity in the fresh B (A) feed, the average boilup over 10 days of operation using RTO is only very slightly (<1%) above the gold standard. On the other hand, for process operation with no change in x_{rxrB} setpoint, the average boilup over 10 days of operation is noticeably (up to ~9%) higher than the corresponding average boilup using RTO. The difference is significant particularly in the direction of a production increase due to steady state process nonlinearity (snowball effect[12]).

The data in the Table also shows that for the fast disturbance of a fresh feed composition change in Mode II, assuming that x_{rxrB} is at its optimum value before the occurrence of the disturbance, the maximum achieved throughput with and without RTO is the same. This is expected as the regulatory control system, CS II, pulls in the appropriate amount of fresh feeds to maintain $V = V^{MAX}$. The achieved production thus remains the same with the fresh *A* and fresh *B* rates readjusting appropriately under CS II inventory control. Even so, the RTO is useful in Mode II to adjust x_{rxrB} to the appropriate value that maximizes production. The value is not known *apriori*. Indeed, if the process is operated at the base-case Mode I optimum value of x_{rxrB} and transitioned to Mode II, the loss in production due to no reoptimization of x_{rxrB} is ~7%, which is significant.

The other fast Mode II disturbance is a quick increase in the V^{MAX} capacity constraint e.g. due to injection of cleaning agents into the column that quickly unclog choked tray valves. The data in the Table shows that the maximum achieved production over 10 days of operation post disturbance using RTO is only 0.5% less than the gold standard. For constant x_{rxrB} setpoint operation, on the other hand, the maximum production is a noticeable 2.2% lower than RTO.

For the very slow disturbance of a 30% ramped decrease in the reaction rate constant over 6 months with Mode I plant operation, the average column boilup using RTO is <0.3% higher than the corresponding gold standard value. On the other hand, if the x_{rxrB} setpoint is maintained at its base-case optimum value, the boil-up continues to increase over time with the column approaching its flooding limit at ~4.7 months. At this point, the overrides switch the control system from CS I to CS II to cut the fresh feed rate and reduce production such that the column operates at V^{MAX}. The total production over 6 months is therefore lower compared to RTO operation by ~6%. Also, the per kg product reboiler duty is higher by about 12%. By adjusting x_{rxrB} to reduce the boilup to near minimum, RTO helps maintain the desired production over 6 months of continuous operation without the column breaching its flooding limit. Compared to constant setpoint operation, RTO achieves both higher total production and lower reboiler steam consumption. Figure 4.7 compares the transient response of salient PVs over 6 months operation using RTO x_{rxrB} updates and constant x_{rxrB} setpoint operation for the very slow reaction rate constant decrease disturbance. Expectedly, for both with and without RTO, the boilup exhibits an increasing trend since maintaining production for a lower kinetic rate constant requires higher recycle. Also, the boilup with RTO updates for x_{rxrB} is consistently lower than for constant x_{rxrB} operation. Further, notice the slow decrease in production post boilup hitting the V^{MAX} constraint for constant x_{rxrB} operation.

In Mode II, quantitative results for the same very slow kinetic rate constant decrease disturbance suggest that the average maximum achieved production using RTO is only 0.07% less than the gold standard (see Table 4.5). On the other hand, for constant setpoint operation with x_{rxrB} = 0.362 (initial plant optimum value), the average achieved maximum production is ~2% lower than for RTO. The transient response of salient PVs for this disturbance scenario is shown in Figure 4.8. Expectedly, the production rate decreases slowly due to the reduction in the rate constant for process operation both with and without RTO. The rate of decrease in production with RTO is however slower as the RTO slowly increases the x_{rxrB} setpoint in response to the slowing reaction rate.

Table 4.5. Economic comparison for disturbance scenarios

	Disturbances	J^{RTO}	J^{opt}	J^{NoRTO}
Mode I	$TP_{+20\%}$	664.81	658.88	723.60
	$TP_{-20\%}$	338.38	336.07	350.40
	CC_{F_B}	400.04	398.91	403.08
	CC_{F_A}	579.89	576.28	592.52
	$k_{100\rightarrow 70\%}$	559.86	558.27	627.00
Mode II	TP^{MAX}	126.62	127.31	118.18
	CC_{F_B}	126.58	127.30	118.11
	CC_{F_A}	126.20	127.29	118.18
	$V^{MAX}_{70\rightarrow 100\%}$	126.61	127.26	123.88
	$V^{MAX}_{100\rightarrow 70\%}$	111.3	111.6	109.2
	$k_{100\rightarrow 40\%}$	101.30	101.37	99.39
Mode I → Mode II → Mode I		V=486.41 P=125.99	V=483.20 P=126.80	V=482.57 P=117.88

$V^{MAX}_{100\%}$ = 822 kmol/h ; $k_{100\%}$ = 2.7×10^8 kmol.m^{-3}.s^{-1}

TP: Throughput change; CC_{F_A} or CC_{F_B}: F_A or F_B composition change; $k_{X\rightarrow Y\%}$: X to Y% catalyst activity change

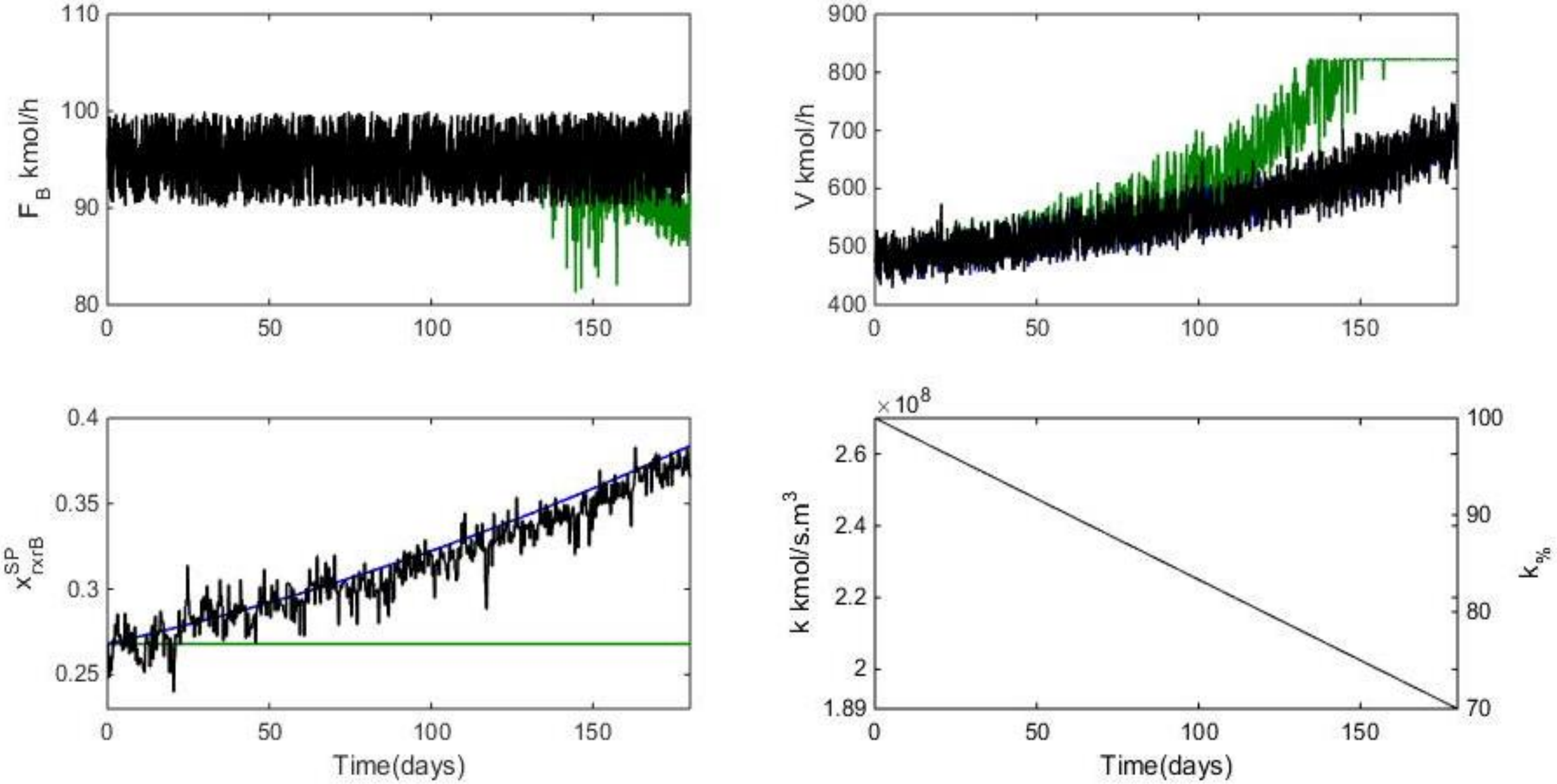

Figure 4.7. Mode I operation for slow decay in catalyst activity over 6 months

— RTO — Gold standard — Constant SP

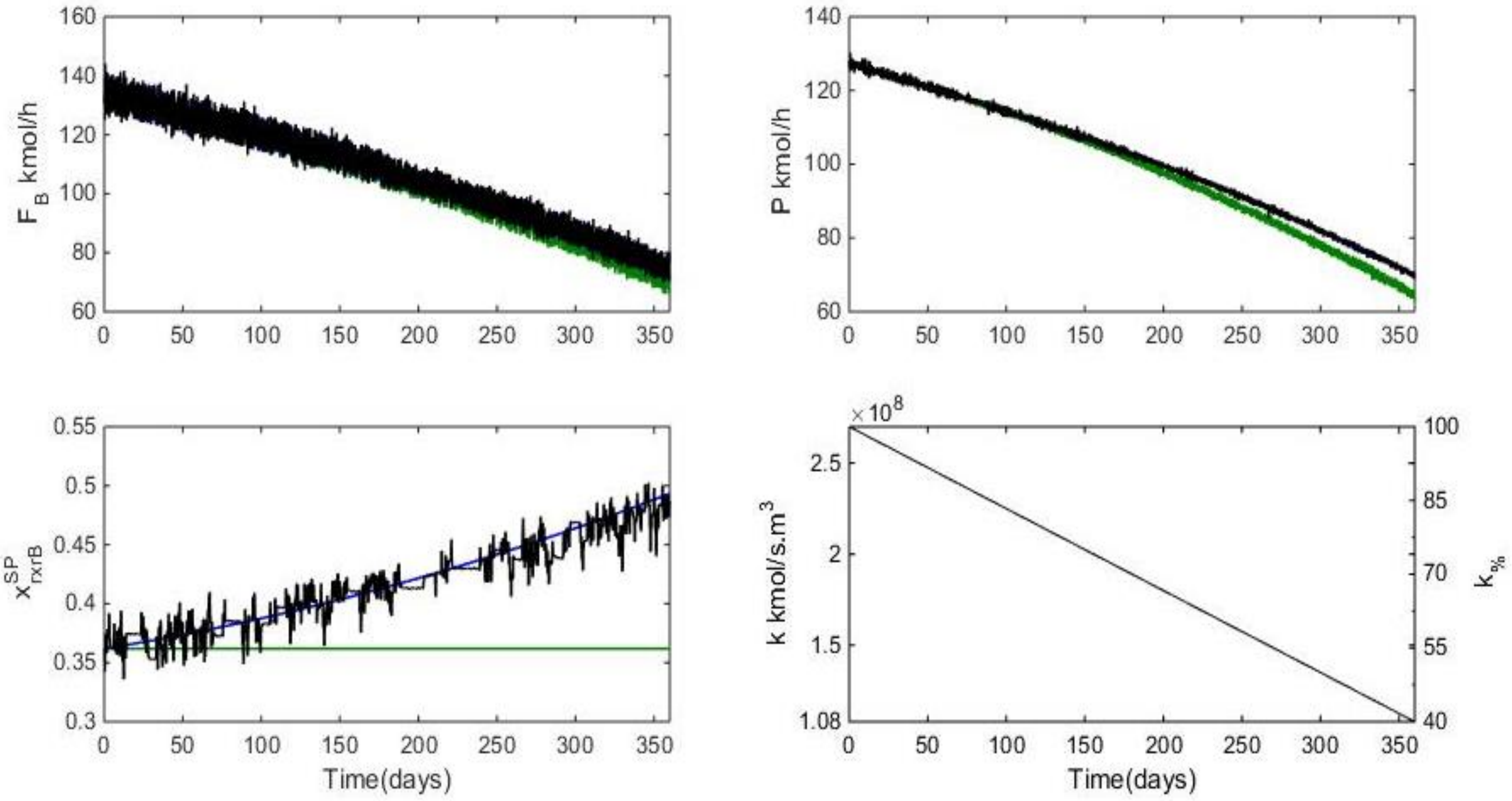

Figure 4.8. Mode II operation for slow decay in catalyst activity over one year

—— RTO —— Gold standard —— Constant SP

The other very slow disturbance considered, applicable to Mode II operation, is a decrease in the bottleneck constraint, V^{MAX}, due to gradual clogging of trays. Specifically, the V^{MAX} constraint is ramped down by 30% from 822 kmol/h to 575 kmol/h over a month with constant V^{MAX} thereafter. The data in Table 4.5 clearly shows that the maximum achieved throughput over a month of operation using RTO is 0.3% lower than the gold standard. On the other hand, if x_{rxrB} is not changed from its initially optimum value of 0.362, the achieved maximum throughput is 1.9% lower than RTO, which again is noticeable.

The final closed loop performance evaluation here is of a transition from Mode I to Mode II and then back to Mode I. Specifically, the process is operated in Mode I (average throughput ≈ 95 kmol/h; due to average 5% A impurity in F_B) for 5 days at which point the CS I fresh B feed rate setpoint (TPM) is increased from 100 kmol/h to 145 kmol/h as a fast ramp at the rate of 10 kmol/h/h to transition to Mode II. In response, the column maximum boilup constraint is hit (maximum production) and the overrides reconfigure the regulatory control system to CS II to appropriately cut the fresh feeds. The process is operated in Mode II for 10 days and then the F_B setpoint is ramped down back to 100 kmol/h to transition back to Mode I operation with the nominal controllers taking back manipulation of control valves from the overrides (CS I). The gold standard x_{rxrB} trajectory here is the Mode I optimum value for the first 5 days followed by an F_B ramp-up synchronized ramp up the Mode II optimum value for the next 10 days and finally an F_B ramp down synchronized ramp down back to the Mode I optimum value for the final 5 days. Figure 4.9 contrasts transient response of salient PVs for the gold standard with RTO based x_{rxrB} updates. The RTO decision logic to distinguish between Mode I vs Mode II optimization remains active throughout. Notice from the Figure that the RTO automatically updates x_{rxrB} to keep it close to the Mode I and Mode II optimum values so that the Mode I operation boilup and the Mode II operation production remain very close to the corresponding gold standard values. Indeed, the average boilup using RTO for the first five days and the last five days is only 0.7% higher than the gold standard.

Similarly, the average production achieved using RTO from day 6 to day 15 is only 0.6% lower than the gold standard. These results highlight the RTO scheme automatically distinguishes between Mode I and Mode II operation and closely tracks the Mode I and Mode II x_{rxrB} optimum.

4.8 Discussion

We note that the TPM in Mode I is at the fresh *B* feed rate. When the V^{MAX} bottleneck constraint is encountered, the inventory control loops upstream of the bottleneck need to be reconfigured to be in the opposite direction of flow. This reconfiguration can be avoided if the TPM is moved to the bottleneck constraint itself, i.e., the boilup, *V,* is used as the TPM. This idea has been explored in the literature[13-14]. To understand the same, consider Mode II process operation with $V = V^{MAX}$ with the control structure in Figure 4.3 being operational. To reduce throughput, we reduce V^{SP} below V^{MAX}. This would cause the column temperature to decrease, which would cause the column temperature controller to reduce the column feed rate. The reactor level would then increase and the reactor level controller would in turn reduce the fresh feed intake to reduce throughput. A complementary argument holds for increasing throughput till V^{MAX}. This has the advantage that the same basic regulatory control structure holds in both Mode I and Mode II and there is no need for reconfiguring inventory loops using overrides or alternatively, a split range controller. We have chosen to take the Mode I TPM at a fresh feed only to reflect prevalent industrial practice, which complicates constraint handling.

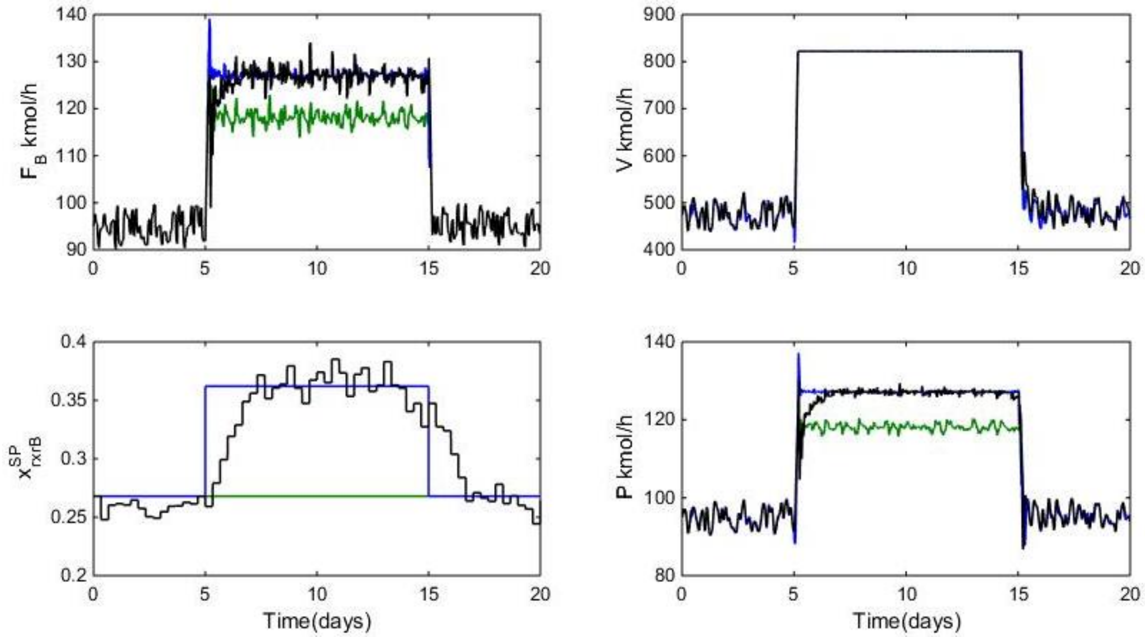

Figure 4.9. Mode I → Mode II → Mode I transition

—— RTO —— Gold standard —— Constant SP

The RTO approach evaluated here consists of the basic regulatory layer loops with overrides for reconfiguring appropriate loops due to the loss in a control degree of freedom as the process hits a capacity constraint. In devising the complete control system with the overrides, one has to necessarily think through the "taking over" and "giving up" of control by the overrides to ensure the reconfigured control strategy moves the process operation appropriately as the constraint is encountered. This is the conventional way of handling constraints. Instead, one may choose to apply MPC where handling constraints is so much easier and natural. Indeed modern practitioners are likely to prefer MPC, a technology that is now well matured, over the conventional approach presented here. The proper formulation of the MPC problem, including prioritization of control objectives in light of a constraint(s) going active, however would still require the control system design engineer to think through the direction in which the process needs to be moved and the appropriate strategy (loop reconfiguration) in order to achieve it. Indeed, in his perspective paper, Downs[15] strongly recommends viewing MPC systems as a "control strategy change agent instead of an algorithm for improved high performance control". The need for control strategy changes is much more persistent to deal with the various operating modes of a plant. A fair comparison between conventional and MPC control systems are quite rare. In their seminal work on comparing the performance of non-linear MPC with a conventional decentralized override control system for the Tennessee Eastman challenge process[16], Ricker and co-workers[17-18] found that the performance of the two systems is very similar. They also found that tuning the overrides and the MPC for handling the constraints was equally important and time consuming in both approaches. In other words, regardless of the approach, MPC or conventional overrides, there is no short cut to carefully thinking through and figuring out the appropriate control strategy to be deployed on encountering a constraint. Thus, in a sense, what this article does is walk the reader through the control strategy design thinking in light of active constraints that must accompany the synthesis of an economic plantwide control system encompassing the lower regulatory and higher supervisory and optimizing layers, regardless of whether conventional overrides or MPC is used for handling constraints.

An issue with the standard two step RTO approach considered here is that the converged RTO optimum and the actual plant optimum may be substantially different in the presence of plant-model mismatch due to model inadequacy or inappropriate parameter fitting strategy. Recent work by Bonvin and coworkers[19-22] has shown that the model optimum can be forced to converge to the plant optimum by solving a modified optimization problem. The so called modifiers are obtained from the difference between the optimality condition for the model and estimated for the plant. The modifiers are added to the constraints and cost objective and the modified optimization problem is solved, which is formulated in a manner that drives the difference between the plant and model optimality conditions to zero via adaptation of the modifiers. The RTO thus converges to the actual plant optimum. We hope to evaluate modifier adaptation based RTO in a future study.

The other popular approach for managing an economically important unconstrained dof is the notion of a self optimizing controlled variable (SOCV)[23-26]. By definition, an SOCV when held constant results in acceptably small loss in the face of expected disturbances[24]. Process operation with the SOCV at constant setpoint thus achieves near optimal management of the unconstrained dof. An optimization problem thus gets transformed into a control problem. We are currently in the process of quantitatively evaluating promising self-optimizing control strategies for the considered process and hope to report the same as a separate article in the near future.

4.9 Conclusions

The dynamic evaluation of the RTO approach shows that even as the plant is never truly at steady state, the developed steady state modeling approach along with bottleneck capacity constraint handling using overrides, drives the unconstrained regulatory layer setpoint very close to the actual plant optimum. The results show that the economic benefit over continuous operation in Mode I (energy minimization) and Mode II (throughput maximization) can be as much as 2-9% over constant setpoint operation for the various fast/slow sustained disturbance scenarios. The proper design of the overrides for control strategy redesign in Mode I ↔ Mode II transitions is particularly important to the success of the approach.

References

(1) Darby, M. L.; Nikolaou, M.; Jones, J.; Nicholson, D. RTO: An overview and assessment of current practice. *J. Process Control* 2011, 21 (6), 874-884.

(2) Forbes, J. F.; Marlin, T. E.; Macgregor, J. F. Model adequacy requirement for optimizing plant operations. *Comput. Chem. Eng.* 1994, 18(6), 497-510.

(3) Duvall, P. M.; Riggs, J. B. On-line optimization of the Tennessee Eastman challenge problem. *J. Process Control* 2000, 10, 19-33.

(4) Mercangöz, M.; Doyle III, F. J. Real-time optimization of the pulp mill benchmark problem. *Comput. Chem. Eng.* 2008, 32, 789-804.

(5) Lid, T.; Strand, S. Real-time optimization of a cat cracker unit. *Comput. Chem. Eng.* 1997, 21, S887-S892.

(6) Zhijiang, S.; Jinlin, W.; Jixin, Q. Real-time optimization of acetaldehyde production process. *Dev. Chem. Eng. Mineral Process* 2005, 13(3/4), 249-258.

(7) Kumar, V.; Kaistha, N. Real time optimization of a reactor-separator-recycle process I: Steady state modelling. *Ind. Eng. Chem. Res.* 2018, 57 (37), 12429-12443.

(8) Jagtap, R.; Pathak, A. S.; Kaistha, N. Economic Plantwide Control of the Ethyl Benzene Process. *AIChE J*. 2013, 59 (6), 1996-2014.

(9) Jagtap, R.; Kaistha, N.; Skogestad, S. Economic plantwide control over a wide throughput range: A systematic design procedure, *AIChE J*. 2013, 59 (7), 2407-2426.

(10) Jagtap, R.; Kaistha, N.; Luyben, W. L. External integral feedback for constrained economic process, *Ind. Eng. Chem. Res.* 2013, 52, 9654-9664.

(11) Shinskey, F. G. *Process Control Systems: Application, Design and Adjustment*. McGraw-Hill, New York, 1967.

(12) Luyben, W. L. Snowball effects in reactor/separator processes with recycle. *Ind. Eng. Chem. Res.* 1994, 33, 299-305.

(13) Kanodia, R.; Kaistha, N. Plant-wide control for throughput maximization: A case study. *Ind. Eng. Chem. Res.* 2010, 49(1), 210-221.

(14) Kumar, V.; Kaistha, N. Hill climbing for plantwide control to economic optimum. *Ind. Eng. Chem. Res.* 2014, 53 (42), 16465−16475.

(15) Downs, J.J. Linking control strategy design and model predictive control, *AIChE Symposium Series* 2002, 98 (326), 328-341.

(16) Downs, J. J.; Vogel, E. F. A plantwide industrial process control problem. *Comput. Chem. Eng.* 1993, 17, 245-255.

(17) Ricker, N. L.; Lee, J. H. Nonlinear model predictive control of the Tennessee Eastman challenge process. *Comput. Chem. Eng.* 1995, 19, 961-981.

(18) Ricker, N. L. Decentralized control of the Tennessee Eastman challenge process. *J. Process Control* 1996, 6, 205-221.

(19) Marchetti, A.; Chachuat, B.; Bonvin, D. Modifier-adaptation methodology for real-time optimization. *Ind. Eng. Chem. Res.* 2009, 48(13), 6022-6033.

(20) Chachuat, B.; Srinivasan, B.; Bonvin, D. Adaptation strategies for real-time optimization. *Comput. Chem. Eng.* 2009, 33(10), 1557-1567.

(21) Marchetti, A.; Chachuat, B.; Bonvin, D. A dual modifier-adaptation approach for real-time optimization. *J. Process Control* 2010, 20(9), 1027-1037.

(22) François, G.; Bonvin, D. Use of convex model approximations for real-time optimization via modifier adaptation. *Ind. Eng. Chem. Res.* 2013, 52(33), 11614-11625.

(23) Skogestad, S. Self-optimizing control: the missing link between steady-state optimization and control. *Comput. Chem. Eng.* 2000, 24, 569-575.

(24) Skogestad, S. Plantwide control: The search for the self-optimizing control structure. *J. Process Control* 2000, 10(5), 487-507.

(25) Larsson, T.; Hestetun, K.; Hovland, E.; Skogestad, S. Self-optimizing control of a large-scale plant: The Tennessee Eastman process, *Ind. Eng. Chem. Res.* 2001, 40(22), 4889-4901.

(26) Jäschke, J.; Skogestad, S. NCO tracking and self-optimizing control in the context of real-time optimization. *J. Process Control* 2011, 21(10), 1407-1416.

Chapter 5

Invariants for Optimal Operation of a Reactor-Separator-Recycle Process

This Chapter is based on the paper "Invariants for Optimal Operation of a Reactor-Separator-Recycle Process" submitted to the Journal of Process Control.

In this Chapter, globally optimal invariants for the one unconstrained degree of freedom in an $A + B \rightarrow C$ reactor-separator-recycle process are derived for four alternative reaction kinetic expressions from an analysis of the overall plant material balance. The derivation is performed for the simplified economic objective of minimizing recycle rate (Mode I) at given production and maximizing production (Mode II) with maximum recycle rate as the capacity bottleneck. For power law kinetics, holding the reactor *A/B* ratio constant is obtained as the invariant while a more complex non-linear expression is obtained for Langmuir-Hinshelwood kinetics. For the more rigorous economic objective of minimizing separation column boilup or maximum column boilup as the capacity bottleneck, the invariant as the controlled variable (CV) achieves near optimal operation with the loss being <0.1% over the envisaged operating space in all cases. The invariants are thus good self-optimizing CVs (SOCVs). The work provides a physical basis for using reactant ratio as an SOCV in plantwide control.

5.1 Introduction

Self optimizing control (SOC) is a practical alternative for near optimal management of an unconstrained controlled variable (CV) setpoint for economic plantwide control of integrated chemical processes. The main idea in SOC is to adjust the unconstrained CV setpoint to hold an appropriately chosen/designed self-optimizing controlled variable (SOCV). An SOCV, when held at an appropriate constant value, results in near optimum steady state operation over the envisaged operating space[1-2]. In other words, SOC assures acceptably small loss from the plant optimum due to no re-optimization of the SOCV setpoint(s) mitigating the need for reoptimization due to sustained disturbances. Figuring out good SOCVs corresponding to unconstrained degrees of freedom (dofs) is however not straightforward and requires process understanding and insight. Several articles in the literature demonstrate the application and economic benefit of SOC in complex chemical plants (see e.g. [3-6]).

SOC is a very appealing concept in that it simplifies an optimization problem to a control problem and thus eliminates/mitigates the need for the optimization layer. A very typical approach to SOC has been to tabulate candidate SOC process variables (PVs), y_{SOC}, obtain the nominal optimum for each and then quantify the loss for the disturbances keeping the candidate PV at its nominal optimum. The one that gives the least economic loss is then deemed the best SOCV from amongst the evaluated candidate CVs. It is also possible to linearly combine available measurements, y_{SOC}, to achieve locally optimal operation using the null-space method [7-8]. Its applicability to integrated chemical processes may however be limited due to high non-linearity such as the snowball effect[9] and infeasibility due to steady state multiplicity[10]. In the absence of a global exact SOCV method, one must resort to proposing candidate SOCVs, usually from process insights, and ranking them in terms of the least economic loss at constant setpoint over the envisaged disturbance space.

Notwithstanding the vast SOC literature where some economic loss is usually accepted due to no setpoint re-optimization, one always wonders if it is possible to fully eliminate the economic loss using a well designed SOCV or alternatively, a globally optimal control law. In other words, find that "magic" CV (or alternatively, control law), which when held constant at the nominal optimum, guarantees optimality over the envisaged disturbance space. Such a globally optimal control policy, which must necessarily correspond to driving the gradient of the economic objective with respect to the unconstrained regulatory CV to zero, is the gold standard for transforming an optimization problem into an equivalent control problem that guarantees zero-loss steady state operation regardless of disturbances. It constitutes the "ideal" management of a regulatory layer unconstrained setpoint.

The idea of optimally invariant variable combinations for non-linear systems has been briefly explored in the extant literature, albeit for simple systems such as an isolated CSTR[11]. To the best of our knowledge, however, globally optimal unconstrained CVs or invariants have not been explored in any depth for a complete plant with recycle. This article does so for a reactor-separator-recycle process that has been the subject of plantwide control system design studies[12-14].

When an optimal operating policy for an unconstrained regulatory setpoint is to be applied in practice, a key requirement is convincing the plant operators on why the recommended solution is preferable over their current way of managing the unconstrained setpoint. Even as quantitative evidence on superior economics is due justification, natural emergence of the globally optimal policy from a direct analysis of the non-linear behaviour of the plant material and energy balances is much more compelling. Such compelling justification is quite rare for complete plants. To provide the same for a reactor-separator-recycle process is the principal motivation behind this work.

In the following, the reactor-separator-recycle process studied is briefly described. Alternative reaction kinetic scenarios are considered for two modes of operation. In Mode I, the recycle rate is minimized at given throughput and in Mode II, the throughput is maximized subject to maximum recycle rate as the bottleneck constraint. A steady state degrees of freedom (dof) analysis with economic optimum operation considerations is then used to show that there is one unconstrained dof that must be optimized for economic optimum operation in both modes. A simple and elegant globally optimal operating policy for this unconstrained dof is obtained via an analysis of the overall plant material balance and the associated optimality condition for both Mode I and Mode II operation. We then consider the practical case of column boil-up (expensive utility) as the rigorous Mode I economic objective and maximum boil-up corresponding to column flooding as the Mode II bottleneck constraint. It is shown that the simplified analysis optimal invariants obtained previously, result near zero loss operation for the practical case in each of the considered reaction kinetic scenarios. The article ends with the customary summary of the main findings from the work.

5.2 Process Description and Optimal Operation

The process flowsheet is shown in Figure 1.8. The irreversible exothermic reaction $A + B \rightarrow C$ occurs in a cooled liquid phase CSTR. The reactor effluent is distilled to take out nearly pure *C* product down the bottoms and unreacted *A* and *B* up the top. The distillate is recycled to the reactor along with the fresh *A* and fresh *B* streams. The hypothetical component properties and four alternative reaction kinetics (including kinetic parameters) are tabulated in Table 5.1 for ready reference. We note that all the considered reaction kinetics are of the general form

$$r = k\frac{{x_{rxrA}}^{a}{x_{rxrB}}^{b}}{(1+K_A x_{rxrA}+K_B x_{rxrB})}$$

Thus e.g., $a, b = 1$, and $K_A, K_B = 0$, gives the elementary reaction kinetic expression $r = k\, x_{rxrA}\, x_{rxrB}$. Similarly, for $a, b \neq 1$, and $K_A, K_B = 0$, the popular power law kinetic expression $r = k\, x_{rxrA}^{\alpha}\, x_{rxrB}^{\beta}$ is obtained. For a, $b = 1$, and K_A, $K_B \neq 0$ the Langmuir-Hinshelwood (LH) kinetic expression is obtained.

Assuming the column is operated at a given design pressure, the process has six steady state operating degrees of freedom (dofs); two for the fresh feeds, two for the reactor (hold-up and temperature) and two for the column. These dofs are to be adjusted for economically optimum operation. We consider two operation modes, Mode I and Mode II.

In Mode I, the production rate is given and the remaining five dofs are to be adjusted to optimize an economic objective function. We consider two alternative Mode I economic objectives, namely, minimize the recycle rate or minimize the column boil-up (expensive utility). Even as the latter is the more usual economic objective, in many processing situations, the simpler objective of minimizing the recycle rate, is equivalent to minimizing the plant operating cost. As will be shown later, elegant globally optimal operating policies can be obtained for this simpler objective.

Table 5.1. Hypothetical component properties and kinetic parameters

Kinetics	$A + B \rightarrow C$	$r = k\, x_{rxrA}^{a}\, x_{rxrB}^{b}/(1+K_A x_{rxrA}+K_B x_{rxrB})$	
Hypotheticals#	MW	NBP(°C)	
A	50	70	VLE: Soave-Redlich-Kwong
B	70	80	
C	120	110	
KM I	$a = 1; b = 1; k = 2.2\times10^{8}.e^{(-70000/RT)}; K_A = K_B = 0$		
KM II	$a = 1; b = 2; k = 7.2\times10^{8}.e^{(-70000/RT)}; K_A = K_B = 0$		
KM III*	$a = 1; b = 1; k = 4.0\times10^{8}.e^{(-70000/RT)}; K_A \neq K_B \neq 0$		
KM IV*	$a = 1; b = 2; k = 12\times10^{8}.e^{(-70000/RT)}; K_A \neq K_B \neq 0$		

Reaction rate units: kmol.m^{-3}.s^{-1}

*: K_A=2.2×10^4.$e^{(-30000/RT)}$, K_B=1.6×10^4.$e^{(-30000/RT)}$

#: Aspen-Hysys hydrocarbon estimation procedure used to estimate parameters for thermodynamic property calculations.

In Mode II, the process is to be operated to maximize production subject to a bottleneck constraint. All six dofs are then to be adjusted for the purpose. Two alternative bottleneck constraints are considered, maximum recycle rate or maximum column boil-up. The latter corresponds to column flooding as the bottleneck, a common occurrence in practice. As shown later, the maximum recycle rate constraint gives an elegant globally optimal operating policy.

Both the Mode I and Mode II optimizations are subject to process constraints such as maximum/minimum material/energy flows, equipment capacity and product quality constraints etc. At the optimum, multiple constraints are likely to be active with a few remaining unconstrained dofs. Engineering common sense is applied to figure out the optimally active constraints.

We consider the fresh *B* feed rate (F_B), the reactor hold-up (U_{rxr}) and temperature (T_{rxr}), the product *C* mol fraction (x_C^P), the recycle *C* impurity mol fraction (x_C^R) and the reactor *B* mol fraction (x_{rxrB}) as the six specification variables corresponding to the six dofs. In Mode I, F_B is specified and this leaves the other five specifications to be chosen for minimum recycle rate or boilup. Clearly, U_{rxr} and T_{rxr} should be specified at their maximum allowed values, U_{rxr}^{MAX} and T_{rxr}^{MAX}, respectively, to maximize single pass conversion and thus minimize the recycle load/boilup. Further $x_C^P = x_C^{P,MIN}$ for as sloppy a split as possible to minimize boilup and also to minimize product give-away. In most processing situations where a heavy product is produced in an addition reaction, too much of the heavy product in the reactant recycle stream is undesirable due to considerations such as accelerated catalyst deactivation, equipment fouling and product side reaction to undesired by-products. Accordingly, we consider $x_C^{R,MAX} = 1$ mol% as an optimally active constraint. This then leaves x_{rxrB} as the only remaining unconstrained dof to be chosen appropriately for optimality.

In Mode II, F_B is an additional dof since F_B is not specified anymore and is to be maximized. The four Mode I active constraints, U_{rxr}^{MAX}, T_{rxr}^{MAX}, $x_C^{P,MIN}$ and $x_C^{R,MAX}$ are likely be active in Mode II also. Further, as F_B is increased to increase production to the maximum achievable, some equipment will hit its maximum processing capacity limit, thus determining the maximum production. This bottleneck capacity constraint then becomes an additional active constraint at maximum production. Due to the high sensitivity of recycle rate to throughput changes, the bottleneck constraint typically corresponds to an equipment in the recycle loop hitting its maximum processing limit. The maximum recycle rate (R^{MAX}) is then a reasonable bottleneck constraint. Alternatively, we consider maximum vapor boilup limit, V^{MAX}, as a bottleneck constraint for this specific process. This would correspond to the onset of entrainment flooding, where significant liquid gets carried along with the vapor, severely compromising column separation efficiency. With R^{MAX} or V^{MAX} as an additional optimally active hard capacity constraint and F_B as an additional dof, x_{rxrB} remains the one unconstrained dof in Mode II (6 dofs - 4 Mode I constraints - 1 bottleneck constraint = 1 unconstrained dof). Thus, in both Mode I and Mode II, *B* mol fraction in the reactor, x_{rxrB}, is an unconstrained dof with a hill / valley shaped optimum. The above conjectures on optimally active Mode I/Mode II active constraints were confirmed via rigorous optimization using Matlab's NLP optimizer, *fmincon*, using the active set method with Aspen Hysys as the background plant steady state solver. The optimization results for the four reaction kinetic systems are summarized in Table 5.2. Mode I results are presented for both recycle rate minimization and boilup minimization. For a nominal throughput of 100 kmol/h and an increased throughput of 120 kmol/h. Mode II results are presented for both R^{MAX} and V^{MAX} as the bottleneck capacity constraint limiting production.

Assuming tight active constraint control in both Mode I and Mode II and x_{rxrB} as the one unconstrained dof, an appropriate control policy that adjusts x_{rxrB} to keep the operation (near) optimal is sought. We first perform steady state analyses to obtain a globally optimal policy for the simpler Mode I objective (minimize recycle rate) and the simpler Mode II bottleneck constraint (R^{MAX}). The performance of these operating policies from the simplified analyses is then evaluated for the rigorous Mode I objective (minimize boil-up) and Mode II bottleneck constraint (V^{MAX}).

Table 5.2. Salient base-case steady state conditions for Mode I/Mode II

Variables	KM I		KM II		KM III		KM IV	
	I	II	I	II	I	II	I	II
No. of Trays	15		15		15		15	
Feed Tray	7		7		7		7	
U_{rxr} (m^3)	6		6		6		6	
T_{rxr} (°C)	110		110		110		110	
V (kmol/h)	390.0	800^{MAX}	432.0	850^{MAX}	402.4	800^{MAX}	451.7	900^{MAX}
R (kmol/h)	130.5	318.3	126.1	282.2	129.0	315.5	129.9	304.1
L (kmol/h)	303.5	585.6	350.3	664.0	317.5	587.7	367.7	699.0
F_{col} (kmol/h)	230.6	469.5	226.2	442.3	229.1	456.5	230	459.9
P (kmol/h)	100.1	151.1	100.1	160.0	100.1	141.1	100.0	155.9
x_{rxrA}	0.3652	0.3989	0.2689	0.2772	0.3361	0.3734	0.2476	0.2591
x_{rxrB}	0.1994	0.2756	0.2876	0.3582	0.2258	0.3138	0.3161	0.3988
$[A/B]$	1.8315	1.4474	0.9350	0.7739	1.4885	1.190	0.7833	0.6497
x_B^R	0.3455	0.4021	0.5083	0.5559	0.3939	0.45	0.5522	0.5983
x_C^R	0.01	0.01	0.01	0.01	0.01	0.01	0.01	0.01
x_B^P	0.0089	0.0091	0.0094	0.0095	0.0091	0.0092	0.0095	0.0096
x_C^P	0.99	0.99	0.99	0.99	0.99	0.99	0.99	0.99
Q_{rxr} (kW)	106.5	288.3	97.3	236.3	103.6	285.5	99.8	256.7
Q_{cnd} (kW)	3483	7269	3845	7647	3590	7275	4021	8116
Q_{reb} (kW)	3447	7069	3817	7509	3556	7068	3990	7951

See Figure 1.8 and Nomenclature for variable descriptions

5.3 Globally Optimal Invariants from Simplified Analysis

The simplified analysis refers to minimizing the recycle rate (R) in Mode I and maximizing the product rate (P) in Mode II with maximum recycle rate (R^{MAX}) as the bottleneck constraint. For convenience, we work with x_{rxrB} and P as the two specifications corresponding to dofs associated with the two fresh feeds. The overall plant balance then requires that the reactor product generation rate equals the product C rate from the column bottoms, i.e.

$$k^{MAX}\frac{{x_{rxrA}}^{a}{x_{rxrB}}^{b}}{(1+K_A x_{rxrA}+K_B x_{rxrB})}U_{rxr}^{MAX}=Px_C^P \tag{1}$$

The rate constant is the maximum possible, k^{MAX}, corresponding to T_{rxr}^{MAX}. Similarly, the reactor hold-up is the maximum allowed, U_{rxr}^{MAX}. Both T_{rxr}^{MAX} and U_{rxr}^{MAX} are optimally active constraints.

Since the Mode I objective and Mode II bottleneck constraint are both related to the recycle rate, R, an explicit expression for R is required in terms of x_{rxrA}, x_{rxrB} and P plus other specified conditions, x_C^P or x_C^R. The expression is obtained as follows. An overall material balance on the column gives the reactor effluent rate (E) as

$$E = P + R \tag{2}$$

The column component balances give the A and B component rates, E_A and E_B, respectively, as

$$E_A = Px_A^P + R_A \tag{3a}$$

and

$$E_B = Px_B^P + R_B \tag{3b}$$

The reactor reactant mol fractions are thus

$$x_{rxrA} = \frac{Px_A^P + R_A}{P+R} \tag{4a}$$

and

$$x_{rxrB} = \frac{Px_B^P + R_B}{P+R} \tag{4b}$$

Adding (4a) and (4b) and rearranging

$$R_A + R_B = (x_{rxrA} + x_{rxrB})(P + R) - P(x_A^P + x_B^P) \tag{5}$$

Since

$$R = R_A + R_B + Rx_C^R \tag{6}$$

we have

$$R(1 - x_C^R) = (R_A + R_B) \tag{7}$$

Substituting for *(R_A + R_B)* in Equation 5 and rearranging, the desired expression for recycle rate is

$$R = P\frac{(x_{rxrA} + x_{rxrB} + x_C^P - 1)}{(1 - x_C^R - x_{rxrA} - x_{rxrB})}$$

where

$$x_A^P + x_B^P = 1 - x_C^P$$

The constrained optimization for both Mode I and Mode II operation can now be solved.

5.3.1 Mode I Globally Optimal Invariant

In Mode I, the objective is to minimize the recycle rate, R, by adjusting the unconstrained dof, x_{rxrB}. The Mode I optimization problem thus is

$$\min_{x_{rxrB}} R \tag{8}$$

subject to the rearranged overall material balance constraint (1)

$$\frac{{x_{rxrA}}^{a}{x_{rxrB}}^{b}}{(1+K_A x_{rxrA}+K_B x_{rxrB})} = \frac{P x_C^P}{k^{MAX} U_{rxr}^{MAX}} \tag{9}$$

and the rearranged recycle rate constraint (7)

$$R(1 - x_C^R - x_{rxrA} - x_{rxrB}) = P(x_{rxrA} + x_{rxrB} + x_C^P - 1) \tag{10}$$

Since the production rate P is given (or known), we have three unknowns, x_{rxrA}, x_{rxrB} and R. At a given x_{rxrB}, both x_{rxrA} and R get calculated by the two constraints, (9) and (10) above. The particular value of x_{rxrB} that minimizes R is thus obtained by setting

$$\frac{dR}{dx_{rxrB}} = 0 \tag{11}$$

subject to constraints (9) and (10) above.

Differentiation and rearrangement of (10) gives

$$(1 - x_C^R - x_{rxrA} - x_{rxrB})dR = (P + R)(dx_{rxrA} + dx_{rxrB})$$

Dividing by dx_{rxrB} and setting dR/dx_{rxrB} to zero for optimality, we get

$$dx_{rxrA} = -dx_{rxrB} \tag{12}$$

Differentiation and rearrangement of (9) at constant P (Mode I) gives

$${x_{rxrA}}^{a}{x_{rxrB}}^{b}\left(\frac{a}{x_{rxrA}}dx_{rxrA} + \frac{b}{x_{rxrB}}dx_{rxrB}\right) = \mu(K_A dx_{rxrA} + K_B dx_{rxrB}) \tag{13}$$

where, μ is the RHS of Equation (9) and is a constant for Mode I (fixed P). Substituting $dx_{rxrA} = -dx_{rxrB}$ and dividing both sides by dx_{rxrB}, we get the global optimality condition as

$$x_{rxrA}{}^{a} x_{rxrB}{}^{b} \left(\frac{a}{x_{rxrA}} - \frac{b}{x_{rxrB}}\right) = \mu(K_A - K_B) \tag{14}$$

For a given P (Mode I) and specified $x_C{}^P$ and $x_C{}^R$, solving (9), (10) and (14) simultaneously gives the values of the three unknowns, x_{rxrA}, x_{rxrB} and R, at the optimum solution.

It is instructive to analyze the form of the global optimality condition in (14) for the simpler reaction kinetics cases considered. For $K_A = K_B = 0$ and $a = b = 1$ (KM I), (14) simplifies to

$$x_{rxrB} = x_{rxrA} \tag{15}$$

This implies that minimum recycle is achieved by holding A and B in equal proportion in the reactor. This is a very simple and elegant optimal operating policy for managing the reactor B mol fraction. For $K_A = K_B = 0$ and $a \neq b$ (KM II), the global optimality condition is

$$x_{rxrB} = \frac{b}{a} x_{rxrA} \tag{16}$$

Again, the elegant policy of holding the reactor B to A ratio at b/a. minimizes the recycle rate. For the standard LH model, the global optimality condition is

$$x_{rxrB} = x_{rxrA} + \mu(K_A - K_B) \tag{17}$$

This simply requires offesetting x_{rxrB} from x_{rxrA}, the offset being a constant at fixed production rate.

For the most general form of the kinetic expression, the optimal Mode I control policy is a more complicated non-linear expression. Replacing μ in (14) by the LHS of (9) and simplifying, the global optimality condition may be rewritten as

$$\left(\frac{a}{x_{rxrA}} - \frac{b}{x_{rxrB}}\right) = \left(\frac{K_A - K_B}{1 + K_A x_{rxrA} + K_B x_{rxrB}}\right) \tag{18}$$

This is a quadratic in x_{rxrB} that can be solved for x_{rxrB} for a measured value of x_{rxrA}. The calculated root in the range $0 < x_{rxrB} < 1$ is implemented in the plant. Eventually, once x_{rxrA} stops changing and the plant settles at steady state, (18) must hold implying minimum recycle operation. In passing we note that between the two alternative control law forms in Equation (18) and Equation (14), the former is preferred since the latter expression contains the reaction rate constant which is known to change slowly due to catalyst deactivation. Repeated estimation of the rate constant will then be required. On the other hand, the adsorption equilibrium constants K_A and K_B are thermodynamic entities that remain fixed at a given temperature, significantly mitigating the need for parameter re-estimation. This also applies to the standard LH kinetics invariant.

5.3.2 Mode II Globally Optimal Invariant

We now consider maximizing production (P) subject to maximum recycle rate (R^{MAX}) as the bottleneck constraint. The optimization problem then is

$$\max_{x_{rxrB}} P \tag{19}$$

subject to the constraints

$$\frac{{x_{rxrA}}^{a}{x_{rxrB}}^{b}}{(1+K_A x_{rxrA}+K_B x_{rxrB})} = \frac{P x_C^P}{k^{MAX} U_{rxr}^{MAX}} \tag{20}$$

$$R^{MAX}(1 - x_C^R - x_{rxrA} - x_{rxrB}) = P(x_{rxrA} + x_{rxrB} + x_C^P - 1) \tag{21}$$

Note that instead of P being constant and recycle rate being variable as in Mode I, we now have recycle rate constant at R^{MAX} with P being variable. There are again three unknowns (P, x_{rxrA} and x_{rxrB}) and two constraints. Enforcing the condition for optimality gives the third constraint that allows the calculation of all three unknowns at the optimum. Without loss of generality, x_{rxrB} is taken as the independent decision variable so that optimality requires

$$\frac{dP}{dx_{rxrB}} = 0 \tag{22}$$

Analogous to Mode I analysis, differentiating (21) with respect to x_{rxrB} and setting $dP/dx_{rxrB} = 0$, we get $dx_{rxrA} = -dx_{rxrB}$

Further, differentiating (20) with respect to x_{rxrB} and substituting $dx_{rxrA} = -dx_{rxrB}$, we get exactly the same global optimality condition as for Mode I, i.e.

$$x_{rxrA}{}^{a}x_{rxrB}{}^{b}\left(\frac{a}{x_{rxrA}}-\frac{b}{x_{rxrB}}\right)=\mu_{(P)}(K_A-K_B) \qquad (23)$$

The only difference is that μ is now no longer a constant but a function of P, as highlighted in (23).

For KM I ($a = b = 1$; $K_A = K_B = 0$), the globally optimal operating policy for maximizing production (Mode II) is to hold $x_{rxrB} = x_{rxrA}$, i.e., ensuring equal proportion of A and B in the reactor. This policy is the same as for minimizing recycle rate at given production (Mode I). Similarly, for KM II ($a \neq b$; $K_A = K_B = 0$), the globally optimal operating policy is again the same as for Mode I, i.e.

$$x_{rxrB}=\frac{b}{a}x_{rxrA}$$

In other words, holding B to A in the ratio b/a in the reactor maximizes production.

For KM III the global optimality condition is

$$x_{rxrB}=x_{rxrA}+\mu_{(P)}(K_A-K_B) \qquad (24)$$

By offsetting x_{rxrB} from x_{rxrA} by a production rate dependent offset, production is maximized. If P and x_{rxrA} are accurately measured, then by setting x_{rxrB} from the above relation and letting the process settle to the eventual steady state, production gets maximized.

For KM IV, the global optimality condition is the same as for Mode I, i.e.

$$\left(\frac{a}{x_{rxrA}}-\frac{b}{x_{rxrB}}\right)=\left(\frac{K_A-K_B}{1+K_A x_{rxrA}+K_B x_{rxrB}}\right)$$

For accurately measured x_{rxrA}, the quadratic in x_{rxrB} can be solved. Of the two roots, only the one for which $0 < x_{rxrB} < 1$ is accepted. Continually implementing this calculated x_{rxrB} and letting the process settle to the eventual steady state maximizes production. As before, the somewhat complicated expression above should be preferred as the unknown parameters (K_A, K_B, a and b) are likely to remain constant over time, unlike the reaction rate constant, which decreases due to catalyst deactivation in the expression for μ. This comment also applies to the invariant for LH kinetics.

The results for the globally optimal invariants from the simplified analysis of the reactor-separator-recycle process are summarized in Table 5.3. In the Table, we also provide simple expressions, where possible, for the Mode I minimum recycle rate and the Mode II maximum production rate. For the specific reaction kinetic parameters (Table 5.1) and process design considered (Figure 1.8) , the values of x_{rxrB}, x_{rxrA}, reactor *A/B* ratio *([A/B]*) and the economic objective at the Mode I / Mode II optimum have already been noted in Table 5.2.

Before closing this section on the simplified optimal operation analysis, we apply engineering common sense to better understand the optimality conditions derived rigorously. The optimal operation argument based on the physics of the process goes as follows. In Mode I, the recycle rate is to be minimized at given production rate. At minimum recycle, the amount of *A* and *B* going around the plant is the least possible. This implies that the concentration of *C* in the reactor, x_{rxrC}, is maximum. In other words, minimizing recycle at given production corresponds to maximizing x_{rxrC}. Since $x_{rxrC} = 1 - x_{rxrA} - x_{rxrB}$, maximizing x_{rxrC} is equivalent to minimizing ($x_{rxrA} + x_{rxrB}$). Taking x_{rxrB} as the independent decision variable, the optimality condition for minimum recycle is

$$\frac{d(x_{rxrA}+x_{rxrB})}{dx_{rxrB}} = 0$$

which directly gives $dx_{rxrB} = -dx_{rxrA}$

Differentiating the overall plant material balance constraint (1) and substituting $dx_{rxrA} = -dx_{rxrB}$ results in the Mode I global optimality invariant in (18).

Table 5.3. Plant globally optimal invariants

Reaction Model	Optimality Condition	Mode I Min (R)				Mode II Min ($-P$)	
		F_B =100* kmol/h		F_B =120* kmol/h		R^{MAX}=300 kmol/h	
		x_{rxrB}^{opt}	R^{opt}	x_{rxrB}^{opt}	R^{opt}	x_{rxrB}^{opt}	P^{MAX}
KM I	$x_{rxrB} = x_{rxrA}$	0.2698	117.65	0.2955	174.92	0.3311	150.73
KM II	$x_{rxrB} = 2x_{rxrA}$	0.3543	113.74	0.3765	156.58	0.4232	170.52
KM III	$\left(\frac{1}{x_{rxrA}} - \frac{1}{x_{rxrB}}\right) = \left(\frac{K_A - K_B}{1 + K_A x_{rxrA} + K_B x_{rxrB}}\right)$	0.2808	118.85	0.317	190.10	0.3524	140.39
KM IV	$\left(\frac{1}{x_{rxrA}} - \frac{2}{x_{rxrB}}\right) = \left(\frac{K_A - K_B}{1 + K_A x_{rxrA} + K_B x_{rxrB}}\right)$	0.3691	120.17	0.3967	170.58	0.4425	157.82

In Mode II, production rate P is to be maximized at given recycle rate, R^{MAX}. Maximum production implies the reactor C generation rate is the highest possible. Thus maximum production corresponds to maximum x_{rxrC} and again the $dx_{rxrB} = -dx_{rxrA}$ condition is directly recovered. Deriving the Mode II global optimality invariant from the overall plant material balance is then straightforward. Indeed, it was these simple physical arguments that lead us to the globally optimal invariants for Mode I and Mode II. We then confirmed from process simulations that these invariants were indeed true and then finally proceeded with the rigorous derivations presented above. Throughout, the simplicity and elegance of the invariant that we initially chanced upon for KM I, was the key motivational driver behind extension of the result to the more complex reaction kinetics reported.

5.4 Evaluation of Optimal Operation Policies for the Rigorous Case

The globally optimal invariants for the four kinetic models have been obtained from the analysis of a simplified problem, where the Mode I objective is minimizing recycle rate while the Mode II objective of maximizing production is limited by a maximum recycle rate bottleneck constraint. In practice, the rigorous optimization objective and constraints can be more complex. Here, we consider the typical case of minimizing reboiler duty (or boilup), which is the expensive utility, as the Mode I objective. For Mode II, the objective remains maximizing production. However, the bottleneck constraint is the commonly encountered case of column entrainment flooding with the boilup hitting a maximum limit, V^{MAX}. Due to the complexity of the multicomponent distillation column model, the existence of an elegant gobally optimal operating policy for managing x_{rxrB} seems very unlikely to us. The next best thing is to quantify the suboptimality resulting from the implementation of operating policies obtained earlier from the simplified analysis. Given that these policies guarantee global optimality for the simplified problem, the expectation is that for the rigorous case, the suboptimality (or economic loss) maybe small enough resulting in near optimal operation over the envisaged operating space.

In both Mode I and Mode II, the simplified analysis optimal operating policy for KM I and KM II corresponds to holding the reactor *A* to *B* ratio *([A/B]*) constant. In other words, the presented simplified analysis provides a physical basis for considering *[A/B]* as a candidate SOCV for managing the unconstrained setpoint x_{rxrB}. We consider a ±20% change in production as the principal Mode I disturbance and a ±30% change in reaction rate constant as the principal Mode II disturbance. The plant economic performance is now compared for the candidate CVs, *[A/B]* or x_{rxrB}, held constant at their nominal optimum value. From the regulatory perspective, both these CVs maintain the stoichiometric feed balance; x_{rxrB} is most commonly applied in the literature (see e.g. [15-16]).

For the economic comparison, Figure 5.1 plots the variation in % economic loss, $L_{\%}$, defined as

$$L_{\%} = \frac{J - J_{opt}}{J_{opt}} \times 100$$

with respect to the Mode I / Mode II principal disturbance with *[A/B]* or x_{rxrB} maintained at its nominal optimum value, for all the four kinetic models considered. The plot has been obtained with the candidate SOCV held constant at its nominal optimum value so that $L_{\%}$ is zero at the nominal condition. Note that the SOCV nominal optimum value for *[A/B]* for the rigorous Mode I objective and Mode II constraint is not the same as for the simplified analysis case. From the plots, it is clearly evident that *[A/B]* is an acceptable SOCV with $L_{\%}$ being less than 0.5% in all cases considered. On the other hand, with x_{rxrB} as the CV, for the largest disturbance magnitude, $L_{\%}$ is consistently above 1% for the different kinetic models. In particular, for KM III, the Mode I $L_{\%}$ is more than 5% for a production rate increase of 20% with x_{rxrB} as the CV. The corresponding figure for *[A/B]* is a very respectable 0.2%. Similarly, in Mode II, the KM IV $L_{\%}$ is 1.8% and 0.1% with x_{rxrB} and *[A/B]*, respectively, as the CVs. These results clearly bring out the self optimizing nature of *[A/B]* as a CV. It is also pertinent to note that even as *[A/B]* is the global optimum invariant for the simplified analysis of only KM I and KM II and not KM III and KM IV, it still behaves as a good SOCV for the rigorous case for all the kinetic models considered. There then may be merit in considering the *A/B* proportion circulating in the recycle loop as an SOCV for more complex reaction kinetics and other similar processes that have two unreacted reactants that are recycled.

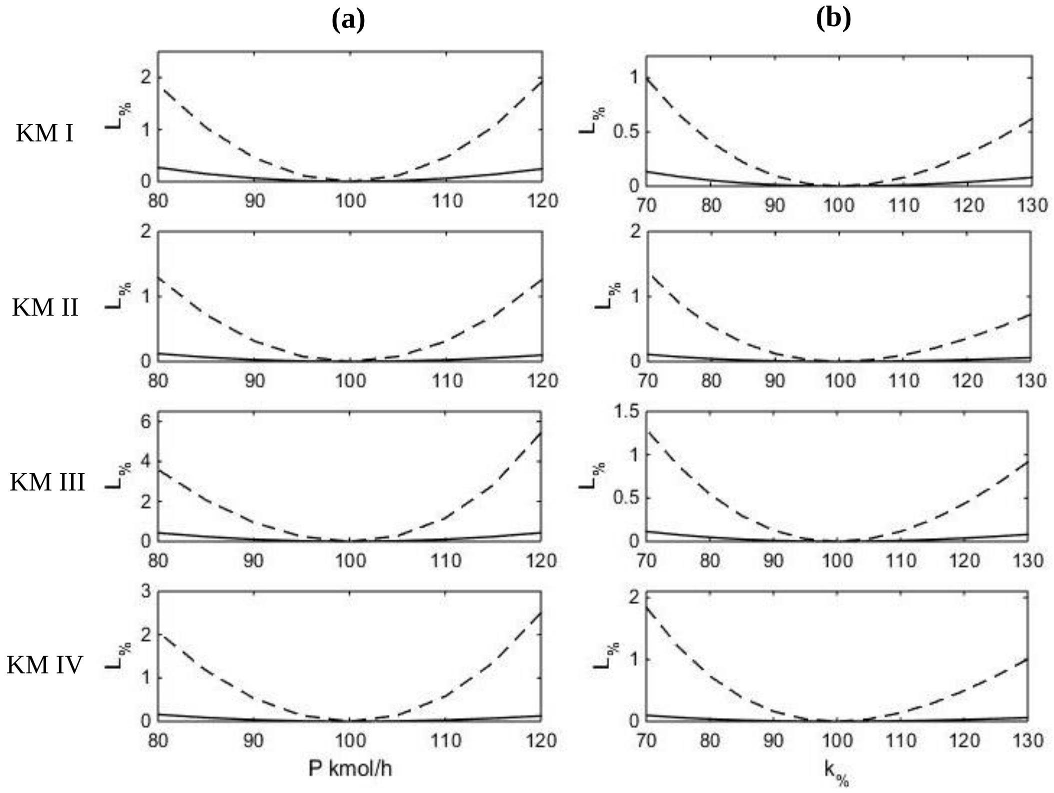

Figure 5.1. % Economic loss with principal disturbance for (a) Mode I (b) Mode II

—— : Nominal optimum *[A/B]* - - - : Nominal optimum x_{rxrB}

Often, processes are required to transition from Mode I to Mode II and vice versa due to anticipated changes in the demand-supply gap. Consider a constant setpoint operating policy with *[A/B]* or x_{rxrB} as the candidate CV. Assume the process is operating at the nominal Mode I optimum when management requests a transition to Mode II (maximize production). The operator would then slowly increase the TPM setpoint until the bottleneck constraint (V^{MAX}) is approached closely from below. Conversely, we may have the process operating at maximum production with *[A/B]* or x_{rxrB} at the Mode II optimum value when the management requests a transition to a much lower Mode II production rate. In response, the operator would slowly decrease the TPM setpoint till the desired lower production rate is achieved. In both cases, for constant setpoint operation, unless the self-optimizing characteristics of the unconstrained CV are good, the suboptimality at the final steady state can be substantial. This is quantified in Table 5.4 for *[A/B]* or x_{rxrB} as the candidate unconstrained CV. The data clearly shows that for both Mode I to Mode II and Mode II to Mode I transition, the economic loss $L_{\%}$ at the final steady state is no more than 1.1% with *[A/B]* as the CV. On the other hand, with x_{rxrB} as the CV, the corresponding loss can be as high as 8.2% in a Mode I to Mode II transition and 9.4% in a Mode II to Mode I transition. This again highlights that *[A/B]* is an excellent SOCV for near optimal operation over a large operating window.

Table 5.4. Quantitative evaluation of candidate unconstrained CV

Mode Transition	Variable	KM I		KM II		KM III		KM IV	
		J	$L_{\%}$	J	$L_{\%}$	J	$L_{\%}$	J	$L_{\%}$
I → II	*[A/B]*	149.99	0.76	159.25	0.48	139.97	0.77	155.05	0.53
	x_{rxrB}	143.63	4.96	151.26	5.48	131.54	6.75	143.13	8.17
II → I	*[A/B]*	393.71	0.94	434.24	0.52	406.61	1.04	454.29	0.58
	x_{rxrB}	415.87	6.62	455.47	5.43	440.06	9.35	486.52	7.72

Given the good self-optimizing performance of *[A/B]* for KM III and KM IV, for which *[A/B]* is not the global invariant from the simplified analysis, it is pertinent to ask if the economic loss can be further reduced for KM III and KM IV by using the simplified analysis global invariant as the candidate SOCV. We analyzed for the performance of both KM III and KM IV simplified analysis global invariants and found that the economic performance is indeed noticeably better than when holding *[A/B]* constant. For quantitative illustration, Figure 5.2 shows the variation in $L_{\%}$ in Mode I and Mode II, with respect to the corresponding principal disturbance, for KM III with the invariant and *[A/B]* as the candidate CVs. When the global invariant is used, $L_{\%}$ is no more than 0.13% over the considered disturbance space, which is much lower than the 0.5% maximum loss when holding *[A/B]* constant. Similar results were also observed for KM IV but are not shown here for brevity. Thus even as the global invariant has been obtained using simplified analysis for KM III and KM IV, its self-optimizing performance over the envisaged operating space for the rigorous case is outstanding with negligible loss. Overall, these results clearly show that the global invariants obtained from the simplified analysis for all the kinetic models considered are excellent SOCVs for the more rigorous Mode I economic objective and Mode II bottleneck constraint.

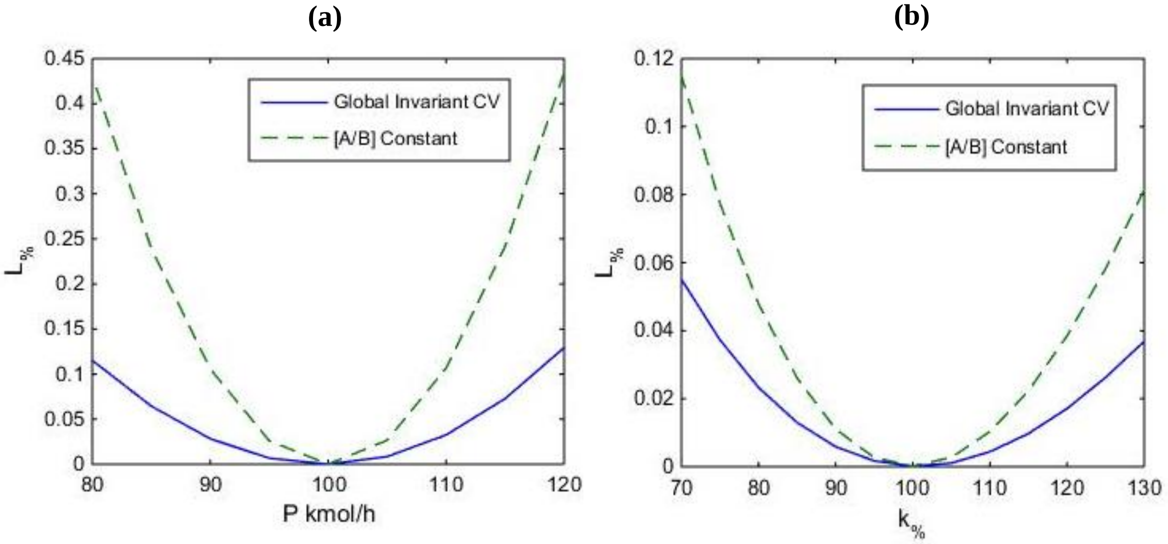

Figure 5.2. Loss% for global invariant and *[A/B]* for KM III for (a) Mode I (b) Mode II

5.5 Discussion

Given the excellent performance of the simplified analysis invariant for the rigorous case for KM III and KM IV, it is tempting to consider controlling a non-linear SOCV which has the same form as the simplified analysis invariant. The problem is identifying the unknown parameters in this nonlinear SOCV. In KM IV, for example, the SOCV will have four unknown parameters, corresponding to a, b, K_A and K_B in the simplified analysis invariant (see Equation 18). Note that since the economic objective or bottleneck constraint are not the same as for the simplified analysis, we expect the "best" value for these parameters to be different than that obtained using the actual reaction kinetic parameter values. This is similar to the "best" value of *[A/B]*, which is the simplified analysis invariant for KM II, being different from *a/b*, for a rigorous economic objective and bottleneck constraint (see Table 5.2). A well fitted kinetic model is then of little avail in obtaining the best value of the SOCV, regardless of whether we are using *[A/B]* or the simplified analysis invariant based process variable as the SOCV.

When using *[A/B]* as the SOCV for any of the kinetic models, including KM III or KM IV, it is quite straight forward to find the optimum value of *[A/B]* at a given production, using for example, hill-climbing[17] or modifier adapted RTO[18]. This optimum value is then applied to all operating conditions with the assurance that the economic loss would remain acceptably small. On the other hand, for the SOCV based on the KM IV invariant, obtaining the four unknown parameters requires driving the process to the economic optimum for at least four different production rates, which is so much more cumbersome and impractical. Nevertheless, purely for illustration purposes, we performed the KM IV invariant parameter fitting using Mode I optimum steady state data at four different production rates of 94, 96, 98 and 100 kmol/h. We have deliberately taken a narrow range of production rates to see the extrapolation ability of the control law. For comparison, we also fitted a third order polynomial, which has four unknown parameters ($x_{rxrB}^{opt} = \alpha + \beta x_{rxrA} + \gamma x_{rxrA}^2 + \delta x_{rxrA}^3$) for these same production rates. Figure 5.3a shows the variation in $L_{\%}$ over a much wider Mode I production rate range of 60 to 125 kmol/h using the invariant based control law and the polynomial control law. For comparison, the curve with *[A/B]* fixed at the nominal optimum is also shown. Notice that the invariant based SOCV further reduces the loss compared to constant *[A/B]* operation to values that are negligible. Given that this SOCV has a physical basis and has been obtained from an analysis of the overall plant material balance, its extrapolation ability far away from the narrow Mode I operating range over which unknown parameters were fitted is reassuring and not surprising. On the other hand, the polynomial control law has very poor extrapolation ability and gives near optimal operation only over the narrow throughput range over which the parameters were fitted. This is again to be expected as the polynomial control law has no physical basis.

Figure 5.3b shows the variation in $L_{\%}$ if the same invariant based fitted SOCV is applied for Mode II operation. The corresponding variation with *[A/B]* fixed at its nominal Mode I optimum (throughput 100 kmol/h) is also shown in the Figure. Again, the excellent extrapolation ability of the invariant based SOCV is self evident. Overall these results highlight that an SOCV with a physical basis provides, by far, the most convincing argument for implementation in industrial settings.

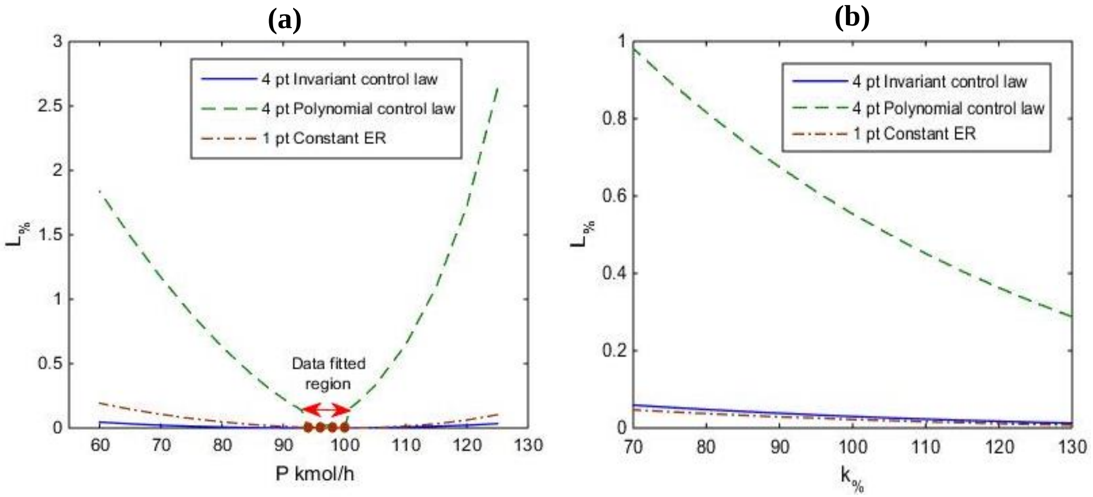

Figure 5.3. Loss% for invariant control law, polynomial control law and constant ER operation for (a) Mode I (b) Mode II

5.6 Conclusion

In conclusion, simplified analysis of the overall plant material balance for a two feed $A + B \rightarrow C$ reactor-separator-recycle process shows that for elementary or power law reaction kinetics, holding the reactor *A/B* ratio constant at an appropriate value minimizes recycle rate at given production (Mode I) or alternatively, maximizes production with maximum recycle rate as the bottleneck constraint. The reactor *A/B* ratio is thus an ideal CV corresponding to the unconstrained dof for the second fresh feed into the process (first fresh feed sets production). A more complex global invariant is obtained for the Langmuir Hinshelwood reaction kinetic expressions. For the more rigorous case of Mode I minimization of column boilup (expensive utility) or Mode II throughput maximization with maximum boilup as the bottleneck constraint, rigorous steady state analysis shows the reactor *A/B* ratio is a good self-optimizing controlled variable (maximum loss % < 0.5%) for all the considered reaction kinetic models. Additionally, if the simplified analysis invariant is used as the CV, the economic loss over the envisaged operating space can be further reduced to <0.13%. Overall, the work highlights the role of the non-linear overall plant material balance as the key determinant of the form of the optimal operating policy corresponding to the unconstrained dof associated with the second fresh feed to the process.

References

(1) Skogestad, S. Plantwide control: The search for the self-optimizing control structure. *J. Process Control* 2000, 10(5), 487-507.

(2) Skogestad, S. Near-optimal operation by Self-optimizing control: from process control to marathon running and business systems. *Comput. Chem. Eng.* 2004, 29, 127-137.

(3) Panahi, M.; Skogestad, S. Economically efficient operation of CO_2 capturing process part I: Self-optimizing procedure for selecting the best controlled variables. *Chem. Eng. and Process.* 2011, 50(3), 247-253.

(4) Larsson, T.; Hestetun, K.; Hovland, V.; Skogestad, S. Self-optimizing control of a large scale plant—The Tennessee Eastman process. *Ind. Eng. Chem. Res.* 2001, 40(22), 4889–4901.

(5) Jensen, J. B.; Skogestad, S. Optimal Operation of Simple Refrigeration Cycles. Part II: Selection of Controlled Variables. *Comput. Chem. Eng*, 2007, 31, 1590-1601.

(6) Araújo, A. C.B. de; Govatsmark, M.; Skogestad, S. Application of plantwide control to the HDA process. I- steady-state optimization and self-optimizing control. *Control Eng. Pract.* 2007, 15, 1222-1237.

(7) Alstad, V.; Skogestad, S. Null space method for selecting optimal measurement combinations as controlled variables. *Ind. Eng. Chem. Res.* 2007, 46(3), 846-853.

(8) Govatsmark, M. S.; Skogestad, S. Selection of controlled variables and robust setpoints. *Ind. Eng. Chem. Res.* 2005, 44(7), 2207–2217.

(9) Luyben, W. L. Snowball effects in reactor/separator processes with recycle. *Ind. Eng. Chem. Res.* 1994, 33, 299-305.

(10) Ojasvi; Kaistha, N. Plantwide control for maximum throughput operation of an ester purification process. *Ind. Eng. Chem. Res.* 2016, 55(47), 12242-12255.

(11) Jäschke, J. E. P.; skogestad, S. Optimally invariant variable combinations for nonlinear systems. *IFAC Papers-OnLine* 2009**,** 7, 530-535.

(12) Larsson, T.; Govatsmark, M.S.; Skogestad, S.; Yu, C. C. Control Structure Selection for Reactor, Separator and Recycle Processes. *Ind. Eng. Chem. Res*. 2003, 42 (6), 1225-1234

(13) Luyben, W. L. Dynamics and control of recycle systems. 1. Simple open-loop and closed-loop systems. *Ind. Eng. Chem. Res.* 1993, 32(3), 466-475.

(14) Wu, K. L.; Yu, C. C. Reactor/separator processes with recycle 1. Candidate control structure for operatibility. *Comput. Chem. Eng.* 1996, *20*, 1291-1316.

(15) Jagtap, R.; Kaistha, N.; Skogestad, S. Plantwide control for economic optimum operation of a recycle process with side reaction. *Ind. Eng. Chem. Res.* 2011, 50(14), 8571-8584.

(16) Sahu, A.; Kumar, V.; Kaistha, N. Conceptual design and plantwide control of an ethyl acetate process. *Chem. Eng. Process. Process Intensif.* 2018, 126, 45-61.

(17) Kumar, V.; Kaistha, N. Hill climbing for plantwide control to economic optimum. *Ind. Eng. Chem. Res.* 2014, 53 (42), 16465−16475.

(18) Marchetti, A.; Chachuat, B.; Bonvin, D. Modifier-adaptation methodology for real-time optimization. *Ind. Eng. Chem. Res.* 2009, 48(13), 6022-6033.

Chapter 6

Inferential Self Optimizing Control of a Reactor-Separator-Recycle Process

This Chapter is based on the paper "Inferential Self Optimizing Control of a Reactor-Separator-Recycle Process" submitted to Industrial Engineering and Chemistry Research.

In this Chapter, self optimizing control of a reactor-separator-recycle process with $A + B \rightarrow C$ reaction chemistry is evaluated for Mode I (minimize recycle rate or boilup at given production) and Mode II (maximize throughput with maximum recycle or boilup as the bottleneck). In both operation modes one unconstrained degree of freedom (dof) remains after accounting for the active constraints. Through an analysis of the overall plant material balance, it is shown that the reactor A to B ratio is a good self-optimizing variable for the unconstrained dof. The separator distillation column top temperature (T_{top}) is directly correlated to this ratio and is a good inferential self-optimizing controlled variable (SOCV) that avoids cumbersome reactor composition measurements. A plantwide control system with column boilup as the throughput manipulator (TPM) is synthesized with two candidate CVs for stoichiometric feed balancing, namely, reactant composition in the reactor (CS1) and separator top temperature (CS2). Steady state and closed loop dynamic results demonstrate that both CS1 and CS2 provide effective process regulation in the face of principal disturbances with CS2 achieving significant economic benefit up to 7% and 0.8% in Mode I and Mode II, respectively. The work emphasizes the substantial economic impact of the CV corresponding to an unconstrained dof.

6.1 Introduction

One of the more appealing approaches for near optimal management of unconstrained regulatory layer setpoints is the self-optimizing control paradigm [1-3]. Here, the unconstrained setpoint is manipulated to hold a self-optimizing CV (SOCV). An SOCV is defined as one which when held constant at an appropriate value, results in acceptably small economic loss in the face of disturbances [3]. The "small economic loss" criteria implies that a constant SOCV setpoint operating policy gives near optimal process operation. An unconstrained optimization problem gets simplified into a control problem. A good SOCV obviates/mitigates the need for reoptimization via real-time optimization (RTO). Since its formalization by Skogestad and coworkers, the SOC approach has been demonstrated on several plantwide control problems (see e.g. [4-8]).

Even as the SOC concept is appealing, obtaining a good SOCV for potentially highly non-linear integrated chemical processes is not straightforward and requires process understanding and insights. Many reported applications simply quantify the economic loss due to no reoptimization for a list of candidate controlled variables (CVs) and then choose the one with the least loss for implementation (see e.g. [4-5]). The null space method [9] gives the best possible combination of measurements for SOC. The combination however is only a local optimum invariant and not a global one. Its usefulness for highly non-linear processes with material and energy integration is not clear. The other issue is the practicality of the SOCV. Not all SOCVs are practical. For example, the costs and delays associated with cumbersome analytical composition measurement based SOCVs may make their implementation infeasible. Also, an SOCV based on several measurement combinations may exhibit strange dynamics requiring significant filtering and controller detuning. Thus, similar to the quest for good models for RTO, the quest for a good SOCV can be an interesting research problem for specific processes.

In this work, we consider self-optimizing control (SOC) of a reactor-separator-recycle process that has been used as a case-study in the PWCS design literature [10-12]. In the previous Chapter, steady state analysis of a reactor-separator-recycle process with the reaction $A + B \rightarrow C$, resulted in a globally invariant control law for minimizing recycle rate at given production or maximizing production with maximum recycle rate as the bottleneck constraint. Here, we extend the work to show that the simplified analysis invariant for power law reaction kinetics, namely reactor *A/B* ratio, is self optimizing for the more complex Langmuir-Hinshelwood kinetics and the rigorous objective of minimizing separator reboiler duty at given production or maximizing production with maximum boilup as the bottleneck constraint, corresponding to onset of column flooding. We further extend the work to consider the dynamic implementation of the self-optimizing control (SOC) policy. Since the policy is based on reactor composition measurements, the scope of the work includes inferring the reactor compositions from available routine online measurements for industrial practicality. The novel contribution is in providing a physical basis for the SOCV and also a practical method for inferential SOC from routine measurements.

In the following, the reactor-separator-recycle process is briefly described. Optimal steady state operation for two common operating modes, Mode I and Mode II is then considered. In Mode Ia, the production rate is given and the steady state dofs are adjusted to minimize the recycle rate. In Mode Ib, the reboiler duty is minimized at given production. In Mode IIa, all degrees of freedom (dofs) are adjusted to maximize production with maximum recycle rate as the bottleneck constraint. In Mode IIb, maximum boilup is taken as the bottleneck constraint. In all cases, after accounting for the optimally active constraints, one unconstrained dof remains. The steady state analysis is then briefly presented to derive the globally optimum invariant for Mode Ia and Mode IIa. We also show that for Mode Ib and Mode IIb, the power law kinetics invariant, which reactor *A/B* ratio is, gives acceptably small loss at a constant value and is therefore self-optimizing. The dynamic implementation of the self-optimizing control policy for realistic Mode Ib and Mode IIb objectives is then considered. An economic PWCS with the TPM at the column boilup (capacity bottleneck) is then synthesized. Two control system variants, CS1 and CS2, are considered. In CS1, the limiting reactant B mol fraction (x_{rxrB}) is used as the CV for the ucnonstrained dof. In CS2, the reactor *A/B* ratio (*[A/B]*), inferred from the column top tray temperature, is used as the CV for the unconstrained dof. The column top tray temperature measurement avoids cumbersome reactor composition measurements. The dynamic economic performance of CS1 and CS2 is then evaluated for Mode Ib and Mode IIb for realistic disturbance scenarios. Post a brief discussion of the results and outstanding issues, the article ends with a summary of the main findings.

6.2 Process Description

A schematic of the reactor-separator-recycle process is shown in Figure 1.8 and base-case operating conditions are noted in Table 6.1. The exothermic, irreversible, liquid-phase reaction $A + B \rightarrow C$ occurs in a cooled continuous stirred tank reactor (CSTR). The reactor effluent is distilled to recover the heavy *C* product down the bottoms and recycle the unreacted reactants up the top. The hypothetical component properties and Langmuir-Hinshelwood reaction kinetics are noted in Table 6.2. The SRK equation of state is used to model the thermodynamic properties. The hypothetical component properties used are also noted in Table 6.2. The base-case salient design and operating conditions are shown in the Figure. These correspond to optimal operating conditions for Mode Ib, as described later.

Table 6.1 The salient base-case process operating conditions

Process Variables	**Temperature (°C)**	**Molar Flow (kmol/h)**	x_A	x_B	x_C
F_A	25	99.1	1	0	0
F_B	25	99.9	0	1	0
F_{col}	96.9	264.8	0.356	0.264	0.38
R	85	164.8	0.571	0.419	0.01
P	124	100	0.001	0.009	0.99
L	85	347.4	0.571	0.419	0.01
Other Variables					
No. of Trays	15				
Feed tray	7				
Pr_{cnd}	140 kPa				
U_{rxr}	6 m^3				
T_{rxr}	110 °C				
Q_{rxr}	129.3 kW				
Q_{cnd}	2705 kW				
Q_{reb}	4016 kW				

See Figure 1.8 and Nomenclature for variable descriptions

Table 6.2. Hypothetical component properties and reaction kinetics

Kinetics	$A + B \rightarrow C$	$r = k.x_{rxrA}.x_{rxrB}/(1+K_A.x_{rxrA}+K_B.x_{rxrB})$ $k = 3.4\times10^8.\exp(-70000/RT)$ $K_A = 2.2\times10^4.\exp(-30000/RT)$ $K_B = 1.6\times10^4.\exp(-30000/RT)$	
Hypotheticals[#]	MW	NBP(°C)	VLE
A	50	70	Soave-Redlich-Kwong
B	70	80	
C	120	110	

Reaction rate units: $kmol.m^{-3}.s^{-1}$

[#]: Hydrocarbon estimation procedure used to estimate parameters for thermodynamic property calculations

6.3 Optimal Operation

Optimal steady process operation is considered for two common operating modes. In Mode I, the throughput is given (for example, target fixed by management) and an economic objective is to be optimized, while in Mode II, the throughput is to be maximized subject to a capacity bottleneck. To facilitate insight into the physics behind the self-optimizing nature of the candidate SOCV that is used here, we first consider the economic objective of minimizing recycle rate at given production (Mode Ia) and maximizing production with maximum recycle rate as the capacity bottleneck (Mode IIa). The more realistic economic objective of minimizing reboiler duty (Mode Ib) and maximizing throughput with maximum boilup as the capacity bottleneck (Mode IIb) are considered subsequently.

The process has 6 steady state degrees of freedom (dofs); two for the fresh feeds, two for the CSTR (hold up and temperature) and two for the column, assuming its operating pressure is fixed. From the operating standpoint, it is always optimal to hold the product purity, x_C^P, at the minimum guarantee given to the customer, $x_C^{P,MIN}$, to avoid free product giveaway[13]. Further, maximizing the reaction rate minimizes the Mode I recycle load so that the reactor should be operated at the maximum allowed temperature T_{rxr}^{MAX} and hold up (U_{rxr}^{MAX}). Thus in Mode I, the given production rate, $x_C^{P,MIN}$, T_{rxr}^{MAX} and U_{rxr}^{MAX} constraints take away four dofs. We also assume that the heavy C leakage in the distillate should not exceed 1 mol% due to operating considerations such as accelerated catalyst deactivation due to the heavy component or accelerated equipment fouling etc. If this constraint is relaxed, large C leakage in the distillate may be optimal, equivalent to the column operating as a simple stripper (no reflux)[14]. However, in view of practical considerations noted above, it is optimal to hold the C leakage in the distillate, x_C^R, at the maximum allowed limit, $x_C^{R,MAX}$, of 1 mol%. In Mode I, the five constraints of given production, $x_C^{P,MIN}$, $x_C^{R,MAX}$, T_{rxr}^{MAX} and U_{rxr}^{MAX} leave only one unconstrained dof. Assuming a fresh feed is used to set production, the unconstrained dof corresponds to the remaining second fresh feed.

In Mode II, the production is to be maximized and is not fixed. It is therefore a dof. The maximum production gets limited by the capacity bottleneck constraint. This capacity bottleneck is considered as maximum recycle rate, R^{MAX}, in Mode IIa or maximum boilup, V^{MAX}, in Mode IIb. All the Mode I active constraints remain active in Mode II so that we again have 5 active constraints, namely, V^{MAX} (or R^{MAX}), $x_C^{P,MIN}$, $x_C^{R,MAX}$, T_{rxr}^{MAX} and U_{rxr}^{MAX}. Thus, in both Mode I and Mode II, we have one unconstrained dof corresponding to the second fresh feed.

Typically, the dof corresponding to one fresh feed gets used to fix the specified production rate in Mode I or to drive the capacity bottleneck to its constraint limit in Mode II. The unconstrained dof corresponding to the other fresh feed gets used for stoichiometric feed balancing for overall plant material balance closure. This is accomplished by holding an appropriate process variable (PV) that is sensitive to stoichiometric imbalance. The most common arrangement is to hold a reactant composition in the reactor by manipulating the flow ratio between the two fresh feeds[15]. There are other possibilities for stoichiometric feed balancing, which shall be discussed later.

Now let us consider the Mode Ia optimal operating policy for the one unconstrained dof corresponding to the second fresh feed. The overall plant material balance closes when the C generation rate in the CSTR exactly matches the specified production rate. In other words, we have

$$k^{MAX}\frac{x_{rxrA}x_{rxrB}}{(1+K_A x_{rxrA}+K_B x_{rxrB})}U_{rxr}^{MAX}=Px_C^P \qquad (1)$$

Assuming U_{rxr}^{MAX}, P and x_C^P are reliably known and good estimates of the reaction kinetic parameters are available, the equation has only x_{rxrA} and x_{rxrB} as unknowns. Since the recycle is essentially unreacted A and B, for the recycle rate to be minimum, the total reactant mol fraction in the reactor, x_{rxrA} + x_{rxrB}, must be minimum. Without loss of generality, let us assume that at a given x_{rxrB}, the overall material balance constraint fixes x_{rxrA}. The optimum x_{rxrB} then is obtained by setting

$$\frac{d(x_{rxrA}+x_{rxrB})}{dx_{rxrB}}=0$$

$$dx_{rxrA} = -dx_{rxrB}$$

Differentiating Equation 1 treating k, K_A, K_B, U, P and x_C^P as constants, then substituting $dx_{rxrA} = -dx_{rxrB}$ and performing necessary algebraic manipulations gives the globally optimal control law as

$$x_{rxrB} = x_{rxrA} + \frac{P x_C^P}{k^{MAX}\, U_{rxr}^{MAX}} (K_A - K_B) \qquad (3)$$

This is equivalent to

$$x_{rxrB} = x_{rxrA} + \alpha P$$

Note that for tightly regulated x_C^P and U (reactor level), which is true in practice, α depends only on the reaction kinetic parameters. Usually, at fixed temperature, the adsorption equilibrium constants, K_A and K_B, will remain fixed. The reaction rate constant, k, however is very likely to decrease significantly over time due to catalyst deactivation. The globally optimal control law above is then problematic in that α cannot be treated as a constant and will require re-estimation. An alternative reaction rate constant independent globally optimal control law may be obtained by substituting of Equation 1 into Equation 3, which gives

$$x_{rxrB} - x_{rxrA} = \frac{x_{rxrA} x_{rxrB} (K_A - K_B)}{1 + K_A x_{rxrA} + K_B x_{rxrB}} \qquad (4)$$

Even as the above is a somewhat more complicated expression, it is independent of the reaction rate constant and contains only two unknown parameters, K_A and K_B. Since the CSTR is operated at the maximum allowed temperature constraint, T^{MAX}, and reactor temperature is tightly regulated, K_B and K_A can be treated as constants so that the globally optimal control law above does not contain any parameters that require re-identification. The two unknown parameters need to be identified only once. This may be done, for example, using data from two optimal steady states at different production rates.

For Mode IIa, the derivation of the globally optimal control law is very similar. At maximum production with $R = R^{MAX}$ (bottleneck), the C mol fraction in the reactor should be as large as possible. This is equivalent to having the total reactant concentration in the reactor, $x_{rxrA} + x_{rxrB}$, as small as possible. We therefore have $dx_{rxrA} = -dx_{rxrB}$ for optimality, as before. Further, differentiation of the overall material balance results in the same globally optimal invariant as in Equation 3 and Equation 4.

Note that for both Mode Ia and Mode IIa, process insight/intuition has been applied to directly derive the optimality condition requiring $dx_{rxrA} = -dx_{rxrB}$. A rigorous proof is provided in chapter 5. We also highlight that for simpler conventional reaction kinetics with $r = k\, x_{rxrA}^{a}\, x_{rxrB}^{b}$, using the procedure above, the globally optimal invariant is

$$\frac{x_{rxrB}}{x_{rxrA}} = \frac{b}{a}$$

This simply requires holding the reactor *A/B* ratio at the appropriate value. Even as this invariant is for the simpler power law kinetics, it provides a physical basis for reactor *A/B* ratio as a potential SOCV.

Armed with the globally optimal invariants from Mode Ia and Mode IIa, we now consider process operation for the more realistic objective of minimizing boilup at given production (Mode Ib) and maximizing production with maximum boilup corresponding to column flooding as the capacity bottleneck. The globally optimal invariant derived previously can no longer be the invariant (zero loss) since the objective function and capacity bottleneck are now different. It is however reasonable to expect that the implementation of the same control law in Mode Ib and Mode IIb gives acceptably small economic loss so that the control law is self-optimizing.

For quantitative evaluation, we consider a change in Mode Ib production rate by up to ±20% and a 40% decrease in catalyst activity in Mode IIb operation as typical disturbances. Figure 6.1 plots the % loss from the actual optimum using candidate self optimizing operating policy of Equation 4, reactor *A/B* ratio, reactor limiting reactant composition (x_{rxrB}). The Figure also shows the % loss for top rectifying tray temperature (T_{top}) as the CV in lieu of x_{rxrB}. As described later, T_{top} is an inferential measure of reactor *A/B* ratio. Note that the difference between the LHS and RHS of Equation 4 is the CV based on the derived invariant from the simplified analysis (Mode Ia and Mode IIa). Its setpoint value then is zero.

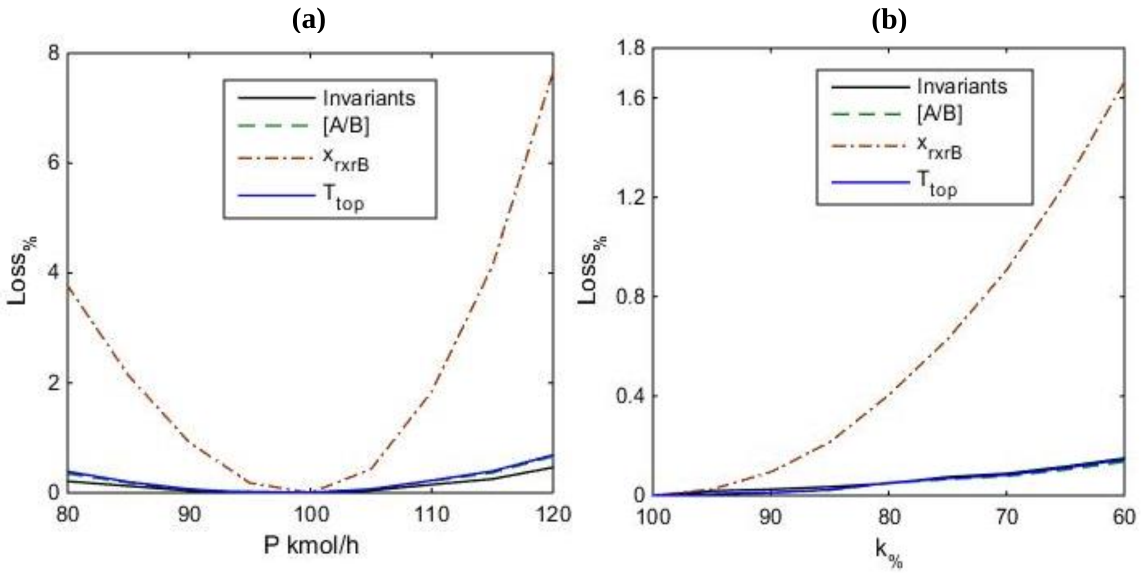

Figure 6.1. % economic loss for four alternative CVs (a) Mode Ib (b) Mode IIb

The Mode IIb data in Figure 6.1 is plotted assuming that the CV is at its optimum value for the nominal reaction rate constant *k*. The economic loss is then calculated for no redjustment in the CV setpoint from this Mode II nominal optimum. Usually, a Mode I to Mode II transition is effected by increasing the TPM setpoint till the bottleneck constraint goes active. It is very likely that the CV setpoint is maintained at its nominal Mode I optimum value. In such a case, the economic loss is from the Mode I nominal optimum, which is likely to be greater than the loss from the Mode II nominal optimum shown in Figure 6.1. Table 6.3 quantifies this greater loss for the four candidate CVs. The data in Figure 6.1 and Table 6.3 clearly suggest that both the invariant (Equation 4) reactor *A/B* ratio and T_{top} are self-optimizing control policies with the Mode Ib loss being within 0.7% and the Mode IIb loss being within 0.2% of the actual optimum. It is quite surprising that the very simple constant reactor *A/B* ratio policy is only slightly worse than the Equation 4 invariant. We therefore consider this simple constant reactor *A/B* ratio self-optimizing control policy, or equivalently, T_{top}, which is a good inferential measure of reactor *A/B* ratio, as described in the following, for implementation.

Table 6.3. % Loss for the four candidate SOCVs

Disturbance	Mode Ib				Disturbance	Mode IIb			
P kmol/h	Invariant	*[A/B]*	x_{rxrB}	T_{top}	$k_{\%}$	Invariants	*[A/B]*	x_{rxrB}	T_{top}
120	0.463	0.665	7.659	0.690	60	0.150	0.136	1.663	0.146
115	0.252	0.365	4.128	0.395	65	0.117	0.104	1.253	0.111
110	0.150	0.216	1.844	0.225	70	0.088	0.078	0.907	0.083
105	0.043	0.066	0.432	0.068	75	0.075	0.066	0.629	0.069
100	0.005	0.010	0.000	0.006	80	0.049	0.049	0.404	0.051
95	0.020	0.003	0.181	0.006	85	0.035	0.022	0.215	0.023
90	0.039	0.056	0.924	0.068	90	0.025	0.011	0.094	0.012
85	0.125	0.185	2.140	0.199	95	0.019	0.005	0.025	0.007
80	0.211	0.348	3.772	0.389	100	0.001	0.001	0.000	0.001

6.4 Inferential SOCV

One of the major issues with the reactor *A/B* ratio as an SOCV is that it requires two analytical composition measurements, namely x_{rxrA} and x_{rxrB}. Given that analytical composition measurements can be quite expensive, cumbersome, unreliable and with potentially large measurement delays, it is worthwhile investigating if routine online measurements can be used to infer/estimate x_{rxrA} and x_{rxrB}. We note that since x_{rxrA}/x_{rxrB} is an SOCV and the product stream is nearly pure with negligible *A* and *B* impurities, essentially all of the unreacted *A* and *B* leaving the reactor ends up in the column distillate stream. In other words,

$$\frac{x_{rxrA}}{x_{rxrB}} \approx \frac{x_A^R}{x_B^R}$$

Since the unreacted *A* and *B* end up at the top of the column, assuming x_C^R is held constant at its active constrained value, then the column top tray temperature, T_{top}, is directly correlated with x_A^R/x_B^R. Thus if x_{rxrA}/x_{rxrB} increases, implying more *A* circulating around the plant (relative to *B*), T_{top} would decrease since *A* is lighter than *B*. Conversely, if x_{rxrA}/x_{rxrB} decreases, the relative proportion of *B* circulating around the plant is higher and T_{top} would increase. This direct correlation between T_{top} and the x_{rxrA}/x_{rxrB}, a good SOCV, implies that T_{top} is also a candidate *SOCV*. Its advantage is that it obviates the need for cumbersome analytical reactor composition measurements for optimal management of the unconstrained dof. Also, given its correlation with the relative *A/B* proportion circulating around the plant, it will stoichiometrically balance the fresh feeds. Controlling T_{top} thus serves two purposes, the regulatory objective of stoichiometric feed balancing and the economic objective of self-optimizing process operation corresponding to the one unconstrained dof in both Mode Ib and Mode IIb. Note that the most common control strategy in the literature for stoichiometric feed balancing is to hold a reactant composition in the reactor by manipulating the fresh reactant feed ratio[15-17].

The self optimizing nature of T_{top} can again be verified from Figure 6.1, which shows the variation in the economic objective when T_{top} is held constant at the nominal optimum. The corresponding variation when x_{rxrA}/x_{rxrB} or x_{rxrB} is held constant at the nominal optimum, is also shown. The plot clearly suggests that T_{top} is a good SOCV with its performance being almost as good as when x_{rxrA}/x_{rxrB} is held constant. On the other hand, x_{rxrB} is a markedly inferior SOCV with noticeably higher economic loss over the envisaged disturbance range.

6.5 Plantwide Control Systems

The plantwide control system is now synthesized. Since the capacity bottleneck is the maximum boilup constraint, boilup is used as the TPM, in line with the heuristic of locating the TPM at the bottleneck constraint[13,18-19]. To hold the boilup constant, the reboiler duty is manipulated. Since the boilup vs production rate relationship is not known *apriori*, a "loose" production rate controller manipulates the boilup controller setpoint in order to hold the product rate at the desired value. Standard level and pressure loops are applied on the column with the sump level regulated by manipulating the bottoms and the reflux drum level regulated by manipulating the distillate rate. The column pressure is regulated by manipulating the condenser duty. A sensitive stripping tray temperature is regulated by manipulating the column feed rate, since the reboiler duty is already paired for throughput regulation. The stripping tray temperature controller setpoint is updated by a product purity controller. On the CSTR, the level is controlled by manipulating the fresh *B* feed rate (F_B) since the reactor effluent is already paired for stripping temperature control. The fresh *A* feed rate (F_A) is maintained in ratio with F_B and the ratio setpoint is manipulated for stoichiometric feed balancing, for which two alternative CVs are considered. The first one holds the reactor *B* mol fraction, x_{rxrB}, which is the conventional practice[15-17], while the second one holds the column top tray temperature, T_{top}, which is also a good SOCV.

The only remaining loop now is the CV to be held constant to hold the recycle stream *C* leakage, x_C^R. We first considered using rectifying section tray temperature control to inferentially hold x_C^R. However, since all three components are present in the rectification section, x_C^R was found to vary between 0.5 to 5 mol% over the envisaged operating space, when the most sensitive rectifying tray temperature is controlled. If the tray temperature setpoint is backed-off so that x_C^R remains below its maximum limit of 1% over the envisaged operating space, the resulting economic loss is very large (>10%). In view of this, we apply the most straightforward method of directly measuring x_C^R and manipulating the reflux rate to hold it constant. Later on, we discuss the possibility of using the difference between two appropriately chosen tray temperatures, ΔT, as an inferential measure of x_C^R. The regulatory control structure as explained above is shown in Figure 6.2. For ease of reference, the control structure with x_{rxrB} as the CV for stoichiometric balancing is referred to as CS1 while the control structure with T_{top} as the CV for the same is referred to as CS2.

For optimal operation, the optimally active constraint setpoints are simply set to the constraint values, i.e., $U_{rxr}^{SP} = U_{rxr}^{MAX}$, $T_{rxr}^{SP} = T_{rxr}^{MAX}$, $x_C^P = x_C^{P,MIN}$ and $x_C^{R,SP} = x_C^{R,MIN}$. In Mode Ib, the production regulator fixes V^{SP} such that the production rate is the desired value. In Mode IIb, we have $V^{SP} = V^{MAX}$ with the desired production rate setpoint being too high so that the low selector (see Figure 6.3) passes V^{MAX} as the setpoint to the boilup controller.

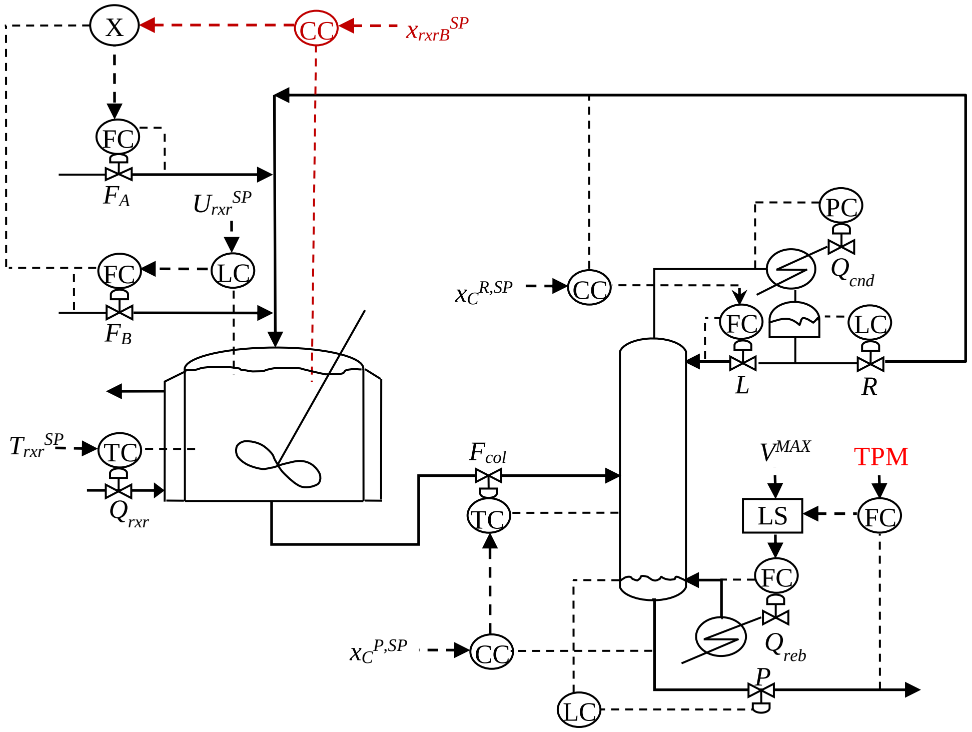
X
CC
x_{rxrB}^{SP}
FC
F_A
U_{rxr}^{SP}
FC
LC
F_B
T_{rxr}^{SP}
TC
Q_{rxr}
$x_C^{R,SP}$
CC
PC
Q_{cnd}
FC
LC
L
R
F_{col}
TC
V^{MAX}
TPM
LS
FC
FC
Q_{reb}
$x_C^{P,SP}$
CC
P
LC

Figure 6.2. Plantwide control structure, CS1

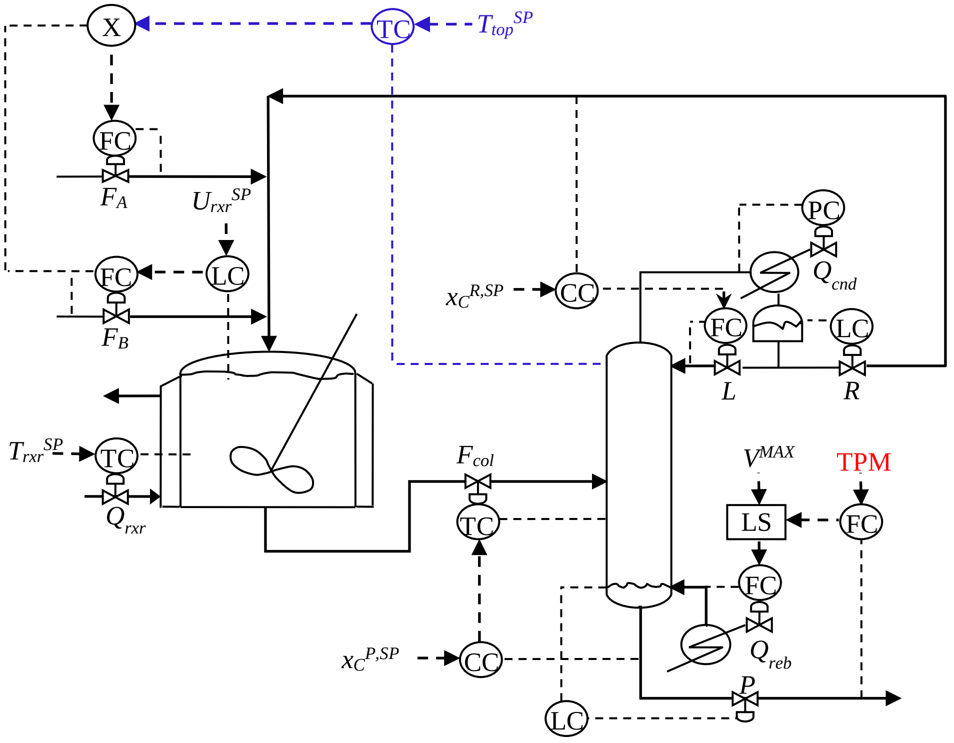
X
TC
T_{top}^{SP}
FC
F_A
U_{rxr}^{SP}
FC
LC
F_B
T_{rxr}^{SP}
TC
Q_{rxr}
$x_C^{R,SP}$
CC
PC
Q_{cnd}
FC
LC
L
R
F_{col}
TC
V^{MAX}
TPM
LS
FC
FC
Q_{reb}
$x_C^{P,SP}$
CC
P
LC

Figure 6.3. Plantwide control structure, CS2

6.6 Closed Loop Dynamic Results

A pressure driven dynamic simulation is built for the PWCS described above. The reflux drum and bottom sump are sized for 5-10 min holdup at the Mode Ib nominal condition at 50% level. The control valves are sized for the nominal flow at 50% opening. The column diameter is sized for nominal operation at 50% flooding velocity. The tray resistance to vapor flow is calculated for the nominal vapor rate and column pressure profile. A 0.5 min lag is applied to all temperature measurements to account for temperature sensor dynamics. Also, a 2 min lag is applied to all direct Q control valves to account for heat exchange equipment dynamics. A 5 minute dead time and sampling time is applied to any composition measurements. All flow controllers are PI and use a gain of 1 and integral time of 0.5 mins for a fast servo response. The column reflux drum and bottom sump level controllers are P only and use a gain between 1-2 (%/%). The column pressure controller is PI and tuned aggressively for tight pressure control. The reactor level controller is PI and uses a gain of 2 (%/%) with the integral time adjusted for a slightly oscillatory servo response. The reactor temperature and column stripping tray temperature controllers are PI and tuned for a slightly underdamped servo response. For stoichiometric feed balancing, the T_{top} or x_{rxrB} controller is tuned by hit and trial for a smooth not-too-oscillatory plantwide response. Lastly, the PI product purity controller is tuned with all other controllers on automatic for a slightly underdamped servo response. The salient parameters of the regulatory loops in CS1 and CS2 simulations are noted in Table 6.4.

The PWCS described above is evaluated for routine disturbances for Mode Ib and Mode IIb operation. Both step changes and sinusoids of varying frequency are considered. The Mode Ib step disturbances are a ±20% change in the production rate, a 10 mol% change in the composition of fresh *B* feed with *A* as impurity and a 20% decrease in the reaction rate constant. The Mode IIb step disturbances are a 30% decrease in reaction rate constant and a 30% decrease in V^{MAX} (bottleneck constraint). The sinusoid disturbances considered are a ±20% production rate sinusoid around the nominal in Mode Ib and in Mode IIb, a reaction rate constant sinusoid between 70% of nominal to 100% of nominal as well as a V^{MAX} sinusoid from 900 kmol/h to 630 kmol/h in Mode IIb. For clarity, these disturbances are explicitly noted in Table 6.5.

Table 6.4. Salient controller parameters for CS1/CS2$^{*,\#,\$}$

CV	CS1/CS2		PV Range$^{\&}$	MV Range$^{\&}$
	K_C	τ_i(min)		
x_{rxrB}/T_{top}	2.2/3.5	150/150	0.05-0.50/75-95°C	0.5-1.5
$P^{\&}$	0.09	5	200kmol/h	250-1000kmol/h
T_{rxr}	2.5	25	90-130°C	$3\text{x}10^6$ kJ/h
U_{rxr}	2	30	0-100%	0-100%
x_C^R	0.2	60	0.005-0.03	100-800kmol/h
T_{Col}^S	0.5	20	110-135°C	0-100%
V	0.5	1	100-1100	$4\text{x}10^7$ kJ/h
x_C^P	0.1	80	0.98-0.999	110-135°C

$^{\&}\tau_D$=10 min for both. * Values for both CS1 and CS2 are same unless otherwise specified. $^{\#}$All level loops use K_C = 1 unless otherwise specified. \$ Pressure/flow controllers tuned for tight control. $^{\$}$ All compositions have a 5 min dead time and sampling time. All temperature measurements are lagged by 2 min.

Table 6.5. Evaluation of disturbances

	Disturbances	**Period/Frequency (h)**	**Type**	**Step Length/ Amplitude**
Mode I	TP	30	Step	+20%
	TP	30	Step	-20%
	CC_{F_B}	30	Step	-10%
	k	30	Step	-20%
	TP	96/48/24/12/6	Sinosoid	±20%
	k	96/48/24/12/6	Sinosoid	±20%
Mode II	V^{Max}	30	Step	-20%
	k	30	Step	-30%
	V^{Max}	96/48/24/12/6	Sinosoid	±30%
	k	96/48/24/12/6	Sinosoid	±30%
Mode I → Mode II → Mode I		120 (60+60)	Ramp	±6 kmol/h

We present the closed loop response of the two plantwide control systems, CS1 and CS2, where in CS1, x_{rxrB} is held constant, and in CS2, T_{top} is held constant. All other loops are as in Figure 6.2. Figure 6.4 contrasts the Mode Ib CS1 and CS2 responses to a ±20% production rate change. In both cases, tight product quality control is achieved in the transient period with the maximum purity deviation being no more than 0.5 mol%. Also the fresh feed, recycle and product stream rates exhibit a smooth response with more oscillatoriness in the direction of a production rate decrease. The response for both CS1 and CS2 completes in about 25 hrs. Notice that the CS1 final steady state boilup is noticeably higher than CS2. Specifically, the final CS1 boilup is 7% and 3.4% higher than CS2 for, respectively, a production rate increase and a production rate decrease.

The Mode Ib transient response of CS1 and CS2 to 10 mol% *A* in fresh *B* feed is shown in Figure 6.5. Overall, the response is smooth with gradual transients in the fresh feeds, boilup, product rate and recycle rate and takes about 20 hrs to complete for both CS1 and CS2. Tight product quality control is observed during the transient period. Since the product rate is the same as the initial steady state (100 kmol/h), the final boilup and recycle rate is the same as the initial steady state. Also, since now *A* is entering the process as an impurity in F_B, the final steady state F_A is lower while the final F_B is higher. Between CS1 and CS2, the transient swing in the boilup, recycle rate and product rate is lower for CS1. This is because CS1 directly regulates x_{rxrB} so that the sudden initial decrease in x_{rxrB} is compensated by a quick decrease in F_A. The action of the corresponding T_{top} controller in CS2 is naturally slower so that the CS2 transients are larger.

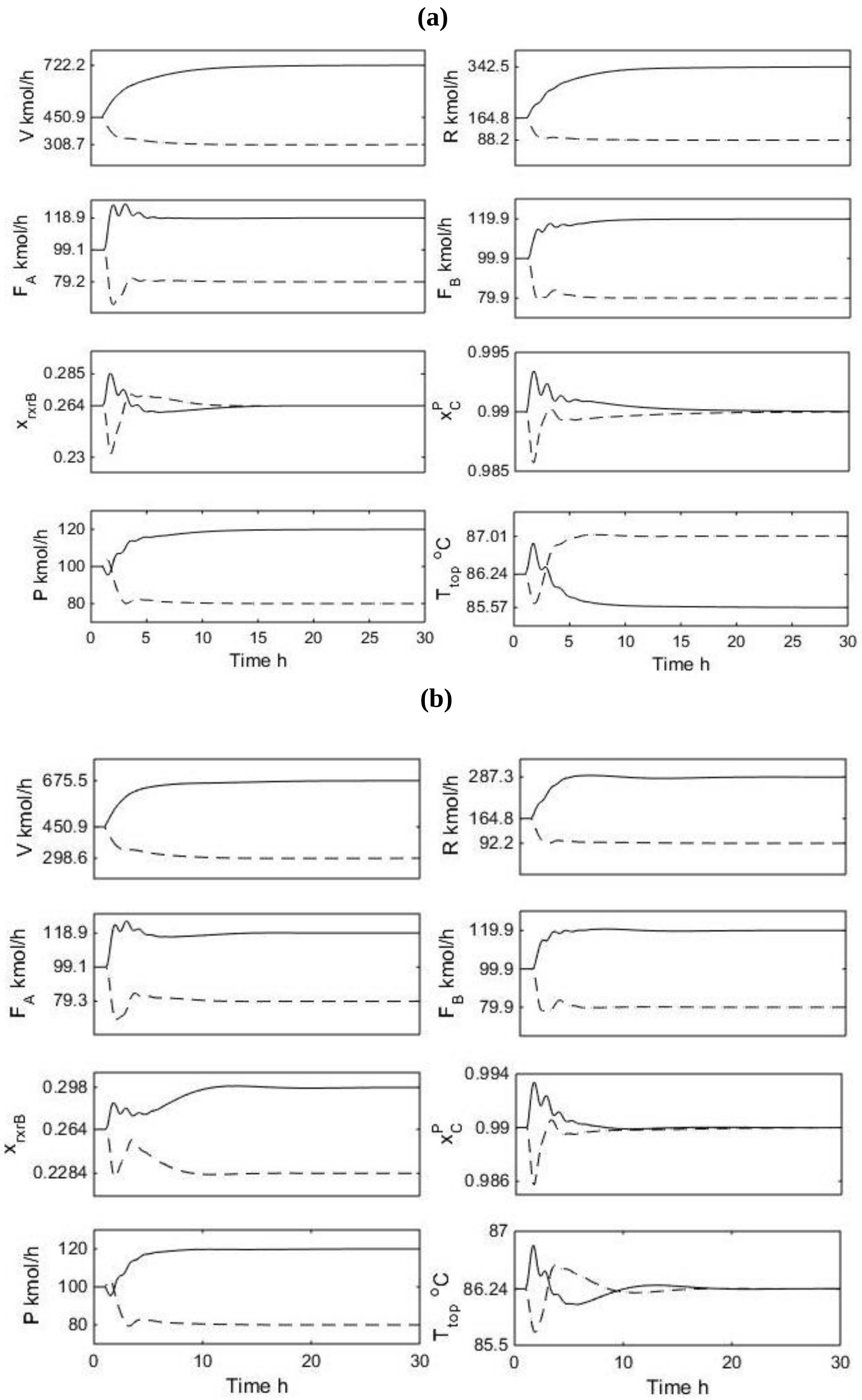

Figure 6.4. Transient response for a ±20% Mode Ib throughput change (a) CS1 (b) CS2

The Mode Ib transient response to a 20% step decrease in reaction rate constant is shown in Figure 6.6. As before, tight product quality control is achieved in the transient period. The decrease in rate constant causes the product rate to decrease initially with the recycle rate increasing due to build-up of unreacted reactants. In response to the decrease in production, the product controller appropriately increases the boilup to drive the production rate back to the desired value (100 kmol/h). Overall, the transient response completes in about 25 hrs for both CS1 and CS2. Notice that the final steady state boilup for CS1 is 12% higher than for CS2 implying significant economic benefit of controlling T_{top}.

The Mode IIb reaction rate constant step decrease response is shown in Figure 6.7. As before, tight product purity control is observed during the transient period with the smooth plantwide response completing in 25 hrs for both CS1 and CS2. Here, since V^{MAX} is the active constraint and the catalyst activity decreases by 30%, the final steady state product rate decreases and settles at a lower value. The CS1 Mode IIb final product rate is 0.75% lower than the corresponding value for CS2.

We also tested CS1 and CS2 for a 20% V^{MAX} step decrease in Mode IIb to obtain smooth plantwide transient response with tight product purity control. Expectedly, the final CS1 product rate is 0.4% lower than CS2. The Mode IIb results suggest that the economic benefit difference between CS1 and CS2 is only marginal. This is probably because the variation in product rate with x_{rxrB} is quite flat so that the economic penalty for not reoptimizing x_{rxrB} is not severe.

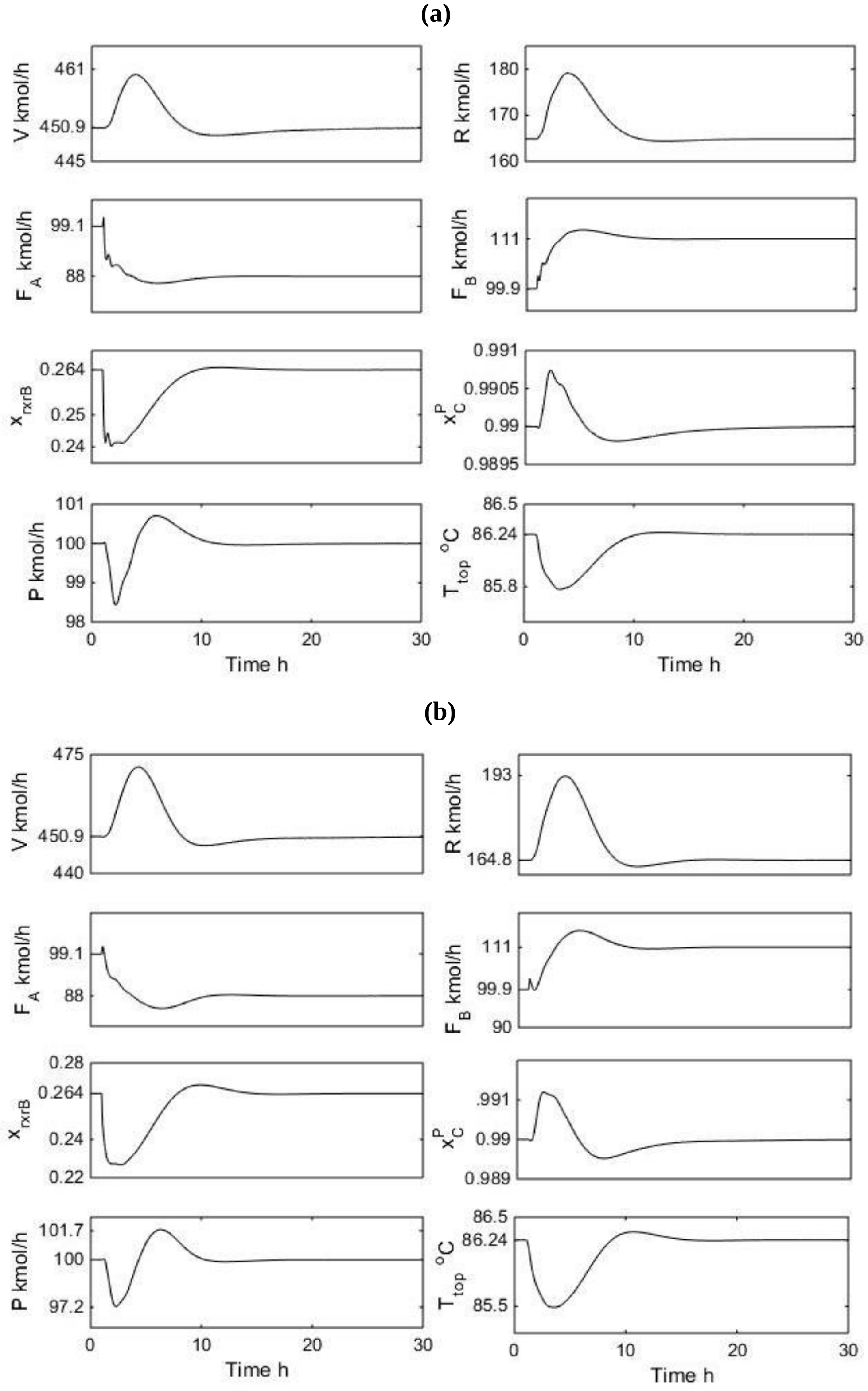

Figure 6.5. Mode Ib transient response for 10 mol% *A* in F_B (a) CS1 (b) CS2

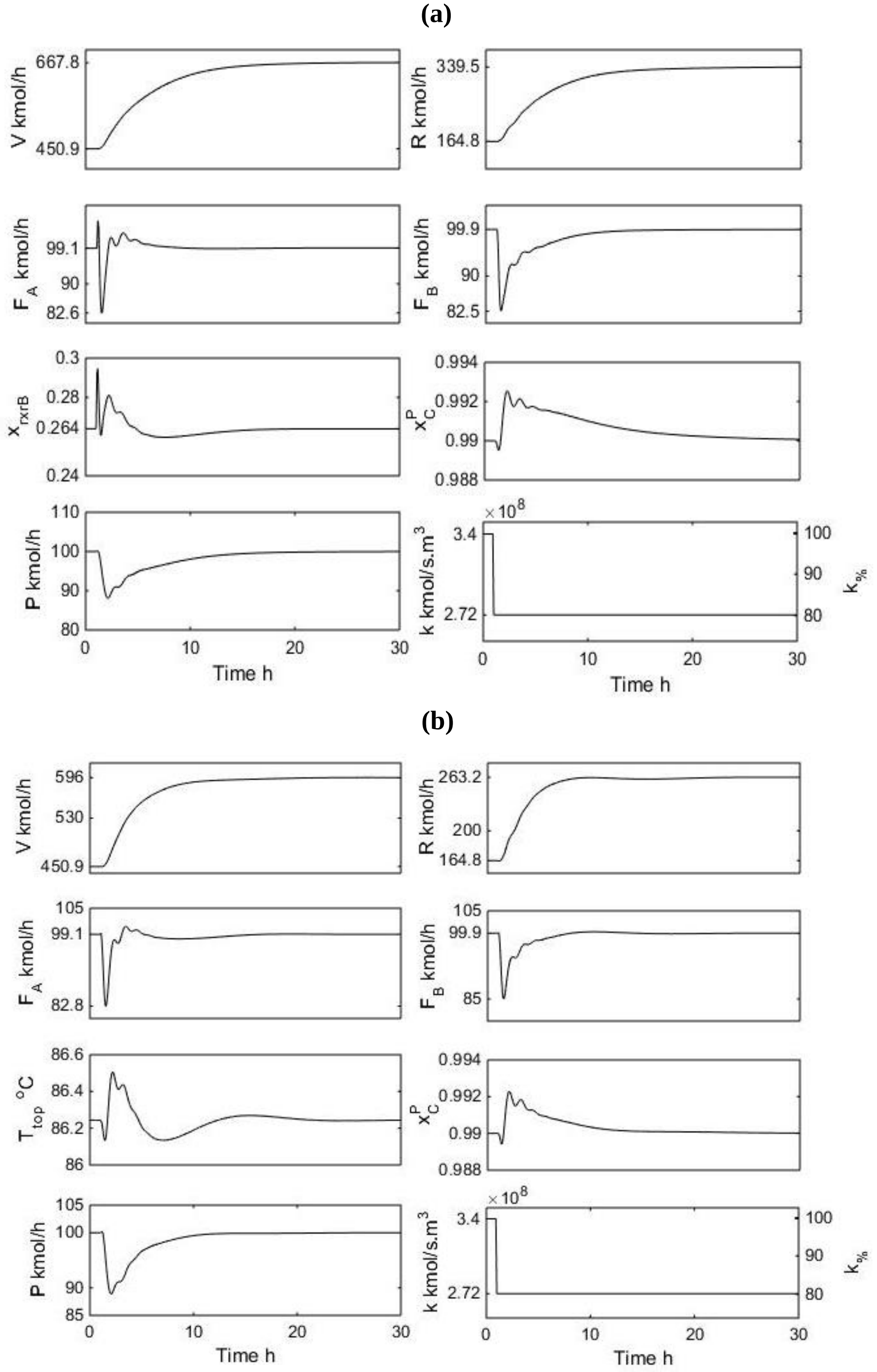

Figure 6.6. Mode Ib transient response for 20% catalyst activity decay (a) CS1 (b) CS2

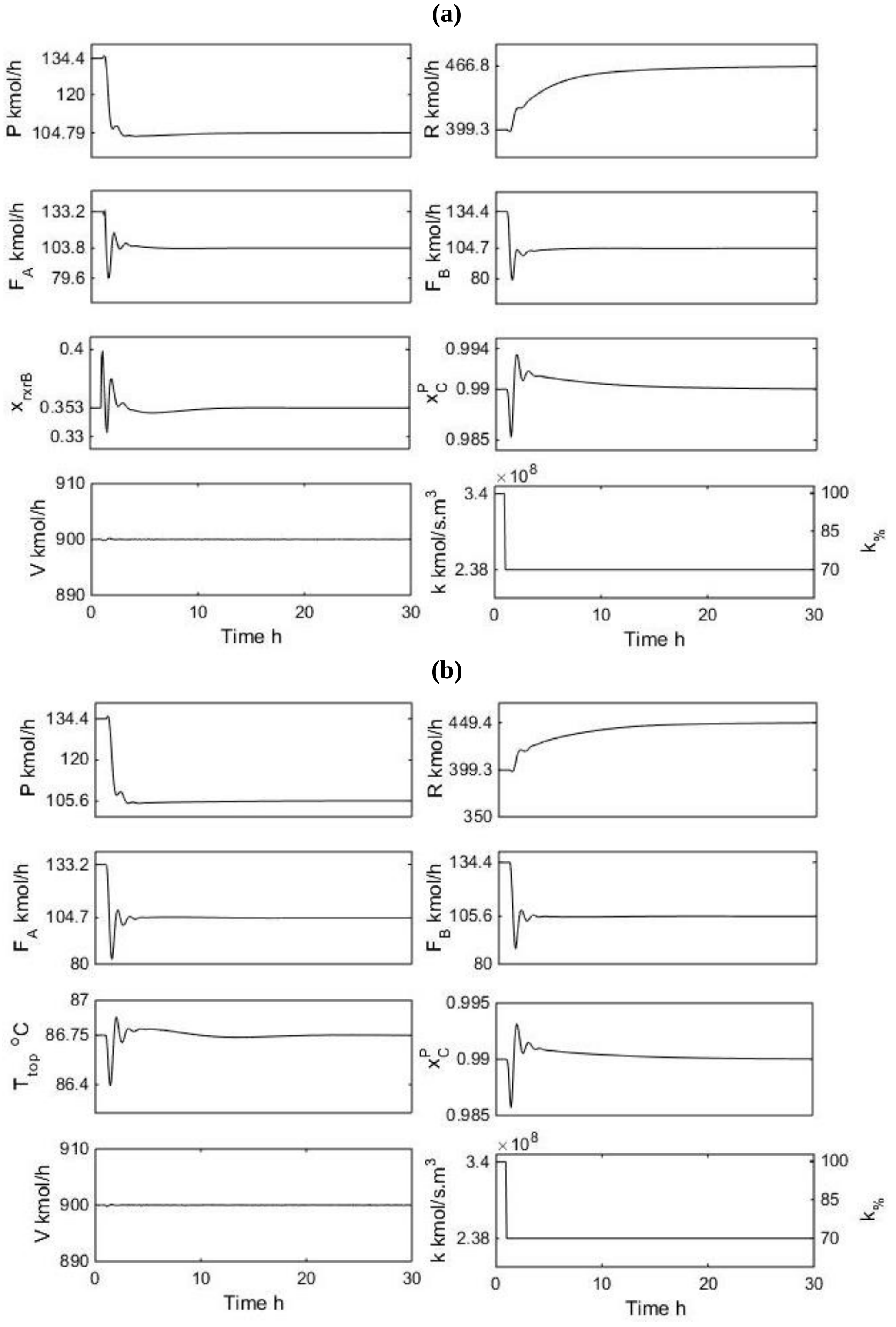

Figure 6.7. 30% activity decay for Mode IIb (a) CS1 (b) CS2

In line with the step change disturbance results, our closed dynamic simulations showed that for sufficiently slow sinusoidal disturbances, CS2 achieves noticeably superior economic performance compared to CS1 in Mode Ib with only a marginal benefit in Mode IIb for all the considered disturbances. However, as the sinusoid becomes fast enough, it is possible that the CS2 outperforms CS1 for specific disturbances. To quantify the economic performance, we simulated 30 days of process operation with the sinusoid disturbance time period being halved from a maximum of 96 hrs (i.e. sinusoid time periods of 96, 48, 24, 12 and 6 h). For Mode Ib, we calculate the average boilup per kg product over the 30 day period defined as

$$[V/P]_{av} = \frac{\int V(t)dt}{\int P(t)dt}$$

For Mode IIb, the average production, P_{av}, over the 30 day period is calculated. To compare between CS1 and CS2 performance at the different sinusoid frequencies, the percentage difference between the two, defined as

$$\text{Mode Ib:} \qquad \Delta[V/P]_{av}\% = \frac{[V/P]_{av}^{CS1} - [V/P]_{av}^{CS2}}{[V/P]_{av}^{CS2}} \times 100$$

$$\text{Mode IIb:} \qquad \Delta P_{av}\% = \frac{P_{av}^{CS2} - P_{av}^{CS1}}{P_{av}^{CS2}} \times 100$$

is obtained.

Figure 6.8 shows the variation in $\Delta[V/P]_{av}\%$ and $\Delta P_{av}\%$ with sinusoid time period for the considered sinusoid disturbances, namely, a Mode Ib ±20% production rate sinusoid, a Mode IIb reaction constant sinusoid and a Mode IIb V^{MAX} sinusoid. In all cases, notice that for sinusoids of period 12 hrs or more, the economic performance of CS2 is consistently superior to CS1 by a few percentage points (2-4%) in Mode Ib and marginally (0.2-0.4%) in Mode IIb. For the fast sinusoid of 6 hr period however, CS1 outperforms CS2 in both Mode Ib and Mode IIb for the considered disturbances. It appears that this difference is caused by the non-linearity between boilup (TPM/ bottleneck constraint) and production rate. A change in boilup required per unit production increase is significantly larger than the corresponding value for a production rate decrease.

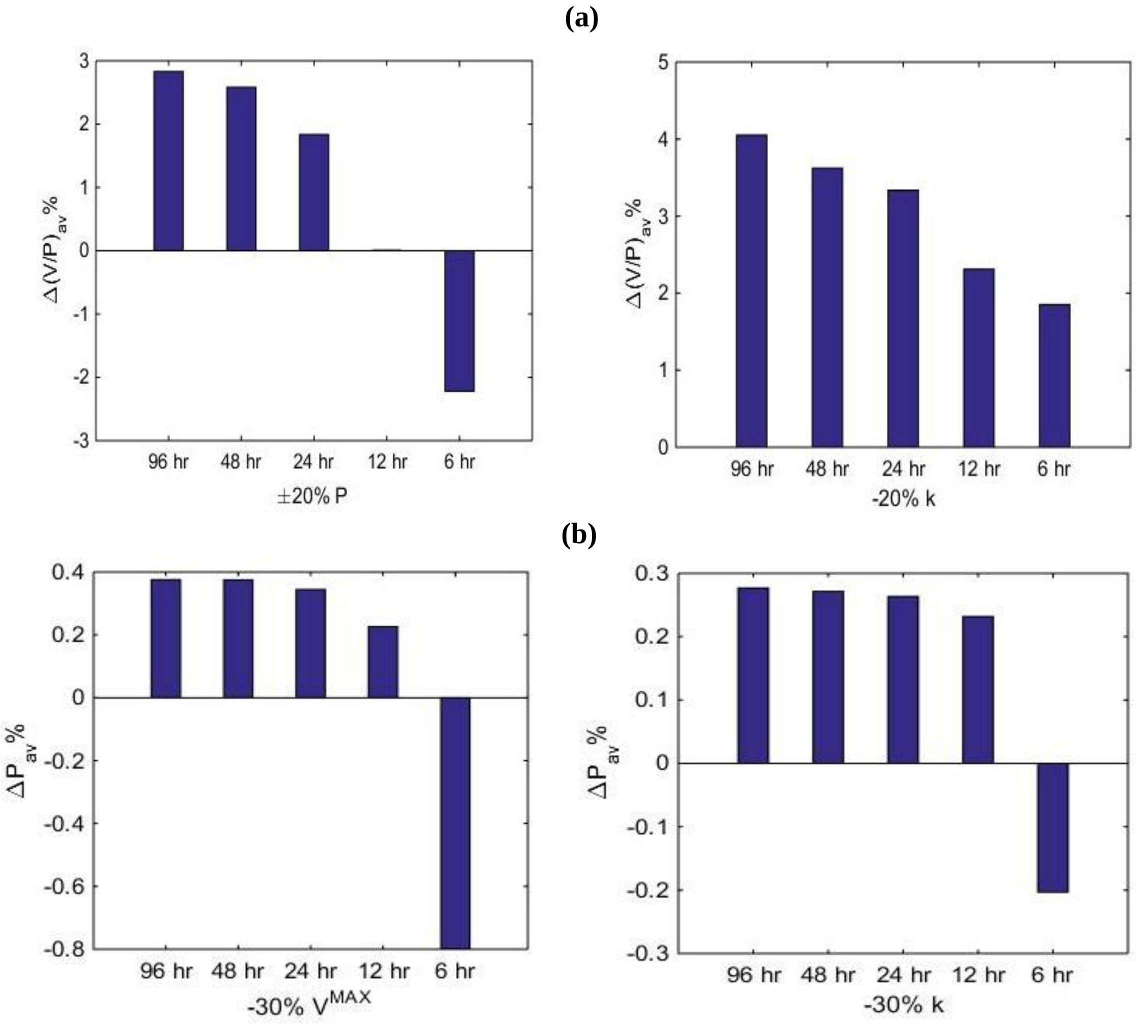

Figure 6.8. Variation in $\Delta[V/P]_{av}$% and ΔP_{av}% for different sinusoid time periods for considered sinusoid disturbances for (a) Mode Ib (b) Mode IIb

As the final illustration of the dynamic performance of the alternative control policies, we consider a tranision from Mode Ib to Mode IIb and then back to Mode Ib. Initially the process is at its nominal production (100 kmol/h; Mode Ib). The product rate regulator setpoint is then ramped up at till 135 kmol/h and held constant there. In response, the column boilup increases and the V^{MAX} constraint goes active (Mode IIb). The process is operated in Mode IIb for 45 hrs and then the production regulator setpoint is ramped back down to nominal. The dynamic responses are obtained for CS1 and CS2 and are shown in Figure 6.9. As expected, holding T_{top} (CS2) gives a Mode IIb product rate that is higher than CS2 by 5.1%. Throughout, x_{rxrB} (CS1) and T_{top} (CS2) are maintained at their Mode Ib nominal optimum values. Since T_{top} is a good SOCV, maintaining it at the nominal value naturally causes x_{rxrB} to increase in proportion to the increase in x_{rxrA} at increased proportion. On the other hand, in CS1, x_{rxrB} is maintained at its nominal value so that x_{rxrA} must increase substantially to achieve higher production. CS1 thus drifts the process significantly away from the optimum reactor *A/B* ratio whereas CS2 maintains it close to the optimum *A/B* ratio. This difference causes the substantial 5% benefit in the achieved maximum product rate in CS2 over CS1 for the same V^{MAX} bottleneck.

Overall, the presented closed loop dynamic results clearly illustrate that T_{top} is a good SOCV that gives substantial economic benefit compared to conventional process operation holding a reactant composition in the reactor. One of the unaddressed questions here is how well would SOC compare with conventional RTO. We intend to take this up in a future study.

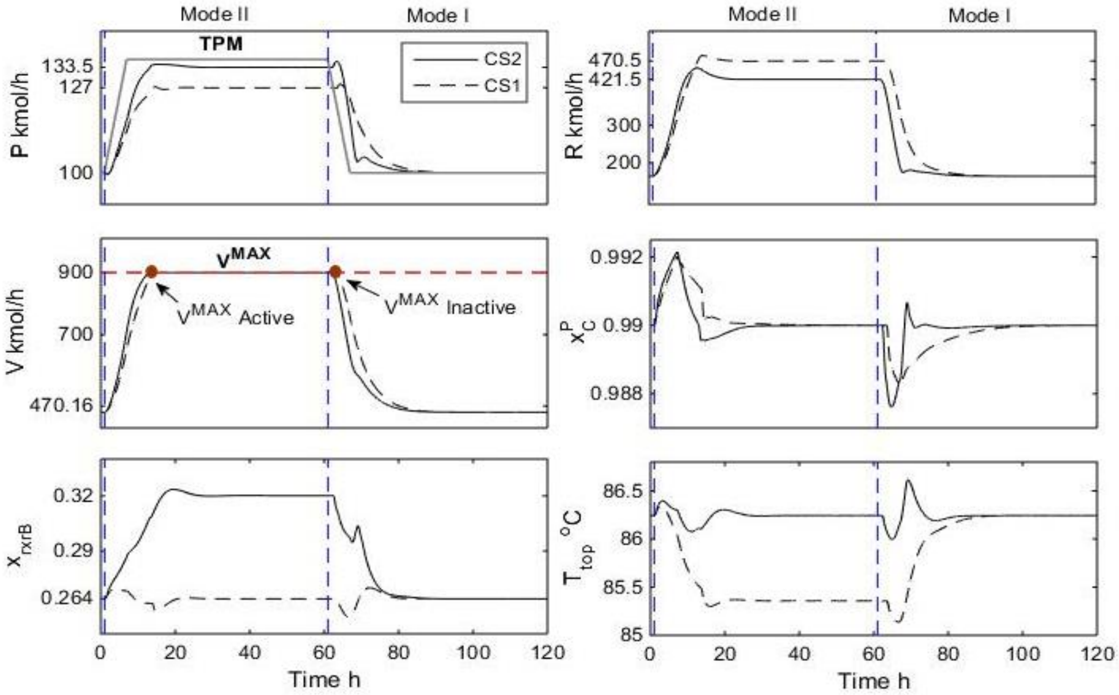

Figure 6.9. Mode Ib → Mode IIb → Mode Ib transition for constant x_C^R

6.7 Discussion

In the presented closed loop results, x_C^R is held constant, which requires a cumbersome analytic composition measurement. Direct rectifying tray temperature control gave unacceptably loose regulation of x_C^R, which is what necessitated direct x_C^R control. In the literature, tray temperature combinations have been used for tighter inferential composition control [20-22]. One of the most commonly applied combinations is the difference between tray temperatures (ΔT) [23]. We explored the possibility of using ΔT as a CV in lieu of direct x_C^R control. Upon trying several combinations, we found that when holding $\Delta T = T_{13} - T_3$, where the column feed is on the seventh tray (top-down numbering), the variation in x_C^R is between 0.6 to 1.5 mol% when throughput is varied from 80 to 120 kmol/h. This range is much smaller than when the most sensitive rectifying tray temperature is controlled at its nominal value, where the corresponding range is 0.5 to 5 mol%. By holding $\Delta T = T_{13} - T_3$ at an appropriate backed-off value, we can ensure that the worst-case x_C^R is at the optimally active constraint limit ($x_C^{R,MIN}$) of 1 mol%. This backed-off ΔT setpoint will create some suboptimality at all other operating conditions.

To analyze for the suboptimality due to backed off ΔT for the alternative operating policies, namely, constant T_{top} and constant x_{rxrB} (CS1$^{\Delta T}$ and CS2$^{\Delta T}$), Figure 6.10 compares the variation in the economic objective with respect to the principal Mode Ib/Mode IIb disturbance using these two policies. The rigorous economic optimum curves are also shown in the Figure. The curves have been obtained for constant ΔT with sufficient back-off such that the worst-case x_C^R does not exceed 1 mol% ($x_C^{R,MAX}$). For comparison, we also plot the curves with $x_C^R = 1$ mol%. It is clearly evident that the constant ΔT operating policy entails significant economic lost of ~29% compared to constant x_C^R of 1 mol%. The moot question then is if this loss is large enough to justify an expensive x_C^R measurement. It is also evident that the constant T_{top} operating policy gives near optimal operation and its benefit over the conventional constant x_{rxrB} operating policy remains substantial regardless of whether ΔT or x_C^R is held constant. T_{top} is thus a good SOCV for managing the unconstrained dof corresponding to the second fresh feed.

(a) **(b)**

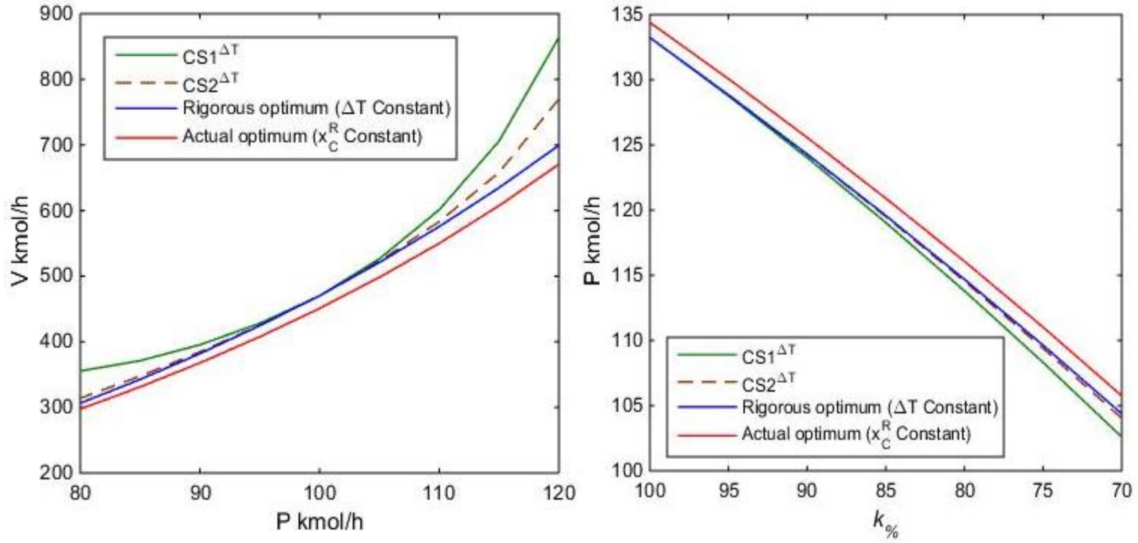

Figure 6.10. Economic objective at backed-off ΔT (a) Mode Ib (b) Mode IIb

For argument's sake, let us assume that the x_C^R measurement is expensive enough to justify controlling ΔT with an appropriate back-off in its setpoint. We tuned such a ΔT controller and tested it for Mode Ib and Mode IIb disturbances. Overall, we observed that when ΔT is controlled instead of x_C^R, the throughput controller requires significant detuning to avoid a highly oscillatory plantwide response. As an illustration, Figure 6.11 compares the response of salient PVs to a ±20% throughput change response in Mode Ib for CS1$^{\Delta T}$ and CS2$^{\Delta T}$. Notice that the response completion time is now noticeably higher at 40 hrs. It is particularly sluggish for a throughput increase. It appears that this may be due to input multiplicity in the ΔT vs L (reflux rate) input-output relation, which is well documented in the literature (see e.g. [24-25]). The sluggish response will naturally reduce the overall economic advantage of CS2 over CS1 in the face of transient disturbances. Given that the back-off required in ΔT itself causes a substantial economic loss (up to 28%), directly regulating x_C^R may be preferred over temperature inferential control, for the specific process evaluated.

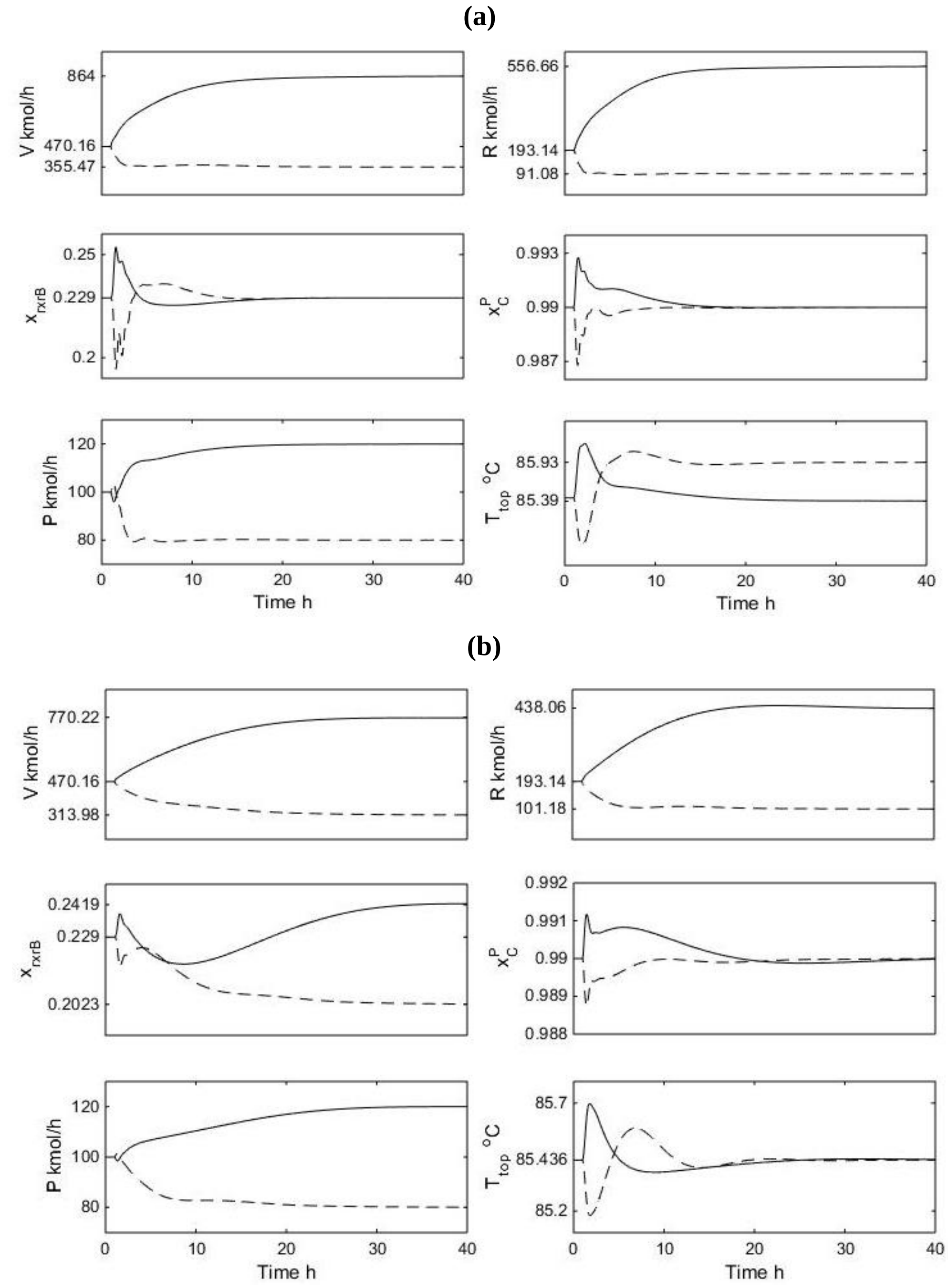

Figure 6.11. Transient response to a ±20% Mode Ib throughput change at backed-off *ΔT* for (a) CS1$^{\Delta T}$ (b) CS2$^{\Delta T}$

6.8 Conclusions

In conclusion, the presented work on the optimal operation of a reactor-separator-recycle process shows that the ratio of A to B circulating around the recycle loop is an unconstrained degree of freedom that significantly affects the process economic performance. Through an analysis of the overall plant material balance, a globally optimal control law relating the reactor A and B mol fractions has been obtained for minimizing the recycle rate (Mode Ia) or maximizing production (Mode IIa) with maximum recycle rate as the bottleneck constraint. The control law is self-optimizing for the more rigorous economic objectives of minimizing column boilup (Mode Ib) and maximizing production with maximum column boilup as the bottleneck (Mode IIb). We have also shown that for the studied process, the reactor A/B ratio is a good SOCV. The separator top tray temperature (T_{top}) has a direct correlation with the reactor A/B ratio and is recommended both for stoichiometric feed balancing and as an equivalent SOCV as it avoids cumbersome analytical reactor composition measurements. Lastly the proposed economic plantwide control system (CS2), that holds T_{top}, is shown to provide robust process regulation with noticeably superior economic performance compared to the conventional practice of holding x_{rxrB} constant, for the considered principal disturbances when they are much slower than the plantwide response time. For the considered disturbances, the steady state economic benefit of CS2 over CS1 is up to 7% and 0.8% for Mode Ib and Mode IIb, respectively. Overall, the work demonstrates how systematically addressing the "what to control" question can achieve significant economic benefit.

References

(1) Skogestad, S. Plantwide control: The search for the self-optimizing control structure. *J. Process Control* 2000, 10(5), 487-507.

(2) Skogestad, S. Self-optimizing control: the missing link between steady-state optimization and control. *Comput. Chem. Eng.* 2000, 24, 569-575.

(3) Skogestad, S. Near-optimal operation by Self-optimizing control: from process control to marathon running and business systems. *Comput. Chem. Eng.* 2004, 29, 127-137.

(4) Halvorsen, I. J.; Skogestad, S.; Morud, J. C.; Alstad, V. Optimal selection of controlled variables. *Ind. Eng. Chem. Res.* 2003, 42(14), 3273–3284.

(5) Govatsmark, M. S.; Skogestad, S. Selection of controlled variables and robust setpoints. *Ind. Eng. Chem. Res.* 2005, 44(7), 2207–2217.

(6) Panahi, M.; Skogestad, S. Economically efficient operation of CO_2 capturing process part I: Self-optimizing procedure for selecting the best controlled variables. *Chem. Eng. and Process.* 2011, 50(3), 247-253.

(7) Larsson, T.; Hestetun, K.; Hovland, V.; Skogestad, S. Self-optimizing control of a large scale plant-The Tennessee Eastman process. *Ind. Eng. Chem. Res.* ***2001***, 40(22), 4889–4901.

(8) Jensen J. B.; Skogestad, S. Optimal Operation of Simple Refrigeration Cycles. Part II: Selection of Controlled Variables. *Comput. Chem. Eng*, 2007, 31, 1590-1601.

(9) Alstad, V.; Skogestad, S. Null space method for selecting optimal measurement combinations as controlled variables. *Ind. Eng. Chem. Res.* 2007, 46(3), 846-853.

(10) Luyben, W. L. Dynamics and control of recycle systems. 1. Simple open-loop and closed-loop systems. *Ind. Eng. Chem. Res.* 1993, 32(3), 466-475.

(11) Wu, K. L.; Yu, C. C. Reactor/separator processes with recycle 1. Candidate control structure for operatibility. *Comput. Chem. Eng.* 1996, *20*, 1291-1316.

(12) Larsson, T.; Govatsmark, M.S.; Skogestad, S.; Yu, C. C. Control Structure Selection for Reactor, Separator and Recycle Processes. *Ind. Eng. Chem. Res*., 2003, 42 (6), 1225-1234.

(13) Minasidis, V.; Skogestad, S.; Kaistha, N. Simple rules for economic plantwide control. *Comp. Aided Chem. Eng*. 2015, 37, 101-108.

(14) Luyben, W. L. Dynamics and control of recycle systems. 2. Comparison of alternative process designs. *Ind. Eng. Chem. Res.* 1993, 32(3), 476-486.

(15) Kanodia, R.; Kaistha, N. Plant-wide control for throughput maximization: A case study. *Ind. Eng. Chem. Res.* 2010, 49(1), 210-221.

(16) Jagtap, R.; Kaistha, N.; Skogestad, S. Plantwide control for economic optimum operation of a recycle process with side reaction. *Ind. Eng. Chem. Res.* 2011, 50(14), 8571-8584.

(17) Sahu, A.; Kumar, V.; Kaistha, N. Conceptual design and plantwide control of an ethyl acetate process. *Chem. Eng. Process. Process Intensif.* 2018, 126, 45-61.

(18) Percell, E.; Moore, C.F. Analysis of the Operation and Control of a Simple Plantwide Module. *Proceed. Amer. Cont. Conf.* 1995, 1, 230-234.

(19) Ojasvi; Kaistha, N. Design and Operating Strategy Innovations for Energy Efficient Process Operations, The Water-Food-Energy-Nexus: Processes, Technologies, and Challenges, CRC Press, Taylor and Francis, 2017, 717-735.

(20) Gupta, R.; Kaistha, N. Role of nonlinear effects in benzene-toluene-xylene dividing wall column control system design. *Ind. Eng. Chem. Res.* 2015, 54(38), 9407-9420.

(21) Luyben, W. L.; Luyben, M. L.; Tyreus, B. D. *Plantwide Process Control*; McGraw-Hill: New York, 1998.

(22) Mejdell, T.; Skogestad, S. Composition estimator in a pilot-plant distillation column using multiple temperatures. *Ind. Eng. Chem. Res.* 1991, 30(12), 2555-2564.

(23) Luyben, W. L. Feedback control of distillation columns by double differential temperature control. *Ind. Eng. Chem. Fundam.* 1969, 8(4), 739-744.

(24) Pavan Kumar, M. V.; Kaistha, N. Decentralized control of a kinetically controlled ideal reactive distillation column. *Chem. Eng. Sci.* 2008, 63, 228-243.

(25) Pavan Kumar, M. V.; Kaistha, N. Role of multiplicity in reactive distillation control system design. *J. Process Control* 2008, 18, 692-706.

Chapter 7

Summary and Future Work

Overall, the work presented in this thesis suggests that (near) optimal management of an unconstrained degree of freedom (dof) can result in significant economic benefit. The application of three techniques for (near) optimal management of a controlled variable (CV) corresponding to an unconstrained dof, namely, hill-climbing, real-time optimization (RTO) and invariant inspired self-optimizing control (SOC), has been considered here. These techniques have been applied to the benchmark $A + B \rightarrow C$ reactor-separator-recycle process for different reaction kinetics. Overall, the results show that the economic benefit can be as high as a few percentage points (up to 10%) compared to constant setpoint operation using conventional CVs. In what follows, the main findings based on the experience with these techniques, particularly emphasizing the suitability of each technique in a specific scenario, are summarized along with pointers for future work.

7.1 Hill Climbing

In the context of plantwide control of continuous integrated chemical processes, hill-climbing control may be used for driving an unconstrained CV setpoint to its optimum value. The case-study results clearly show that the hill-climber drives the unconstrained reactor composition setpoint to its actual optimum in about 6-8 moves with significant economic benefit over the conventional constant setpoint operating policy. The method is however effective only in the absence of unmeasured disturbances that can confound the economic objective gradient estimate with respect to the unconstrained CV and move the CV in the wrong direction. It should therefore be applied to obtain the optimum CV setpoint value during relatively calm and undisturbed periods of process operation.

Given that the open loop plantwide response times can be quite large in recycle systems, the 6-8 hill climber moves and also the reduction in the hill-climber open loop gain as the process gets closer to the optimum (gradient approaches zero near optimum), the hill climber takes a long time to reach close to the CV setpoint optimum. Also, in the first few iterations where the gradient is not known, it can move the CV setpoint in the wrong direction before reliable gradient estimates cause the setpoint to move in the right direction. Since the hill-climber obtains gradient estimates through explicit plant perturbations, it guarantees approach to the actual optimum in the presence of a static disturbance.

In view of all of the above, the hill-climber appears to be an ideal tool for application in conjunction with self-optimizing control. Since the appropriate SOCV setpoint value is not known *apriori*, the hill-climber may be used for obtaining it during relatively calm periods of operation. Once the value is obtained, the hill-climber can be switched off with self-optimizing control ensuring near optimal operation at constant SOCV setpoint.

One of the limitations of the current work is the use of a one dof hill-climber. Future work may consider its extension to multivariable optimization problems, where there are more than one economically important unconstrained CVs. The hill climber may also be tested for other more complex integrated chemical processes with multiple material recycle loops as well as energy recycle loops.

7.2 Real Time Optimization

Real time optimization remains the preferred method for optimizing an unconstrained CV setpoint in the industry as it does not require perturbing the plant to estimate the economic objective gradient and approaches the plant optimum by repeatedly fitting a model to recent plant data, calculating the model optimum and implementing the model calculated optimum setpoints in the plant. The feedback is through the repeated parameter fitting and model reoptimization. The problem however is that the RTO converged optimum is only as good as the plant model. Thus, an inadequate process model or an inappropriate parameter fitting strategy can result in the converged RTO optimum being significantly away from the actual plant optimum. In the presented case-study, the inability of the elementary reaction kinetic model (KM I) to converge close to the actual plant optimum is a compelling illustration of this.

Given an adequate process model and appropriate parameter fitting strategy, the case-study results show that RTO converges very close to the actual plant optimum in about 4-5 RTO iterations but not the exact plant optimum. Very simple time averages over a sufficiently large time window of transient process data are appropriate for estimating the process variables required in the model fitting exercise. Even in the presence of large variability in the process feed composition, the developed RTO approach for the reactor-separator recycle process effectively compensates for slow disturbances. The approach however may not be useful for compensating fast disturbances.

Given the possibility of large offset in the RTO converged optimum from the actual plant optimum, combining model based RTO with hill-climbing so that the offset gets driven to zero via feedback, is a promising avenue for further research. It appears that the modifier adaptation method recently developed by Bonvin and coworkers[1-4], that ensures RTO convergence to the actual plant optimum is one such method combining model based RTO with feedback. Its application to plantwide control problems needs immediate further investigation.

7.3 Invariants and Self Optimizing Control

The ideal way of managing an economically dominant unconstrained CV setpoint is by holding a globally optimal invariant. The invariant corresponds to the economic optimality condition with respect to the CV. In this work, it was possible to derive an elegant invariant for the one unconstrained dof corresponding to the second fresh feed in the reactor-separator-recycle process. The derivation was made possible by directly solving the plant overall material balance constraint and the optimality condition. For power law kinetics, holding the reactor *A/B* ratio constant at an appropriate value minimizes the recycle rate (Mode I) or maximizes production (Mode II) with maximum recycle rate as the capacity bottleneck. Somewhat more complicated invariants are obtained for Langmuir Hinshelwood kinetics. Results show that regardless of the kinetic expression, holding the reactor *A/B* ratio constant is a good self-optimizing policy for the unconstrained dof for the rigorous objective of minimizing column boilup and maximizing production with maximum boilup as the capacity bottleneck. The work thus provides a sound physical basis for using reactor *A/B* ratio as a SOCV.

For the reactor-separator-recycle process, the *A/B* ratio can be directly inferred from the column top temperature (T_{top}) to avoid cumbersome analytical composition measurements. Dynamic results not only confirm the economic benefit of T_{top} control over constant reactor composition operation, but also show that for not-too-slow sinusoidal disturbances with time periods of 12hrs or more, controlling T_{top} achieves economic benefit of a few percentage points over conventional reactor composition control. From the practical standpoint, invariant inspired SOCVs seem like the best bet for achieving better plant economics in the face of not-too-slow disturbances.

Overall, a combination of SOC and RTO/hill-climbing appears to be the most prudent way of managing an economically important unconstrained CV. Given the appropriate SOCV setpoint value, holding it constant ensures an acceptably small loss for moderate disturbances. A hill-climber or RTO may be used to obtain the appropriate SOCV setpoint value. In case of a significant change in the plant characteristics, the hill-climber/RTO may be invoked again to readjust the SOCV setpoint.

7.4 Concluding Remarks

Optimal operation of chemical plants has been researched for over four decades now. In addition to the techniques evaluated here, other variants such as evolutionary operation (EVOP)[5-6] and response surface methods too exist but have not been explored here. In addition, recent literature proposes direct economic model predictive control[7-9]. An evaluation of these other techniques may be explored in the future. It is however worth noting the economic MPC is mathematically very complex and the computations may not be tractable for typically large plantwide control problems.

In terms of the research imperatives based on the current work, it is highlighted that the three techniques have been evaluated in isolation here and no effort has been made directly compare their performance for typical disturbance scenarios. Such an evaluation would be of much interest to the academic and industrial community and should be taken up on priority. Additionally, it would be desirable to explore economic plantwide control problems with multiple unconstrained CVs that are economically dominant.

In the end, it is pertinent to highlight that regardless of the technique used for economic plantwide control, it is essential to understand the reasons as to why a particular CV is economically dominant based on the physics of the process and also why/how the proposed method for managing the CV ensures (near) optimality. In the absence of such physical insights and understanding, all of the economic plantwide control work risks being only a fancy number crunching game with little/no practical utility. In the pursuit of better plant economics, it is important to guard against the temptation of fancy number crunching replacing solid process engineering based on insights and understanding of the physics of the process.

References

(1) Marchetti, A.; Chachuat, B.; Bonvin, D. Modifier-adaptation methodology for real-time optimization. *Ind. Eng. Chem. Res.* 2009, 48(13), 6022-6033.

(2) Chachuat, B.; Srinivasan, B.; Bonvin, D. Adaptation strategies for real-time optimization. *Comput. Chem. Eng.* 2009, 33(10), 1557-1567.

(3) Marchetti, A.; Chachuat, B.; Bonvin, D. A dual modifier-adaptation approach for real-time optimization. *J. Process Control* 2010, 20(9), 1027-1037.

(4) Costello, S.; François, G.; Bonvin, D. A directional modifier-adaptation algorithm for real-time optimization. *J. Process Control* 2016, 39, 64-76.

(5) George, E. P. B.; Draper, N. R. *Evolutionary Operation: A Statistical Method for Process Improvement*. John Wiley & Sons, Inc., New York, 1969.

(6) Zhang, Y.; Nadler, D.; Forbes, J. F. Results analysis for trust constrained real-time optimization. *J. Process Control* 2001, 11 (3), 329-341.

(7) De Souza, G.; Odloak, D.; Zanin, A. C. Real-time optimization (RTO) with model predictive control (MPC). *Comput. Chem. eng.* 2010, 34 (12), 1999-2006.

(8) Marchetti, A. G.; Ferramosca, A.; González, A. H. Steady-state target optimization designs for integrating real-time optimization and model predictive control. *J. Process Control* 2014, 24 (1), 129-145.

(9) D'Jorge, A.; Ferramosca, A.; González, A. H. A robust gradient-based MPC for integrating real time optimizer (RTO) with control. *J. Process Control* 2017, 54, 65-80.

Nomenclature

E	Reactor effluent flow rate, kmol/h
F_A	Fresh *A* feed flow rate, kmol/h
F_B	Fresh *B* feed flow rate, kmol/h
F_{col}	Column feed rate, kmol/h
F_{rxr}	Reactor feed rate, kmol/h
J	Economic objective function
k	Reaction rate constant, kmol/s.m^3
K	Absorption equilibrium constant
L	Column reflux rate, kmol/h
P	Column bottom product rate, kmol/h
Pr	Pressure, kPa
Q	Heating or cooling duty, kW
r	Specific reaction rate, kmol/s.m^3
R	Recycle rate, kmol/h
T	Temperature, °C
u	Regulatory layer setpoint manipulated by hill-climber
U	Hold-up, m^3
V	Column boilup, kmol/h
v_S	Column vapor superficial velocity, m/s
x_i^j	Component i (i: A, B, C) mol fraction in stream j (j: P, R, E, F_{col}, F_{rxr} etc)
x_{rxri}	Component i (i: A, B, C) mol fraction in reactor
$y_{estimated}$	Estimated hill slope
y_{SOC}	Self optimizing control process variables
ΔPr_{col}	Column pressure drop, kPa

Greek Symbols

α	Kinetic model reaction order with respect to component *A* mol fraction
β	Kinetic model reaction order with respect to component *B* mol fraction
η_R	Rectifying section tray Murphree efficiency
η_S	Stripping section tray Murphree efficiency
ρ	Column vapor density, kg/m^3

Superscripts

*	Plant process variable (PV) measurement
e	Estimated PV/parameter
m	Model PV/parameter
MIN	Minimum constraint value
MAX	Maximum constraint value
opt	optimum
S	Column stripping tray
SP	Controller setpoint

Subscripts

A, B, C	For components A, B or C
bot	PV for bottom sump
cnd	PV for condensor
col	PV for column
rxr	PV for reactor
reb	PV for reboiler
rd	PV for reflux drum

Vivek Kumar

Email: vivekiit09@gmail.com
Mobile: 8574854047

117/Q/38 R.K. Housing Society
Sharda Nagar, Kanpur, U.P.
208025 (INDIA)

PERSONAL

DOB: 28th August 1983 *Marital Status*: Married *Sex*: Male *Nationality*: Indian

RESEARCH INTERESTS

- Economic plantwide control of integrated chemical processes
- Modelling, simulation and control of chemical systems

EDUCATION

Indian Institute of Technology (IIT), Kanpur (Thesis submitted)
Ph.D., Chemical Engineering (July 2011- Till date) **9.33/10**
Dissertation: Economic Plantwide Control Techniques Applied to a Reactor-Separator-Recycle Process

Indian Institute of Technology (IIT), Kharagpur
M.Tech., Chemical Engineering (2009-2011) **8.95/10**
Dissertation: Energy Integration in an ETBE Reactive Distillation Column

Institute of Engineering & Technology (IET), Lucknow
B.Tech., Chemical Engineering (2004-2008) **74.92%**

Dr. C. L. Rastriya Inter College, Kanpur
Intermediate, U.P. Board, 2001 **71.60%**

Dr. C. L. Rastriya Inter College, Kanpur
High School, U.P. Board, 1999 **75.10%**

JOURNAL PUBLICATIONS

- **V. Kumar** and N. Kaistha, "Real time optimization of a reactor-separator-recycle process I: Steady state modelling", *Ind. Eng. Chem. Res.*, 2018, 57 (37), 12429-12443.
- **V. Kumar** and N. Kaistha, "Real time optimization of a reactor-separator-recycle process II: Dynamic evaluation", *Ind. Eng. Chem. Res.*, Accepted.
- **V. Kumar** and N. Kaistha, "Invariants for optimal operation of a reactor-separator-recycle process", *J. Process Control,* under review.
- **V. Kumar** and N. Kaistha, "Inferential self optimizing control of a reactor-separator-recycle process: Self optimizing control and real time optimization", *Ind. Eng. Chem. Res.*, under review.

- **V. Kumar** and N. Kaistha, "Hill Climbing for plantwide control to economic optimum", *Ind. Eng. Chem. Res.*, 53, 16465-16475 (2014).
- **V. Kumar**, B. Kiran, A. K. Jana, and A. N. Samanta, "A Novel Multi-stage Vapor Recompression Reactive Distillation with Intermediate Reboilers", *AIChE J.*, 59, 761-771 (2013).
- A. Sahu, **V. Kumar** and N. Kaistha, "Conceptual design and plantwide control of an ethyl acetate process", *Chem. Eng. Process. Process Intensif.*, 126, 45-61 (2018).
- S. S. Thakur, Ojasvi, **V. Kumar** and N. Kaistha, "Continuous diisobutylene manufacturing: conceptual process design and plantwide control", *Comp. Chem. Eng.*, 97, 59-75 (2017).

CONFERENCES

- AIChE Annual Meeting: V. Kumar and **N. Kaistha**, "Steady-State Real Time Optimization of Reactor-Separator-Recycle Process" (poster presentation) Oct 2017, Minneapolis, MN
- IFAC World Congress: V. Kumar and **N. Kaistha**, Hill-Climbing for Economic Plantwide Control (Oral presentation) Aug 2014, Capetown, South Africa

INDUSTRIAL EXPERIENCE

July 08-Aug 09 Process Engineer Jubilant Organosys Limited, Gajraula

- Supervised production plant of Acetic Anhydride and Ethyl Acetate.

AWARDS

- Best oral talk award in computational and simulation category in Research scholar day'2017 at IIT Kanpur

OTHER RELEVANT INFORMATION

Organized intensive short courses on plantwide control, Jun 2014 at IIT Kanpur for design/control engineers in the industry.

REFERENCES

Prof Nitin Kaistha	nkaistha@iitk.ac.in +91-512-2597432 Chemical Engineering Indian Institute of Technology Kanpur Kanpur, U.P., India-208016
Prof Nishith Verma	nishith@iitk.ac.in +91-512-2596767 Chemical Engineering Indian Institute of Technology Kanpur Kanpur, U.P., India-208016
Dr. Amiya K. Jana	akjana@che.iitkgp.ernet.in +91-3222-283918 Chemical Engineering Indian Institute of Technology Kharagpur Kharagpur, W.B., India-721302